NPS ARCHIVE
1969
BANNING, M.

THE UNSTEADY NORMAL FORCE ON AN AIRFOIL IN OSCILLATING FLOW

by

Maurice Roy Banning

Thesis
B214
c.1

DUDLEY KNOX LIBRARY
NAVAL POSTGRADUATE SCHOOL
MONTEREY, CALIFORNIA 93943-5002

DUDLEY KNOX LIBRARY
NAVAL POSTGRADUATE SCHOOL
MONTEREY, CA 93943-5101

United States
Naval Postgraduate School

THESIS

THE UNSTEADY NORMAL FORCE ON AN
AIRFOIL IN OSCILLATING FLOW

by

Maurice Ray Banning

December 1969

This document has been approved for public release and sale; its distribution is unlimited.

T135683

DUDLEY KNOX LIBRARY
NAVAL POSTGRADUATE SCHOOL
MONTEREY, CA 93943-5101

The Unsteady Normal Force on an Airfoil in Oscillating Flow

by

Maurice Ray Banning
Captain, United States Marine Corps
B.S., Oregon State University, 1962

Submitted in partial fulfillment of the
requirements for the degree of

AERONAUTICAL ENGINEER

from the

NAVAL POSTGRADUATE SCHOOL
December 1969

NPS ARCHIVE
1969
BANNING, M.

ABSTRACT

The effects of oscillating flow on the pressure force normal to the chord of a symmetrical airfoil were investigated experimentally employing a remote pressure transducer to measure the instantaneous pressure distribution.

An open circuit wind tunnel having a set of rotating shutter blades located down stream of the test section was used to produce the oscillating flow. Electrical signals analogous to the free stream velocity and surface pressure were recorded simultaneously on separate tracks of a magnetic tape. The recorded data were converted to digital representation, and numerical techniques utilized to evaluate the spectral composition of the measured pressure distribution, from which the normal force was calculated.

It was found that the magnitude of the total normal force at high angles of attack is significantly greater in oscillating flow than in steady flow and is frequency dependent; while at low angles of attack no significant differences were observed. Moreover it was found that higher order harmonics of the fundamental free-stream frequency constitute a significant fraction of the normal force, and these fractions are also frequency dependent. The observed results are not adequately predicted by quasi-steady aerodynamic analysis.

ARY
L POSTCRADUATE SCHOOL
EREY, CALIF. 93940

DUDLEY KNOX LIBRARY
NAVAL POSTGRADUATE SCHOOL
MONTEREY, CA 93943-5101

TABLE OF CONTENTS

I. INTRODUCTION 15

II. BASIC APPROACH 16

A. ALTERNATIVES AVAILABLE FOR MEASUREMENT 16

B. BRIEF DESCRIPTION OF EXPERIMENTAL METHOD 17

III. EXPERIMENTAL EQUIPMENT 18

A. WIND TUNNEL 18

1. General Description 18

2. Rotating Shutter Valve 18

3. Test Section 22

B. MODEL 22

C. PRESSURE MEASURING SYSTEM 27

1. Pressure Transducers 27

2. Power Supplies and Amplifier 31

D. HOT WIRE ANAMOMETER 31

E. TAPE RECORDER 37

F. MISCELLANEOUS 37

IV. PROCEDURES 39

V. DATA ANALYSIS 40

A. ANALOGUE TO DIGITAL CONVERSION 40

B. TAPE CONVERSION 43

C. ADDITIONAL ASSUMPTIONS 43

D. NON-DIMENSIONALIZATION 44

1. Pressure Coefficients 44

2. Normal Force Coefficients 44

3. Center of Pressure 45

DUDLEY KNOX LIBRARY
NAVAL POSTGRADUATE SCHOOL
MONTEREY, CA 93943-5101

E. COMPUTATIONAL PROCEDURES 45

VI. RESULTS AND DISCUSSION 48

A. CONDITIONS INVESTIGATED 48

B. STEADY FLOW RESULTS 48

C. UNSTEADY FLOW RESULTS 49

1. Run 5 49

2. Run 7 51

D. COMPARISON OF RESULTS AT DIFFERENT FREQUENCIES 52

1. Normal Force and Center of Pressure 52

2. Pressure Distributions 53

E. COMPARISON OF UNSTEADY FLOW RESULTS WITH STEADY FLOW ANALYSIS 54

F. SUMMARY OF RESULTS 55

VII. CONCLUSIONS 57

APPENDIX A - Transducer Calibration 128

APPENDIX B - Analogue to Digital Conversion 132

APPENDIX C - Numerical Analysis of Data 137

APPENDIX D - Evaluation of Experimental Techniques 140

COMPUTER PROGRAM LISTINGS 144

A. DATA ANALYSIS 144

B. TAPE CONVERSION 160

C. DISPLAY 162

LIST OF REFERENCES 170

INITIAL DISTRIBUTION LIST 171

FORM DD 1473 173

LIST OF TABLES

Table		Page
I	Typical Tape Recorder Calibration	37
II	Typical Recorded D. C. Voltage and Corresponding Digital Mean Value	43
III	Experimental Conditions for which Data was Taken	58
IV	Chordwise Variation in Amplitude Ratio, Run 5	142
V	Chordwise Variation in Amplitude Ratio, Run 7	143

LIST OF ILLUSTRATIONS

Figure		Page
1	Plan View of Wind Tunnel	19
2	Photograph of Rotating Shutter Valve	21
3	Photograph of Wind Tunnel Test Section	23
4	Typical Wind Tunnel Test Section Velocity Profile	24
5	Overall Photographic View of Wind Tunnel	25
6	Schematic Diagram of Airfoil Model Showing Pressure Tap Location	26
7	Photograph of Airfoil Model Mounted in Tunnel	28
8	Sectional Drawing of Pressure Transducer	29
9	Photograph of Transducer Components	30
10	Transducer Gain	32
11	Transducer Phase Angle	33
12	Schematic Diagram of Pressure Measuring System	34
13	Typical Pressure Measuring System Static Calibration Curve	35
14	Photograph of Pressure Measuring System Installed	36
15	Schematic Diagram of Data Acquisition System	38
16	Filter Gain	41
17	Filter Phase Angle	42
18	Abbreviated Flow Chart of Computer Program Used to Analyze Data	47
19	$\overline{C}_N$ vs. α, Steady Flow	59
20	Mean Pressure Distribution on Airfoil, Run 2 α = 5 Degrees, Steady Flow	60
21	Mean Pressure Distribution on Airfoil, Run 3 α = 10 Degrees, Steady Flow	61

Figure		Page
22	Mean Pressure Distribution on Airfoil, Run 4 α = 15 Degrees, Steady Flow	62
23	PSD of Unsteady Pressure Coefficient, Run 1 ξ = 0.0	63
24	PSD of Unsteady Pressure Coefficient, Run 1 ξ = 0.250, Upper Surface	64
25	PSD of Unsteady Pressure Coefficient, Run 2 ξ = 0.0	65
26	PSD of Unsteady Pressure Coefficient, Run 2 ξ = 0.150, Lower Surface	66
27	PSD of Unsteady Pressure Coefficient, Run 3 ξ = 0.0	67
28	PSD of Unsteady Pressure Coefficient, Run 3 ξ = 0.450, Upper Surface	68
29	PSD of Unsteady Pressure Coefficient, Run 3 ξ = 0.5, Lower Surface	69
30	PSD of Unsteady Pressure Coefficient, Run 4 ξ = 0.0	70
31	PSD of Unsteady Pressure Coefficient, Run 4 ξ = 0.500, Upper Surface	71
32	PSD of Unsteady Pressure Coefficient, Run 4 ξ = 0.125, Lower Surface	72
33	Mean Square of Unsteady Pressure Coefficient vs. ξ, Run 3	73
34	Mean Square of Unsteady Pressure Coefficient vs. ξ, Run 4	74
35	Typical Unfiltered PSD, Steady Flow	75
36	Velocity and Pressure Analogue Waveforms, Run 5, f_0 = 94 Hertz, α = 15 Degrees, ϵ = 0.085	76
37	Velocity and Pressure Analogue Waveforms, Run 5, (continued)	77
38	PSD of Unsteady Velocity, Run 5	78
39	PSD of Unsteady Pressure Coefficient, Run 5 ξ = 0.0, Upper Surface	79

Figure		Page
40	PSD of Unsteady Pressure Coefficient, Run 5 ξ = 0.025, Upper Surface	80
41	PSD of Unsteady Pressure Coefficient, Run 5 ξ = 0.075, Upper Surface	81
42	PSD of Unsteady Pressure Coefficient, Run 5 ξ = 0.125, Upper Surface	82
43	PSD of Unsteady Pressure Coefficient, Run 5 ξ = 0.175, Upper Surface	83
44	PSD of Unsteady Pressure Coefficient, Run 5 ξ = 0.225, Upper Surface	84
45	PSD of Unsteady Pressure Coefficient, Run 5 ξ = 0.300, Upper Surface	85
46	PSD of Unsteady Pressure Coefficient, Run 5 ξ = 0.350, Upper Surface	86
47	PSD of Unsteady Pressure Coefficient, Run 5 ξ = 0.400, Upper Surface	87
48	PSD of Unsteady Pressure Coefficient, Run 5 ξ = 0.450, Upper Surface	88
49	PSD of Unsteady Pressure Coefficient, Run 5 ξ = 0.500, Upper Surface	89
50	PSD of Unsteady Pressure Coefficient, Run 5 ξ = 0.600, Upper Surface	90
51	PSD of Unsteady Pressure Coefficient, Run 5 ξ = 0.700, Upper Surface	91
52	PSD of Unsteady Pressure Coefficient, Run 5 ξ = 0.750, Upper Surface	92
53	PSD of Unsteady Pressure Coefficient, Run 5 ξ = 0.0, Lower Surface	93
54	PSD of Unsteady Pressure Coefficient, Run 5 ξ = 0.050, Lower Surface	94
55	PSD of Unsteady Pressure Coefficient, Run 5 ξ = 0.100, Lower Surface	95
56	PSD of Unsteady Pressure Coefficient, Run 5 ξ = 0.150, Lower Surface	96
57	PSD of Unsteady Pressure Coefficient, Run 5 ξ = 0.200, Lower Surface	97

Figure		Page
58	PSD of Unsteady Pressure Coefficient, Run 5 ξ = 0.250, Lower Surface	98
59	PSD of Unsteady Pressure Coefficient, Run 5 ξ = 0.350, Lower Surface	99
60	PSD of Unsteady Pressure Coefficient, Run 5 ξ = 0.450, Lower Surface	100
61	PSD of Unsteady Pressure Coefficient, Run 5 ξ = 0.600, Lower Surface	101
62	PSD of Unsteady Pressure Coefficient, Run 5 ξ = 0.750, Lower Surface	102
63	PSD of Unsteady Pressure Coefficient, Run 5 ξ = 0.850, Lower Surface	103
64	PSD of Unsteady Pressure Coefficient, Run 5 ξ = 0.950, Lower Surface	104
65	Mean Square of Unsteady Pressure Coefficient vs. ξ, Run 5	105
66	Unsteady Normal Force Coefficient and Unsteady Velocity vs. Time, Run 5	106
67	PSD of Unsteady Normal Force, Run 5	107
68	Mean Presuure Distribution on Airfoil, Run 5, α = 15 Degrees, f_0 = 94 Hertz, ϵ = 0.085	108
69	Time Dependent Pressure Distributions on Airfoil, Run 5	109
70	Time Dependent Pressure Distributions on Airfoil, Run 5 (continued)	110
71	PSD of Unsteady Pressure at the Center of Pressure, Run 5	111
72	Velocity and Pressure Analogue Waveforms, Run 7, f_0 = 11 Hertz, α = 15 Degrees, ϵ = 0.072	112
73	Velocity and Pressure Analogue Waveforms, Run 7 (continued)	113
74	PSD of Unsteady Velocity, Run 7	114
75	PSD of Unsteady Pressure Coefficient, Run 7 ξ = 0.0, Upper Surface	115
76	PSD of Unsteady Pressure Coefficient, Run 7 ξ = 0.100, Upper Surface	116

Figure		Page
77	PSD of Unsteady Pressure Coefficient, Run 7 ξ = 0.500, Upper Surface	117
78	PSD of Unsteady Pressure Coefficient, Run 7 ξ = 0.900, Upper Surface	118
79	PSD of Unsteady Pressure Coefficient, Run 7 ξ = 0.100, Lower Surface	119
80	PSD of Unsteady Pressure Coefficient, Run 7 ξ = 0.500, Lower Surface	120
81	Mean Square of Unsteady Pressure Coefficient vs. ξ, Run 7	121
82	Unsteady Velocity vs. Time, Run 7	122
83	Unsteady Normal Force Coefficient vs. Time, Run 7	123
84	PSD of Unsteady Normal Force, Run 7	124
85	PSD of Unsteady Pressure at the Center of Pressure, Run 7	125
86	Mean Pressure Distribution on Airfoil, Run 7, α = 15 Degrees, f_0 = 11 Hertz, ϵ = 0.072	126
87	Mean Normal Force Coefficient vs. Frequency α = 15 Degrees, $\bar{U}$ = 100 feet/sec, ϵ = 0.08	127
88	Mean Center of Pressure vs. Frequency α = 15 Degrees, $\bar{U}$ = 100 feet/sec, ϵ = 0.08	127
89	Pressure Transducer Static Calibration Instrumentation	130
90	Pressure Transducer Dynamic Calibration Instrumentation	131
91	Logic and Analogue Circuitry for Steady Flow Analogue to Digital Conversion	135
92	Logic and Analogue Circuitry for Unsteady Flow Analogue to Digital Conversion	136

LIST OF SYMBOLS

Symbol	Definition	Units
C_N	Normal Force Coefficient, $\frac{N}{1/2\rho\bar{U}^2 c}$	
$\bar{C}_N$	Mean Normal Force Coefficient, $\frac{\bar{N}}{1/2\rho\bar{U}^2 c}$	
C_P	Pressure Coefficient, $\frac{P}{1/2\rho\bar{U}^2}$	
$\bar{C}_P$	Mean Pressure Coefficient, $\frac{\bar{P}}{1/2\rho\bar{U}^2}$	
F_c	Nyquist Cutoff Frequency	Hertz
G(f)	Complex Transducer Transfer Function	
G_K	Complex Value of G(f) at kth Discrete Frequency Increment	
H(f)	Complex Filter Transfer Function	
H_k	Complex Value of H(f) at kth Discrete Frequency Increment	
N	Aerodynamic Force Normal to Airfoil Chord, $\bar{N}+n$	lb/ft
$\bar{N}$	Mean Aerodynamic Force Normal to Airfoil Chord	lb/ft
P	Absolute Pressure, $\bar{P}+p$	lb/ft^2
$\bar{P}$	Mean Absolute Pressure	lb/ft^2
P_A	Atmospheric Pressure	lb/ft^2
P_1	Directly Measured Calibration Chamber Pressure	lb/ft^2
P_2	Indirectly Measured Calibration Chamber Pressure	lb/ft^2
t	Time	sec
U	Free Stream Velocity, $\bar{U}+u$	ft/sec
$\bar{U}$	Mean Free Stream Velocity	ft/sec
c	Chord Length	ft

Symbol	Definition	Units
c_n	Unsteady Normal Force Coefficient, $\frac{R}{1/2\rho\bar{U}^2 c}$	
c_p	Unsteady Pressure Coefficient, $\frac{P}{1/2\rho\bar{U}^2 c}$	
f	Frequency	hertz
f_0	Fundamental Oscillatory Frequency of Free Stream Velocity	hertz
n	Unsteady Normal Force	lb/ft
p	Unsteady Pressure	lb/ft^2
$\bar{q}$	Free Stream Stagnation Pressure Defined with Mean Free Stream Velocity, $1/2\rho\bar{U}^2$	lb/ft^2
u	Unsteady Velocity	ft/sec
$\bar{u}^2$	Mean Square of Unsteady Velocity	ft^2/sec^2
x	Chordwise Coordinate of Point on Airfoil Surface Measured from Leading Edge	ft
y	Coordinate of Point on Surface of Airfoil Measured Normal to Chord	ft
α	Angle of Attack	degrees
ϵ	Amplitude Ratio of Free Stream Oscillation, $\frac{2\cdot\sqrt{\bar{u}^2}}{\bar{U}}$	
ξ	Nondimensional Chordwise Coordinate, x/c	
η	Nondimensional Coordinate Normal to Chord, y/c	
ρ	Air Density	$slug/ft^3$
Subscripts		
$_l$	Refers to Lower Surface of Airfoil	
$_u$	Refers to Upper Surface of Airfoil	
Superscript		
*	Denotes Complex Conjugate	

I. INTRODUCTION

The aerodynamic forces associated with unsteady flows have attracted great interest in recent times. With the rapid development of the helicopter and advances in gas turbine technology, more detailed knowledge of unsteady phenomona is required than can be obtained from quasi-steady flow analysis.

Experimental investigations of unsteady flow problems have been hampered by lack of adequate facilities, i.e. lack of wind tunnels that are capable of establishing a controlled unsteady flow. Consequently the majority of previous investigations have been concerned with the starting process or have utilized programmed model motion rather than an oscillating flow [Ref. 1, 2, and 3]. Analytical investigations of the problem have been restricted to linearized solutions that are not applicable for airfoils at large angles of attack [Ref. 4 and 5].

The objective of the work reported here was to measure the time-dependent pressure distribution on an airfoil at constant angle of attack in a controlled oscillating stream and from these measurements to calculate the time-dependent forces acting on the airfoil surface.

II. BASIC APPROACH

A. ALTERNATIVES AVAILABLE FOR MEASUREMENT

There are two obvious methods one might use to measure the instantaneous pressure distribution on the surface of an airfoil model in an unsteady flow. The most direct technique would be to mount many transducers in the model in such a manner that the pressure at discrete points on the surface could be measured directly. The difficulties involved in applying this method are the cost of the miniature transducers required and the possibility that the dynamics of the test installation would influence the response of the transducers.

A less direct method would be to connect remote transducers to pressure taps on the surface of the airfoil with tubing. This would eliminate the dynamic interference likely to be encountered with the more direct method, but would add to the complexity of the system because of the transfer functions associated with the tubing.

In the case of oscillating flows, however, both the free stream velocity and the pressure at a point on the surface of the airfoil are periodic functions of time having some fixed phase relation between them. Knowledge of the phase relations existing between the free stream velocity and the pressure at various points on the surface of the airfoil, assuming that this phase relation remains constant, would allow the pressure distribution to be reconstructed from temporal records of the pressures and velocities taken over different intervals of time. A remote transducer then could be utilized to measure pressure and, if the leads from each tap were identical, only a single transfer function would have to be known.

B. BRIEF DESCRIPTION OF EXPERIMENTAL METHOD

The technique utilized in this investigation was based on the last alternative described above. Electrical signals analogous to the free stream velocity and surface pressure at a point were recorded simultaneously on separate tracks of magnetic tape. The pressure analogues recorded were the electrical output of a single remote transducer connected in turn by tubing to each of the pressure taps on the surface of the airfoil. The velocity analogues recorded were the output of a linearized hot-wire anemometer.

The transfer function of the tubing was experimentally measured and applied in digital form to the Fourier Transform of the digitized pressure analogue in order to obtain the Fourier Transform of the pressure at the surface of the airfoil. The inverse of the pressure Fourier Transform was then taken to obtain the pressure-time relation.

III. EXPERIMENTAL EQUIPMENT

A. WIND TUNNEL

1. General Description

The experimental work was conducted in the low-speed, oscillating flow wind tunnel located in the Aeronautics Laboratories of the Naval Postgraduate School. This wind tunnel is of open circuit design, with a 24-inch square by 223-inch long test section. A plan view of the tunnel is presented in Figure 1. The tunnel inlet is eight feet square, resulting in a 16:1 contraction ratio. Three high solidity screens located in the inlet section just upstream of the nozzle produce measured free stream turbulence intensities of 0.261 to 0.413 percent for the velocities encountered in the present work.

The wind tunnel drive consists of two Joy Axivane Fans in series, each of which has an internal, 100 horsepower, direct connected, 1750 rpm motor. The fan blades are internally adjustable through a pitch range of 25 to 55 degrees, providing a wide operating base. Two sets of variable inlet vanes, located immediately upstream of each fan, are externally operated to provide control of test section velocity. These vanes are of multileaf design, and preswirl the air in the direction of fan rotation to reduce fan capacity. The total range of tunnel velocity is from 10 to 250 feet per second.

2. Rotating Shutter Valve

Two fundamental methods of creating an oscillating flow environment have been employed in the past. Both Nickerson [Ref. 6] and Hori [Ref. 7] introduced oscillations by oscillating their models in a steady flow environment. This method severely restricts the range of attainable

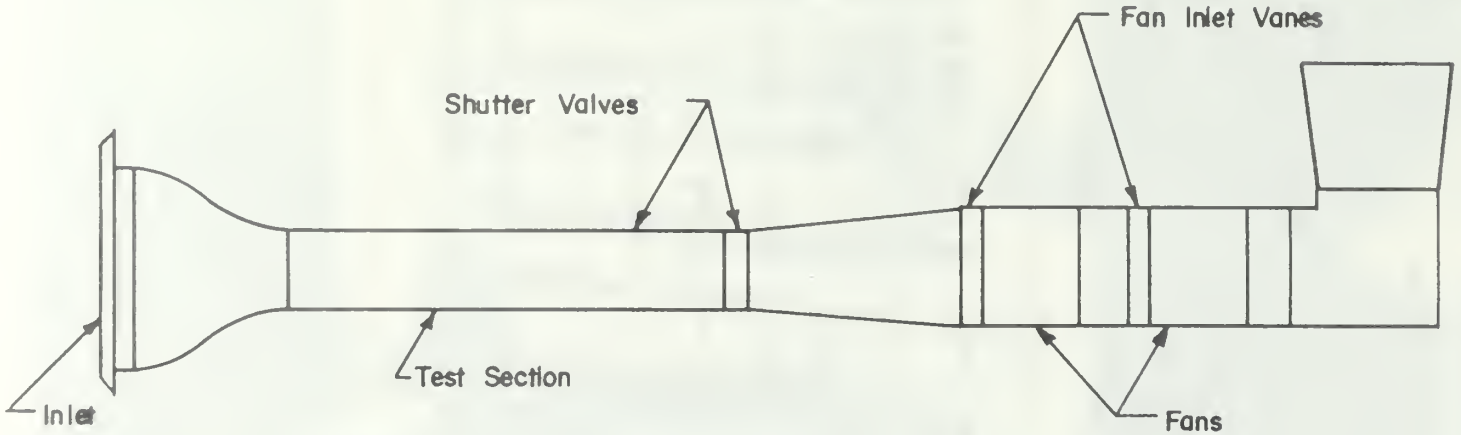

FIGURE 1

PLAN VIEW OF WIND TUNNEL

frequencies because of mechanical complications, and also introduces measurement difficulties. The other approach is to actually oscillate the flow over a stationary model. Hill [Ref. 8] used a sliding shutter to impose oscillations on the free stream but was restricted by mechanical limitations to low frequencies.

The most successful method of obtaining an oscillating flow with large ranges of frequency and amplitude was that employed by Karlsson [Ref. 9], and later by Miller [Ref. 10] in his investigation of transition. A rotating shutter valve, immediately downstream of the test section, is employed to superimpose a periodic variation of velocity on the mean flow. The method used in the present investigation is virtually identical to that employed by Miller. The shutter valve consists of four horizontal steel shafts equally spaced across the test section. The shafts are slotted to accommodate flat blades of various widths, forming a set of four butterfly valves spanning the test section. Figure 2 is a photograph of the shutter valve. Each blade is driven from its immediate neighbor by means of a timing belt and pulley arrangement. The bottom shaft is driven by a five horsepower variable speed electric motor, through a timing belt and pulley. An intermediate shaft between the motor and shutter valve permits a wide variety of pulley ratios. This drive arrangement provides a frequency range of two cycles per second to the first critical frequency of 933 cycles per second. The electric motor presently in use, however, restricts the oscillation frequency to a maximum of 240 cycles per second. The amplitude of oscillation is controlled by blade width. Test section closure may be varied from 25 to 100 per cent. The resulting amplitude of oscillation of test section velocity is a function of frequency, mean velocity and pressure gradient. In this

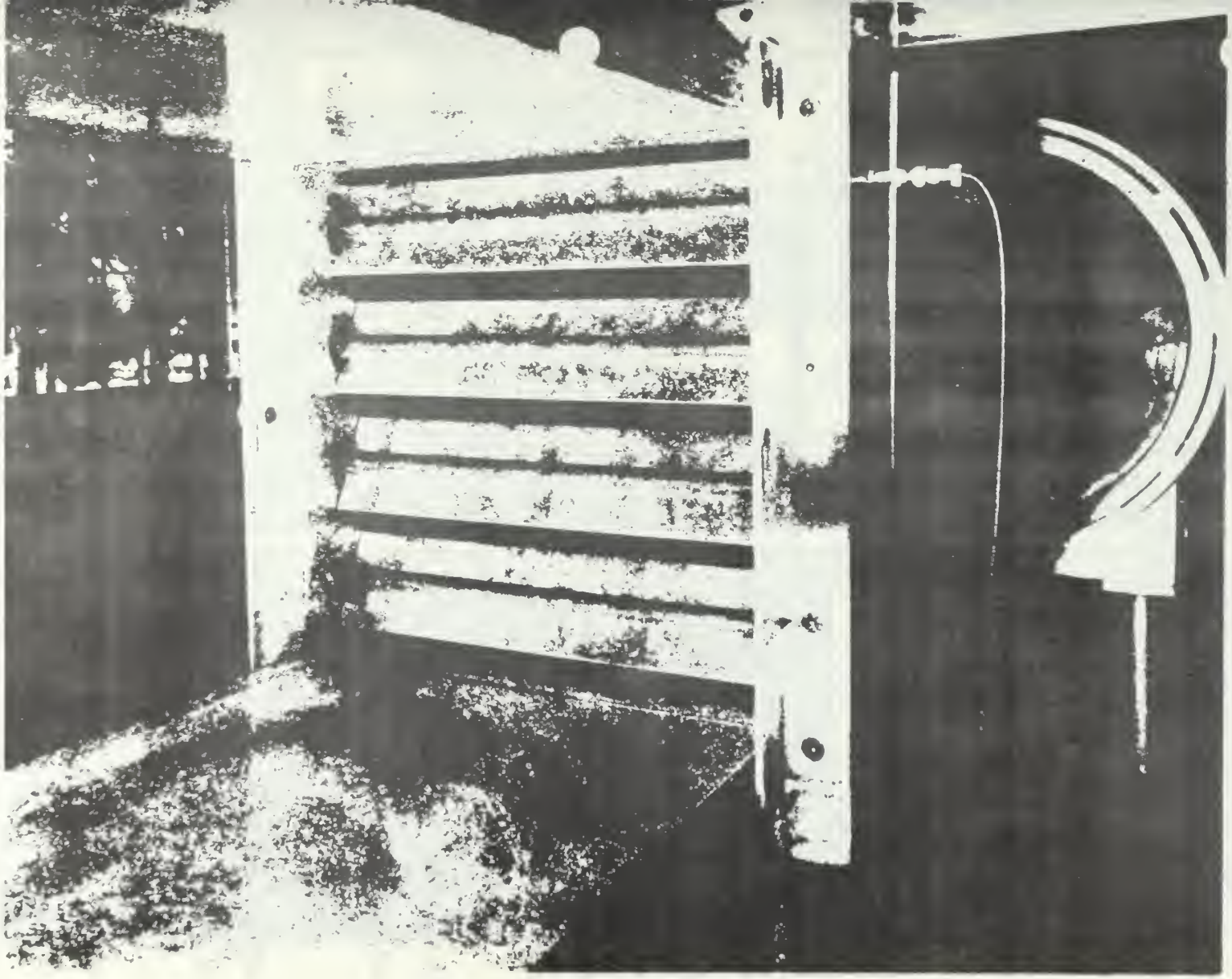

FIGURE 2 PHOTOGRAPH OF ROTATING SHUTTER VALVE

investigation, blades producing 50.0 per cent closure were used, resulting in an amplitude range of from 3 to 40 per cent of the local mean free stream velocity.

3. Test Section

The wind tunnel test section is shown in Figure 3. Continuous pieces of two-inch thick aluminum, 24 inches wide and 223 inches long, form the upper and lower test section walls. Each of the side walls consists of three two-inch thick panels of stress-relieved Lucite. For this investigation, the central side wall panel on the opposite side of the tunnel from the control console was replaced with two-inch thick plywood to facilitate the mounting of instrumentation. The Lucite panels on the console side of the test section are hinged and may be raised hydraulically, providing access to the test section. The heavy construction of the test section is intended to minimize deflections induced by rapid changes in static pressure.

Figure 4 is a typical test section velocity profile. Velocity variation is less than one per cent from the mean to within three inches of any wall.

Figure 5 is an overall photographic view of the wind tunnel.

B. MODEL

The airfoil model used in this investigation was that employed by Allen [Ref. 11]. It is a NACA 63-010 section modified by straight line fairing from 60 per cent chord to the trailing edge. The model has a 24 inch span and a constant 6 inch chord. Twenty three pressure taps are located chordwise across the upper surface and two on the lower surface at midspan. Figure 6 is a schematic drawing of the model showing the location of the pressure taps.

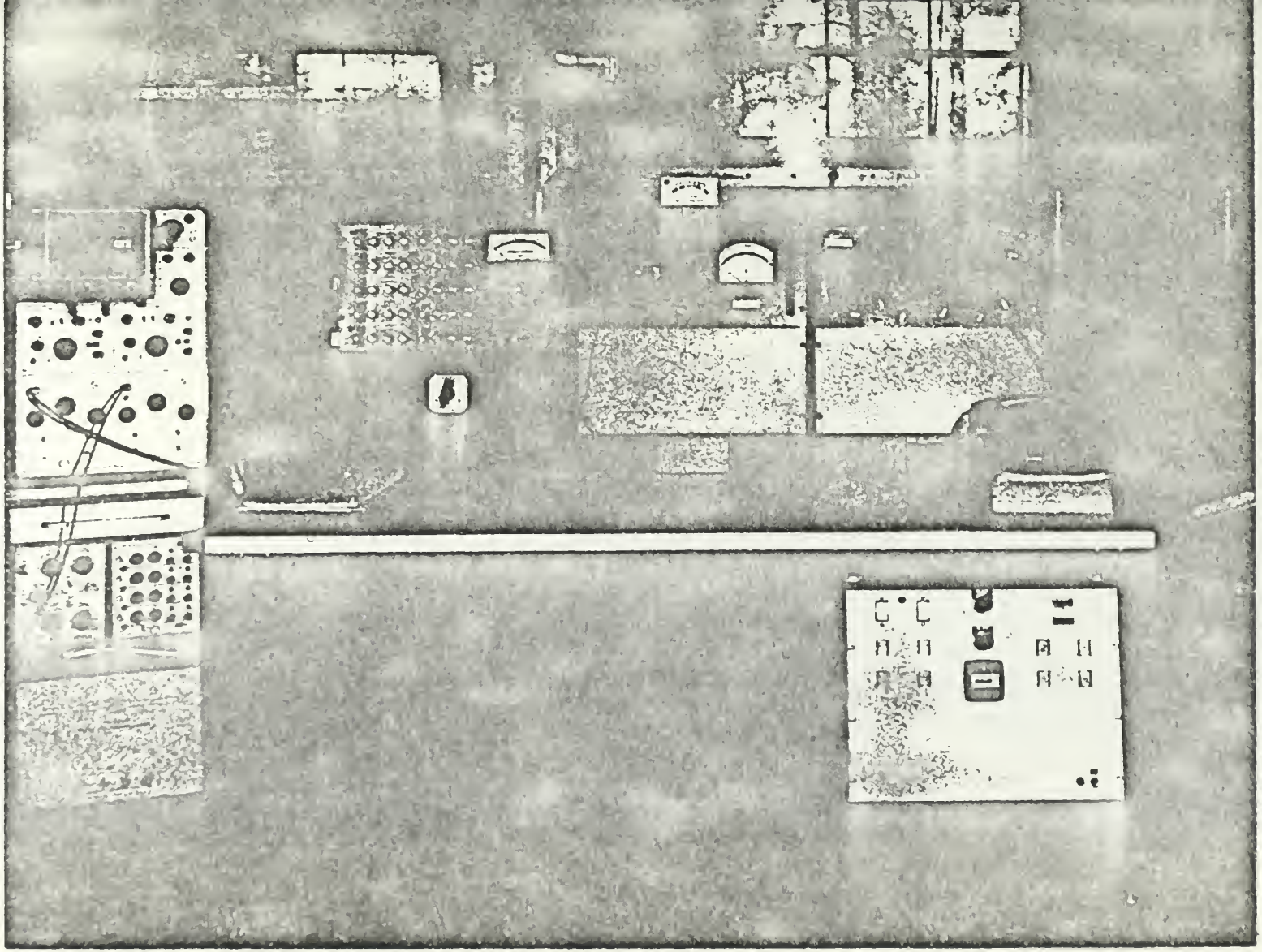

FIGURE 3 PHOTOGRAPH OF WIND TUNNEL TEST SECTION

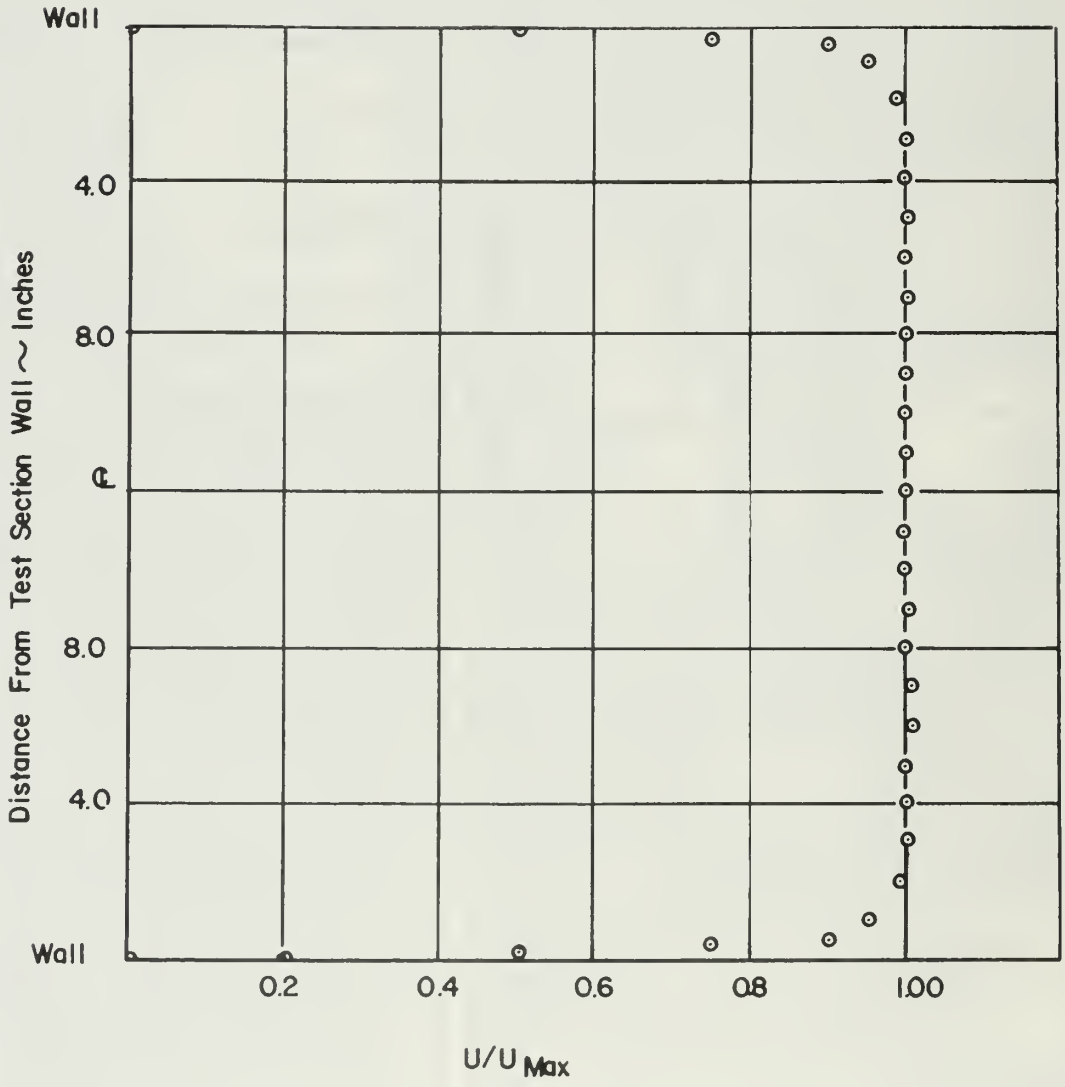

FIGURE 4

TYPICAL WIND TUNNEL TEST SECTION VELOCITY PROFILE

24 INCHES UPSTREAM OF MODEL

U_{Max} = 20ft/sec

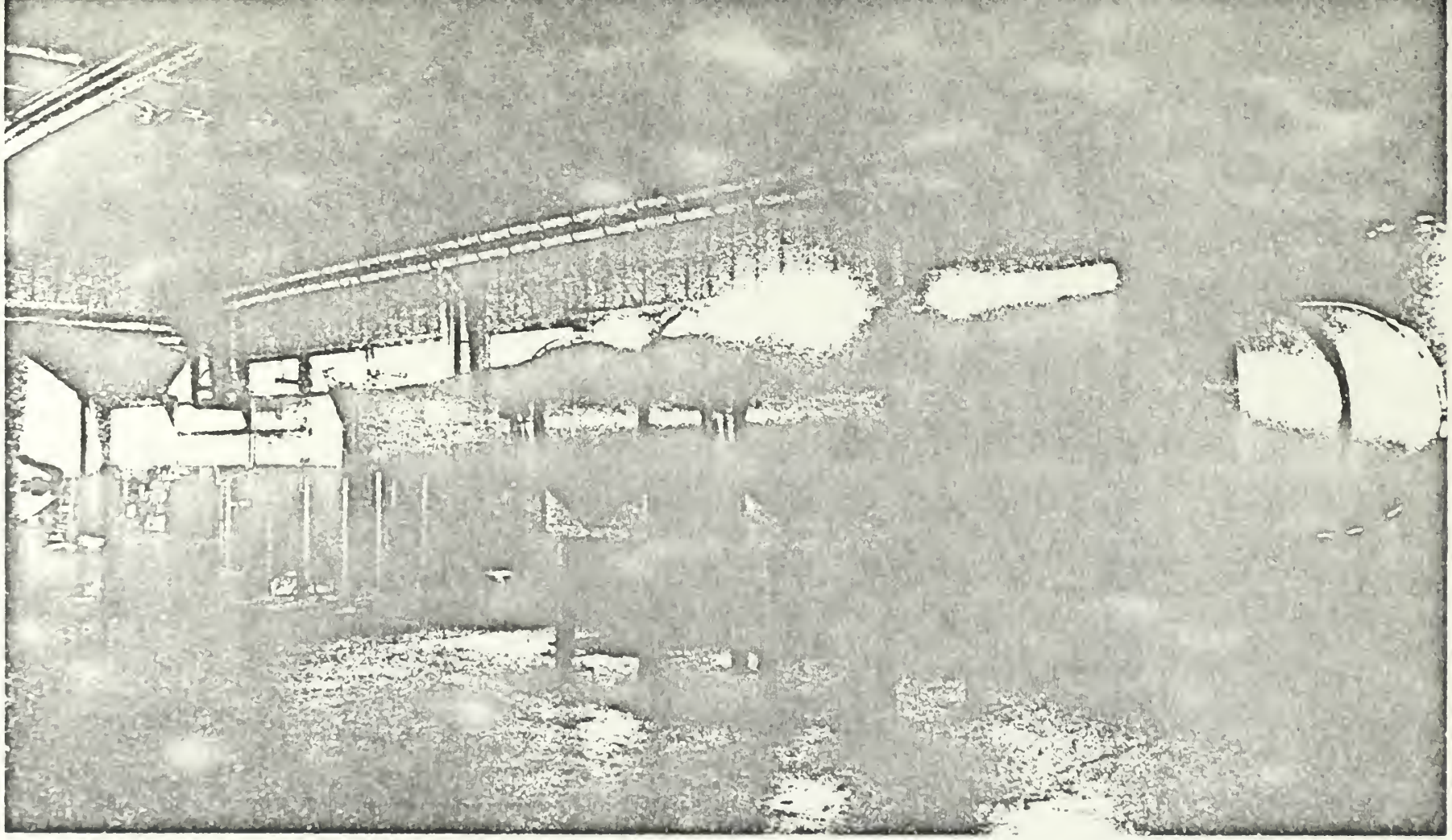

FIGURE 5. OVERALL VIEW OF WIND TUNNEL

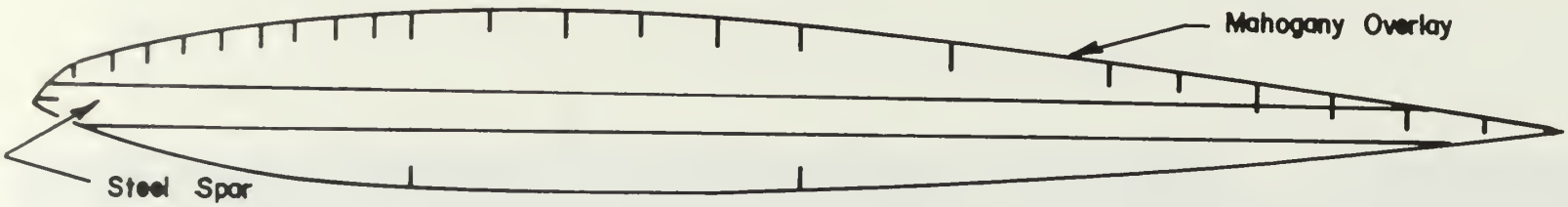

STATION	DISTANCE (x/c)
1	.00
2	.025
3	.050
4	.075
5	.100
6	.125
7	.150
8	.175
9	.200
10	.225
11	.250
12	.300
13	.350

STATION	DISTANCE (x/c)
14	.400
15	.450
16	.500
17	.600
18	.700
19	.750
20	.800
21	.850
22	.900
23	.950
*24	.250
*25	.500

*Taps 24 & 25 Are On Lower Surface

FIGURE 6. PRESSURE TAPS ON WIND TUNNEL MODEL

The model was mounted spanwise across the test section on a mechanism which allowed measuring the angle of attack about the midchord line. The pressure tap leads were brought through the tunnel walls with stainless steel tubing. Figure 7 shows the model mounted in the tunnel test section.

C. PRESSURE MEASURING SYSTEM

1. Pressure Transducers

Limitations on size and expense lead to the selection of a remote pressure transducer designed by Professor L. V. Schmidt of the Naval Postgraduate School. The design is shown in Figure 8. Two transducers were built, one to measure pressures on the model and the other to be used as a reference.

The transducer system consisted basically of a Bently Detector System, a 0.003 inch thick annealed brass diaphragm mounted in an aluminum housing, and plastic and steel tubing enabling the pressure on the airfoil to be transmitted to the transducer diaphragm cavity. The diaphragm thickness was selected so as to provide a useable instrument in the pressure range of $\pm$ 0.75 psia. The disassembled transducer is shown in Figure 9.

The Bently Detector System provides a voltage signal which is linear with respect to the distance change detected by its probe. For small pressure differentials across the brass diaphragm, the deflection is proportional to pressure. By putting a known pressure differential across the diaphragm, the transducer can be calibrated yielding a linear calibration curve for small differentials. The details of this procedure are given in Appendix A.

The stainless steel and plastic tubing act as transmission lines from the pressure taps to the transducer. The unsteady pressure components

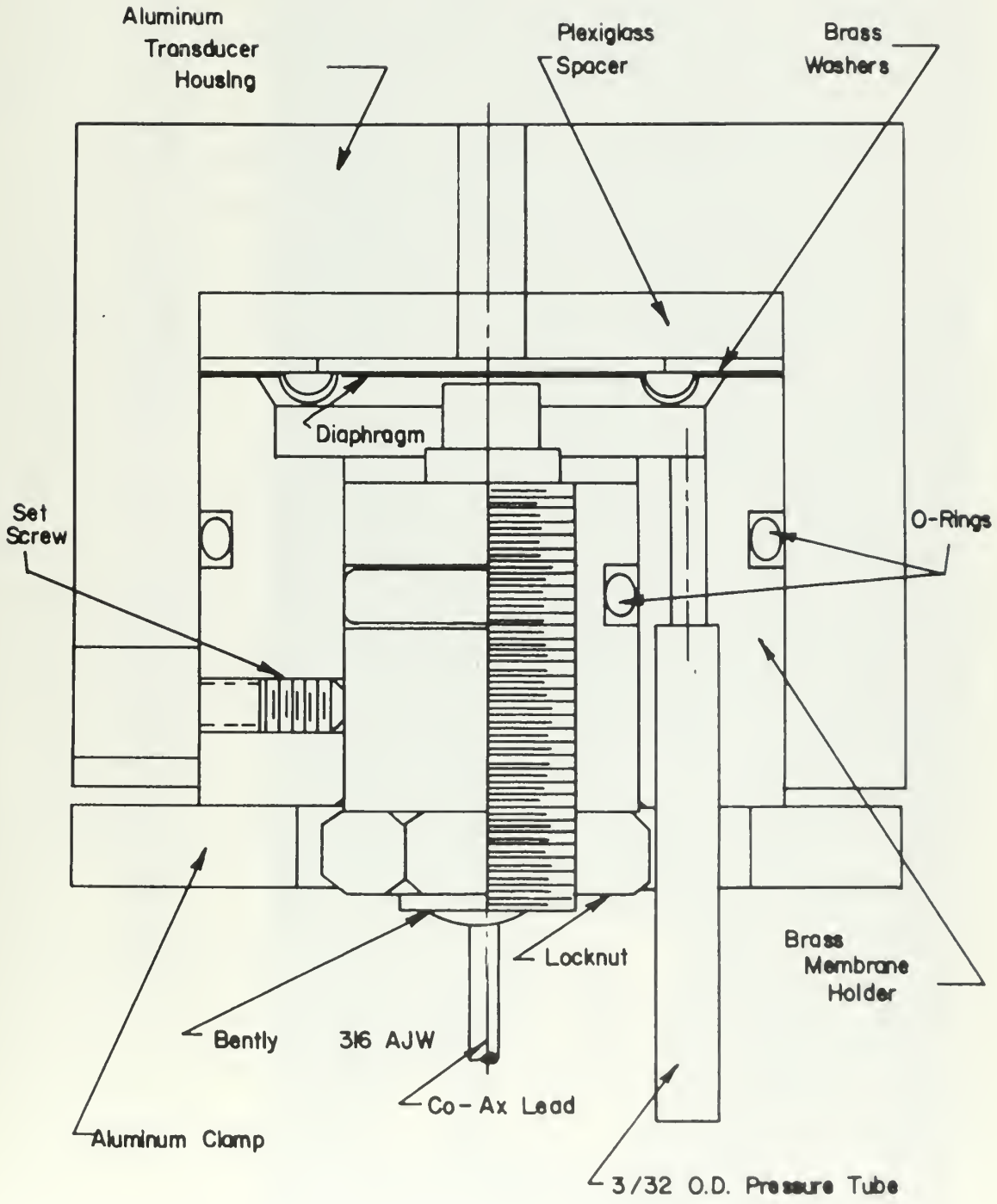

FIGURE 8. SECTIONAL DRAWING OF PRESSURE TRANSDUCER

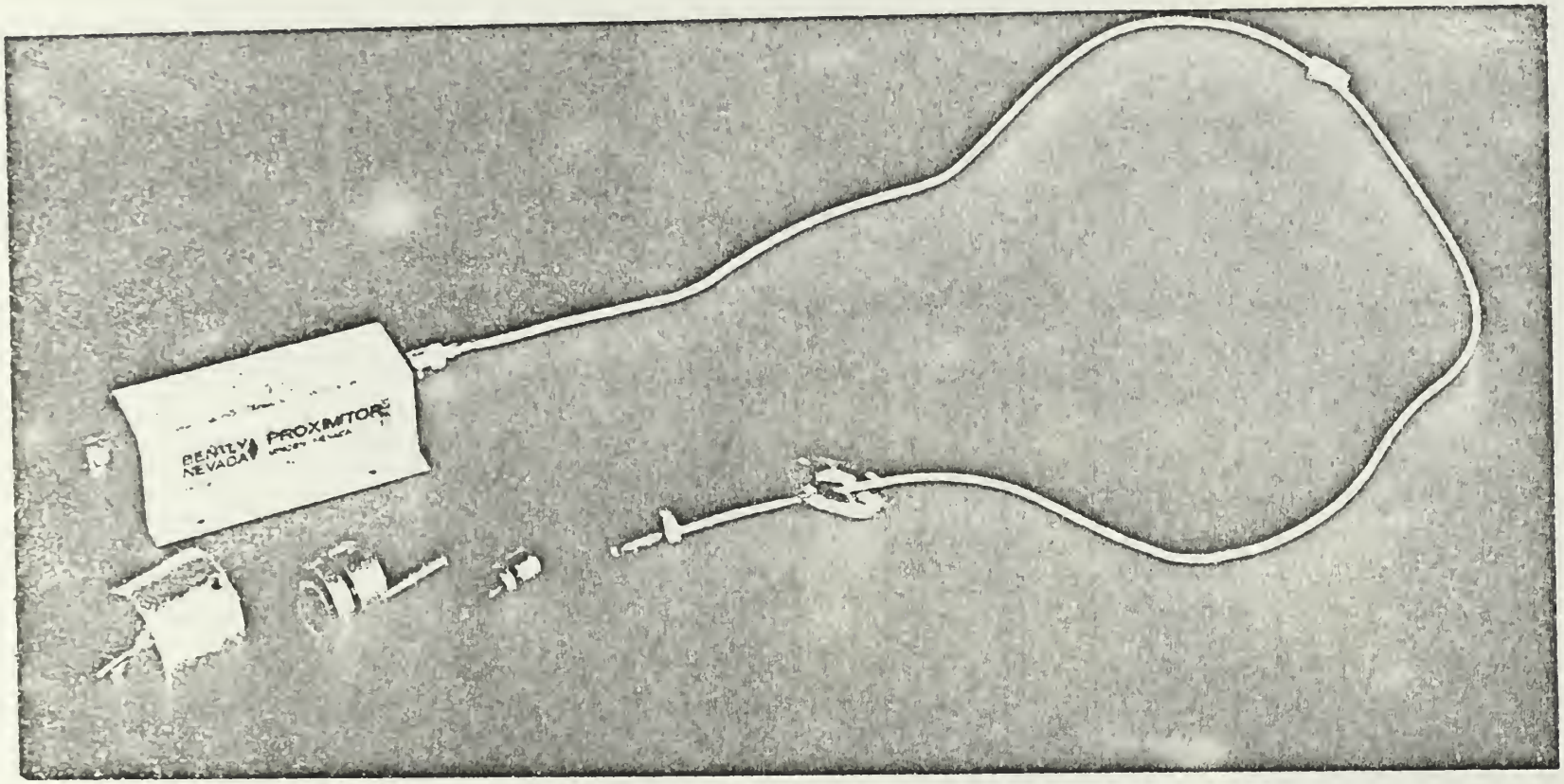

FIGURE 9. PHOTOGRAPH OF TRANSDUCER COMPONENTS.

undergo frequency-dependent phase shift and attenuation through the tubing. A dynamic calibration (Appendix A) was performed at 5 hertz increments and intermediate values at 1 hertz increments were obtained by linear interpolation and extrapolation. The results may be seen in Figures 10 and 11.

2. Power Supplies and Amplifier

A Power Design Transistorized Power Supply, Model 2051R was used to power the Bently Proximeter. The Proximeter output at zero pressure differential was in the neighborhood of + 5.73 Volts as installed in the pressure measuring system. A Kepco Model OPS 21-1 Operational Power Supply/Amplifier was used to amplify the Proximeter signal. The output of the operational amplifier was adjusted to zero volts at zero pressure differential by means of a suitable bias voltage. The gain of the operational amplifier at a given feedback resistance was verified to be constant with input frequency over the frequency range of interest. The phase shift due to the operational amplifier was a constant -180 degrees over the same frequency range. Figure 12 is a schematic diagram of the pressure measuring system and Figure 13 is a typical static calibration. Figure 14 shows the pressure measuring system installed.

D. HOT WIRE ANAMOMETER

A constant temperature, transistorized, hot wire anamometer was used to measure the free stream velocity. The electrical output of the hot wire anamometer was proportional to the velocity. A micromanometer connected to a pitot-static tube was used to measure the mean free stream velocity and to statically calibrate the hot wire anamometer.

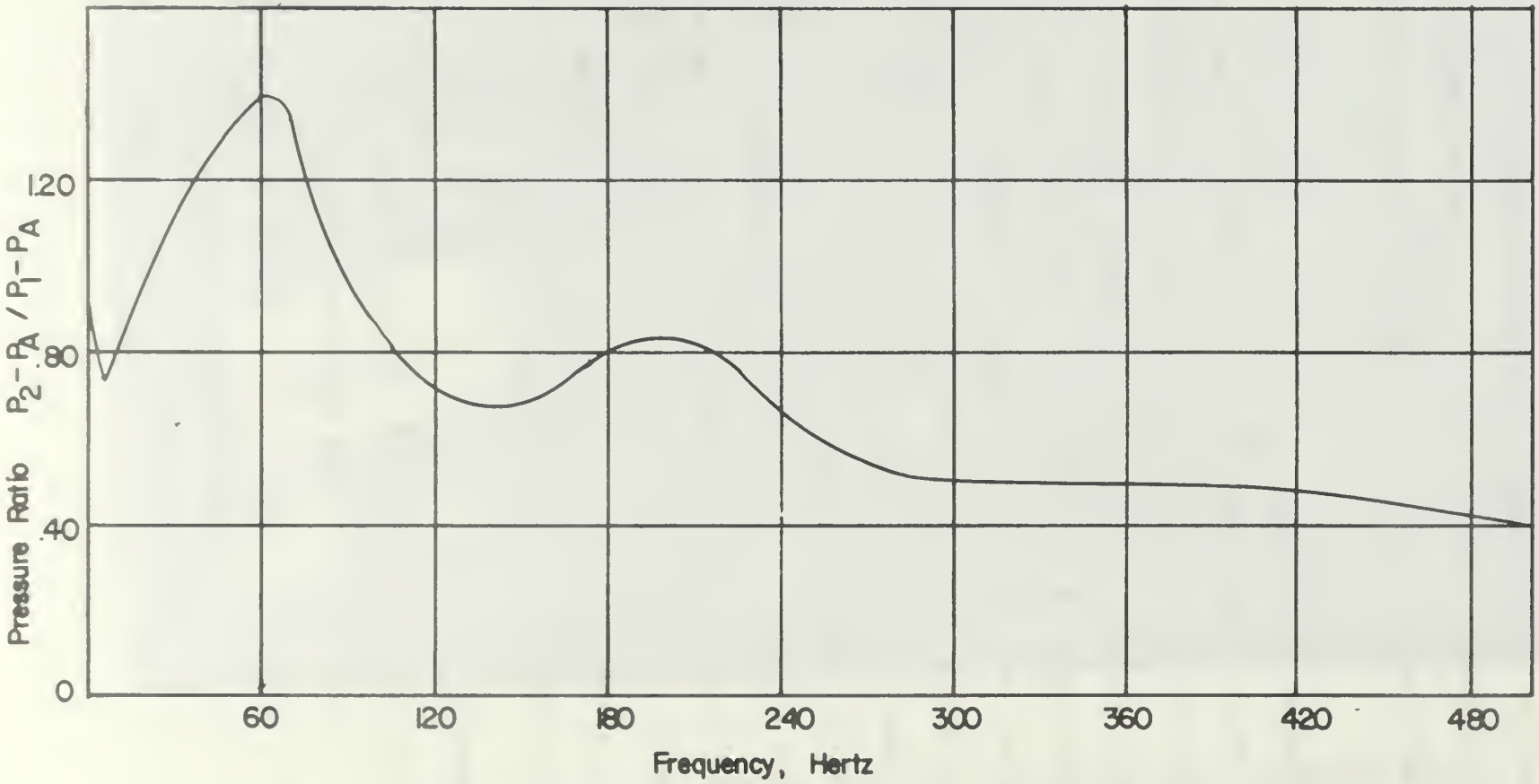

FIGURE 10. TRANSDUCER GAIN AS A FUNCTION OF FREQUENCY

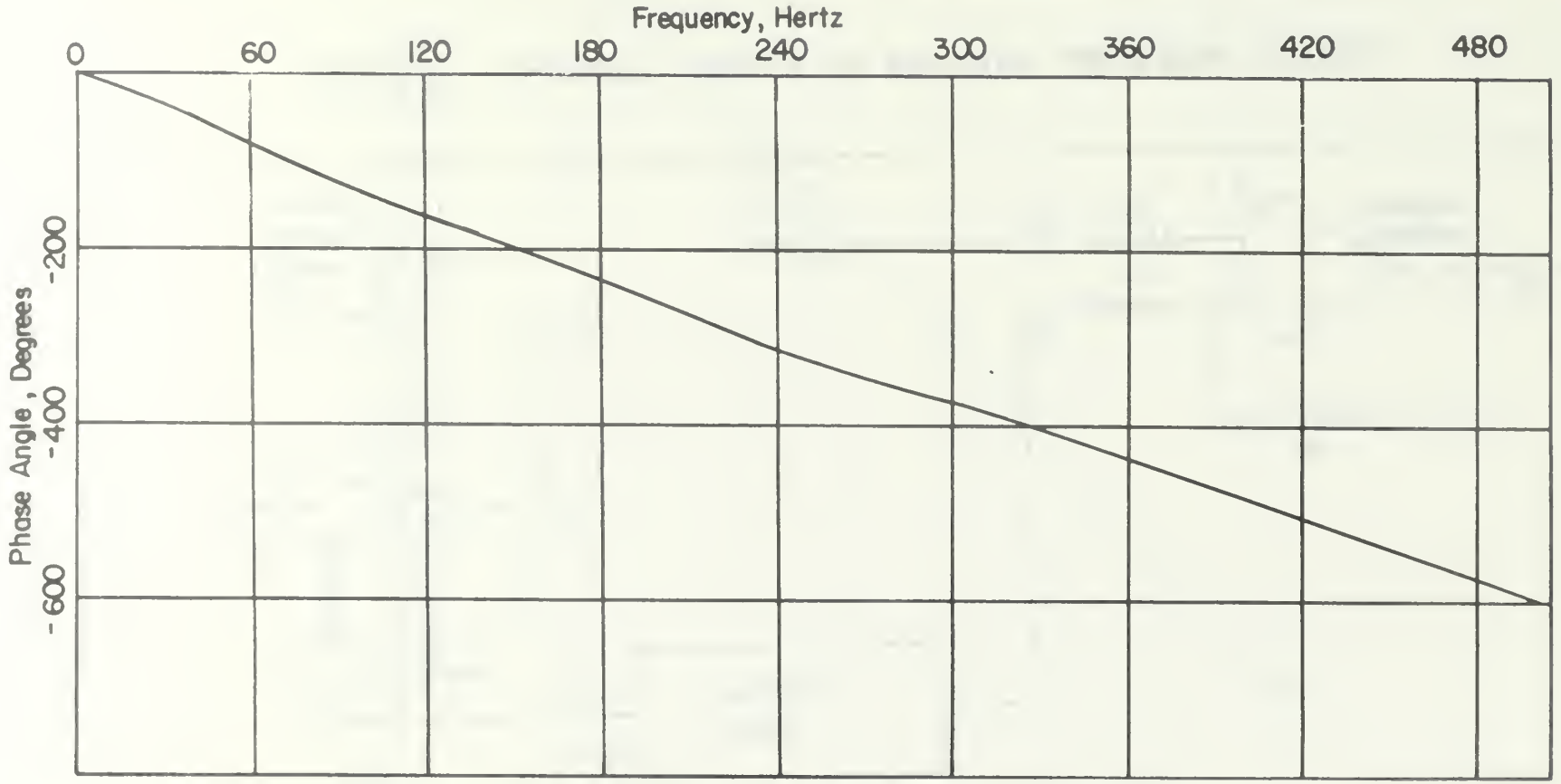

FIGURE 11. TRANSDUCER PHASE ANGLE, AS A FUNCTION OF FREQUENCY.

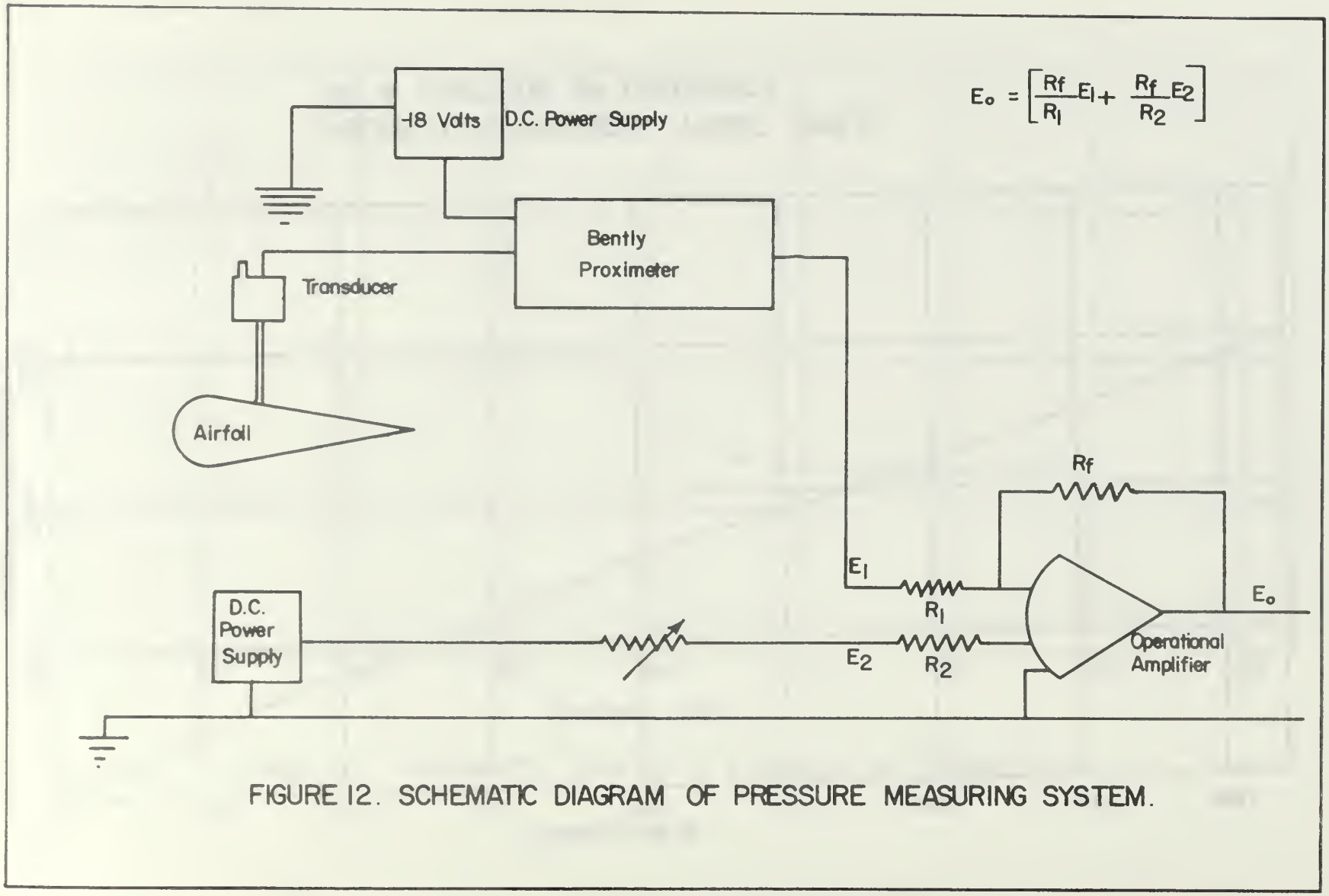

FIGURE 12. SCHEMATIC DIAGRAM OF PRESSURE MEASURING SYSTEM.

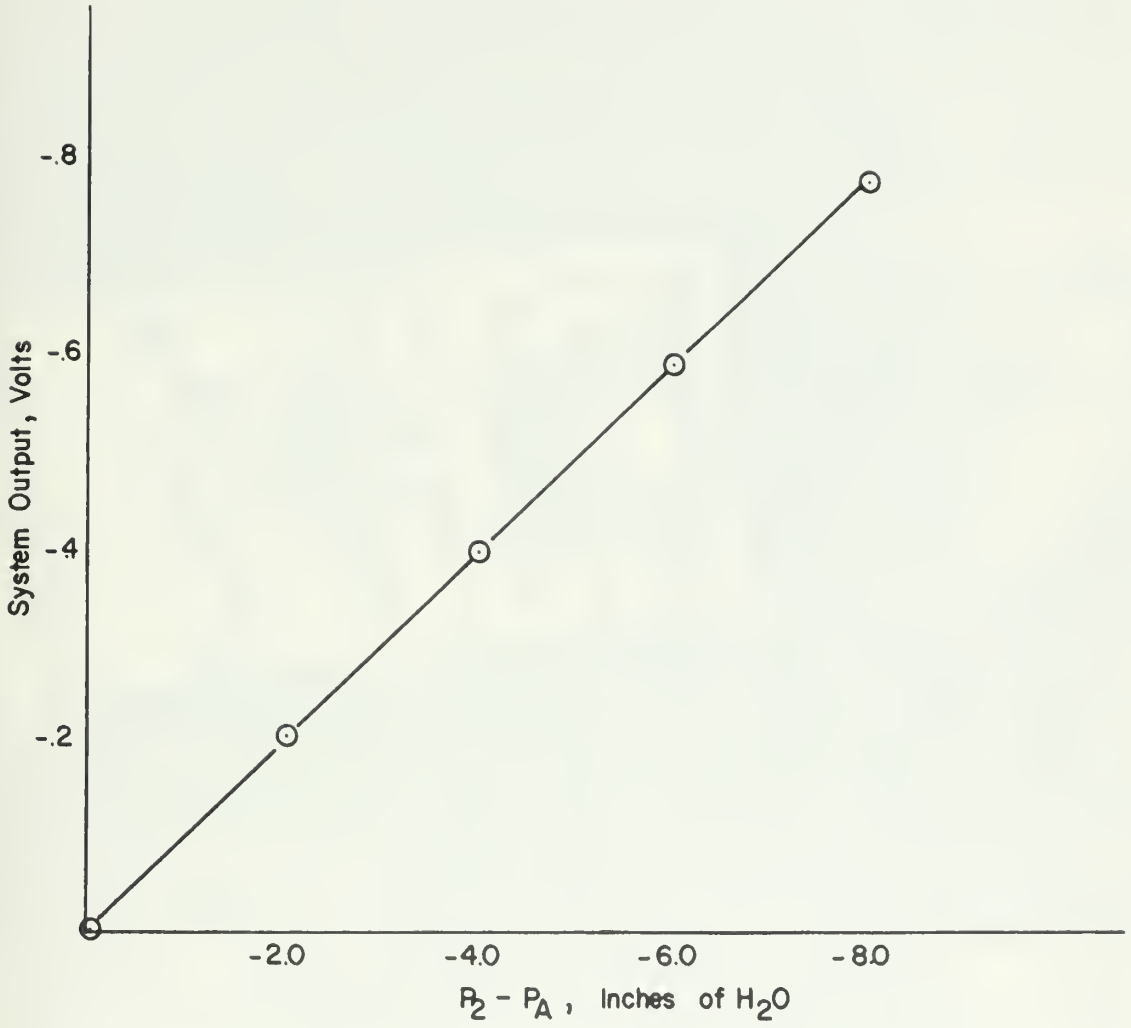

FIGURE 13. TYPICAL STATIC CALIBRATION CURVE OF PRESSURE MEASURING SYSTEM

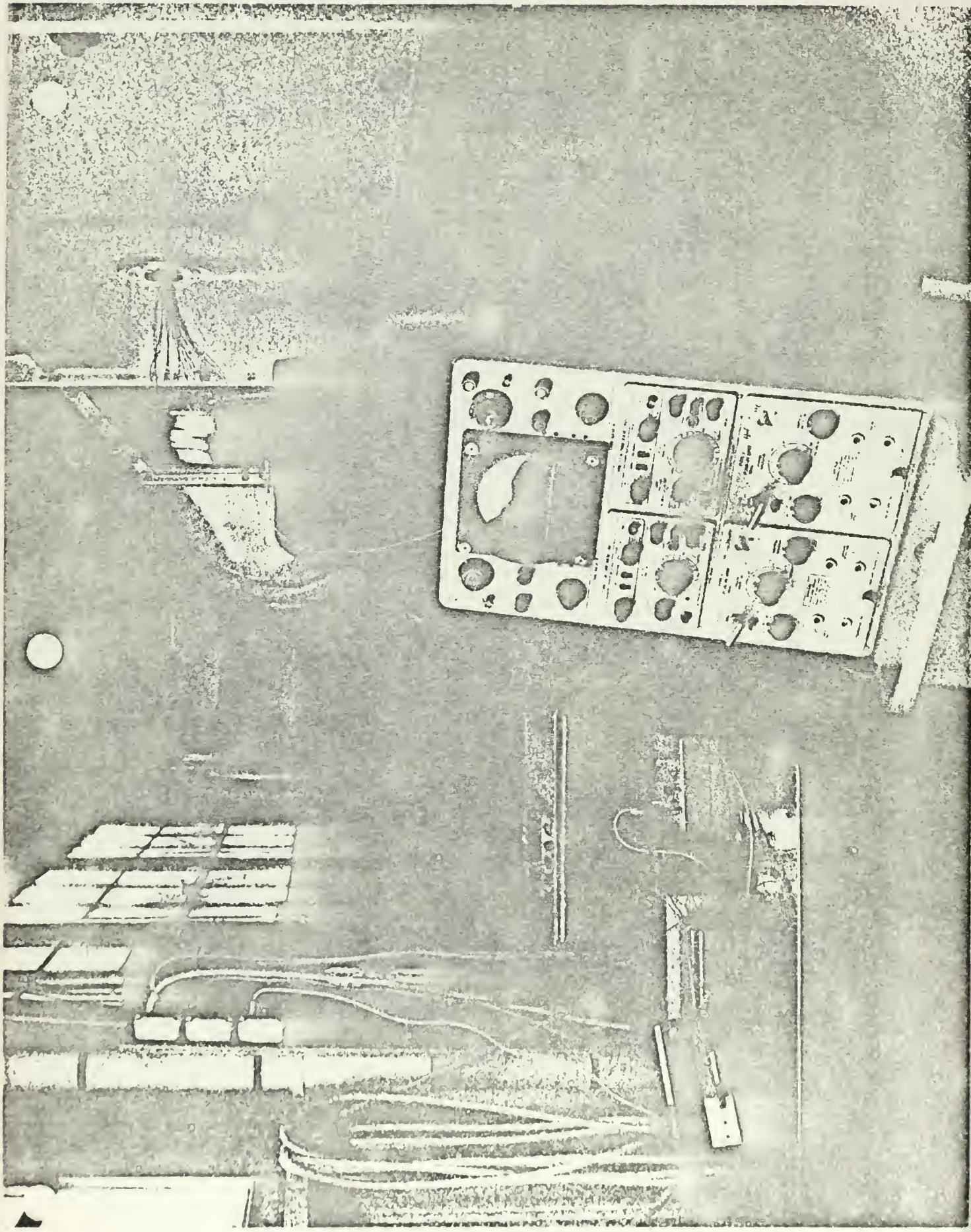

E. TAPE RECORDER

The outputs of the hot wire anamometer and pressure transducer were recorded on an Ampex CP-100 Portable Instrumentation Magnetic Tape Recorder/Reproducer. Typical record and reproduce calibration values for the recorder at a tape speed of 3-3/4 inches per second are shown in Table I.

TABLE I

TYPICAL TAPE RECORDER CALIBRATION

Record

D.C. INPUT (VOLTS)	FREQUENCY (HERTZ)
1.414	9448
0	6748
-1.414	4047

Reproduce

FREQUENCY INPUT (HERTZ)	D.C. OUTPUT (VOLTS)
9450	1.420
6750	0.0
4050	-1.409

F. MISCELLANEOUS

The velocity and pressure analogues were monitored on a Tektronix Dual Beam Oscilloscope. Pictures of representative velocity and pressure outputs were recorded photographically from oscilliscope traces.

The shutter valve frequency was measured with a magnetic pickup located outboard of the upper shutter valve blade shaft. The output of the pickup was read on a decade counter. A schematic diagram of the complete data aquisition system is shown in Figure 15.

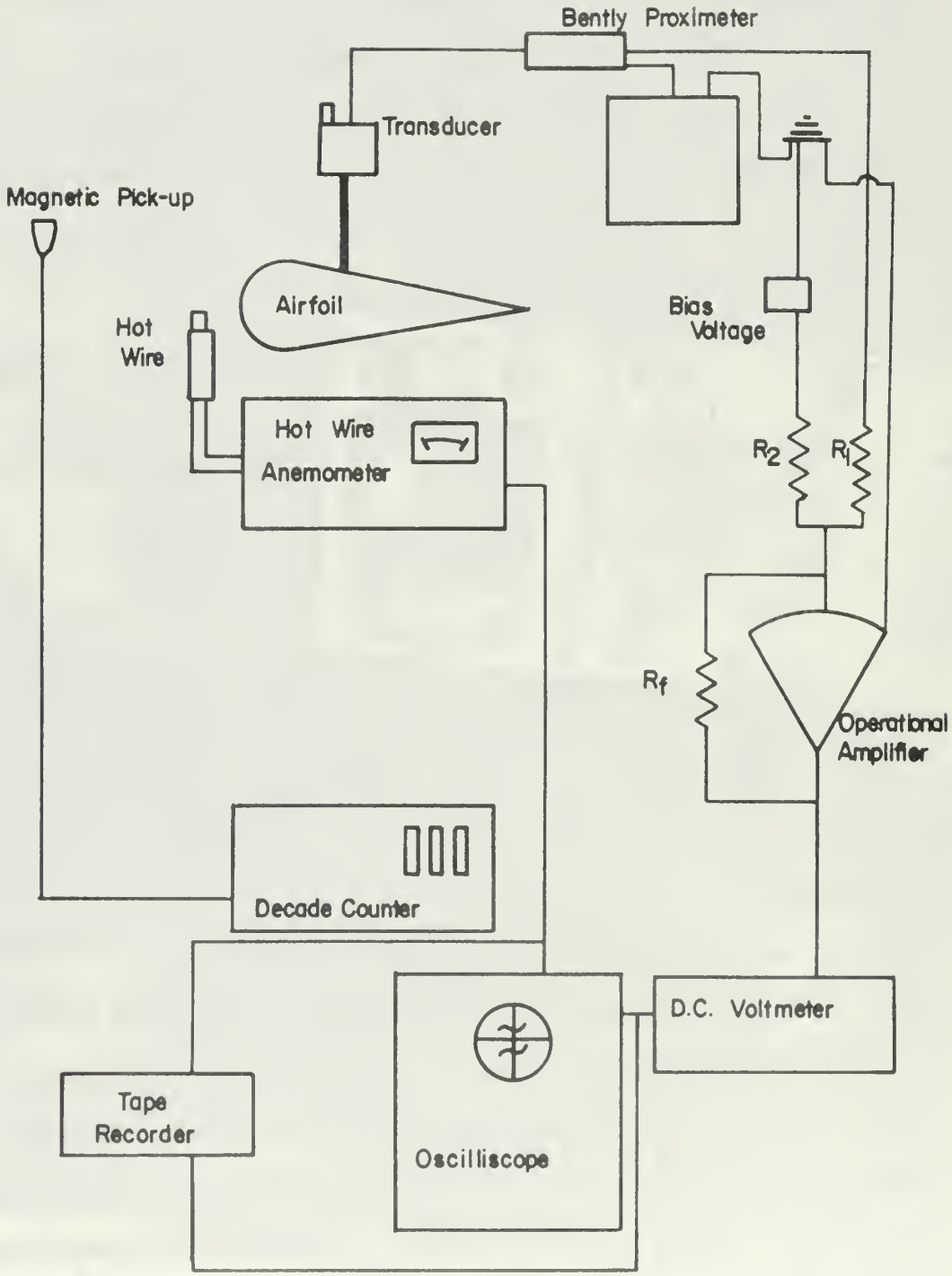

FIGURE 15. SCHEMATIC DIAGRAM OF DATA ACQUISITION SYSTEM

IV. PROCEDURES

Prior to each run, a static calibration of the transducer was made in order to ensure that no drift had occurred since the previous calibration.

The desired free stream mean velocity was established in steady flow and the hot wire anamometer set to give the desired output at the free stream mean velocity. The oscillations were then adjusted to the required frequency.

The angle of attack vernier was calibrated by comparing the transducer output of the taps on the lower surface with those at corresponding locations on the upper surface. The angle of attack vernier was accurate to $\pm$ .05 degrees when calibrated on this basis at zero degrees angle of attack.

Apparent regularity of the free stream wave-form on the oscilloscope was used to establish the desired oscillating frequencies. Subsequent Fourier analysis of the free stream velocity wave-form showed this procedure to be adequate in establishing clean wave-forms.

The airfoil was placed at the desired positive angle of attack and recording began. The output of the transducer connected to each pressure tap in turn was recorded on tape simultaneously with the output of the hot wire anamometer. Since the airfoil was symmetrical, the pressure on the lower surface was assumed to correspond to the pressure on the upper tapped surface at negative angle of attack. The airfoil was rotated to a negative angle of attack in order to obtain the pressure distribution on the lower surface.

V. DATA ANALYSIS

A. ANALOGUE TO DIGITAL CONVERSION

The recorded data were converted from analogue to digital representation on the Naval Postgraduate School's Hybrid Computer. Details of the data conversion process are given in Appendix B.

The analogue signals were filtered through two low-pass R. C. filters in series prior to digitization. The filter was used to improve signal to noise ratios of the analogue data. Preliminary investigations had shown that some high frequency noise was picked up in the data recording process from both the transducer and the tape recorder. ("High frequency", for the purposes of this investigation, means frequencies greater than 500 hertz.) The filters were built around the existing high gain amplifiers on the analogue side of the hybrid. The filter transfer function was measured at 10 hertz increments and intermediate values at 1 hertz increments obtained by linear interpolation. Figures 16 and 17 give the transfer function of the filtering system.

All sampling was done at the rate of 1024 samples per second. The analogous pressure and velocity signals associated with each pressure tap were sampled for 4 seconds for a total sample size of 4096 samples per digital record.

Prior to each run a D. C. reference voltage measured with a digital voltmeter was recorded. These reference voltages were then digitized as a check on the tape recorder and digitizing process. Typical values of voltmeter measured D. C. voltages and the corresponding digital mean value are shown in Table II.

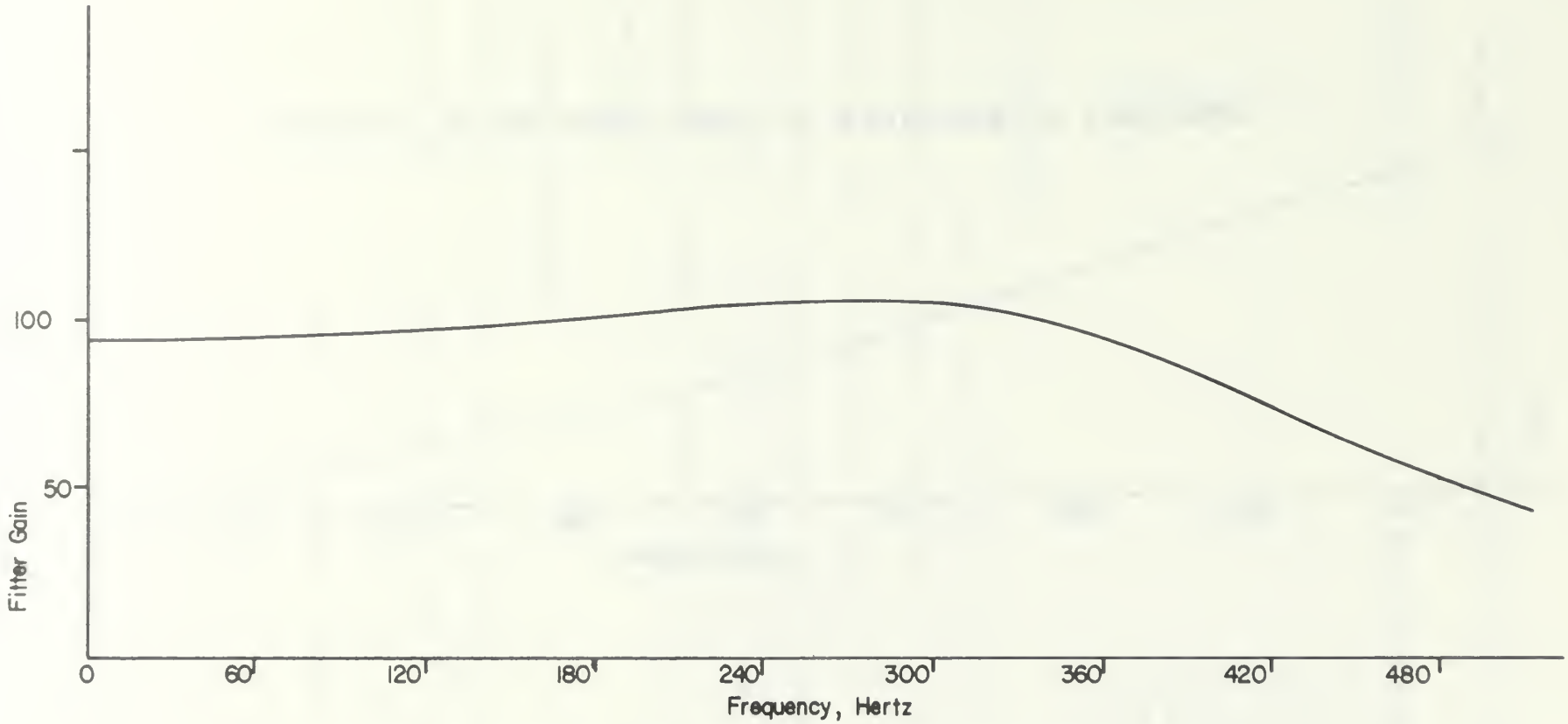

FIGURE 16. FILTER GAIN AS A FUNCTION OF FREQUENCY

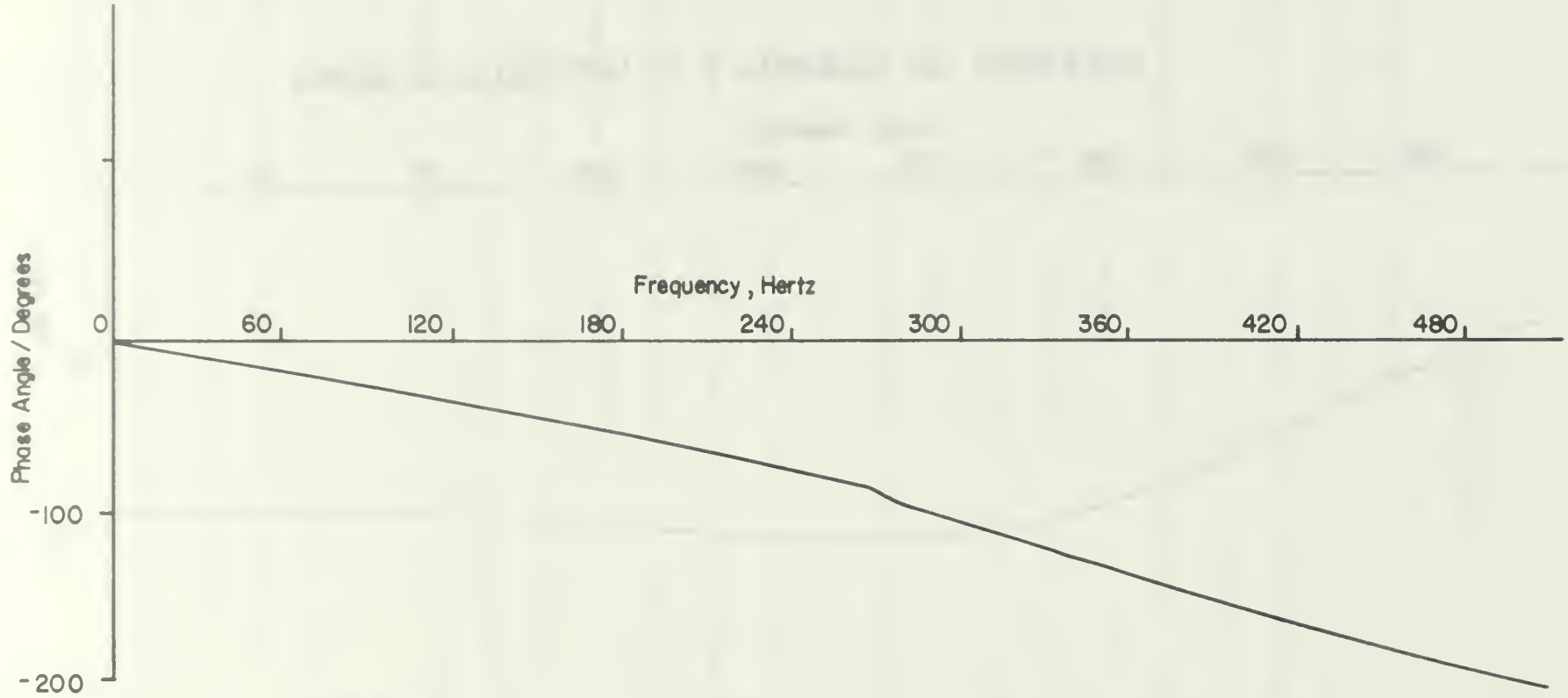

FIGURE 17. FILTER PHASE ANGLE AS A FUNCTION OF FREQUENCY

TABLE II

RECORDED D.C. VOLTAGE AND CORRESPONDING DIGITAL MEAN VALUE

RECORDED (VOLTS)	DIGITAL MEAN VALUE (VOLTS)
+1.414	+1.409
1.0	0.995
0.5	0.496
0.1	0.104
0.0	0.002
-0.1	-0.100
-0.5	-0.496
-1.0	-0.994
-1.414	-1.415

B. TAPE CONVERSION

The arrays of digitized data obtained from the analogue to digital conversion process were stored on 7 track, 200 bit per inch magnetic tape in 24 bit words. A conversion to 9 track, 800 bit per inch tape and 32 bit words was necessary in order to analyze the data on the IBM 360 Series Computer. The computer program used to make the conversion is included as an appendage to this thesis under the title "TAPE CONVERSION PROGRAM".

C. ADDITIONAL ASSUMPTIONS

Ideally, phase information between the free stream velocity and pressure analogues at a given tap would have been preserved during the analogue to digital conversion process. Because of equipment limitations discussed in Appendix B, this was not possible. However, measurements from photographs of oscilloscope traces of the velocity and pressure analogues corresponding to given pressure taps indicated that the phasing between the free stream velocity and the pressure on the surface of the airfoil was essentially independent of the surface coordinate. This measured time difference between a negatively-sloped zero crossing

of the corresponding pressure analogue was therefore taken as constant for a given run.

D. NON-DIMENSIONALIZATION

1. Pressure Coefficients

The pressure data corresponded to the difference between atmospheric pressure and the surface pressure. It was therefore convenient to define a non-dimensional pressure coefficient referenced to atmospheric pressure as:

$$C_p(x,y,t) = \frac{P(x,y,t)-P_A}{\bar{q}}$$

where:

$P(x,y,t)$ = pressure at time t at a point (x,y) on the surface of the airfoil,

P_A = atmospheric pressure, and

$\bar{q}$ = mean free stream dynamic pressure.

The mean pressure coefficient, $\bar{C}_p(x,y)$, is then defined as:

$$\bar{C}_p(x,y) = \frac{\bar{P}(x,y)-P_A}{\bar{q}} \qquad \text{and}$$

the "unsteady pressure coefficient" is defined as:

$$c_p(x,y,t) = \frac{p(x,y,t)}{\bar{q}},$$

where:

$p(x,y,t)$ = "unsteady pressure" at time t at a point (x,y) on the surface of the airfoil.

2. Normal Force Coefficients

The time dependent force per unit span acting normal to the chord of a two-dimensional airfoil is approximated by:

$$N(t) = \int_0^c [P(x,-y,t)-P(x,y,t)]\, dx$$

if the airfoil is symmetrical. The normal force coefficient can be defined in terms of the non-dimensional pressure coefficient as:

$$C_N(t) = \int_0^1 [C_P(x,-y,t)-C_P(x,y,t)]\, d\xi$$

where:

$$\xi = x/c.$$

In terms of the mean and unsteady pressure coefficients this becomes:

$$C_N(t) = \int_0^1 [\bar{C}_P(\xi,-\eta) - \bar{C}_P(\xi,\eta)]\, d\xi + \int_0^1 [C_P(\xi,-\eta,t)-C_P(\xi,\eta,t)]\, d\xi$$

which leads to:

$$C_N(t) = \frac{\bar{N}}{qc} + \frac{R(t)}{qc} = \bar{C}_N + c_n(t)$$

where:

$\bar{C}_N$ = mean normal force coefficient

$c_n(t)$ = "unsteady normal force coefficient".

3. Center of Pressure

The center of pressure may be defined in terms of non-dimensional parameters in a manner similar to that used above. The result is:

$$\xi_{c.p.} = \frac{\int_0^1 [C_P(\xi,-\eta,t) - C_P(\xi,\eta,t)]\, \xi\, d\xi}{C_N(t)}$$

E. COMPUTATIONAL PROCEDURES

The numerical techniques used in the calculations are discussed in Appendix C. A flow chart of the computer program used to analyze the

digitized data is shown in Fig. 18. A listing of the program is included as an appendage to this thesis.

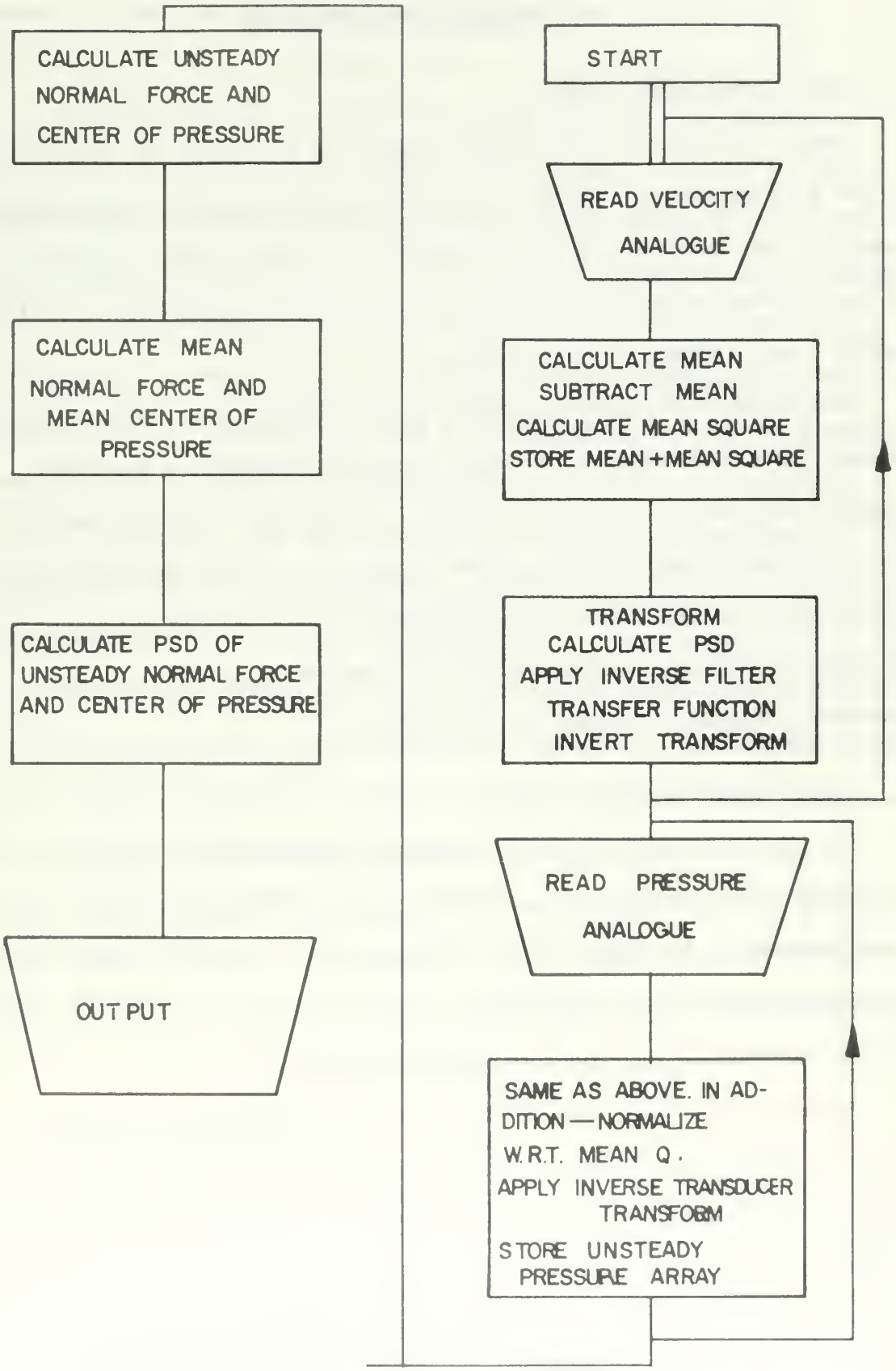

FIGURE 18. ABBREVIATED COMPUTER PROGRAM FLOW CHART

VI. RESULTS AND DISCUSSION

A. CONDITIONS INVESTIGATED

Table III lists the freestream conditions and angles of attack at which data was taken. A "Run" consisted of recording the pressure at each tap for 30 seconds with the airfoil at a given angle of attack in a free stream velocity with a given mean velocity, amplitude of oscillation, and frequency of oscillation.

The steady flow Runs were made and the pressure distribution and normal force coefficients presented in order to provide a basis for comparison with the non-steady results. Power spectral densities of the turbulent pressure fluctuations in steady flow were calculated to investigate the possibility of any harmonic coupling that might occur between the forced oscillations of the free stream and the vortex shedding phenomona observed in steady flow.

B. STEADY FLOW RESULTS

The measured pressure distributions on the airfoil at angles of attack of 5, 10, and 15 degrees in a steady flow of approximately 100 feet per second are shown in Fig. 19 through 21. Figure 22 shows the resulting normal force coefficients. The lift curve of a NACA 63-009 airfoil section is included for comparison [Ref. 12].

Power spectral densities of the turbulent pressure fluctuations at representative taps are shown in Fig. 23 through 32. These power spectrums and subsequent power spectrums shown have been normalized with respect to their mean squares.

At angles of attack of 0 and 5 degrees a distinct periodic component in the neighborhood of 21 to 22 hertz was discernable at all chordwise

locations investigated. The corresponding Strouhal Number taken with respect to chord and the frequency of the periodic component is:

$$N_{ST} = 0.105.$$

At 10 degrees angle of attack the spectrum of the fluctuating pressure on the upper surface appears to be broadened over the lower frequencies. Periodic components are discernable along the lower surface at about the same frequency as was noted at lower angles of attack.

At 15 degrees angle of attack the airfoil was fully stalled as evidenced by the pressure distribution. Figures 30 through 32 show a distinct periodic component between 21 and 22 hertz just as the runs at lower angle of attack. This periodicity was visible at all pressure taps on the surface. The tendency of the spectrum to spread more towards lower frequencies at downstream stations on the upper surface is apparent when Fig. 30 and 31 are compared.

Figures 33 and 34 show the mean square of the fluctuating pressure coefficients for Runs 3 and 4 plotted as a function of chord. Discussion of the possible significance of the resulting distribution will be deferred to the unsteady flow section.

Noise at 60 hertz was filtered from the spectral and mean square distributions shown in Fig. 23 through 34 by setting the computed value of the spectrum at 60 hertz equal to the average of the values at 59 and 61 hertz. A typical unfiltered spectrum is shown in Fig. 35.

C. UNSTEADY FLOW RESULTS

1. Run 5

Run 5 was made at a fundamental frequency of 94 hertz, an angle of attack of 15 degrees, and a free stream velocity with mean of approximately 100 feet per second and amplitude ratio of 0.085. Figures 36 and

37 show typical oscilloscope traces of the velocity and pressure analogue wave-forms at selected pressure taps for this Run.

It is apparent from these photographs that the time between a negatively sloped zero crossing on the velocity analogue wave and a positive sloped zero crossing on the pressure analogue wave is essentially constant at a given tap even though the wave-form is obviously not the same for every period. These same pictures show that the change in the above time-difference with chordwise location is small.

The time-difference mentioned above was measured at two sample time-increments from photographs similar to those shown in Fig. 36 and 37, but on an expanded time scale. Expressed in terms of a phase angle at the fundamental frequency of 94 hertz, the two sample time-increments are equivalent to 66 degrees. This measurement served to establish the phasing that was used in reducing the data.

Figure 38 shows the power spectrum of the oscillating free stream velocity for Run 5. The spectral quality of the oscillations produced by the tunnel is immediately apparent from the manner in which the fundamental frequency dominates the spectrum.

Figures 39 through 64 are power spectral densities of the unsteady pressures associated with the indicated chordwise locations. They were selected to indicate the complete trend of the pressure spectrum on the surface of the airfoil. The spectrums appear to be essentially the same along the upper surface to about 30 per cent chord at which point the spectral component at the fundamental harmonic begins to decrease and the second and third order harmonic components increase. These effects appear to be maximized at or near the mid-chord point where the second order harmonic dominates the unsteady pressure. (It is unfortunate that the

spacing between pressure taps near the mid-chord point increases but the observed pressure spectrums were not anticipated before the model was constructed.) Less than 20 per cent chord downstream from the mid-chord point the spectrum again takes on the appearance noted near the leading edge.

Figure 65 shows the measured mean square of the unsteady pressure coefficient at each tap. There is a decrease in the mean square as mid-chord is approached and a definite increase as the downstream edge is approached, implying some sort of spatial correlation between the mean square of the pressure fluctuation and chordwise distance downstream.

Figure 66 shows the calculated time dependent normal force coefficient and the free stream velocity plotted with common time origins as determined by the previously described photographic measurement.

Figure 67 is the power spectrum of the calculated unsteady normal force.

Figure 68 shows the mean pressure distribution as calculated for Run 5. Figures 69 and 70 are photographs of the time dependent pressure distribution displayed on an IBM 2250 Visual Display Unit. The computer program used to create the display is attached as an appendage under the title "DISPLAY PROGRAM".

Figure 71 is the power spectrum of the calculated unsteady center of pressure for Run 5.

2. Run 7

Run 7 was made at a fundamental frequency of 11 hertz, an angle of attack of 15 degrees, and a free stream velocity with a mean of approximately 100 feet per second and amplitude ratio of 0.072. Figures 72 and 73 show typical oscilloscope traces of the velocity and pressure analogue

wave-forms at selected pressure taps for Run 7. Note the regularity of the pressure analogue wave-forms with time for a given tap and the similarities of the wave-forms for the different taps. The time difference between a negatively sloped zero crossing on the velocity analogue wave-form and a positively sloped zero crossing on the pressure analogue wave-form was measured at approximately 24 sample time-increments. At the fundamental frequency of 11 hertz, 24 sample time-increments is approximately given in terms of a phase angle as 93 degrees. This measurement was used as described previously to establish the phasing between the free stream velocity and pressure in data reduction.

The power spectral density of the unsteady free stream velocity for Run 7 is shown in Fig. 74. The quality of the oscillation should again be noted.

Power spectrums of the unsteady pressure associated with representative taps are shown in Fig. 75 through 80. The wave-form similarity noted in the oscilloscope pictures is also apparent in the power spectrums. The similarity of the spectrums to each other should also be noted.

Figure 81 gives the mean square of the unsteady pressure coefficient associated with each tap as a function of the non-dimensional chord.

The unsteady velocity and normal force coefficient are given as functions of time from a common time origin in Fig. 82 and 83. The power spectrum of the unsteady normal force is given in Fig. 84 and the power spectrum of the center of pressure in Fig. 85. Figure 86 shows the mean pressure distribution on the airfoil for Run 7.

D. COMPARISON OF RESULTS AT DIFFERENT FREQUENCIES

1. Normal Force and Center of Pressure

The most obvious difference between the results presented is in the mean normal force coefficients. This is illustrated in Fig. 87 which

shows the mean normal force coefficient at 15 degrees angle of attack as a function of frequency. Recall that the mean velocities for the steady flow Run and the oscillating Runs 5 and 7 were all about 100 feet per second. Run 5 had a fundamental frequency of 94 hertz while Run 7 had a fundamental frequency of 11 hertz. The amplitude ratio for the two oscillatory Runs was about the same, that for Run 5 being 0.085 and that for Run 7 being 0.072.

The harmonic composition of the unsteady normal force coefficient for the two oscillatory Runs under consideration was also much different. A comparison of Fig. 67 and Fig. 84 shows that the second harmonic of 94 hertz is much more predominant than the second harmonic of 11 hertz.

Center of pressure calculations also reflect the difference in harmonic composition that was found in the normal force results. The unsteady center of pressure at 94 hertz is dominated by the second harmonic and the first and third harmonics are about the same, while at 11 hertz little difference between the spectrum of the unsteady normal force and unsteady center of pressure was noted.

2. Pressure Distributions

The spectral composition of the unsteady pressure reflects the difference noted in the normal force and center of pressure results. The presence of higher order harmonics is apparently not just related to increasing frequency. Allen [Ref. 11] showed oscilloscope traces of the pressure analogues associated with the same airfoil used in this investigation at a fundamental frequency of 128 hertz and about the same mean and mean square velocity. His traces did not give an indication of any significant higher order harmonics.

There are apparent spatial periodicities evident in the instantaneous pressure distributions shown in Fig. 69 and 70 for Run 5. The

mean pressure distribution for Run 7 shown in Fig. 86 also clearly indicates a spatial periodicity. The mean square distributions of the unsteady pressure plotted in Fig. 65 and 81 show a similar trend.

A hint as to the cause of these periodic trends may be obtained by considering the chordwise distribution of the mean square of the pressure fluctuation in steady flow. One would normally expect vortices shed at or near the separation point on the airfoil to immediately begin to dissipate as they travel downstream from their point of origin. A resulting decrease in the mean square of the fluctuations in velocity and pressure would be expected with chordwise distance downstream as is shown in Fig. 33 for the airfoil at 10 degrees angle of attack in steady flow. The mean square of the pressure fluctuation on the airfoil at 15 degrees angle of attack in steady flow shows a definite increase toward the trailing edge as shown in Fig. 34. This suggests that the spatial periodicity observed in the unsteady runs was a result of the combination of the oscillatory effects and the effects of the stalled airfoil.

The instantaneous pressure distributions shown for Run 5 in Fig. 69 and 70 also suggest that the second harmonic component of the normal force could be due to a delay of separation near the leading edge associated with the minimum of the velocity or change in sign of the acceleration of the free stream. Reference to the instantaneous pressure distribution associated with the minimum of the velocity demonstrates the more favorable spatial pressure distribution that occurs at that point on the velocity waveform.

E. COMPARISON OF UNSTEADY FLOW RESULTS WITH STEADY FLOW ANALYSIS

Steady flow results have traditionally been used to estimate aerodynamic forces acting on airfoils in unsteady environments. Such analysis

usually involves assuming that the lift coefficient of an airfoil section is constant at a given angle of attack within a given range of Reynolds Number.

The normal force coefficient found for the airfoil used in this investigation at 15 degrees angle of attack and a Reynolds Number based on chord of approximately 3×10^6 was 0.681. Assuming the normal force coefficient to be constant for a given angle of attack leads to the following estimates for the mean normal force coefficient and mean square of the unsteady normal force coefficient for the same airfoil at 15 degrees angle of attack in an oscillating flow with amplitude ratio $\epsilon = 0.08$:

$$\overline{C}_N = C_{N_s}\left(1 + \frac{\epsilon^2}{2}\right) \approx 0.683$$

$$\overline{c_n^2} = C_{N_s}\left(2\epsilon^2 + \frac{\epsilon^4}{8}\right) \approx 0.0128$$

where C_{N_s} is the normal force coefficient in steady flow.

Note that assuming a constant normal force coefficient leads to results that depend only on the amplitude ratio of the oscillating free stream and are independent of frequency.

The experimentally measured mean normal force coefficients for the airfoil at 15 degrees angle of attack in a free stream oscillating at 11 and 94 hertz were 0.851 and 1.401 respectively. The mean squares of the unsteady normal force coefficients for the two cases were 0.075 and 0.100 respectively. The difference between the experimentally derived values and the values predicted by assuming a constant normal force coefficient at a given angle of attack are considered by the author to be significant.

F. SUMMARY OF RESULTS

Figure 87 gives the measured mean normal force coefficient as a function of frequency for the airfoil at an angle of attack of 15 degrees

in a free stream with a mean velocity of approximately 100 feet per second and amplitude ratio of approximately 0.08. Figure 88 gives the measured mean center of pressure under the same conditions.

Due to lack of computing time and a machine malfunction in the digitization process, the data taken for Runs 6 and 8 were not reduced.

VII. CONCLUSIONS

From the results presented, the following conclusions may be drawn for the conditions investigated:

1. The magnitude of the pressure force acting normal to the chord of an airfoil at high angle of attack in oscillating flow is frequency dependent and is significantly greater than that observed in steady flow and is not adequately predicted by quasi-steady analysis.

2. Higher order harmonic components of the fundamental free stream frequency of oscillation are of significant order of magnitude in the normal force and their relative magnitude is frequency dependent.

3. Distinct periodic components are observable in the pressure acting on an airfoil in steady flow.

TABLE III

EXPERIMENTAL CONDITIONS FOR WHICH DATA WERE TAKEN

Run No.	Angle of Attack (degrees)	Mean Velocity (ft/sec)	Frequency of Oscillation (hertz)	Amplitude Ratio of Oscillation
1	0	100	steady	--
2	5	100	steady	--
3	10	100	steady	--
4	15	100	steady	--
5	15	100	94	0.08
6	15	150	94	0.08
7	15	100	11	0.08
8	15	70	9	0.25

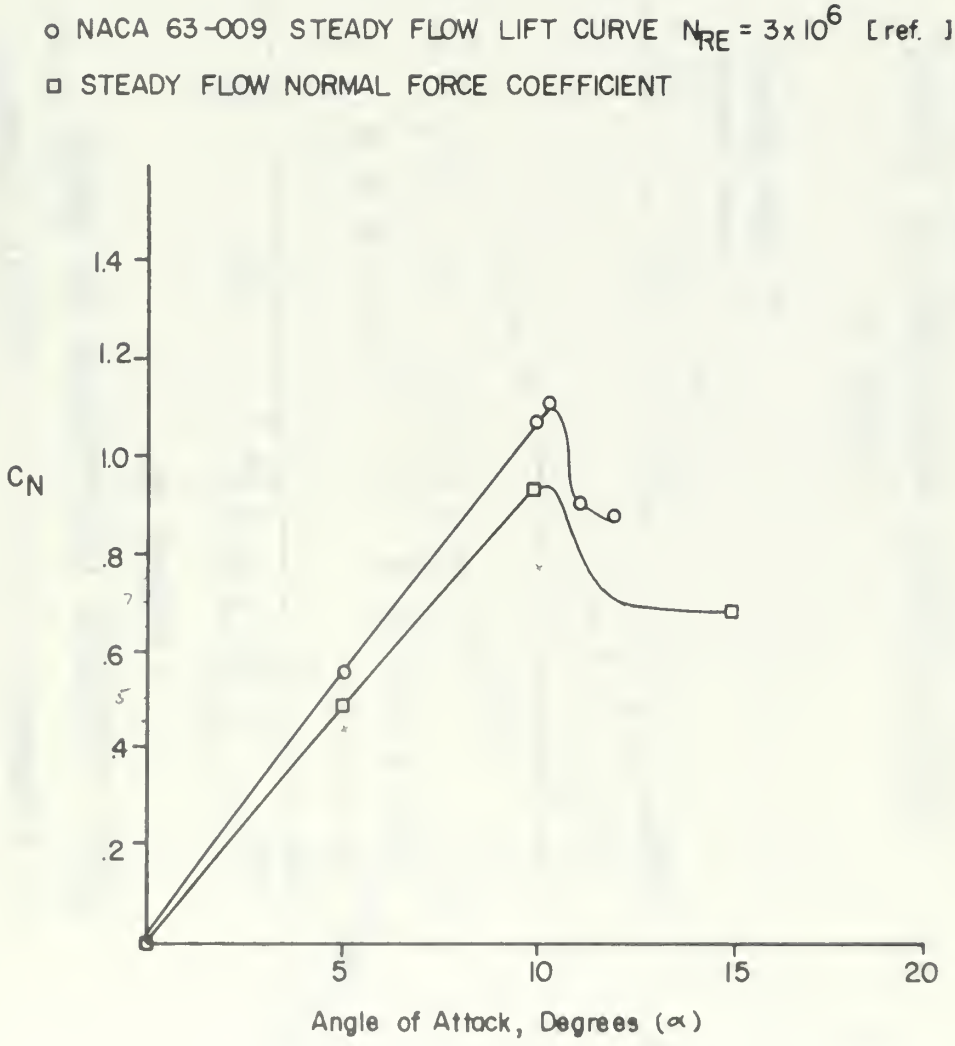

FIGURE 19. STEADY FLOW C_N VS α

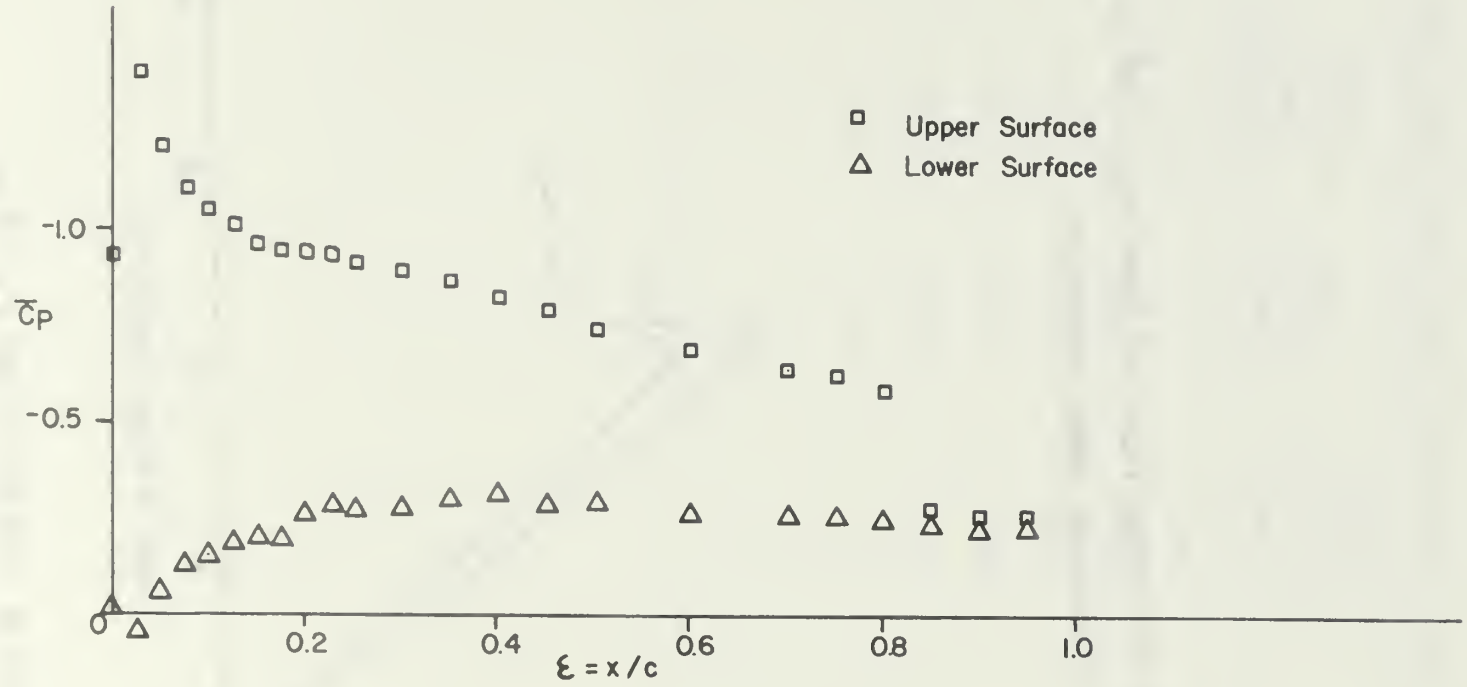

FIGURE 20.

MEAN PRESSURE DISTRIBUTION ON AIRFOIL

α = 5 degrees STEADY FLOW

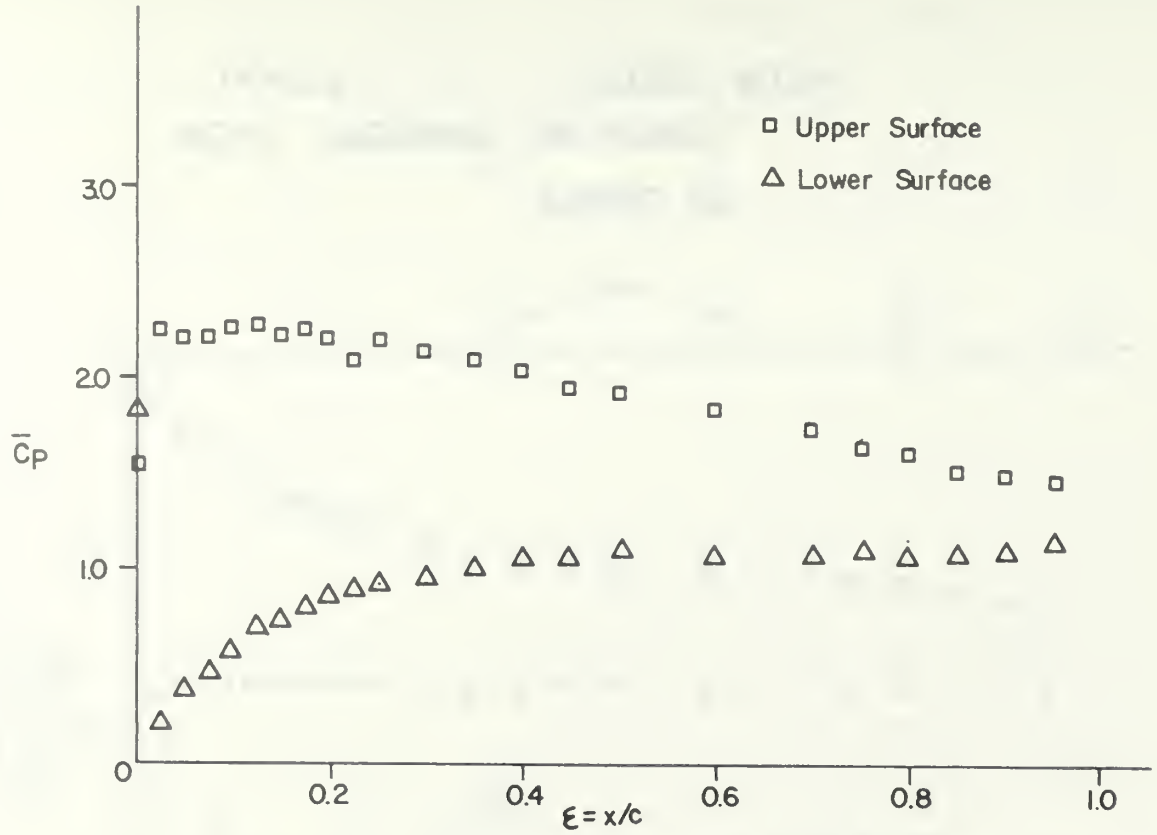

FIGURE 21

MEAN PRESSURE DISTRIBUTION ON AIRFOIL

α = 10 degrees STEADY FLOW

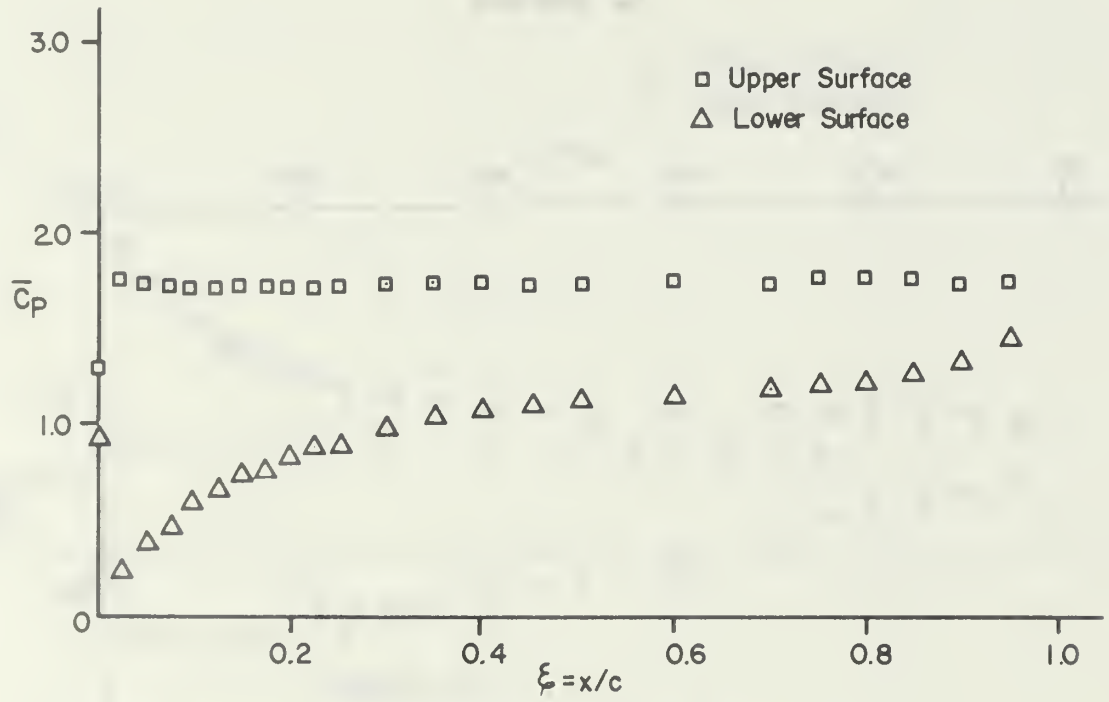

FIGURE 22

MEAN PRESSURE ON AIRFOIL

$\alpha = 15°$ STEADY FLOW

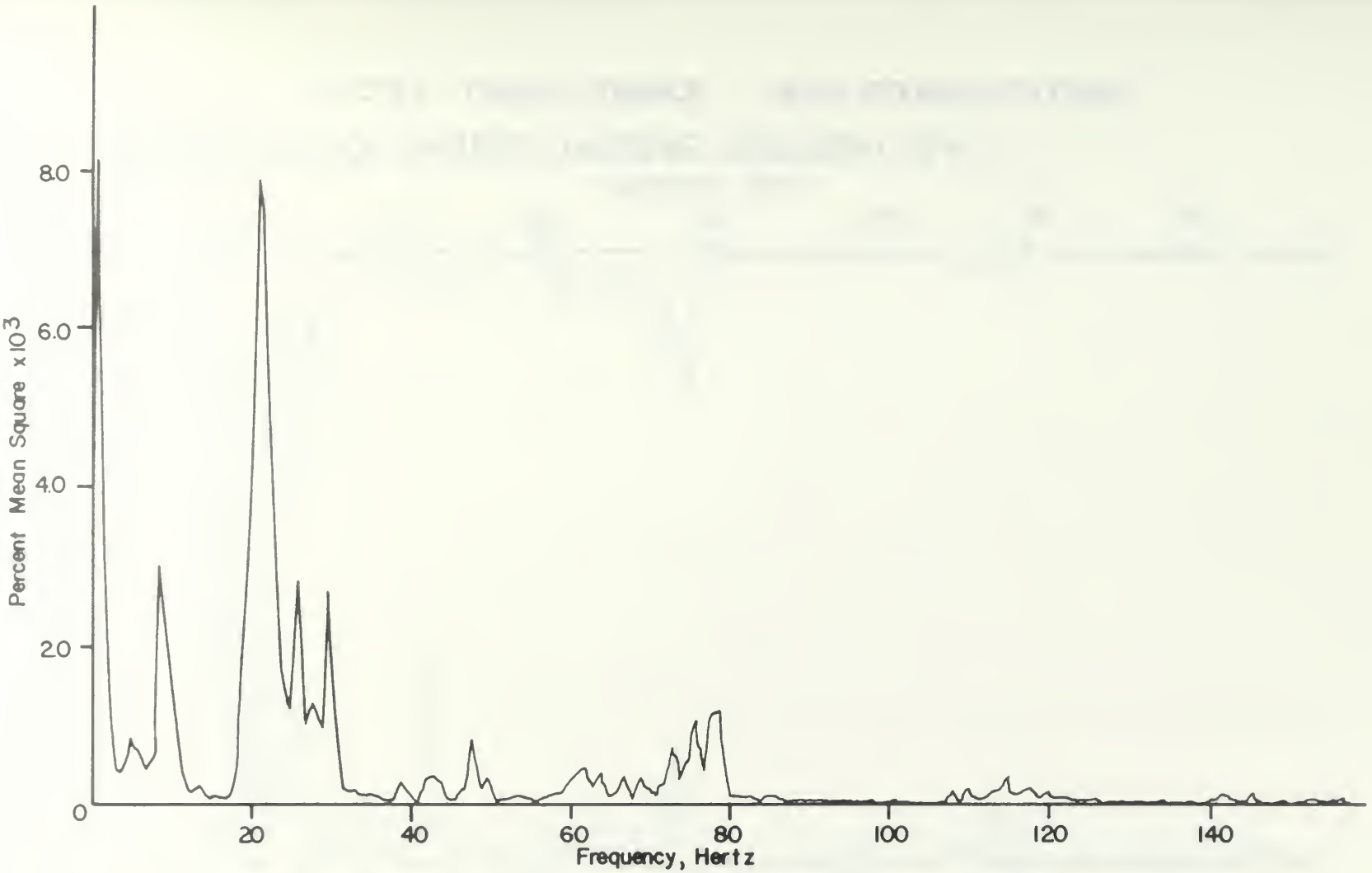

FIGURE 23. PSD OF UNSTEADY PRESSURE COEFFICIENT, RUN 1

ζ=0.0 MEAN SQUARE =0.00804

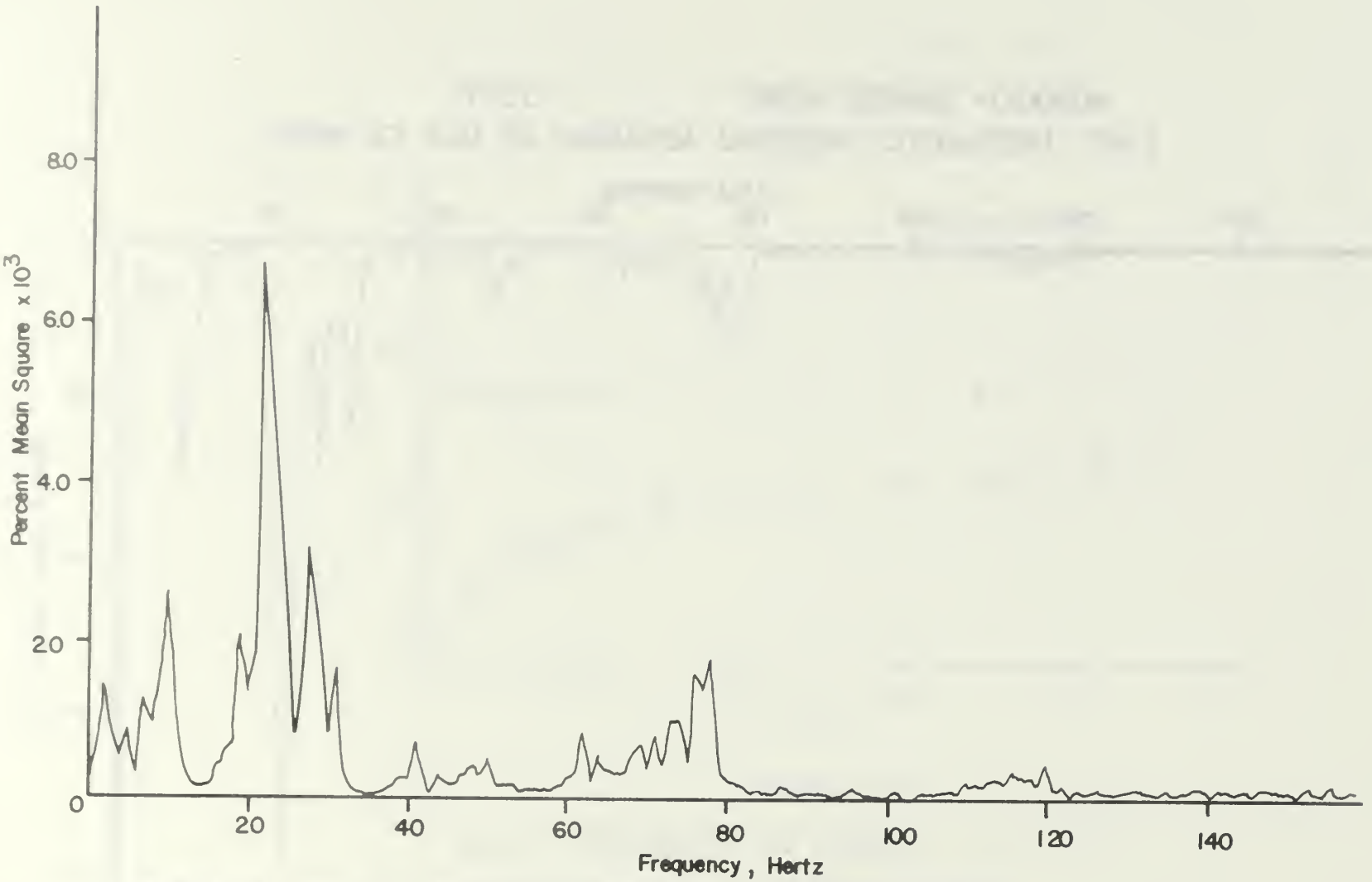

FIGURE 24. PSD OF UNSTEADY PRESSURE COEFFICIENT, RUN 1

$\xi = 0.25$, UPPER SURFACE MEAN SQUARE = 0.00785

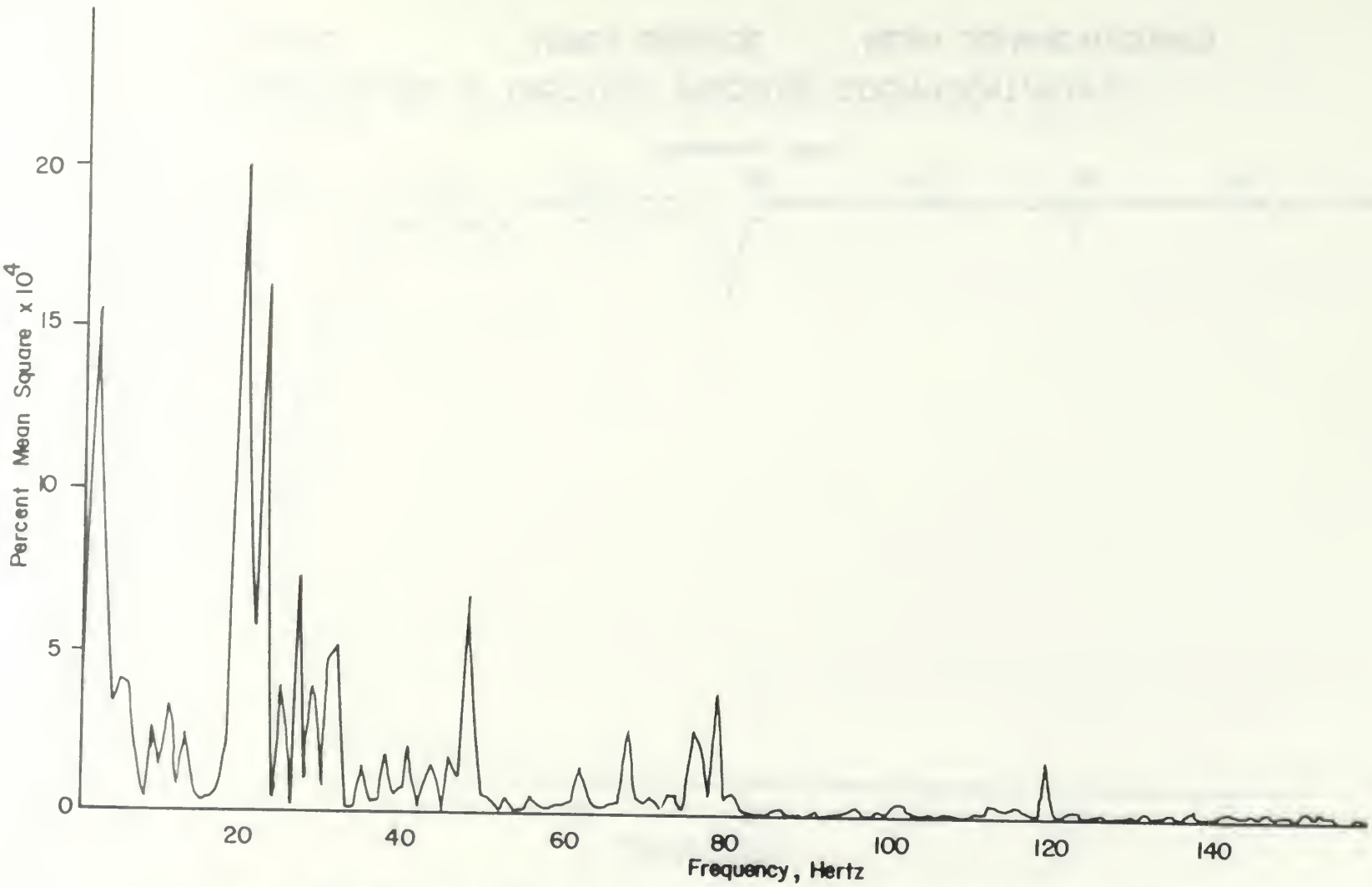

FIGURE 25. PSD OF UNSTEADY PRESSURE COEFFICIENT, RUN 2

ζ=0.0 MEAN SQUARE =0.00334

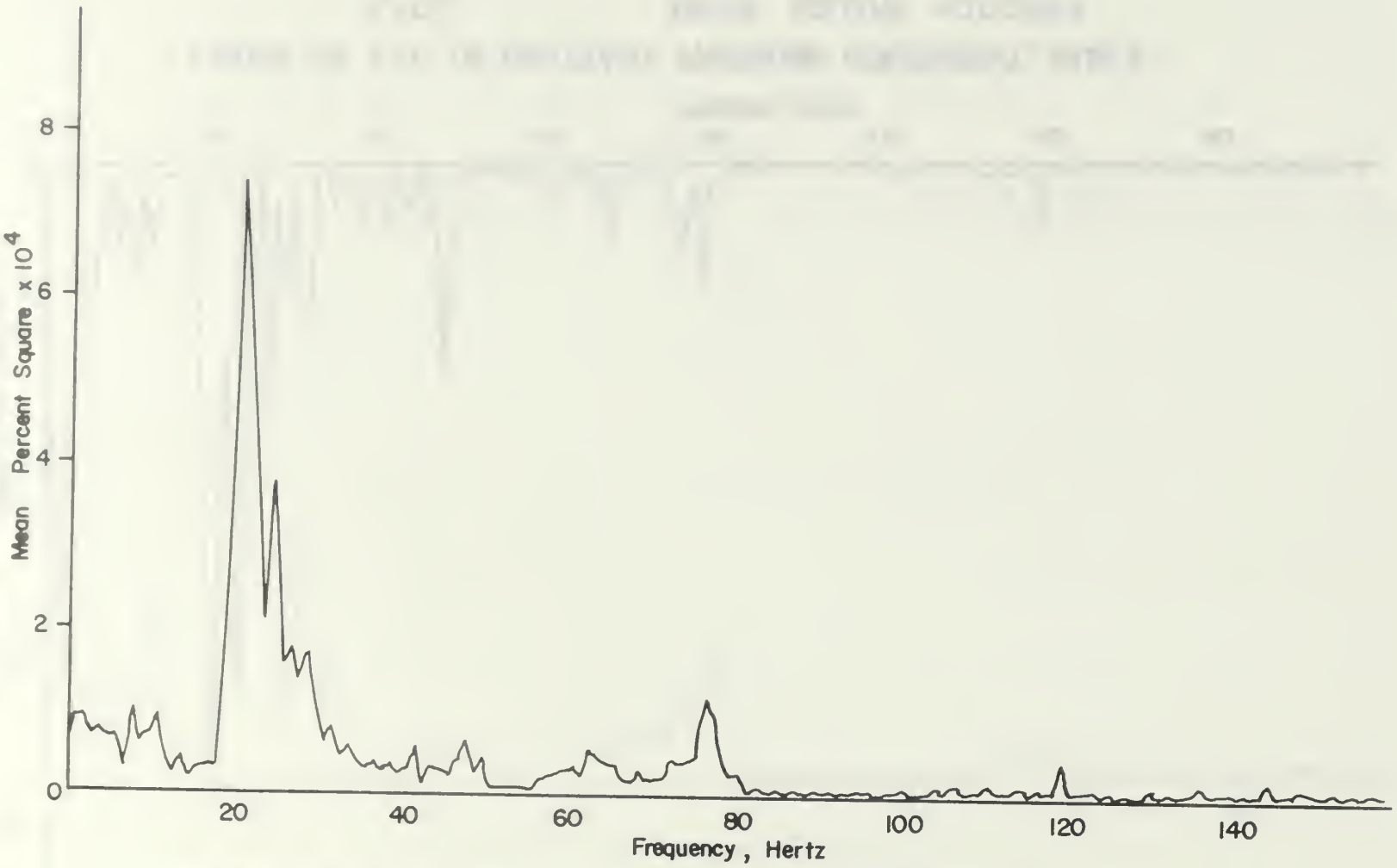

FIGURE 26. PSD OF UNSTEADY PRESSURE COEFFICIENT, RUN 2

$\zeta = 0.15$ UPPER SURFACE MEAN SQUARE = 0.00993

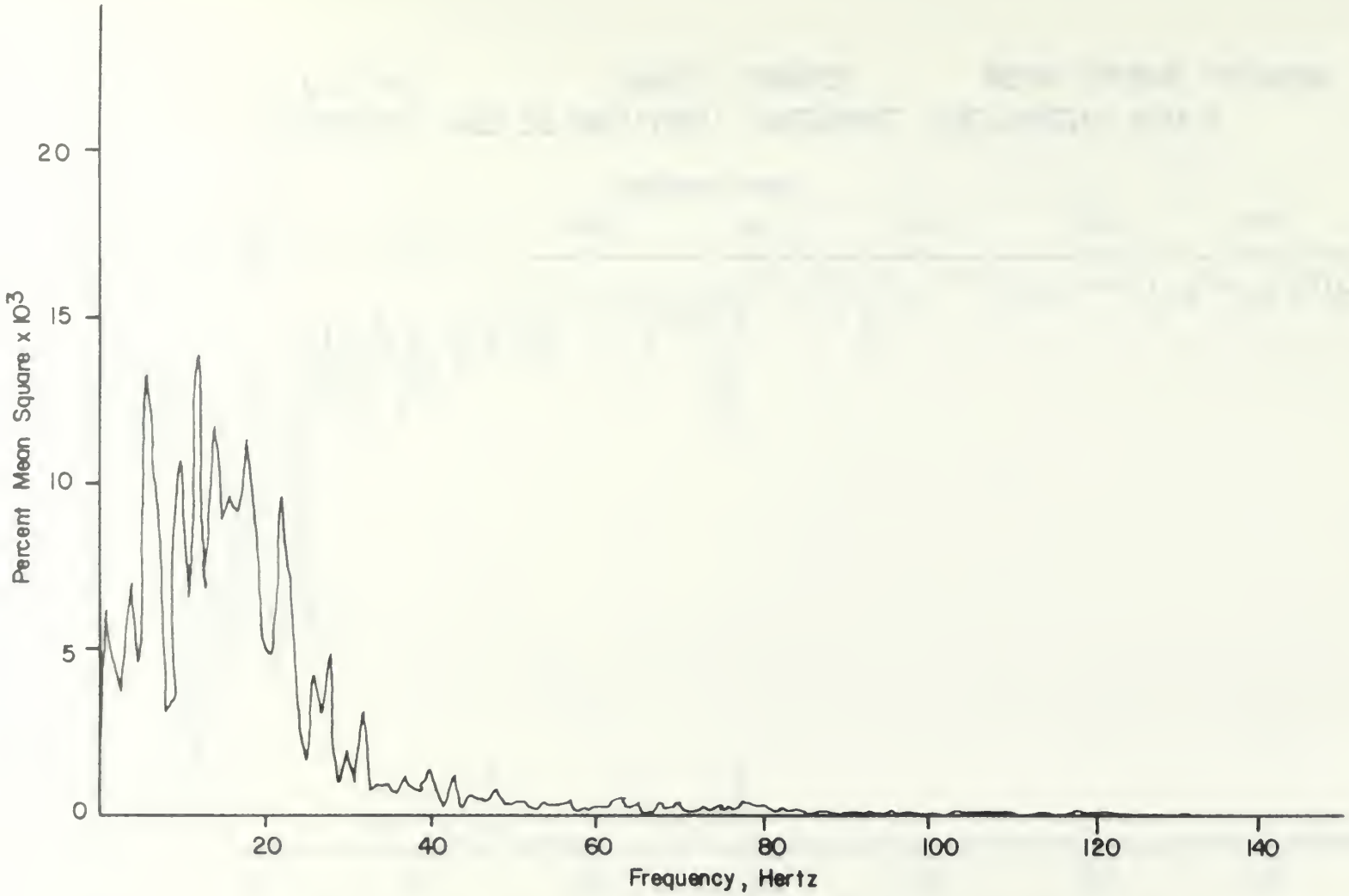

FIGURE 27. PSD OF UNSTEADY PRESSURE COEFFICIENT, RUN 3
$\varepsilon = 0.0$ MEAN SQUARE = 0.0727

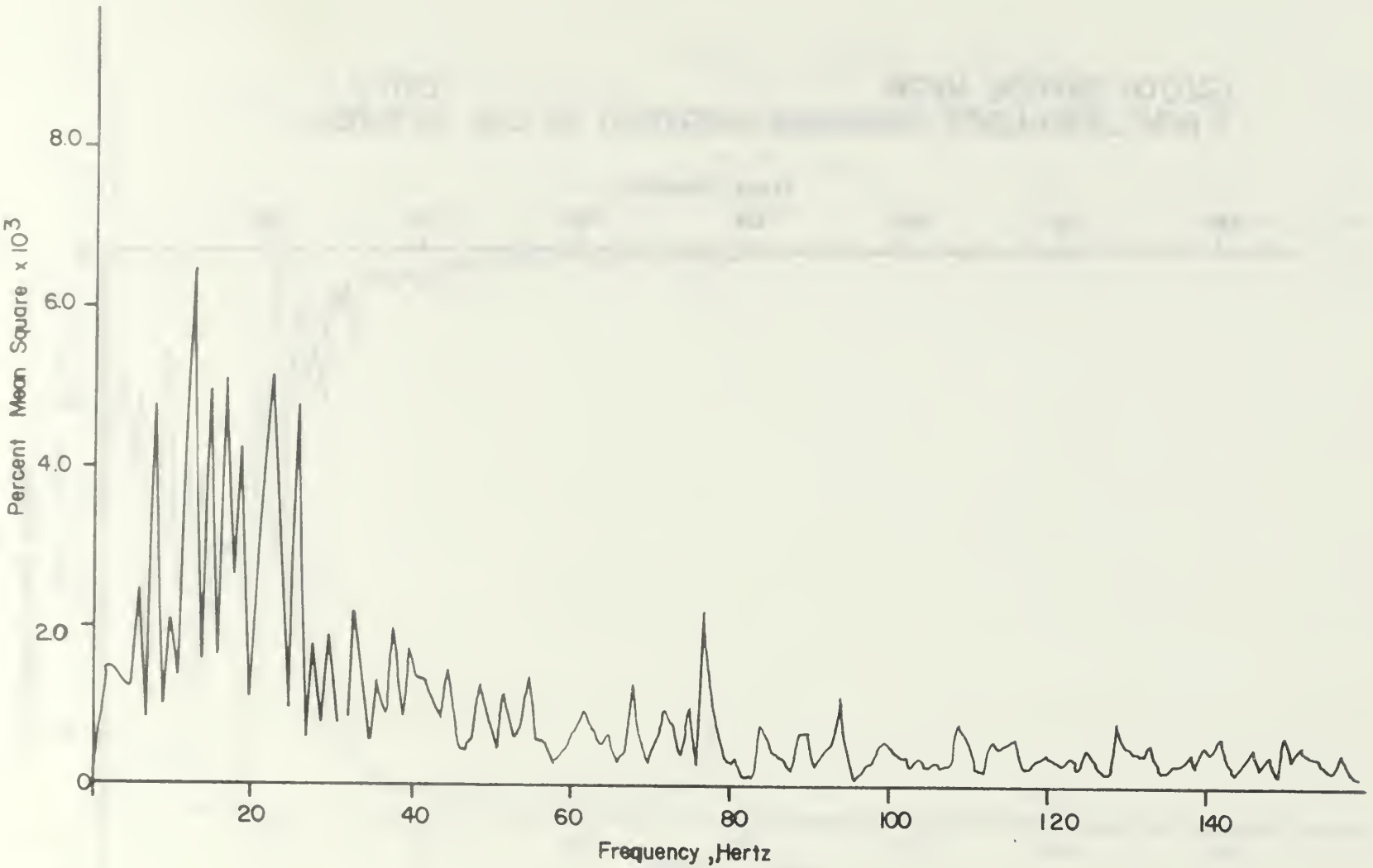

FIGURE 28. PSD OF UNSTEADY PRESSURE COEFFICIENT, RUN 3
ϵ = 0.45 UPPER SURFACE MEAN SQUARE = 0.0448

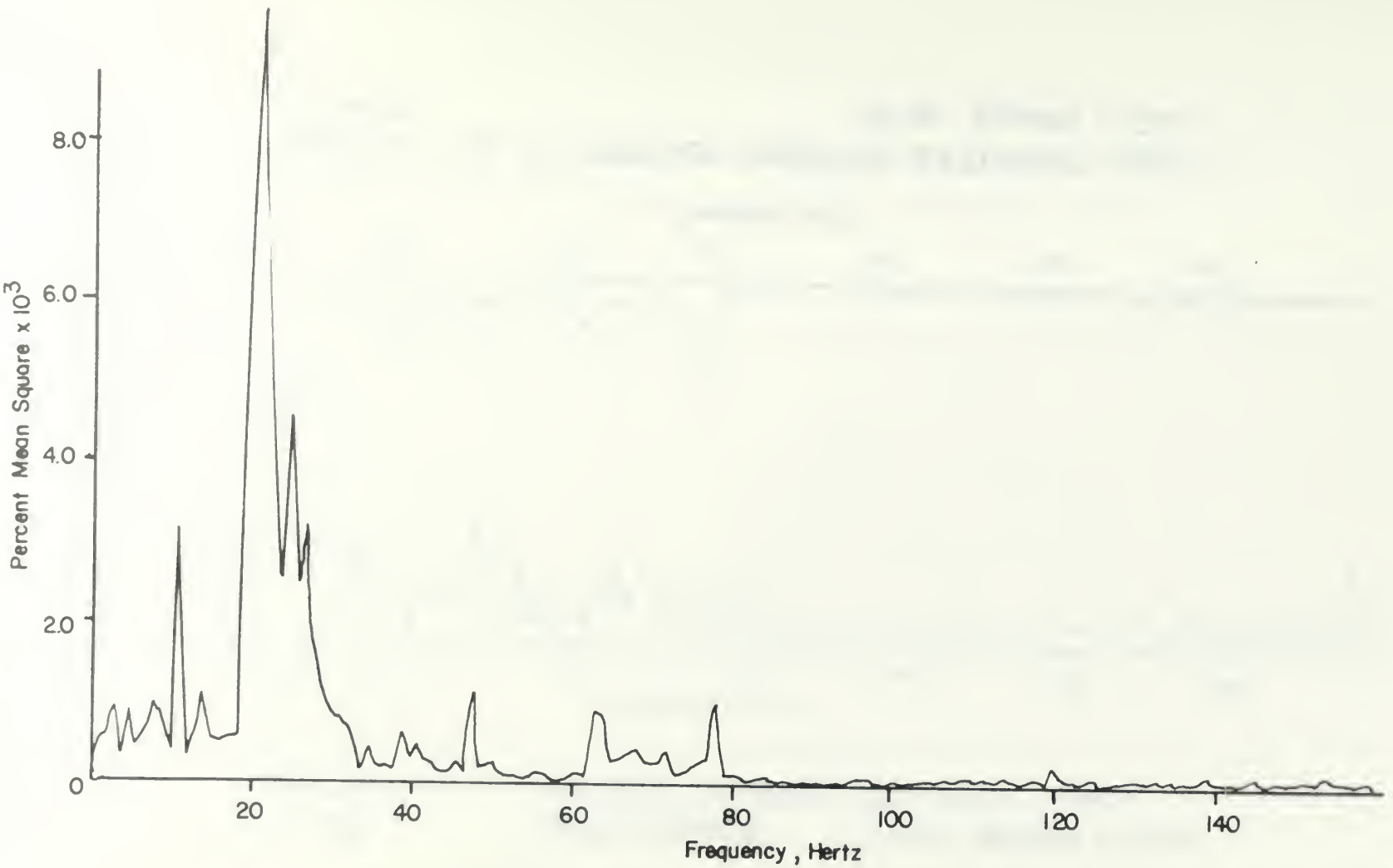

FIGURE 29. PSD OF UNSTEADY PRESSURE COEFFICIENT, RUN 3
ζ=0.5 LOWER SURFACE MEAN SQUARE =.00116

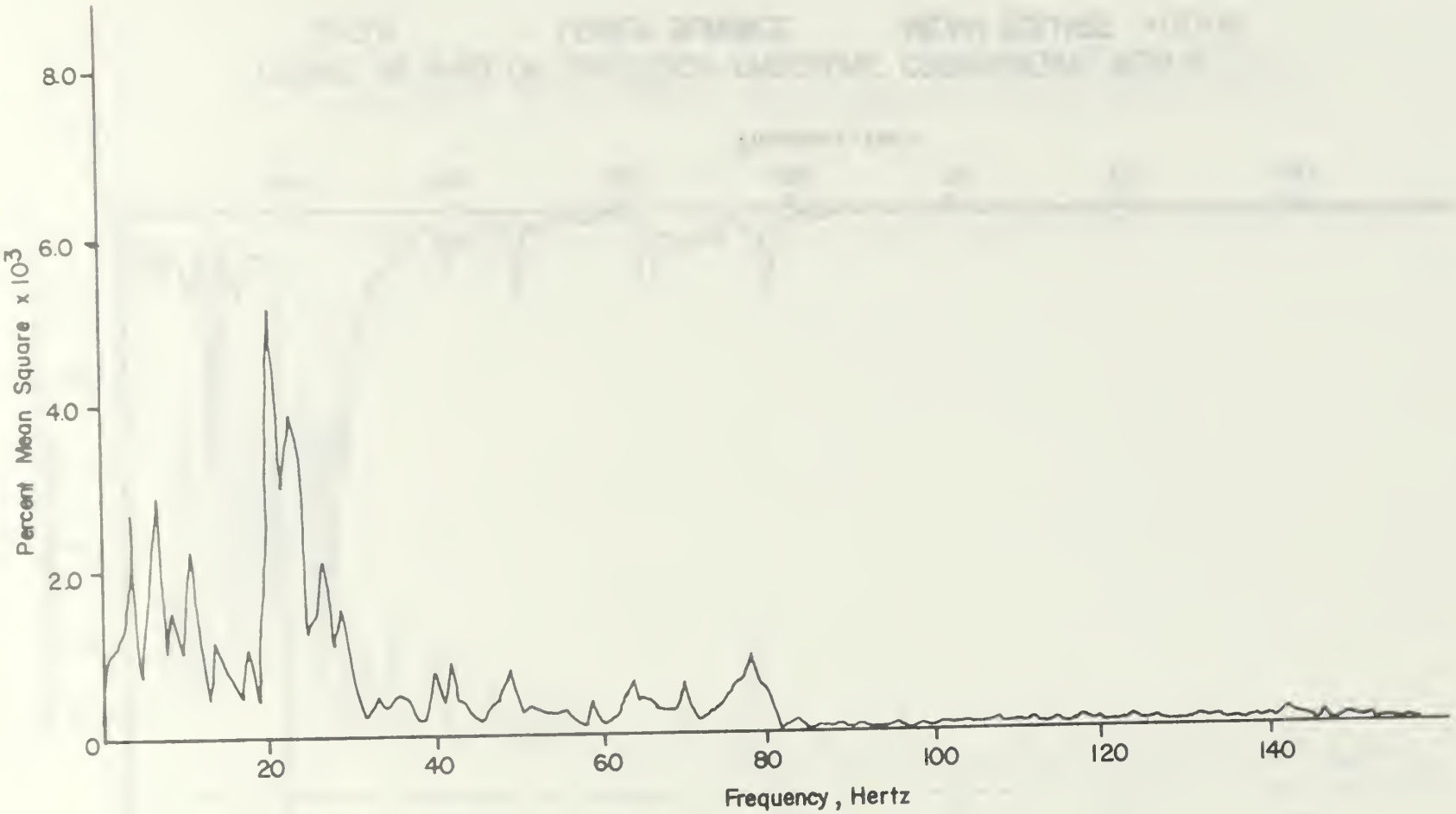

FIGURE 30. PSD OF UNSTEADY PRESSURE COEFFICIENT, RUN 4
$\epsilon = 0.0$ MEAN SQUARE = 0.0131

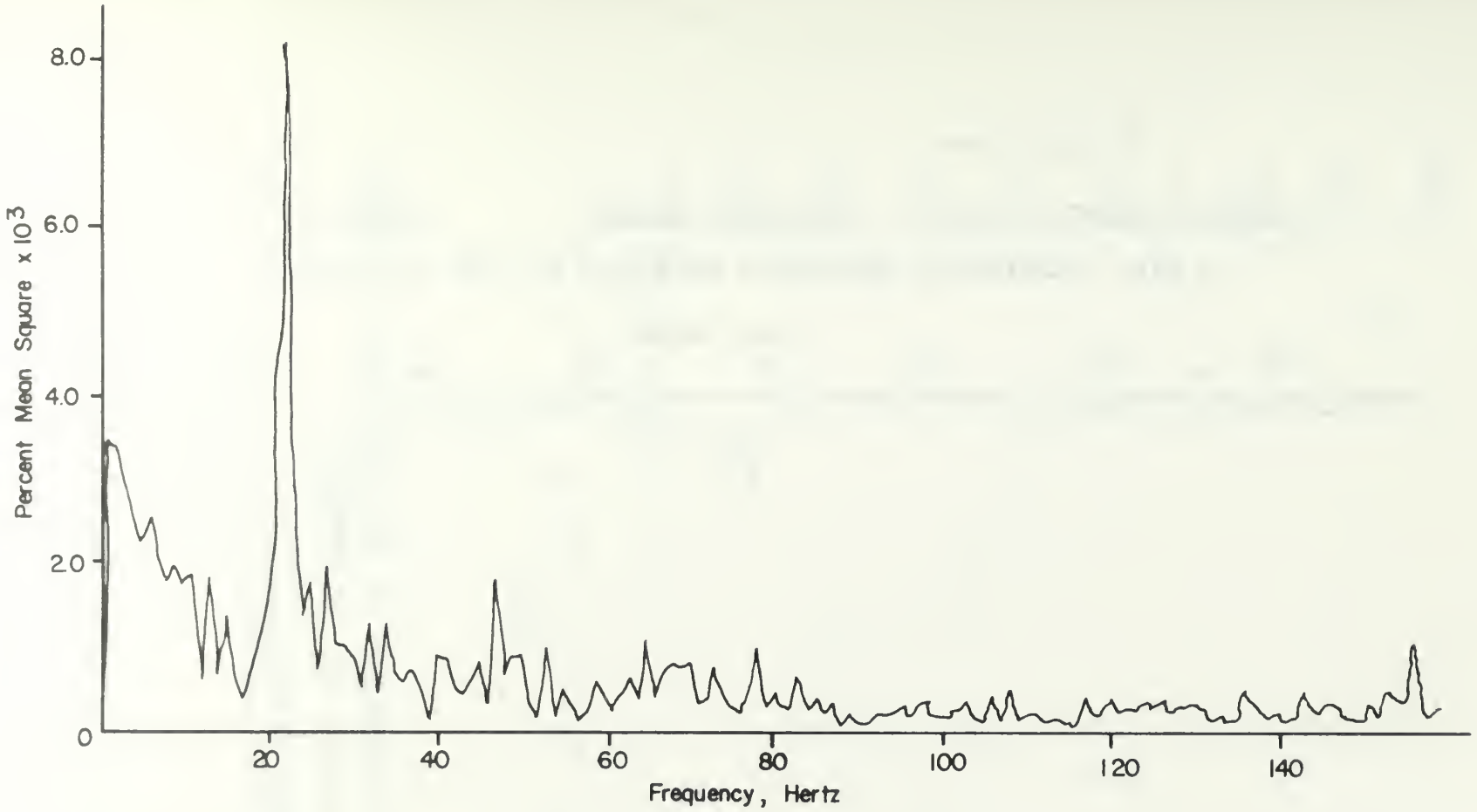

FIGURE 31. PSD OF UNSTEADY PRESSURE COEFFICIENT, RUN 4
$\xi = 0.5$ UPPER SURFACE MEAN SQUARE = 0.0172

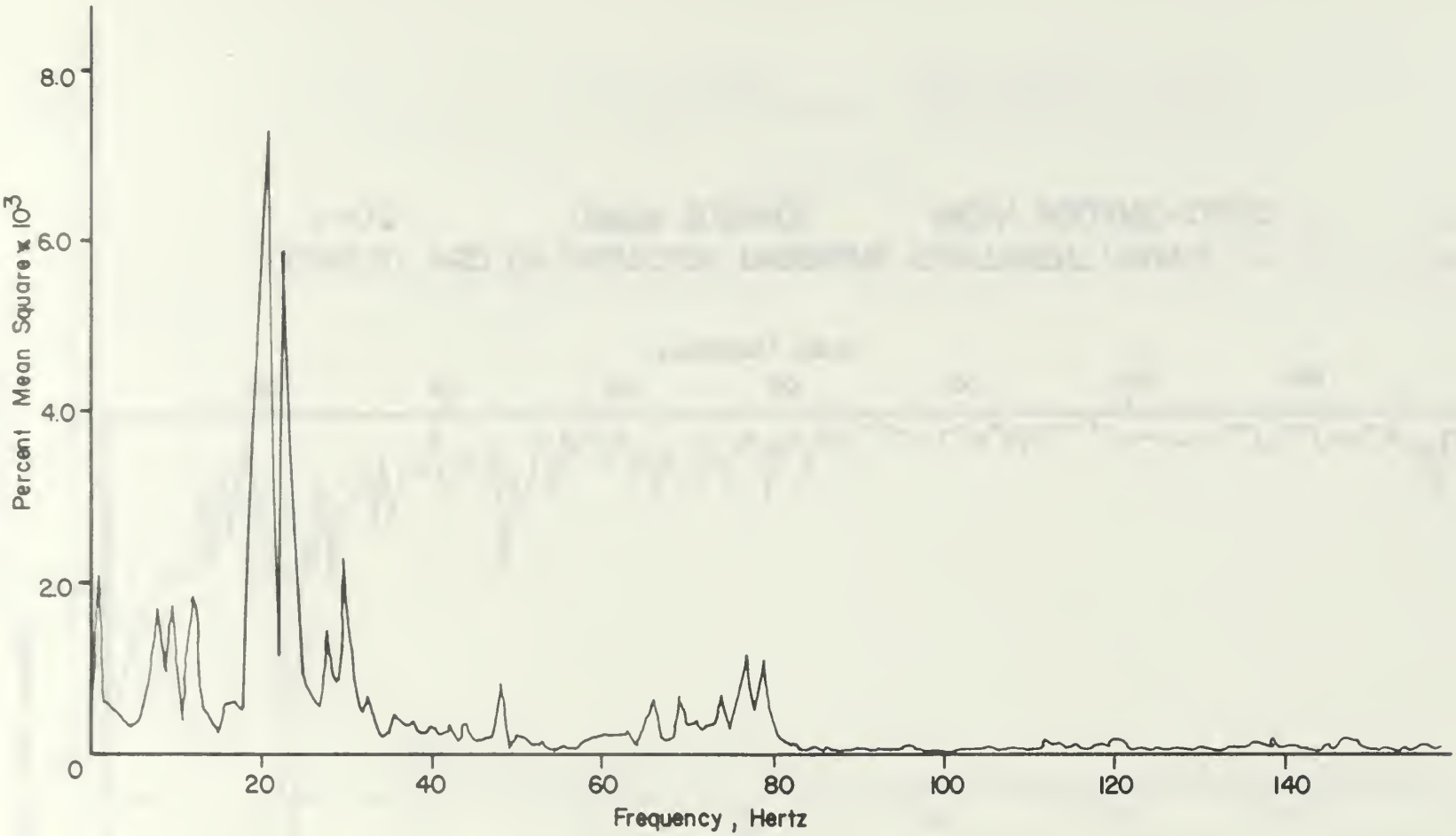

FIGURE 32. PSD OF UNSTEADY PRESSURE COEFFICIENT, RUN 4

$\varepsilon = 0.125$ LOWER SURFACE MEAN SQUARE = 0.0104

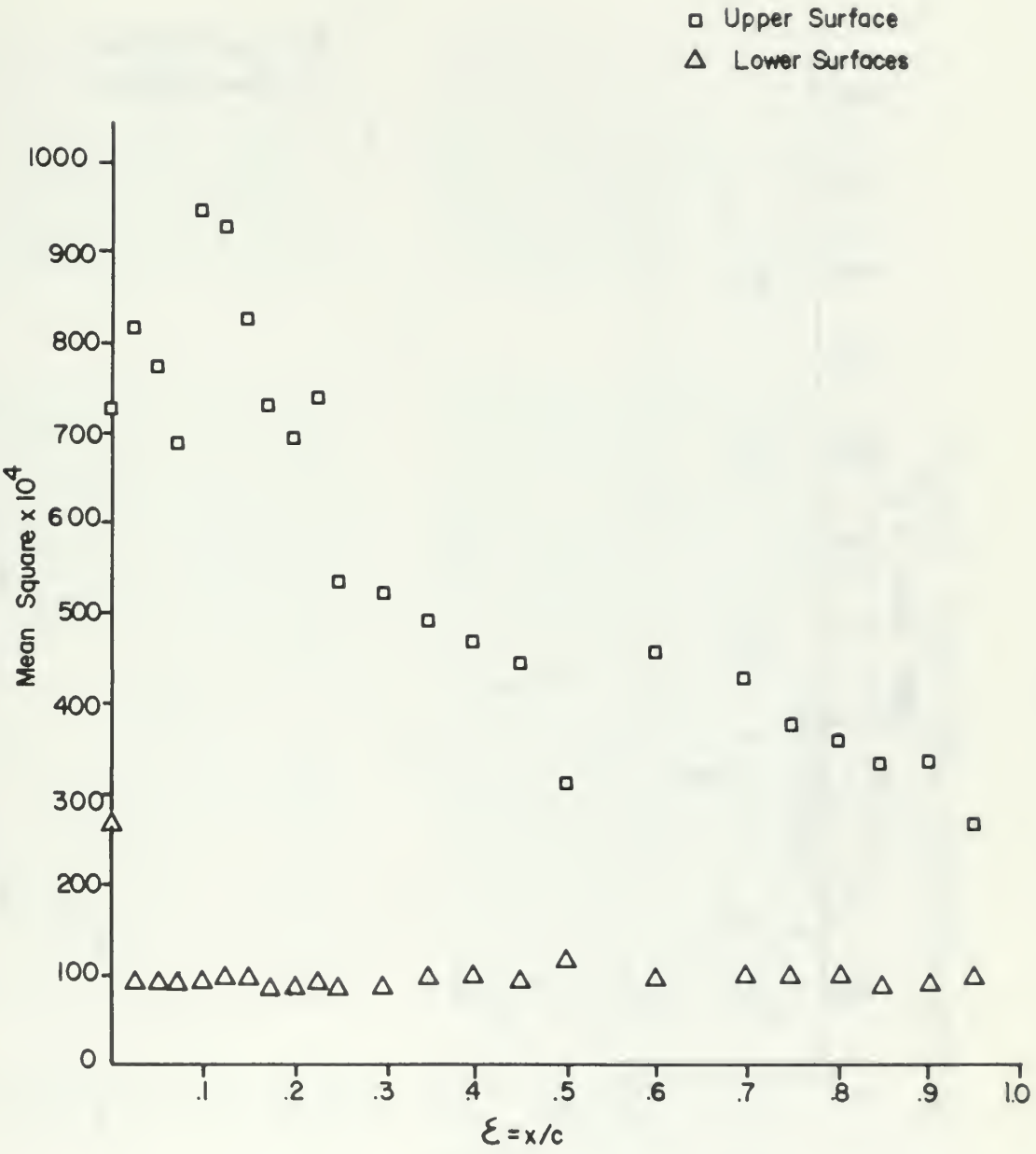

FIGURE 33. MEAN SQUARE OF UNSTEADY PRESSURE COEFFICIENT ON AIRFOIL

RUN 3 $\alpha = 10°$ $\overline{U} \approx 100$ ft / sec STEADY FLOW

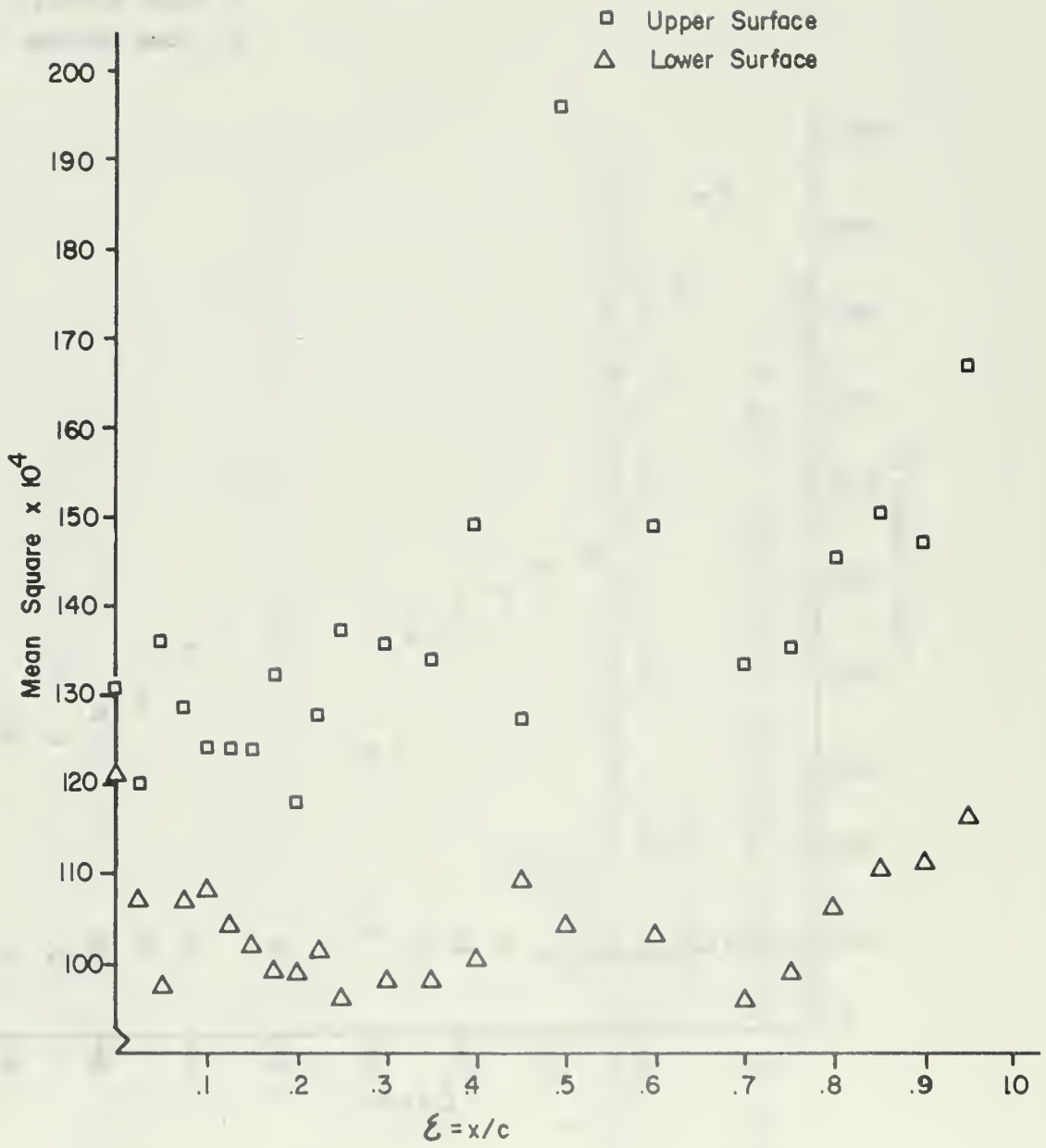

FIGURE 34. MEAN SQUARE OF UNSTEADY PRESSURE COEFFICIENTS ON AIRFOIL

RUN 4 $\alpha = 15°$ $\bar{U} \approx 100$ ft/sec STEADY FLOW

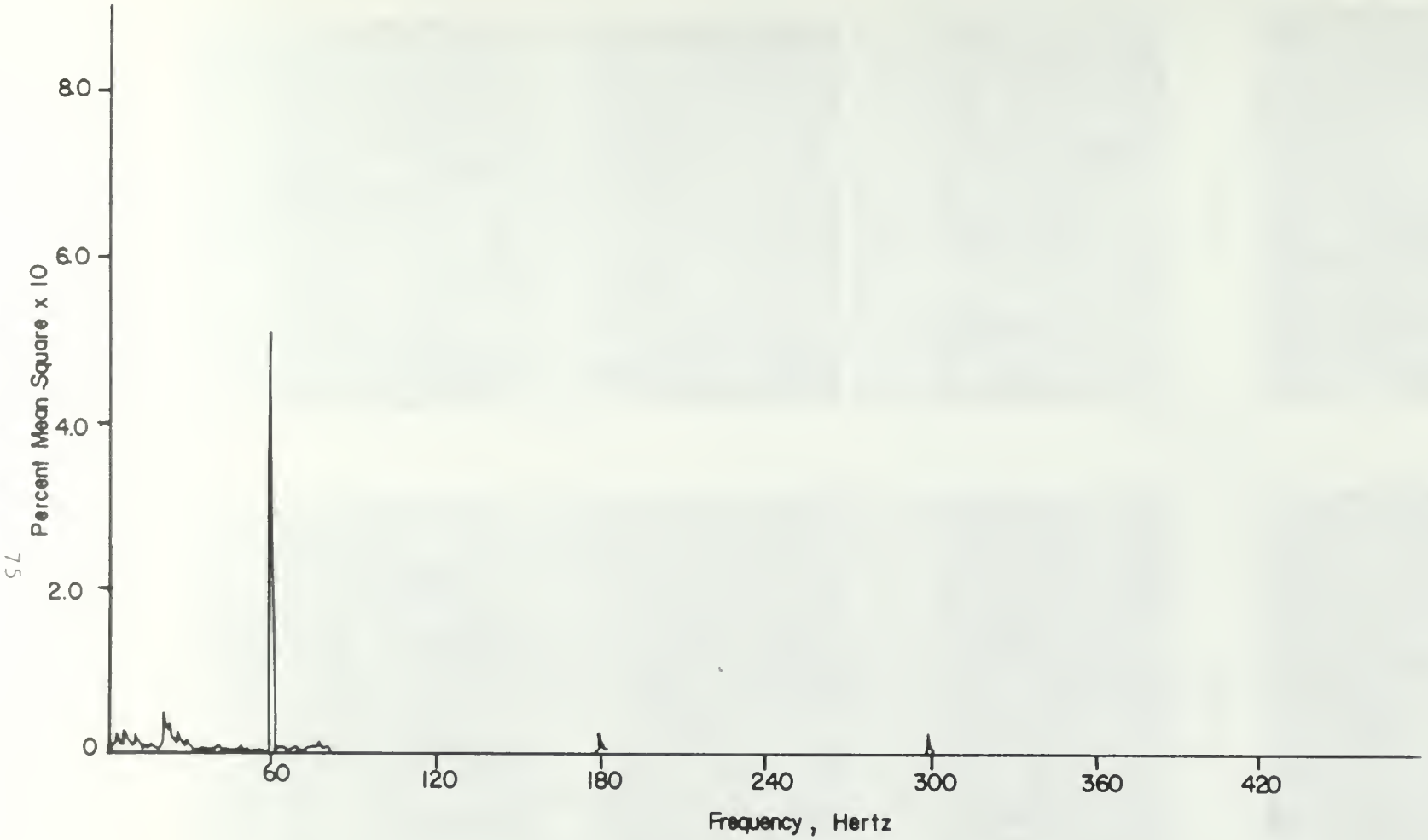

FIGURE 35

TYPICAL UNFILTERED PSD, RUN 4, $\zeta = 0.0$

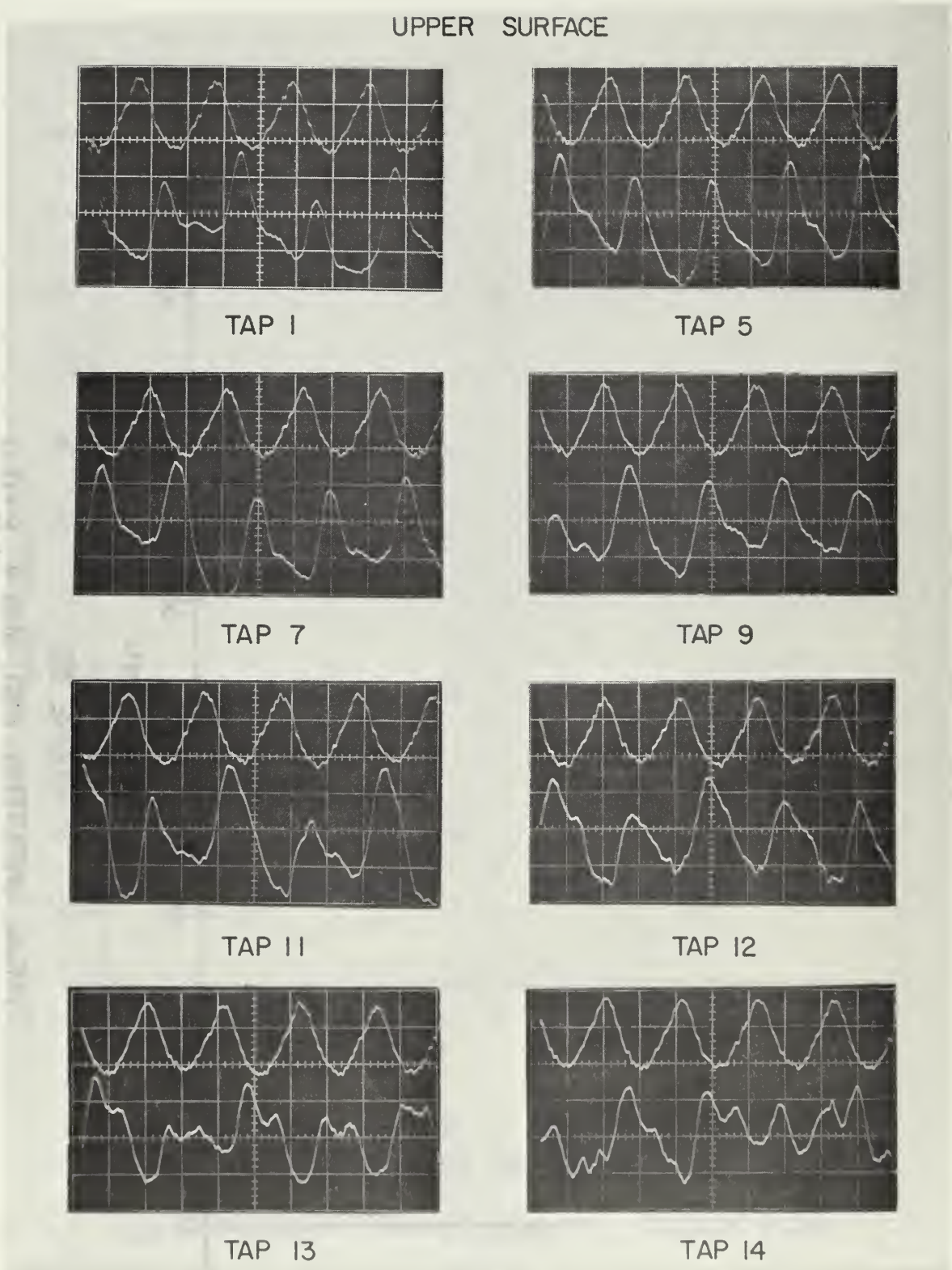

Figure 36. Selected Oscilloscope Traces, Run 5

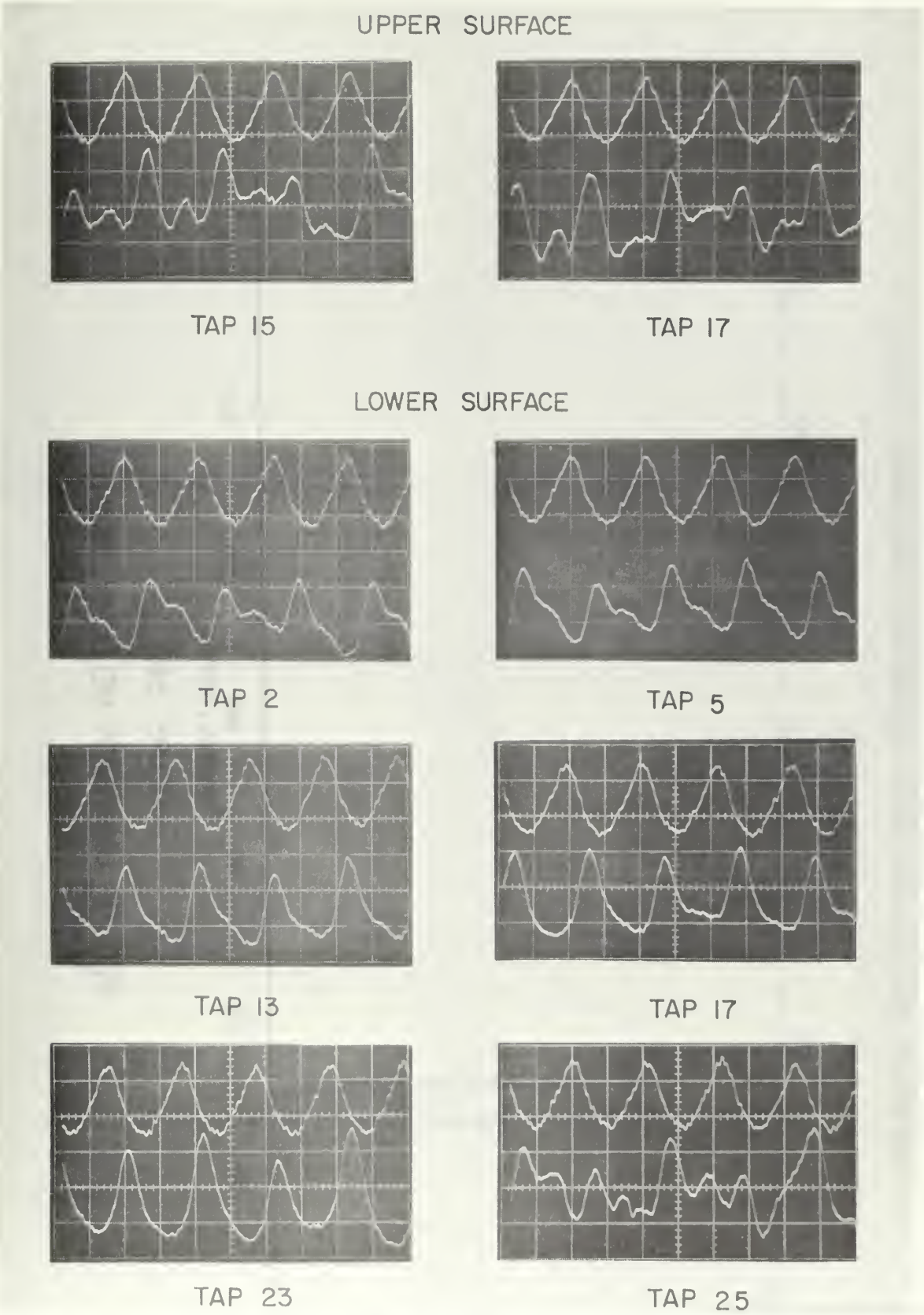

Figure 37. Selected Oscilloscope Traces, Run 5

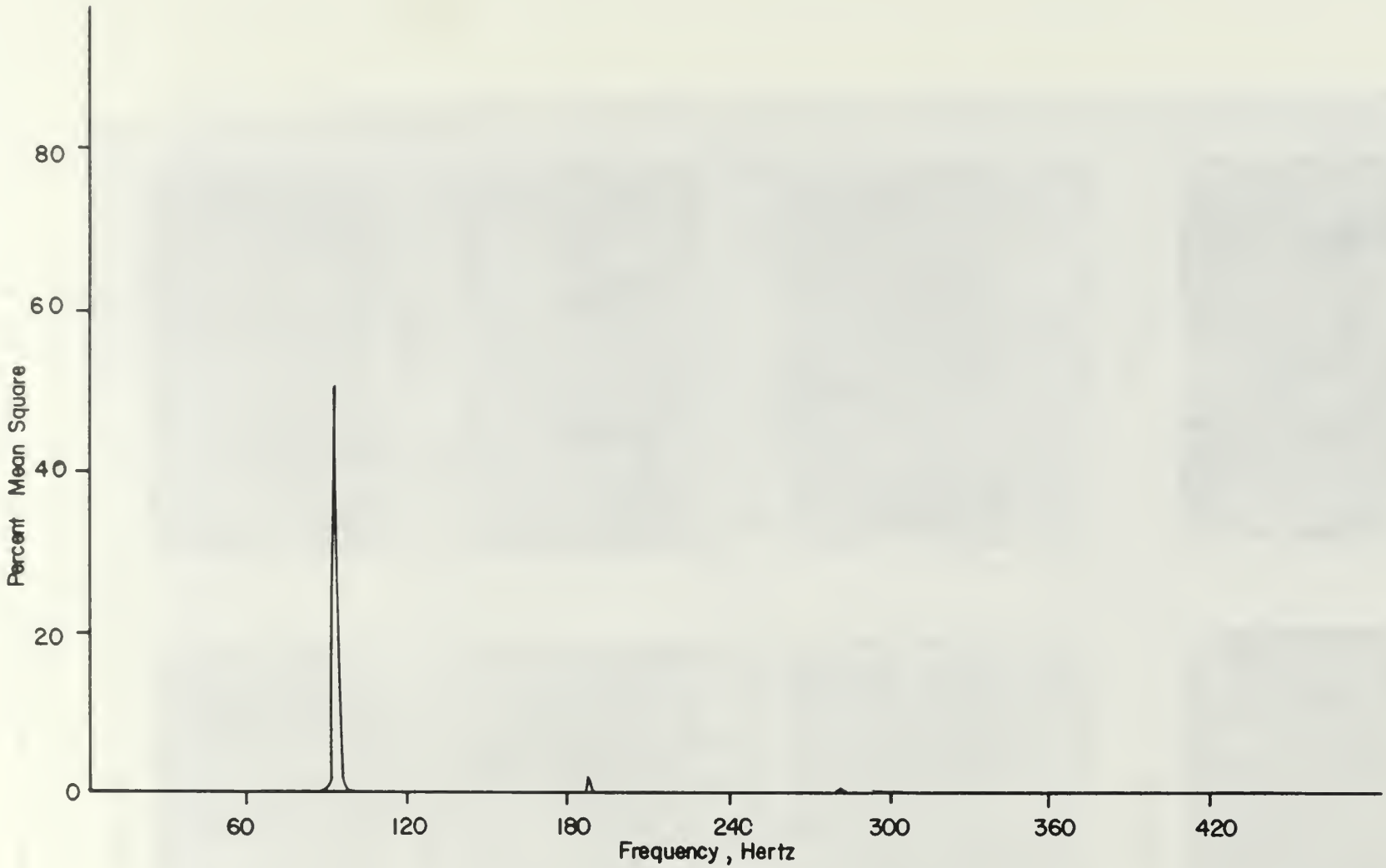

FIGURE 38

PSD OF UNSTEADY VELOCITY, RUN 5
$\overline{U} = 102.66$ $\overline{U}^2 = 38.43$

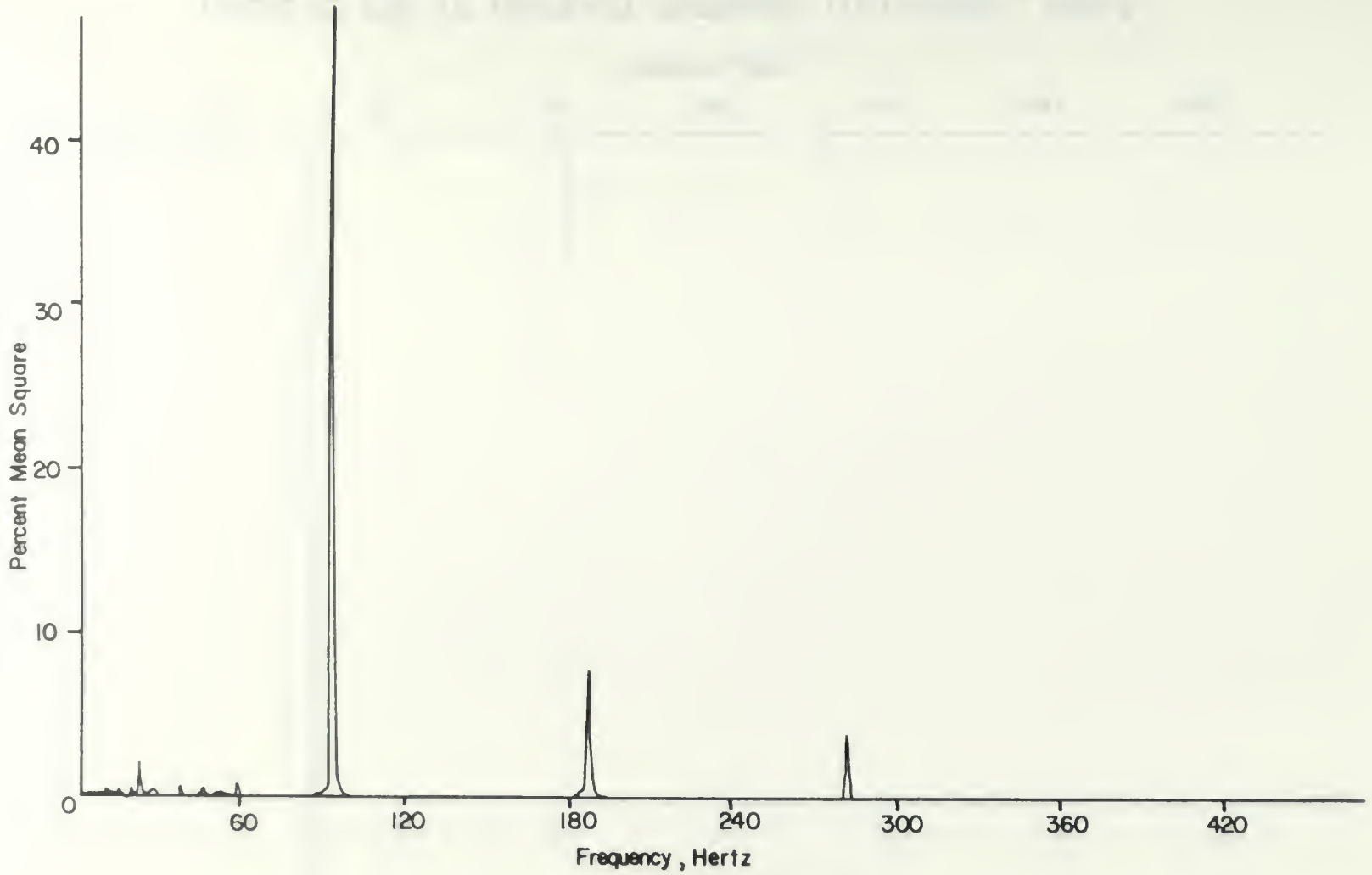

FIGURE 39. PSD OF UNSTEADY PRESSURE COEFFICIENT, RUN 5
$\xi = 0.0$ UPPER SURFACE

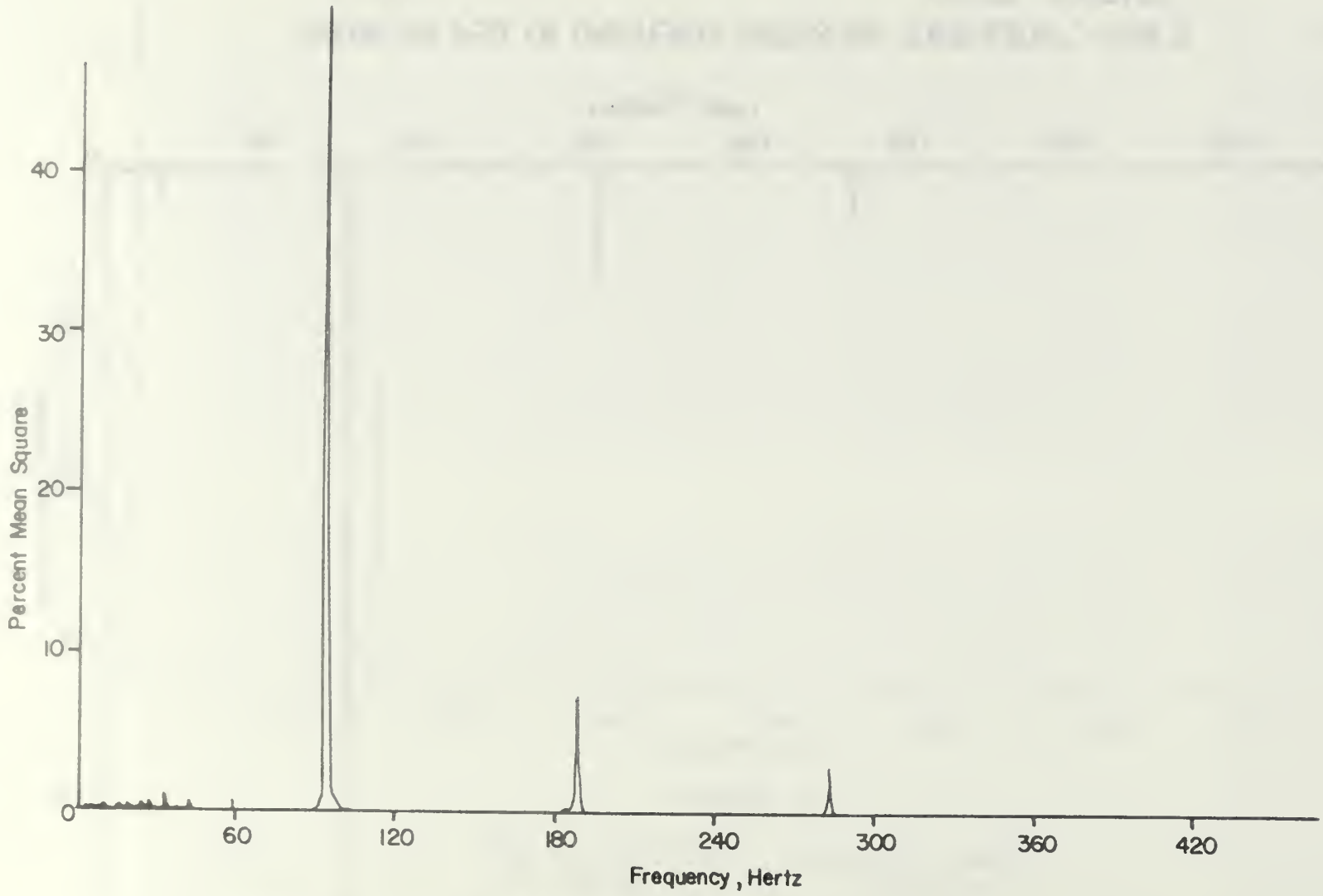

FIGURE 40. PSD OF UNSTEADY PRESSURE COEFFICIENT, RUN 5
ζ=0.025 UPPER SURFACE

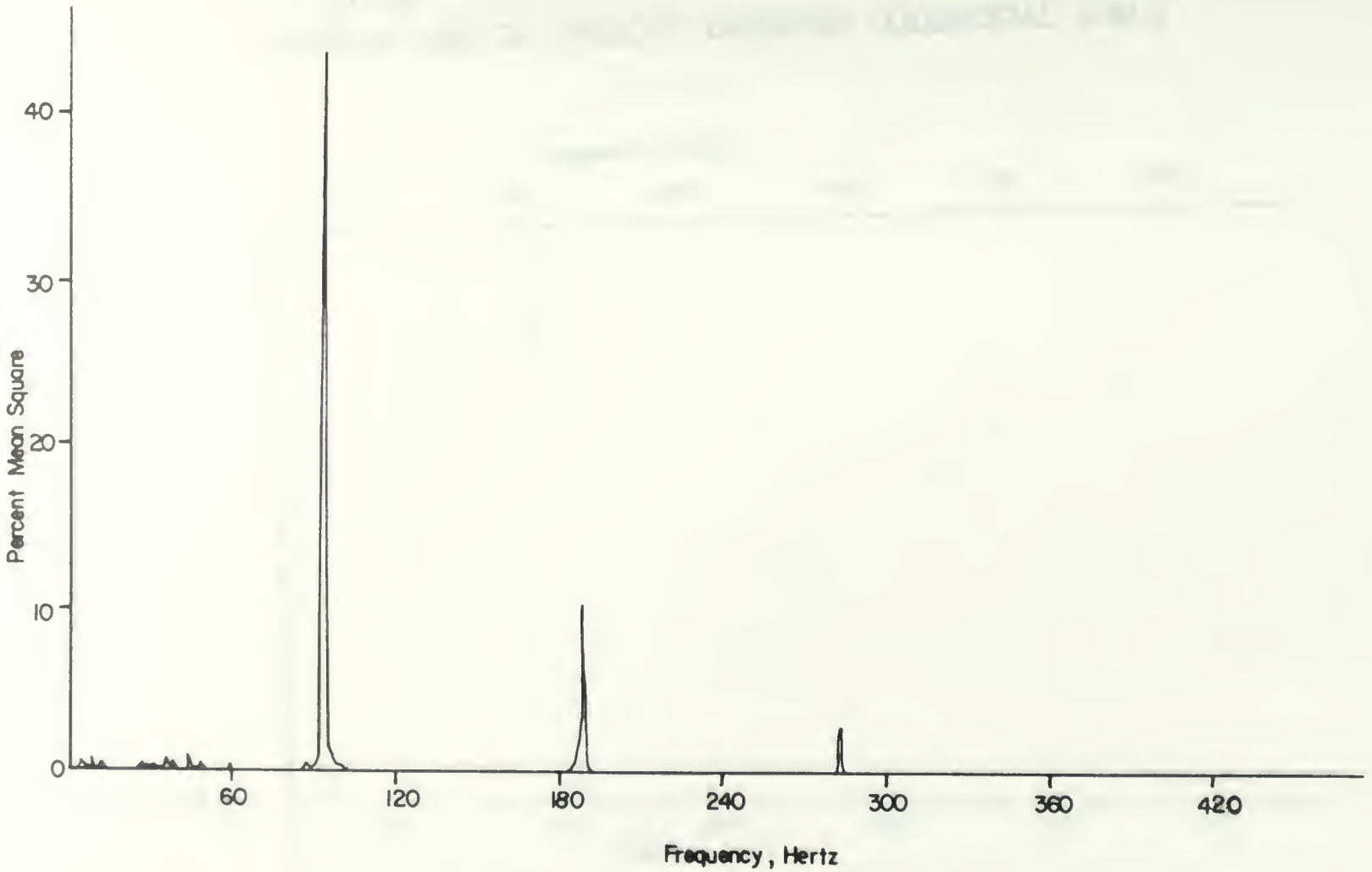

FIGURE 41. PSD OF UNSTEADY PRESSURE COEFFICIENT, RUN 5

ϵ=0.075 UPPER SURFACE

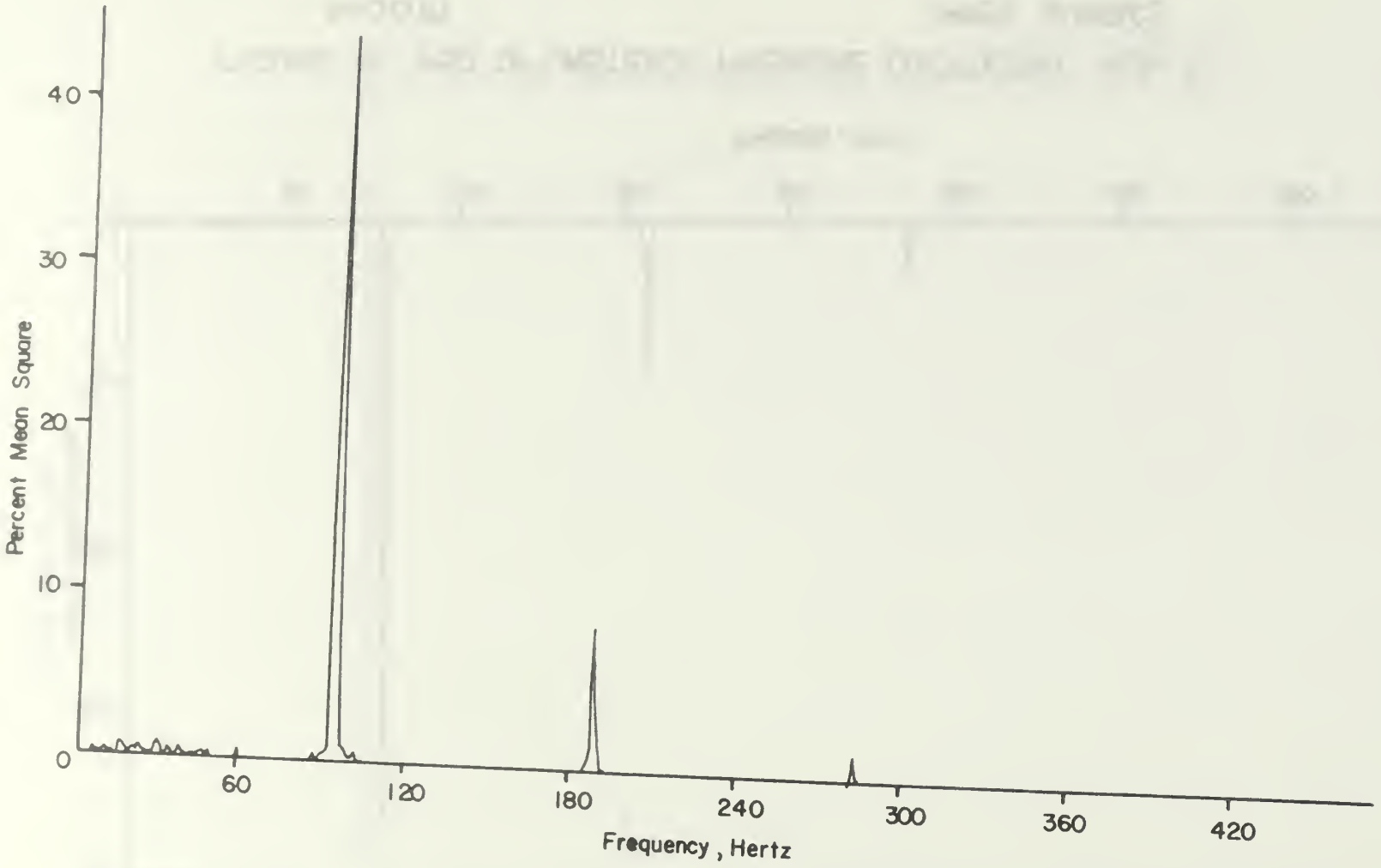

FIGURE 42. PSD OF UNSTEADY PRESSURE COEFFICIENT, RUN 5
ϵ =0.125
UPPER SURFACE

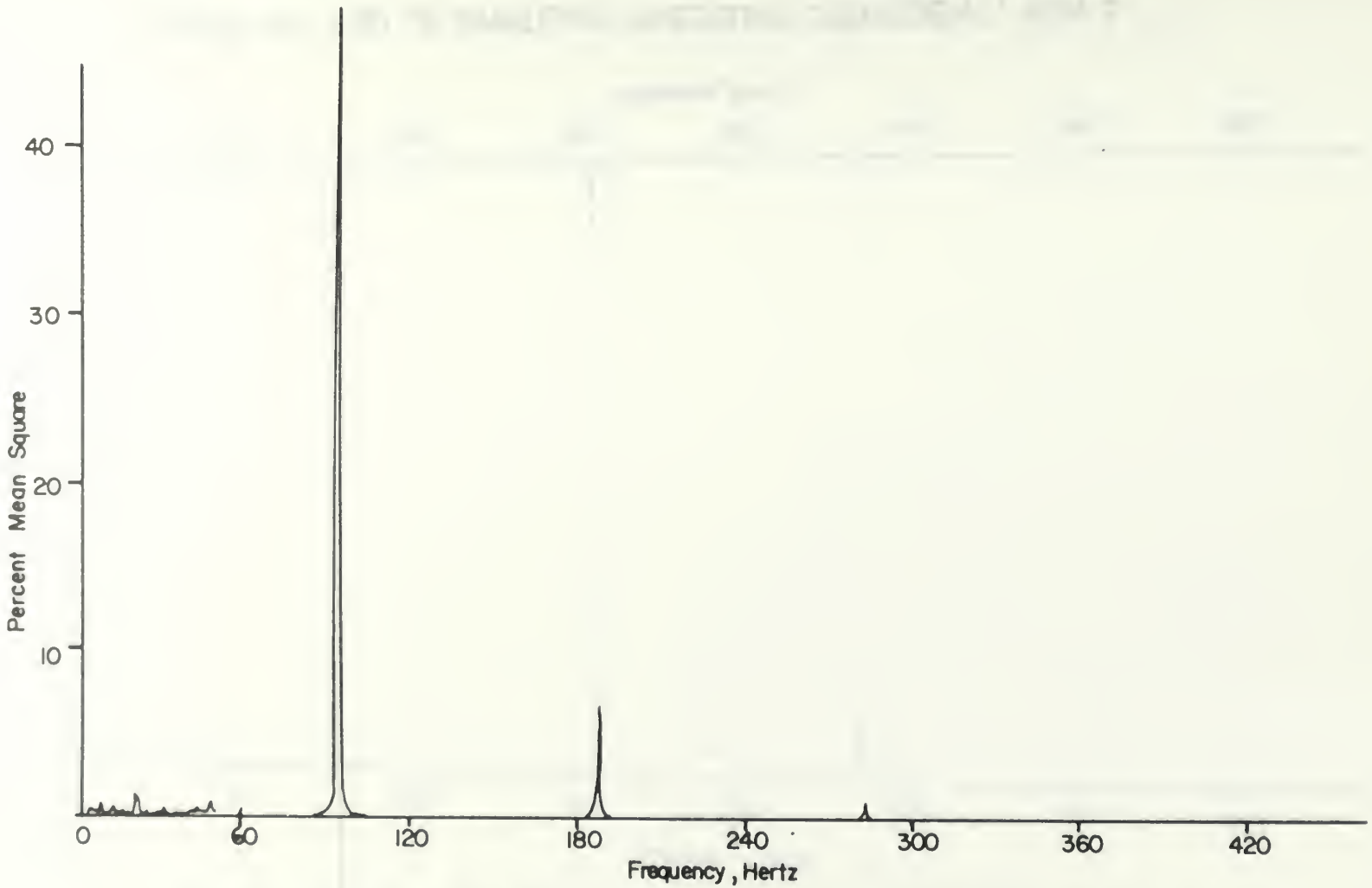

FIGURE 43. PSD OF UNSTEADY PRESSURE COEFFICIENT ,RUN 5

ε=0.175 UPPER SURFACE

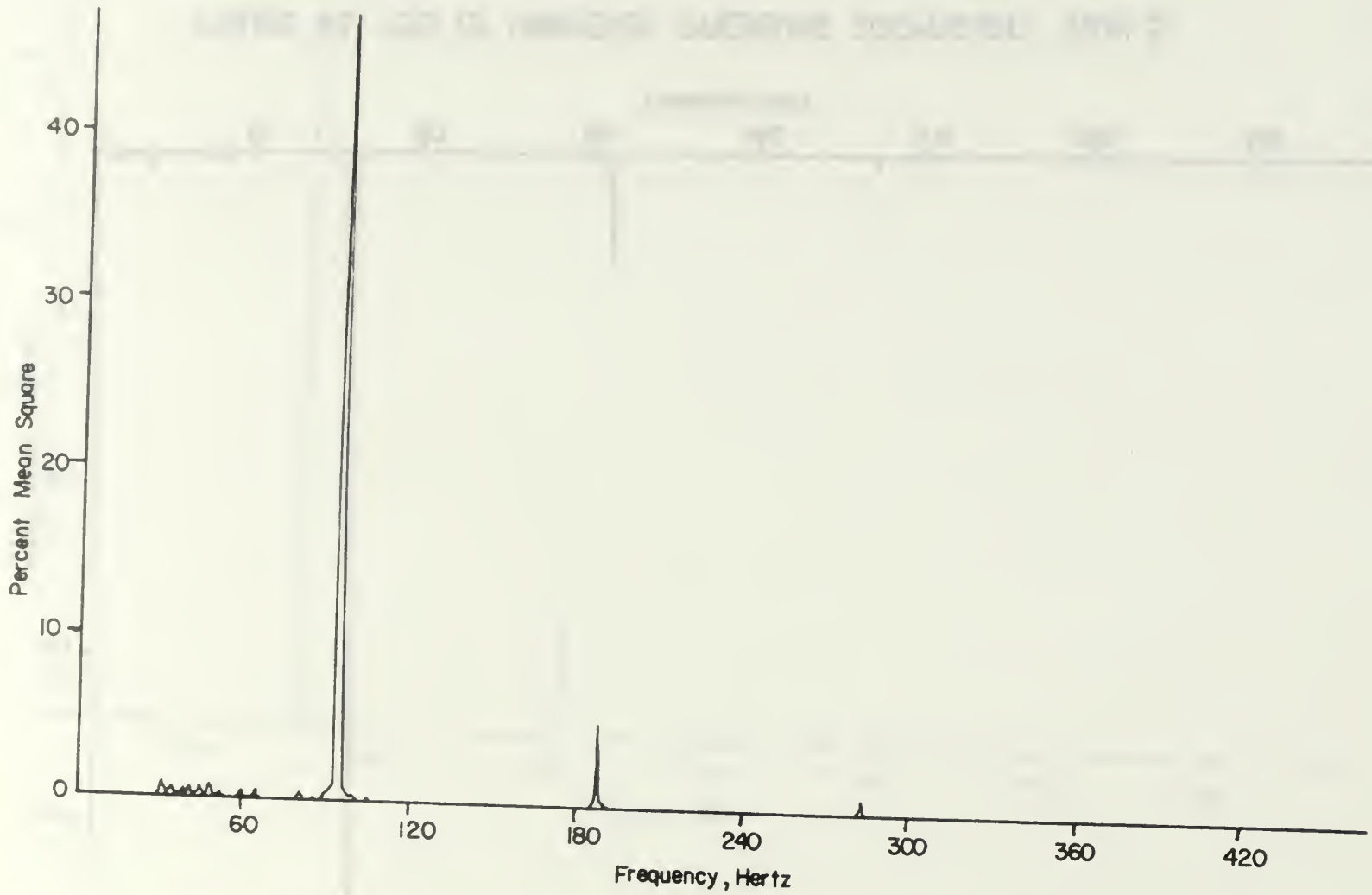

FIGURE 44. PSD OF UNSTEADY PRESSURE COEFFICIENT, RUN 5

$\epsilon = 0.225$

UPPER SURFACE

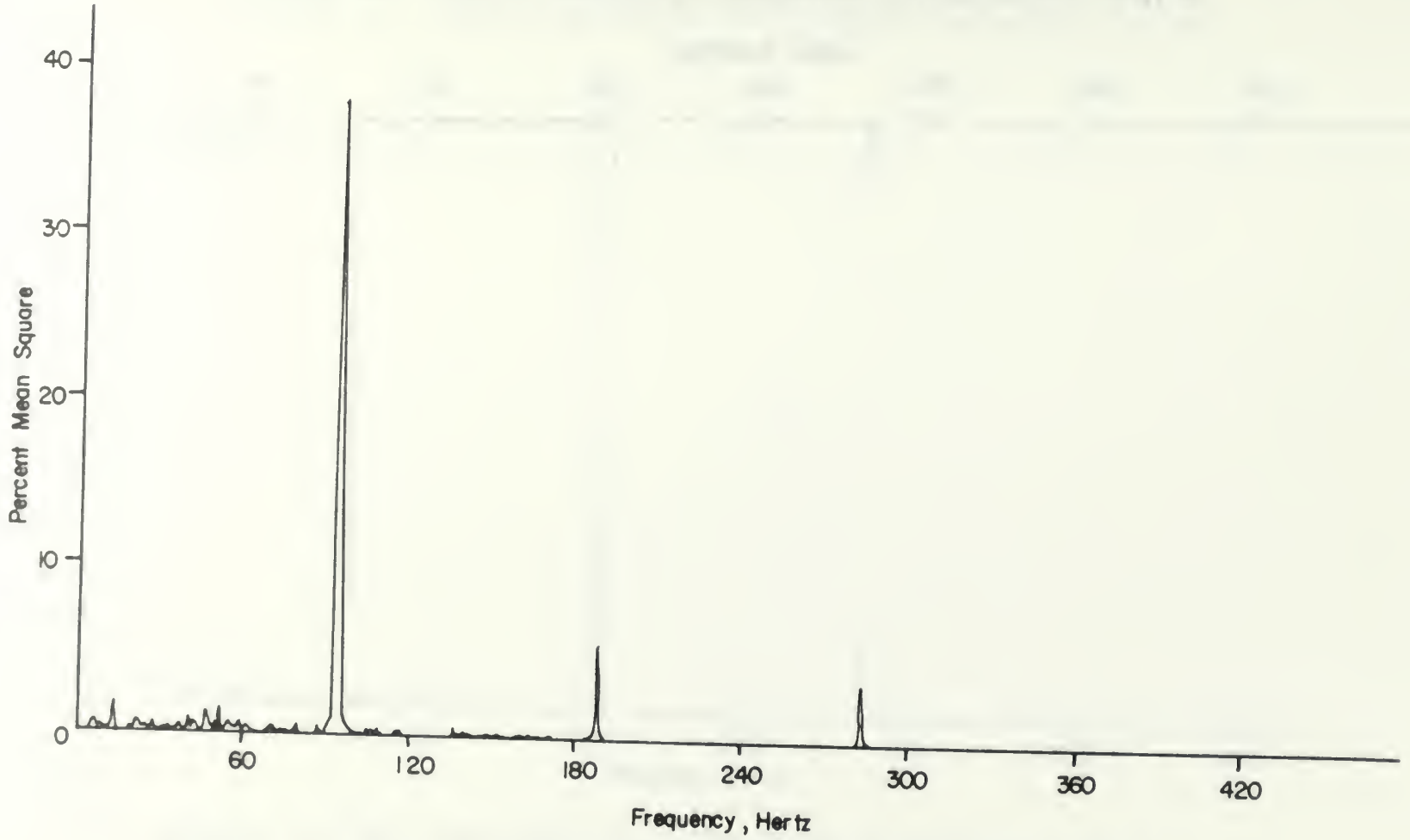

FIGURE 45. PSD OF UNSTEADY PRESSURE COEFFICIENT , RUN 5

ξ=0.300 UPPER SURFACE

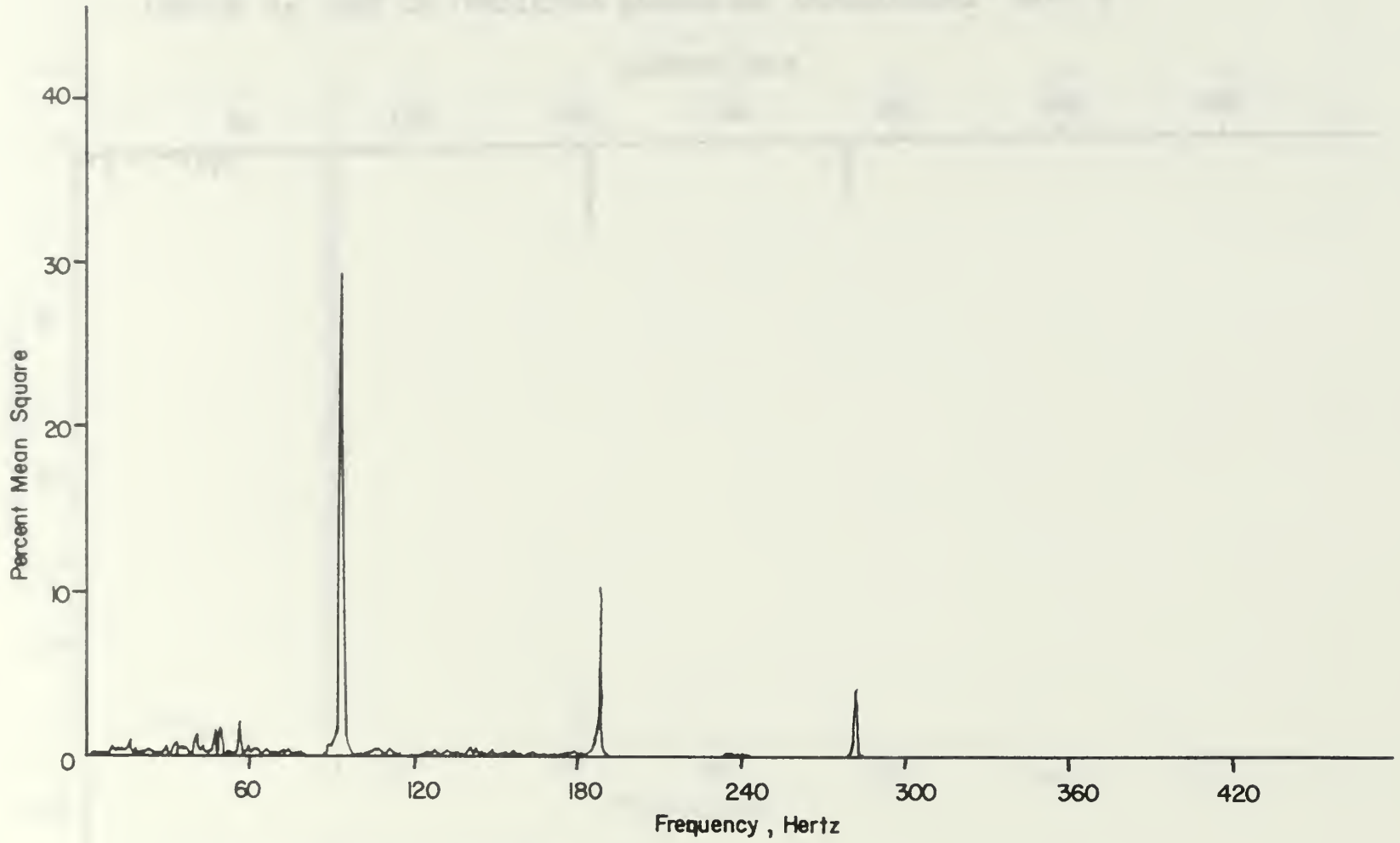

FIGURE 46 PSD OF UNSTEADY PRESSURE COEFFICIENT, RUN 5
ζ=0.350 UPPER SURFACE

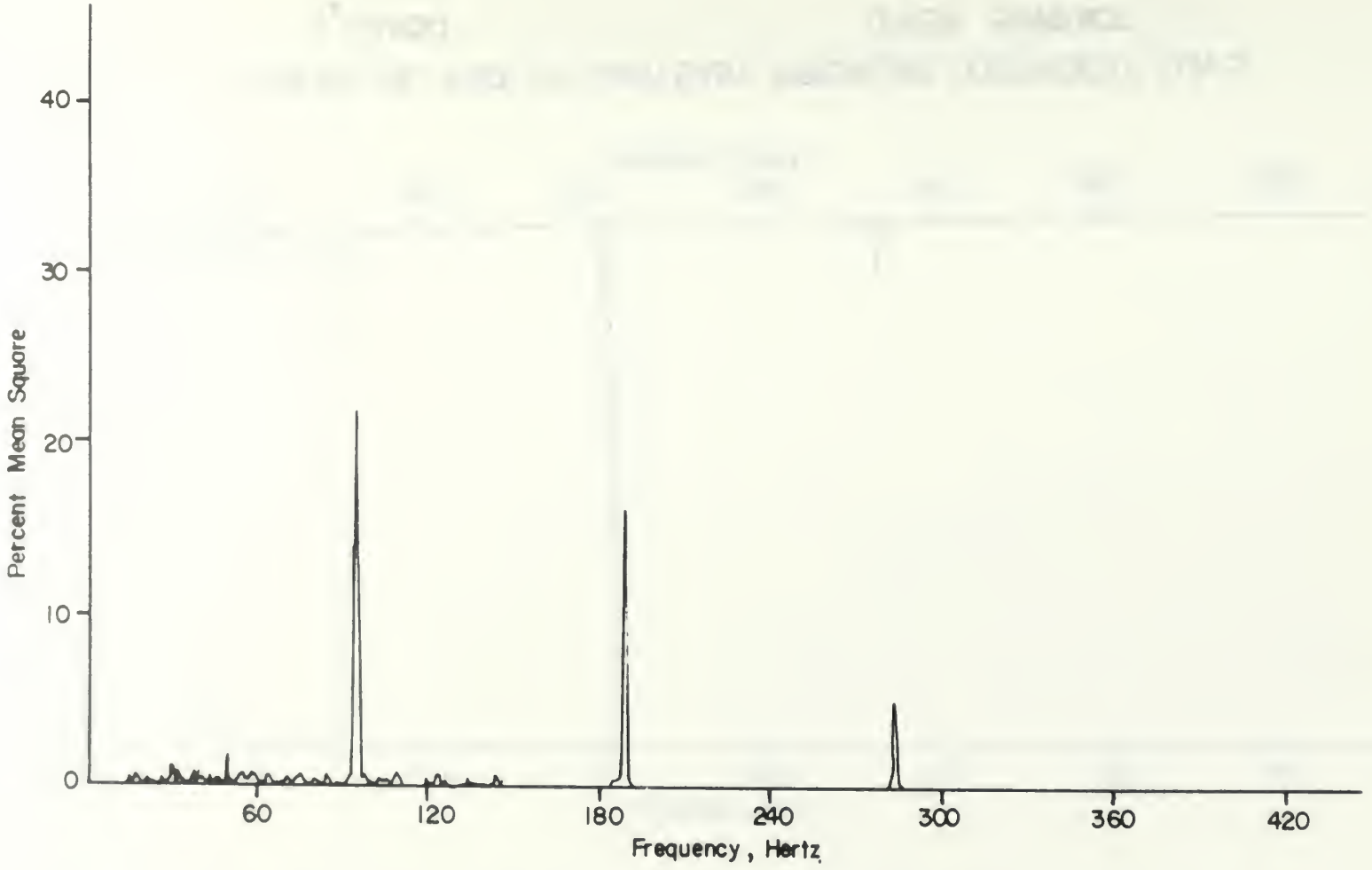

FIGURE 47. PSD OF UNSTEADY PRESSURE COEFFICIENT, RUN 5
ξ=0.400 UPPER SURFACE

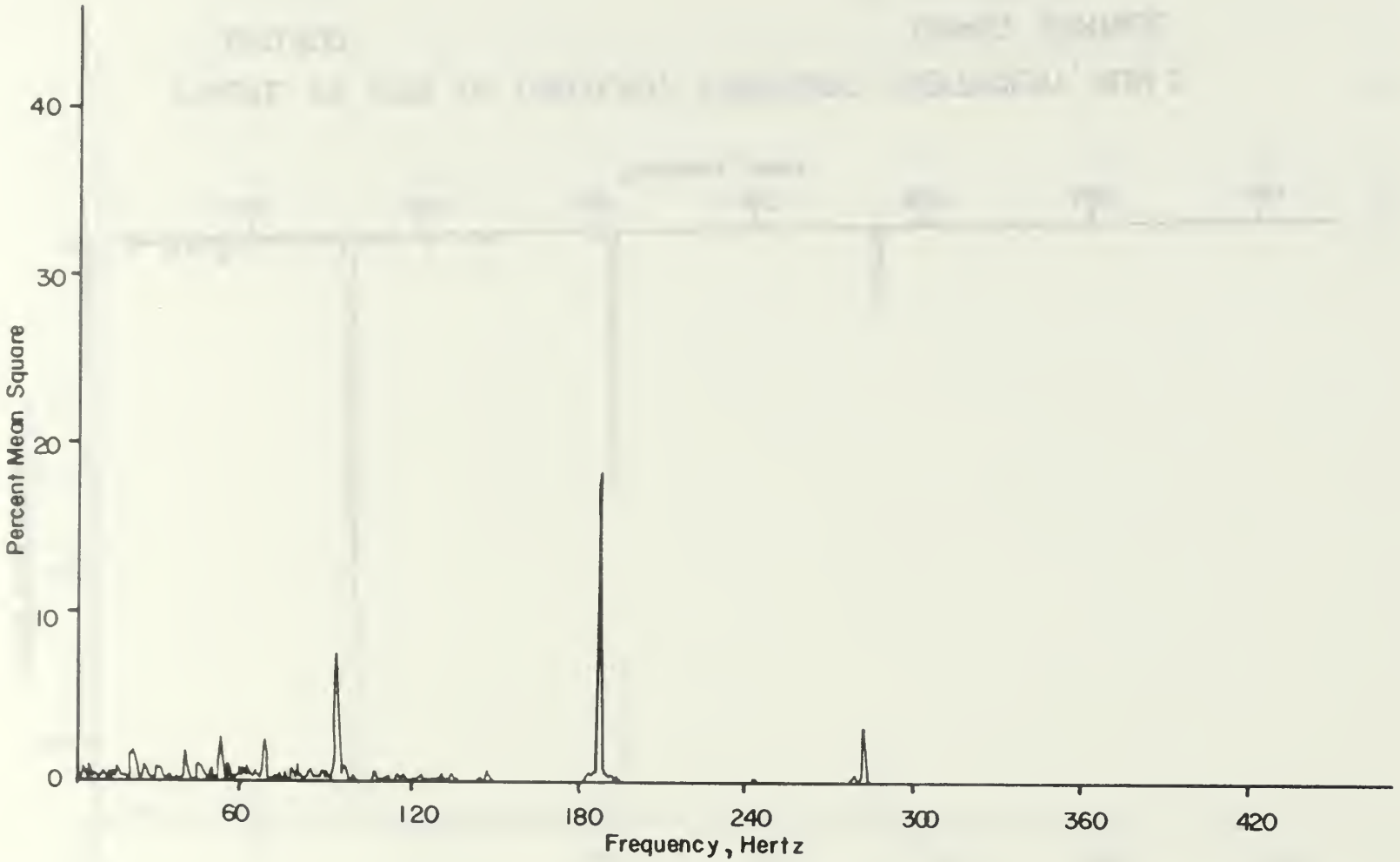

FIGURE 48. PSD OF UNSTEADY PRESSURE COEFFICIENT, RUN 5

ξ=0.450 UPPER SURFACE

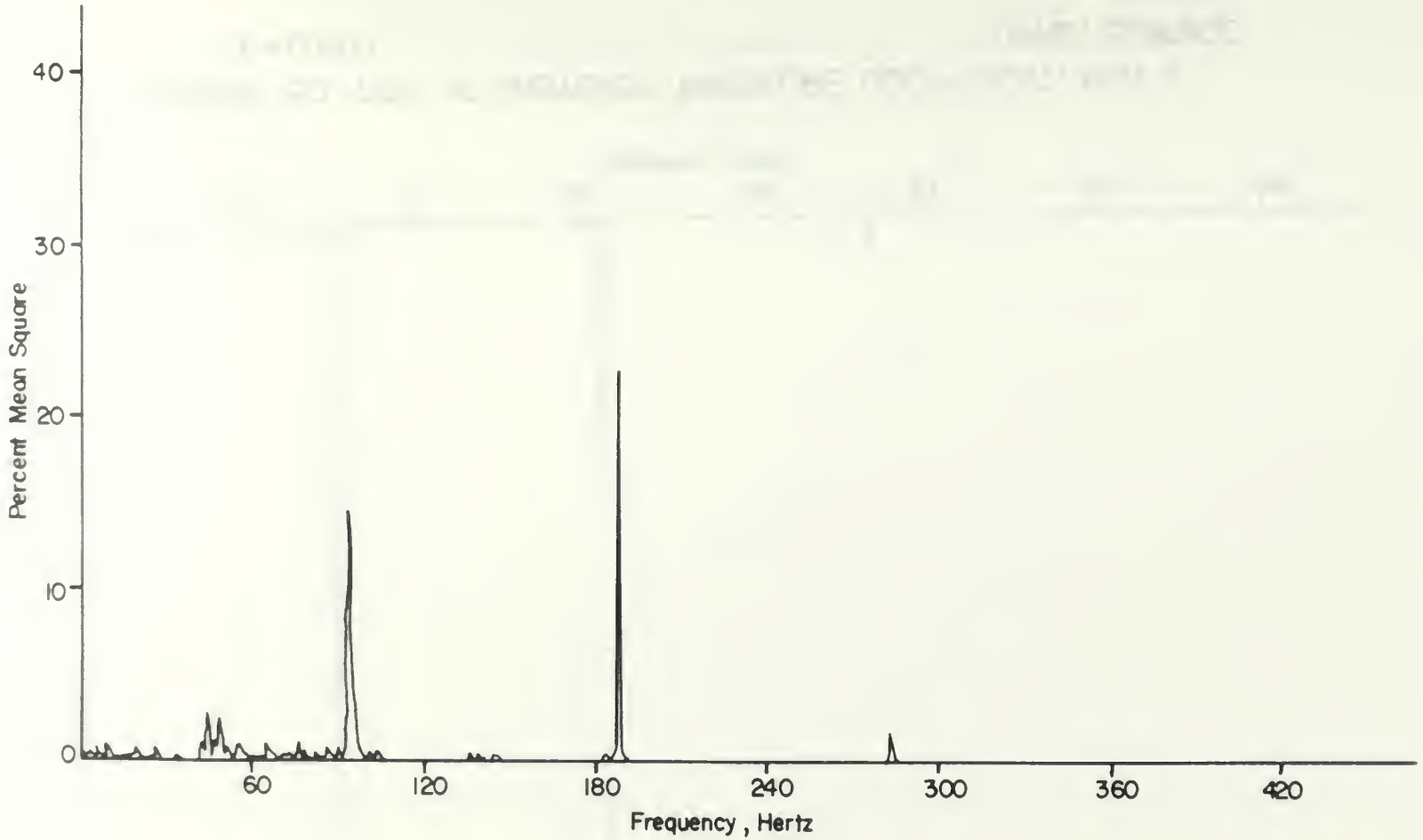

FIGURE 49. PSD OF UNSTEADY PRESSURE COEFFICIENT , RUN 5

$\zeta = 0.500$ UPPER SURFACE

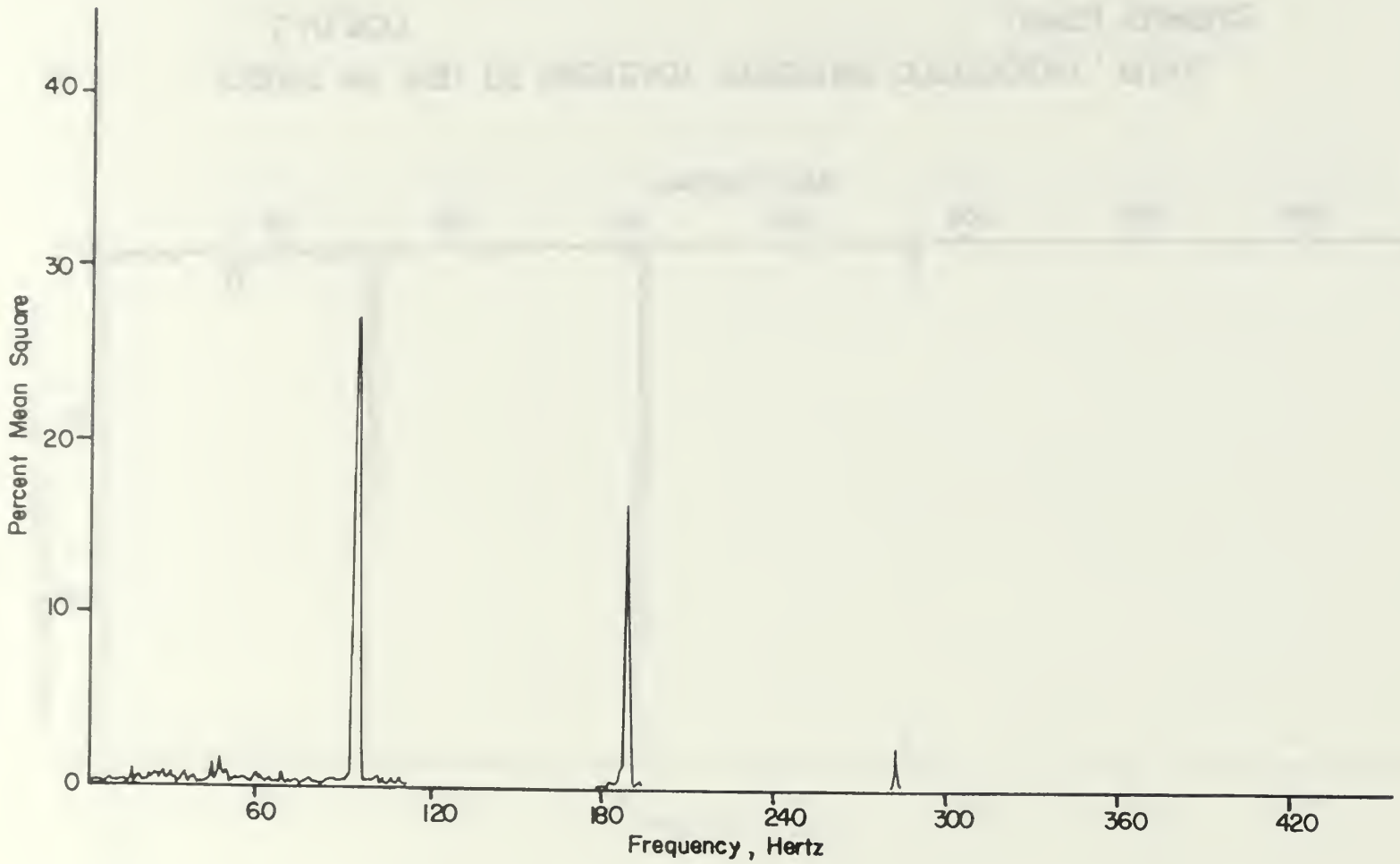

FIGURE 50. PSD OF UNSTEADY PRESSURE COEFFICIENT, RUN 5
ϵ=0.600
UPPER SURFACE

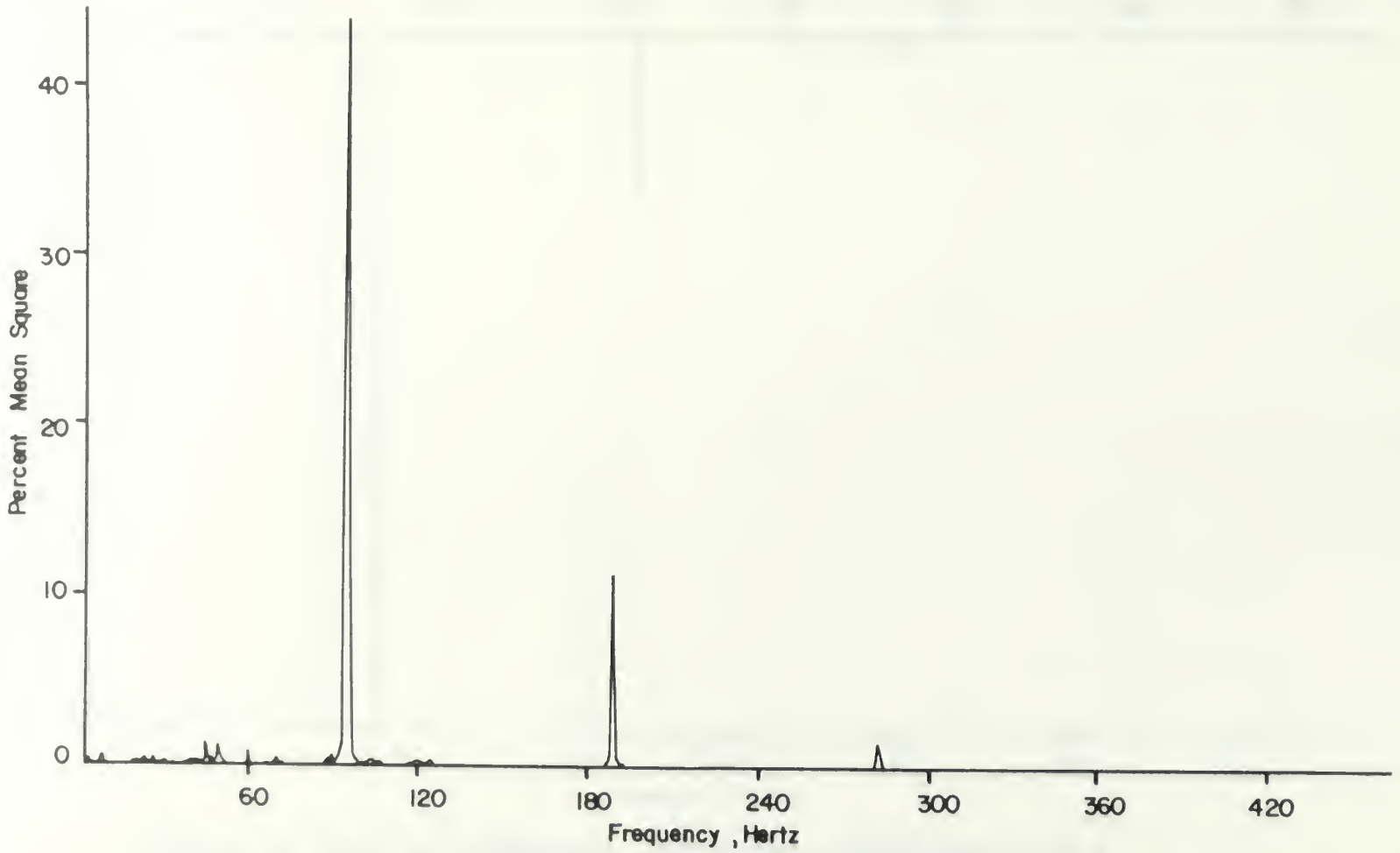

FIGURE 51. PSD OF UNSTEADY PRESSURE COEFFICIENT, RUN 5

$\delta = 0.700$ UPPER SURFACE

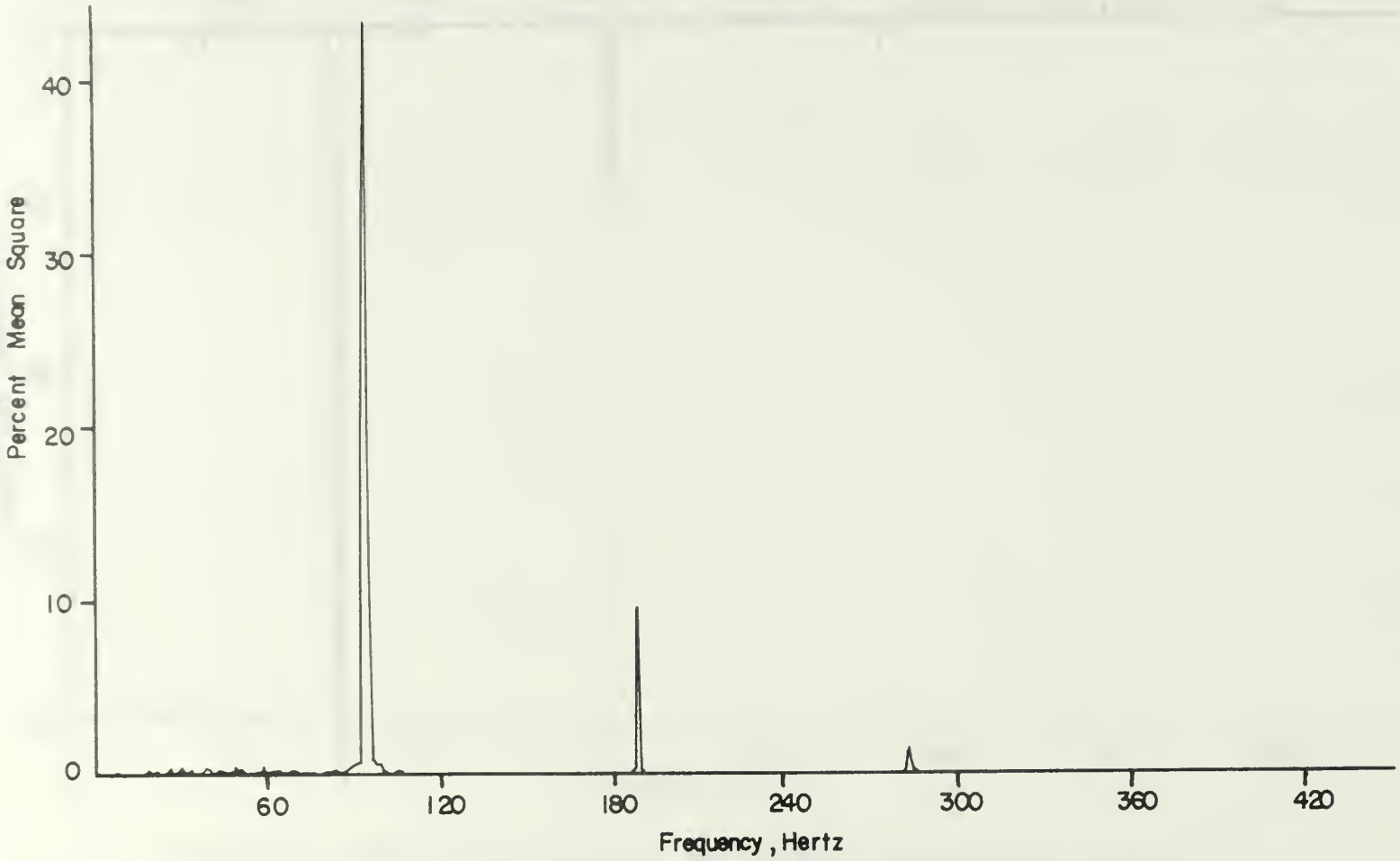

FIGURE 52. PSD OF UNSTEADY PRESSURE COEFFICIENT, RUN 5
ξ=0.750 UPPER SURFACE

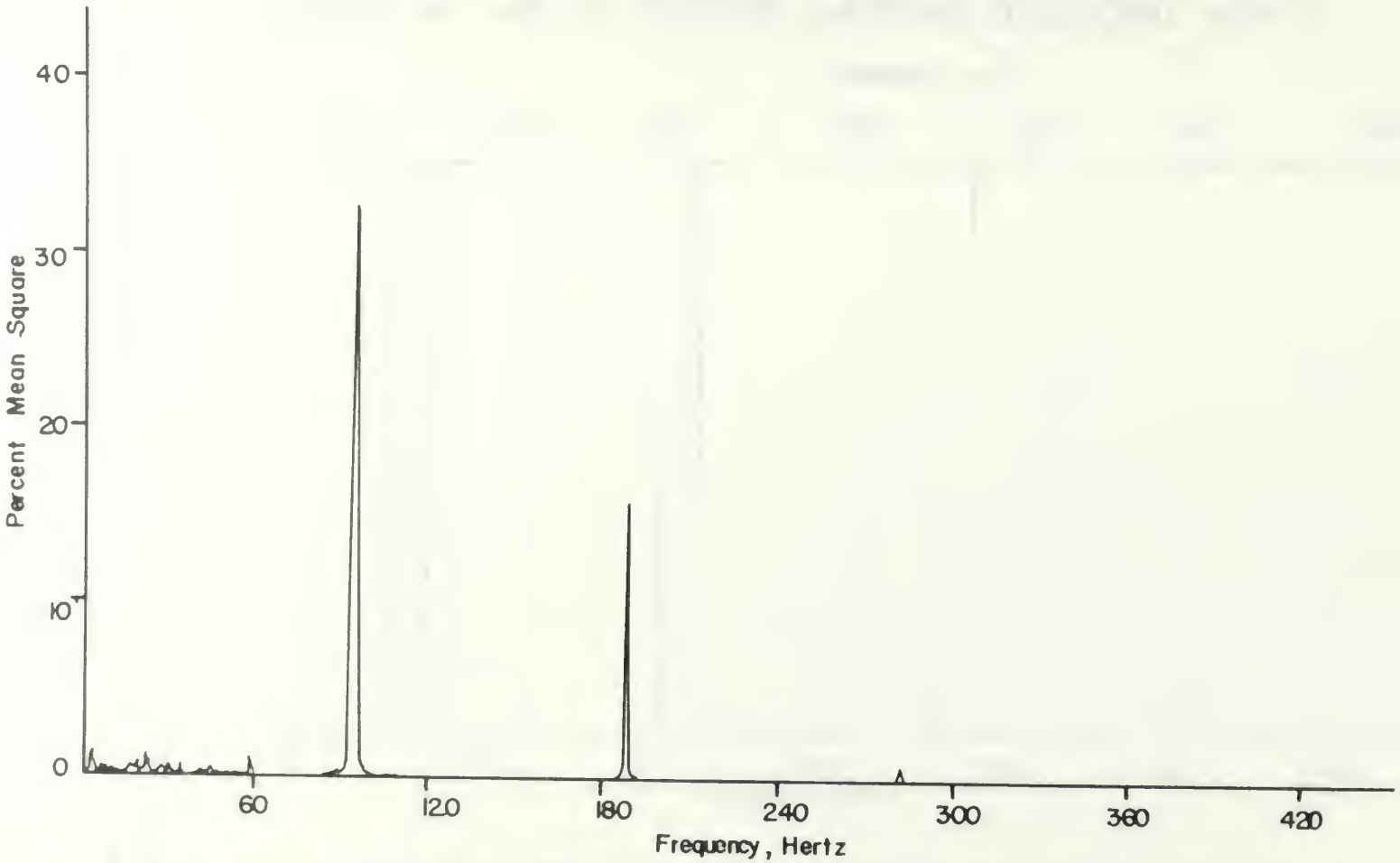

FIGURE 53. PSD OF UNSTEADY PRESSURE COEFFICIENT, RUN 5
$\xi = 0.0$ LOWER SURFACE

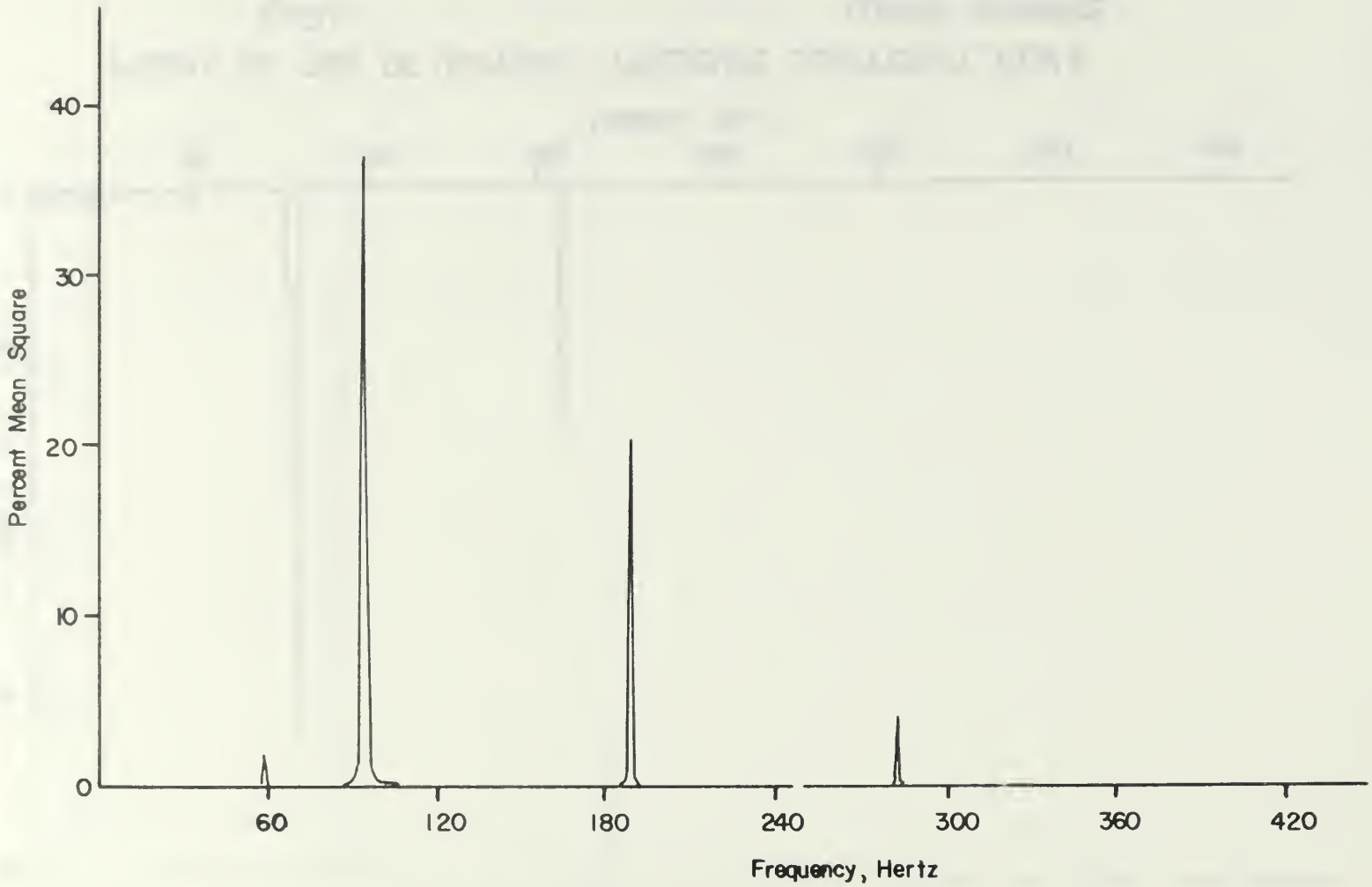

FIGURE 54. PSD OF UNSTEADY PRESSURE COEFFICIENT, RUN 5

ε=0.050 LOWER SURFACE

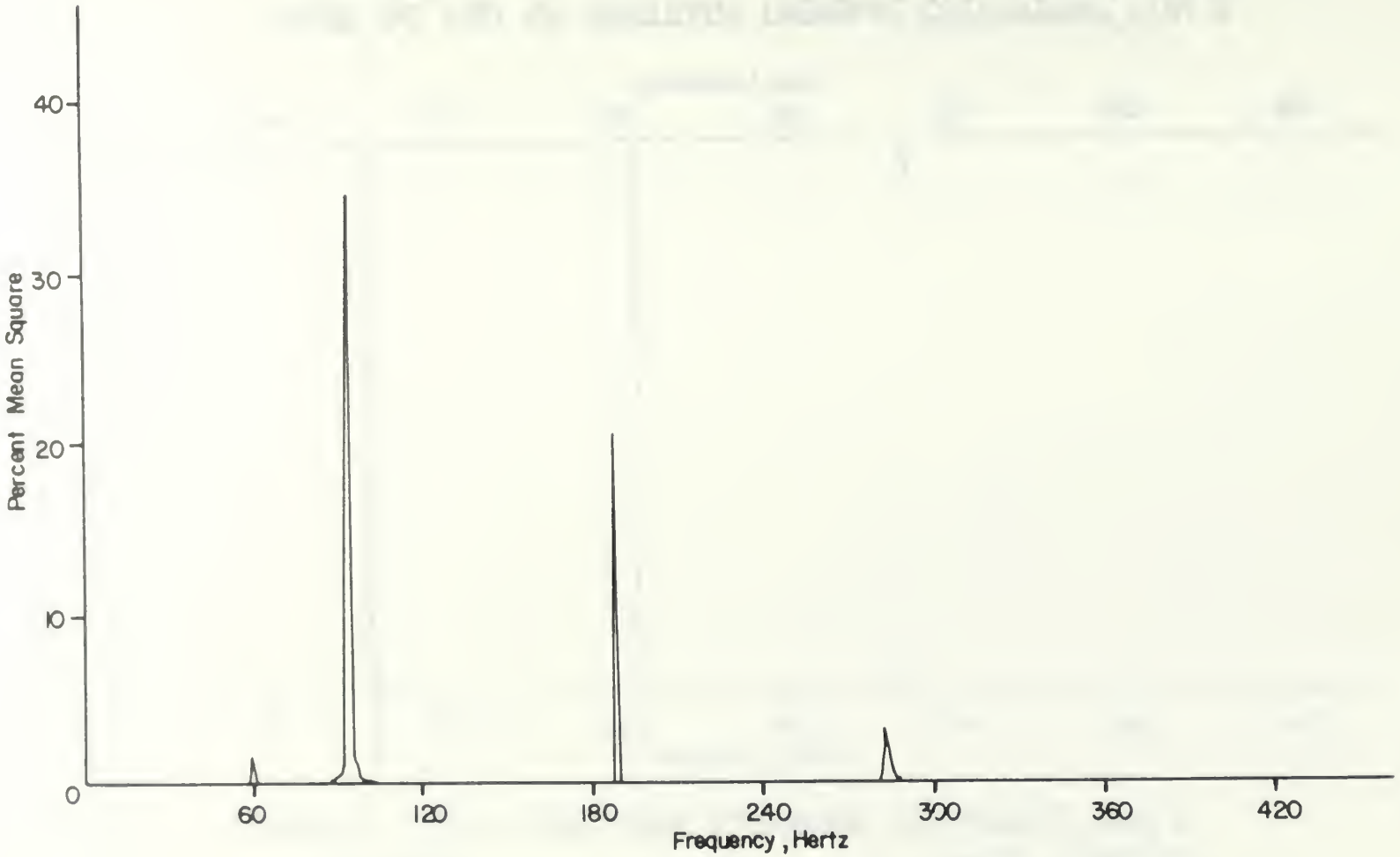

FIGURE 55. PSD OF UNSTEADY PRESSURE COEFFICIENT, RUN 5
$\varepsilon = 0.100$ LOWER SURFACE

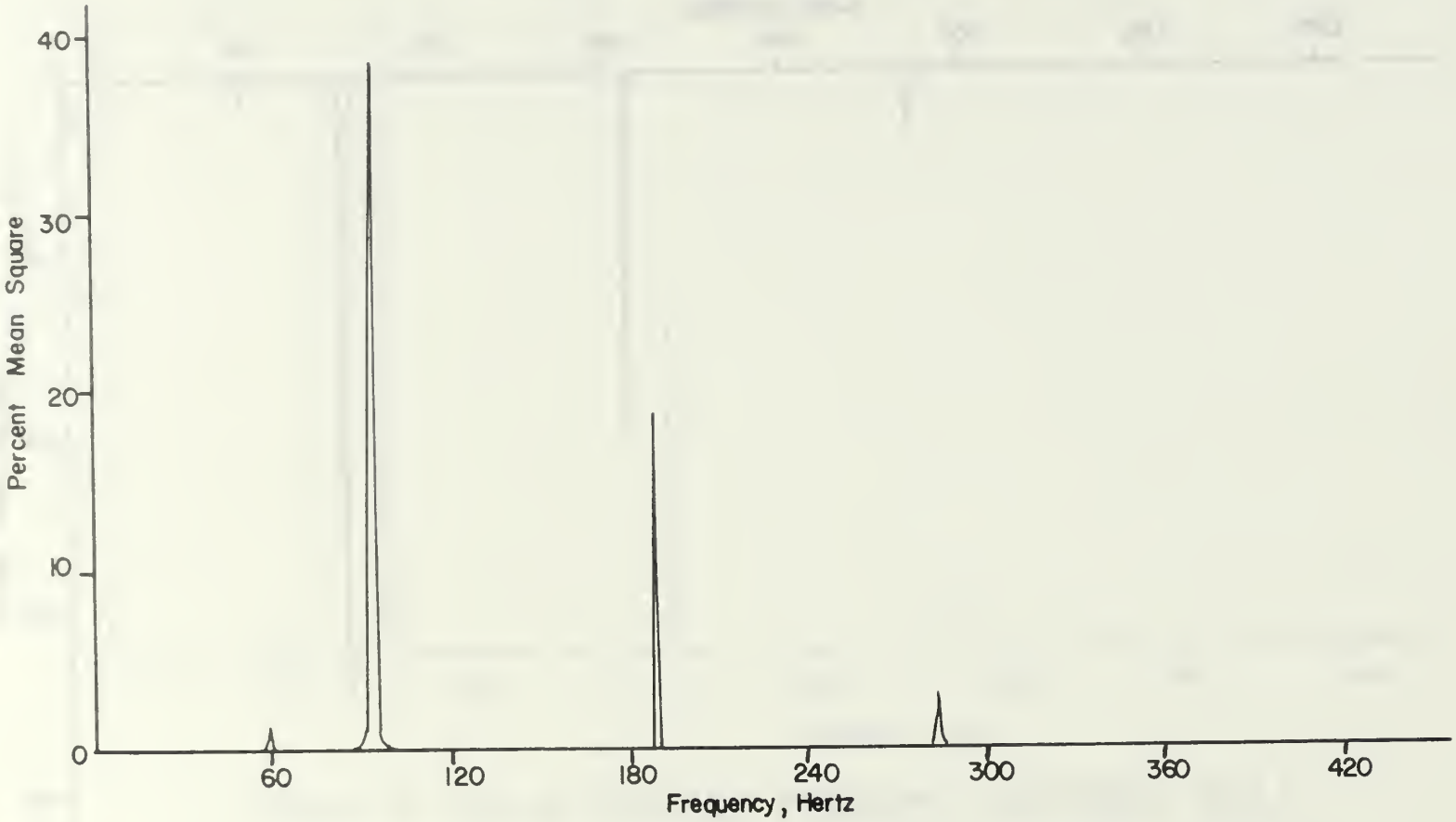

FIGURE 56. PSD OF UNSTEADY PRESSURE COEFFICIENT, RUN 5
$\epsilon = 0.150$ LOWER SURFACE

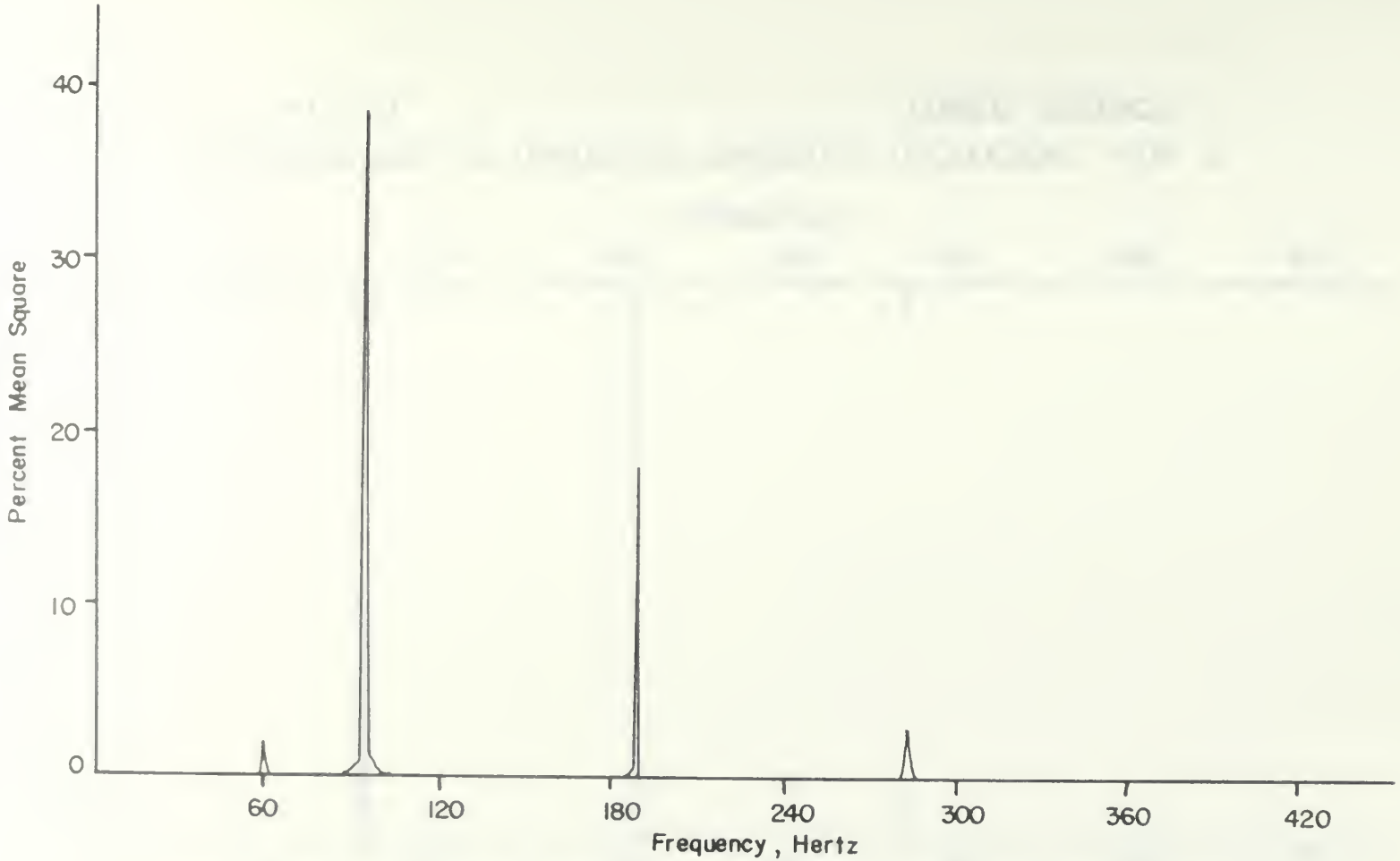

FIGURE 57. PSD OF UNSTEADY PRESSURE COEFFICIENT, RUN 5
ζ=0.200 LOWER SURFACE

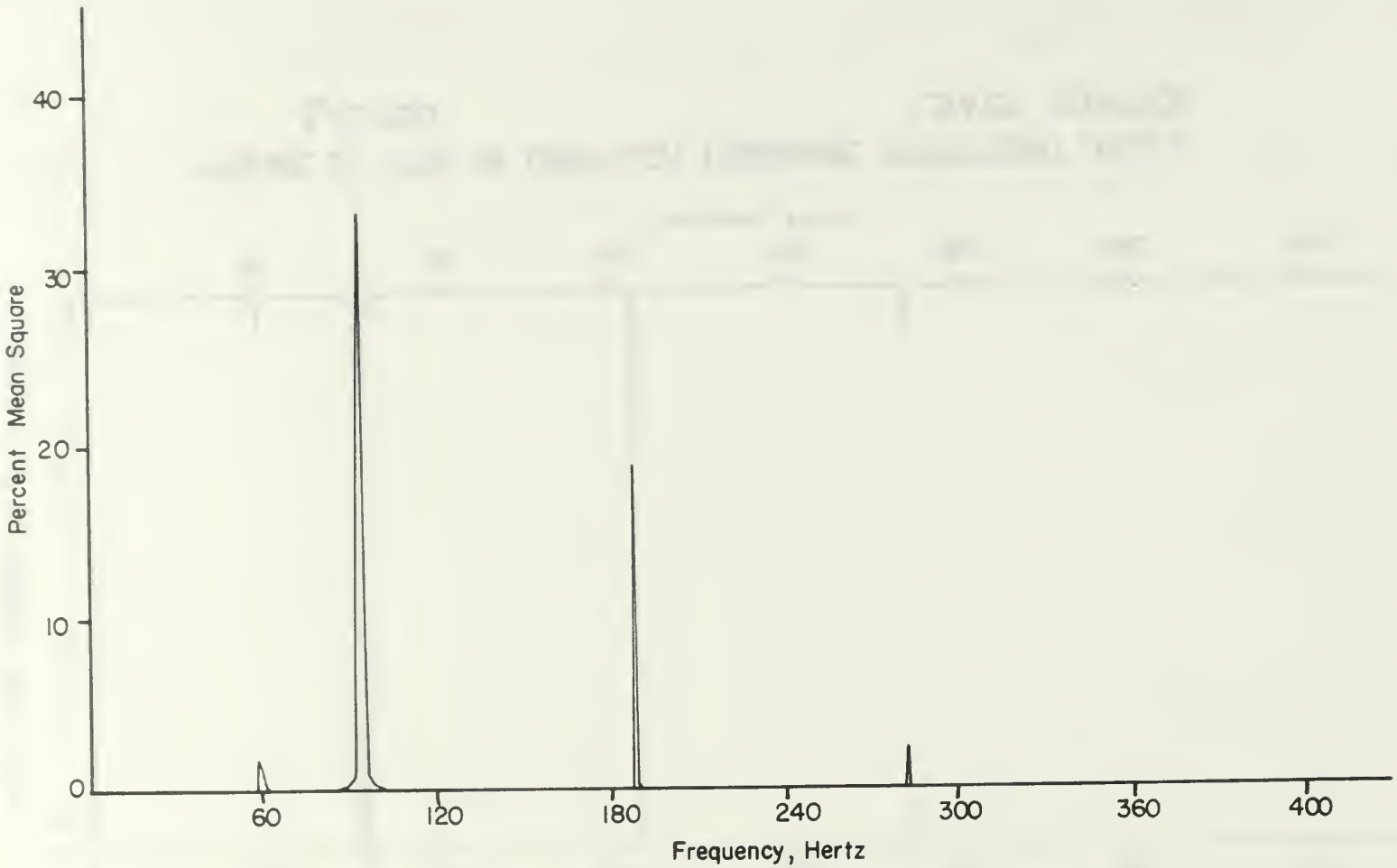

FIGURE 58. PSD OF UNSTEADY PRESSURE COEFFICIENT, RUN 5
$\mathcal{E}$=0.250 LOWER SURFACE

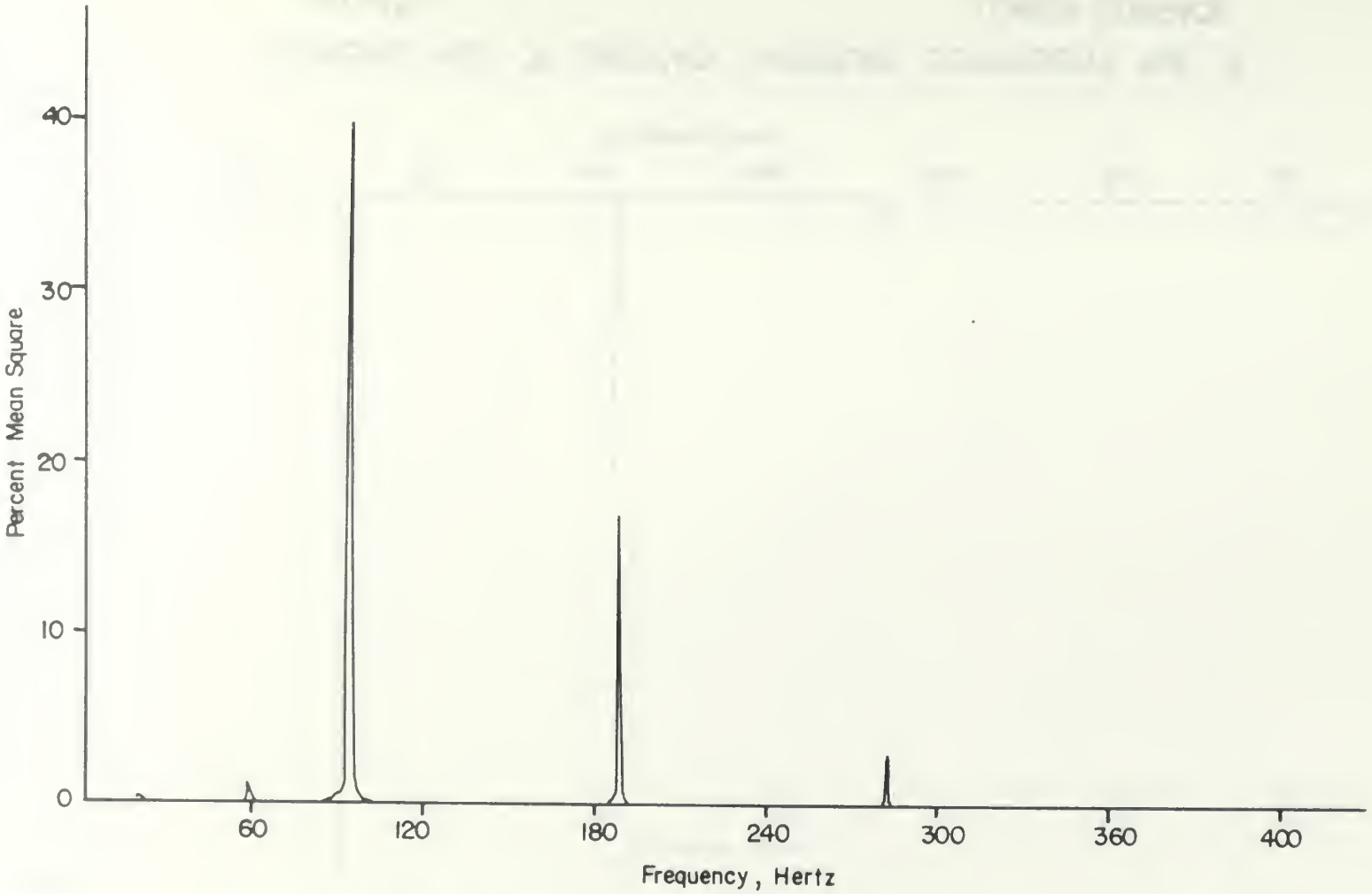

FIGURE 59. PSD OF UNSTEADY PRESSURE COEFFICIENT, RUN 5
$\mathcal{E} = 0.350$ LOWER SURFACE

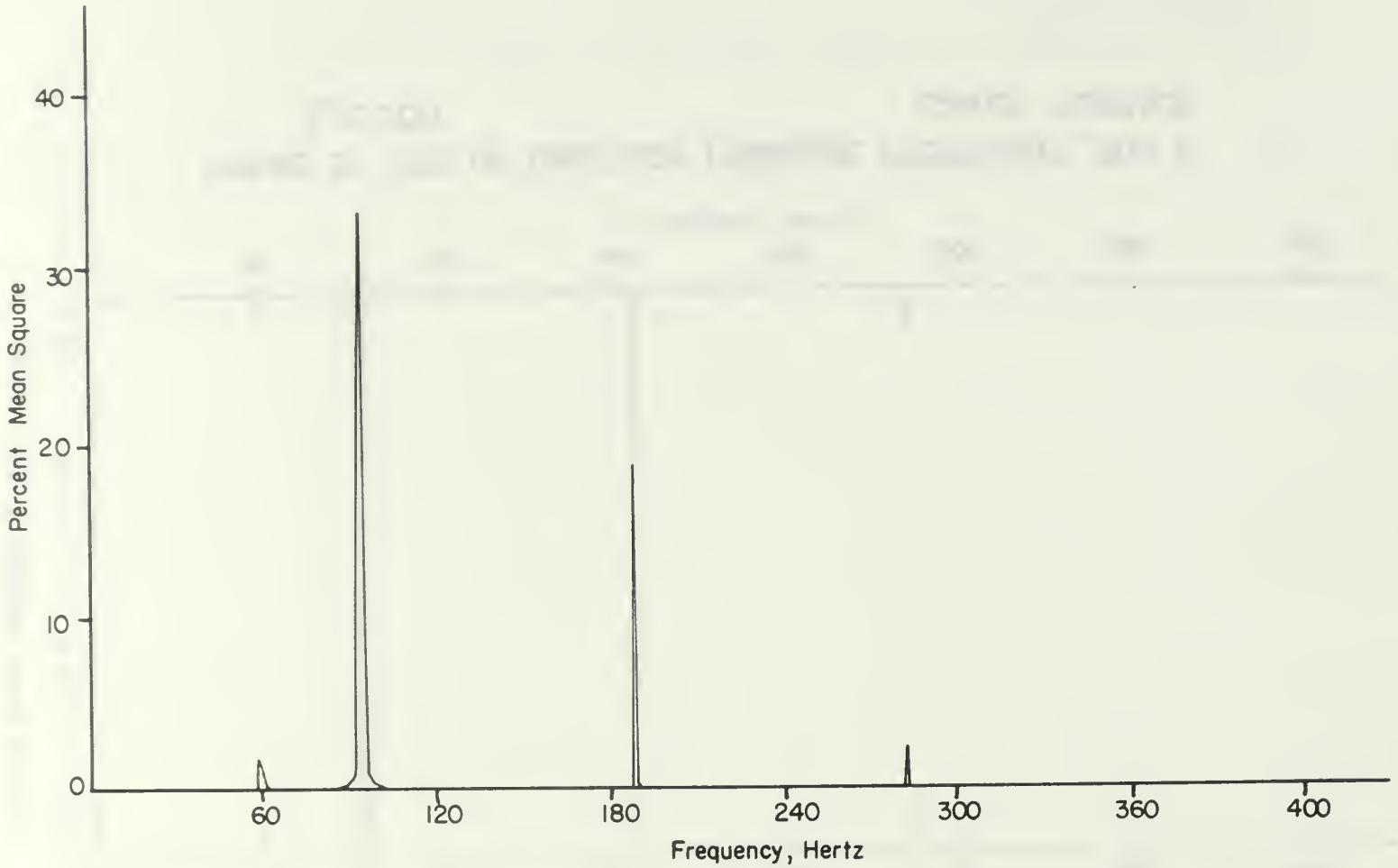

FIGURE 58. PSD OF UNSTEADY PRESSURE COEFFICIENT, RUN 5
$\xi = 0.250$ LOWER SURFACE

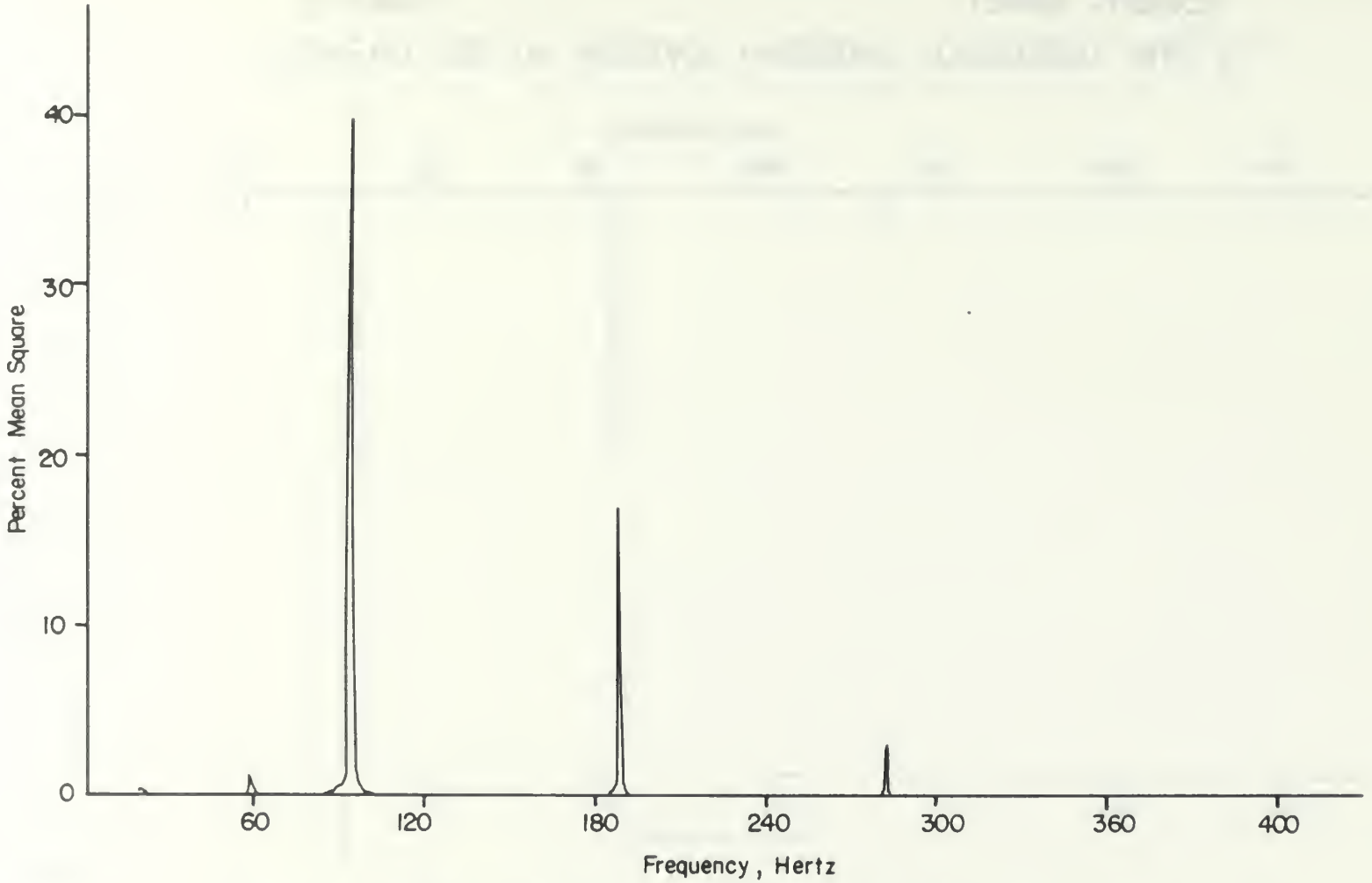

FIGURE 59. PSD OF UNSTEADY PRESSURE COEFFICIENT, RUN 5
$\mathcal{E}$ = 0.350 LOWER SURFACE

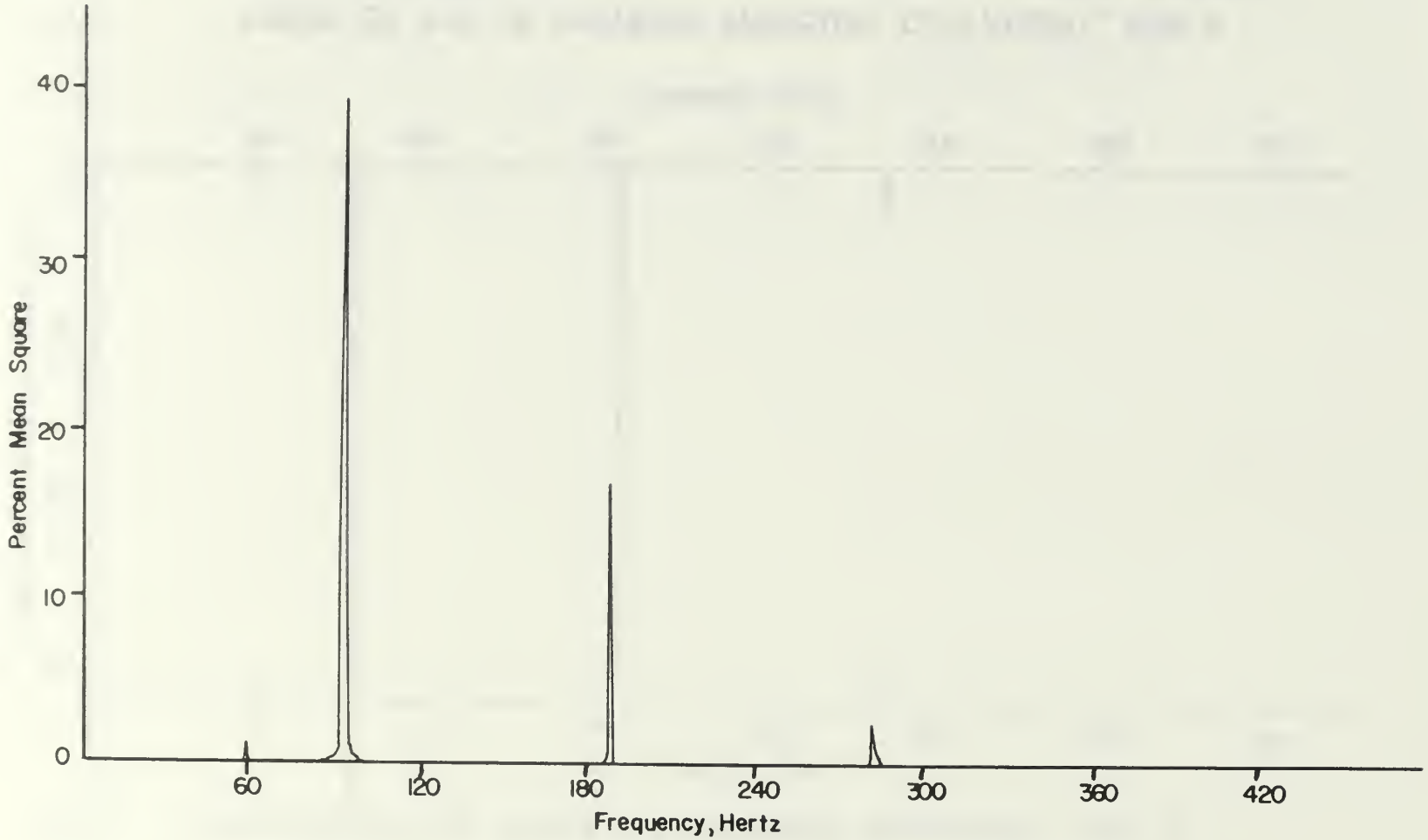

FIGURE 60. PSD OF UNSTEADY PRESSURE COEFFICIENT, RUN 5

$\mathcal{E}$=0.450 LOWER SURFACE

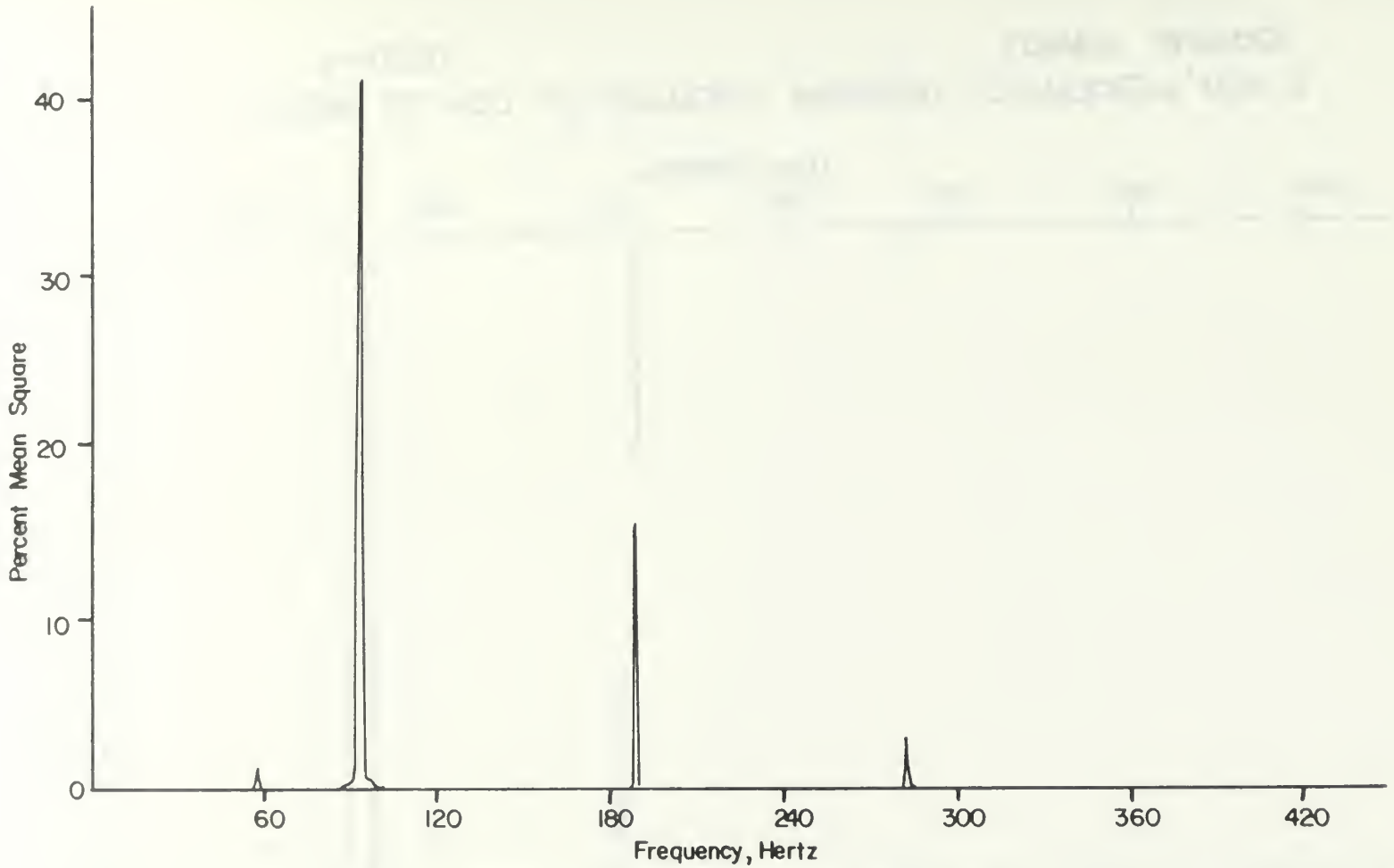

FIGURE 61. PSD OF UNSTEADY PRESSURE COEFFICIENT, RUN 5

$\mathcal{E}$ = 0.600 LOWER SURFACE

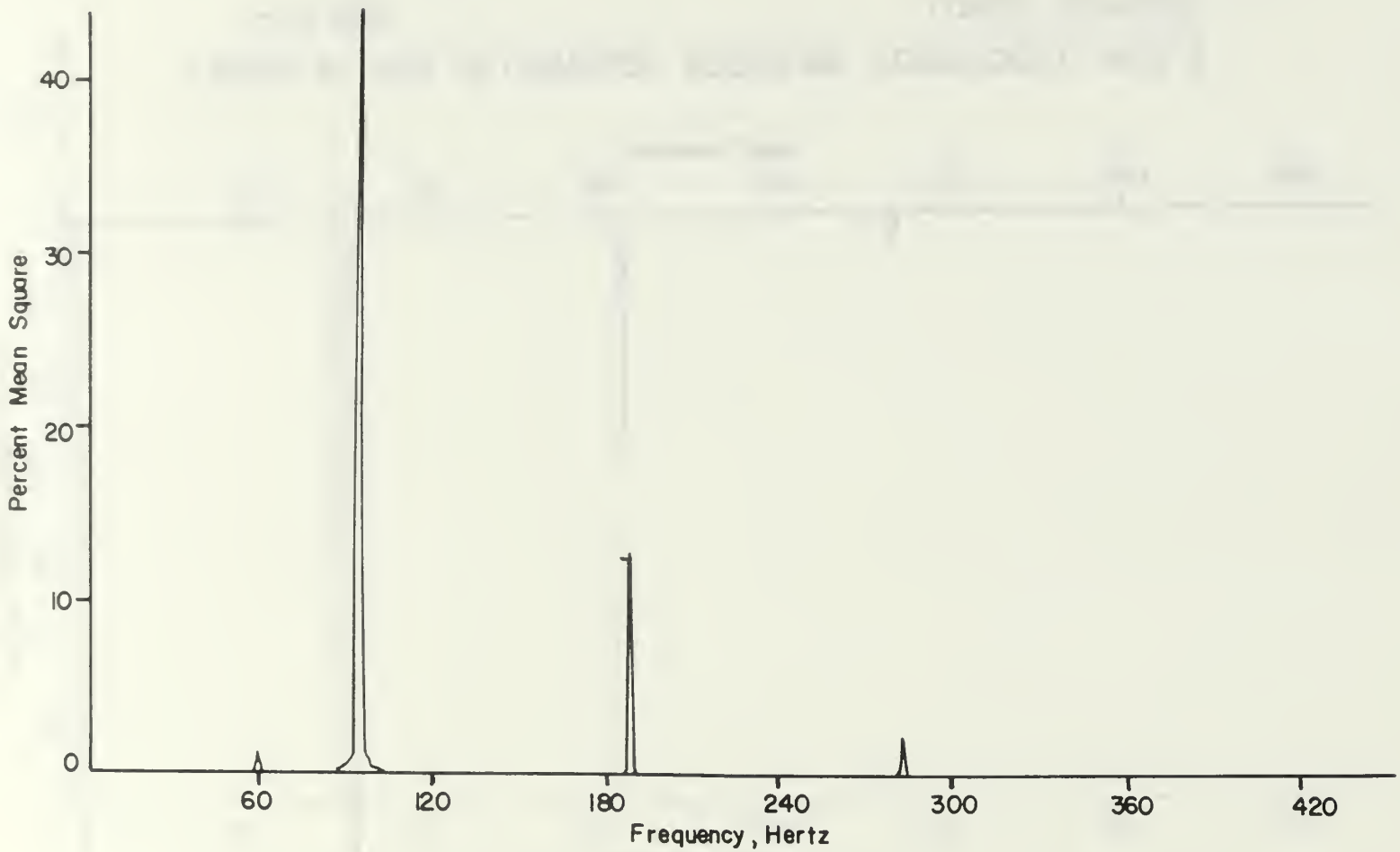

FIGURE 62. PSD OF UNSTEADY PRESSURE COEFFICIENT, RUN 5
ξ=0.750 LOWER SURFACE

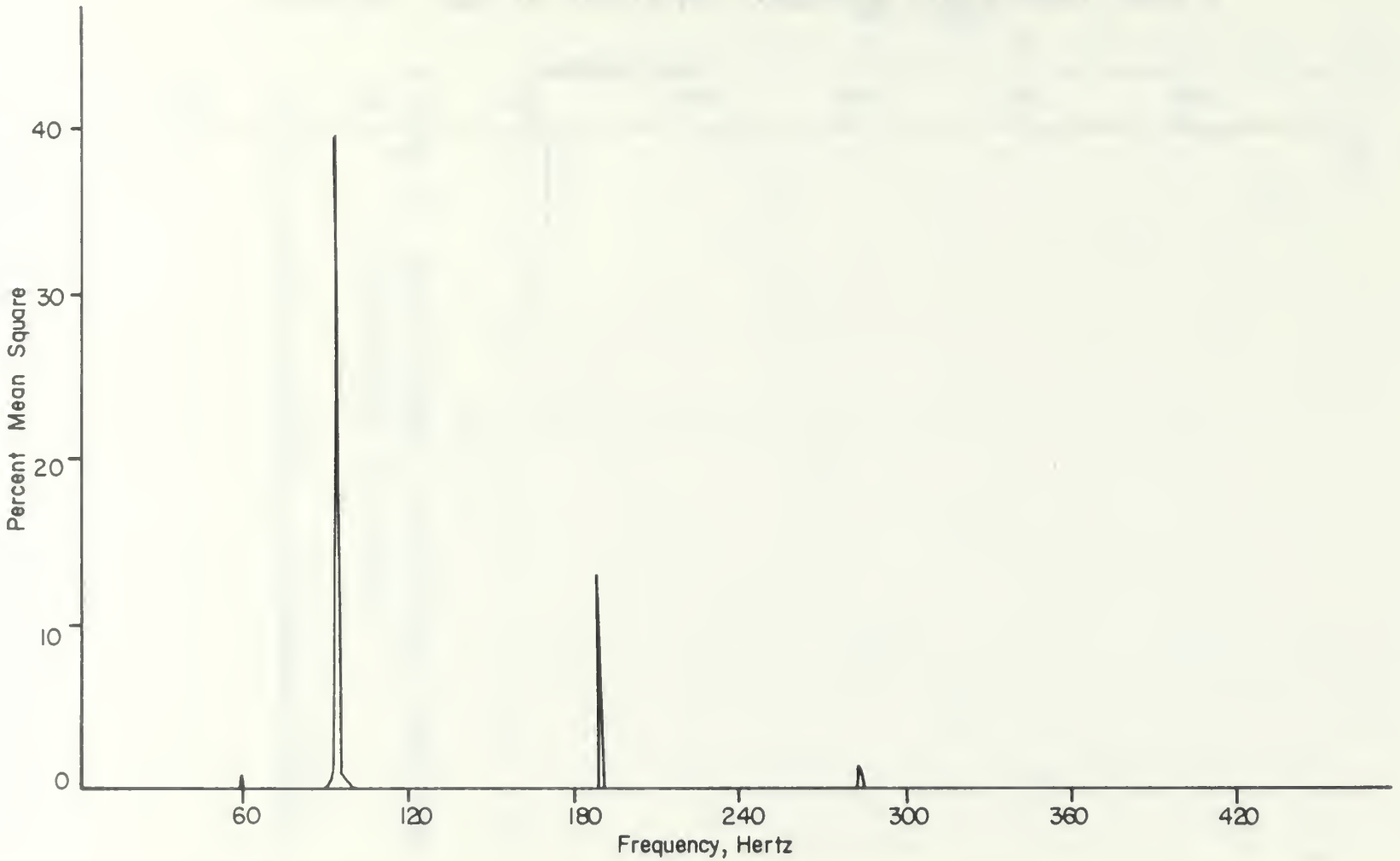

FIGURE 63. PSD OF UNSTEADY PRESSURE COEFFICIENT, RUN 5

$\bar{\epsilon}$=0.850 LOWER SURFACE

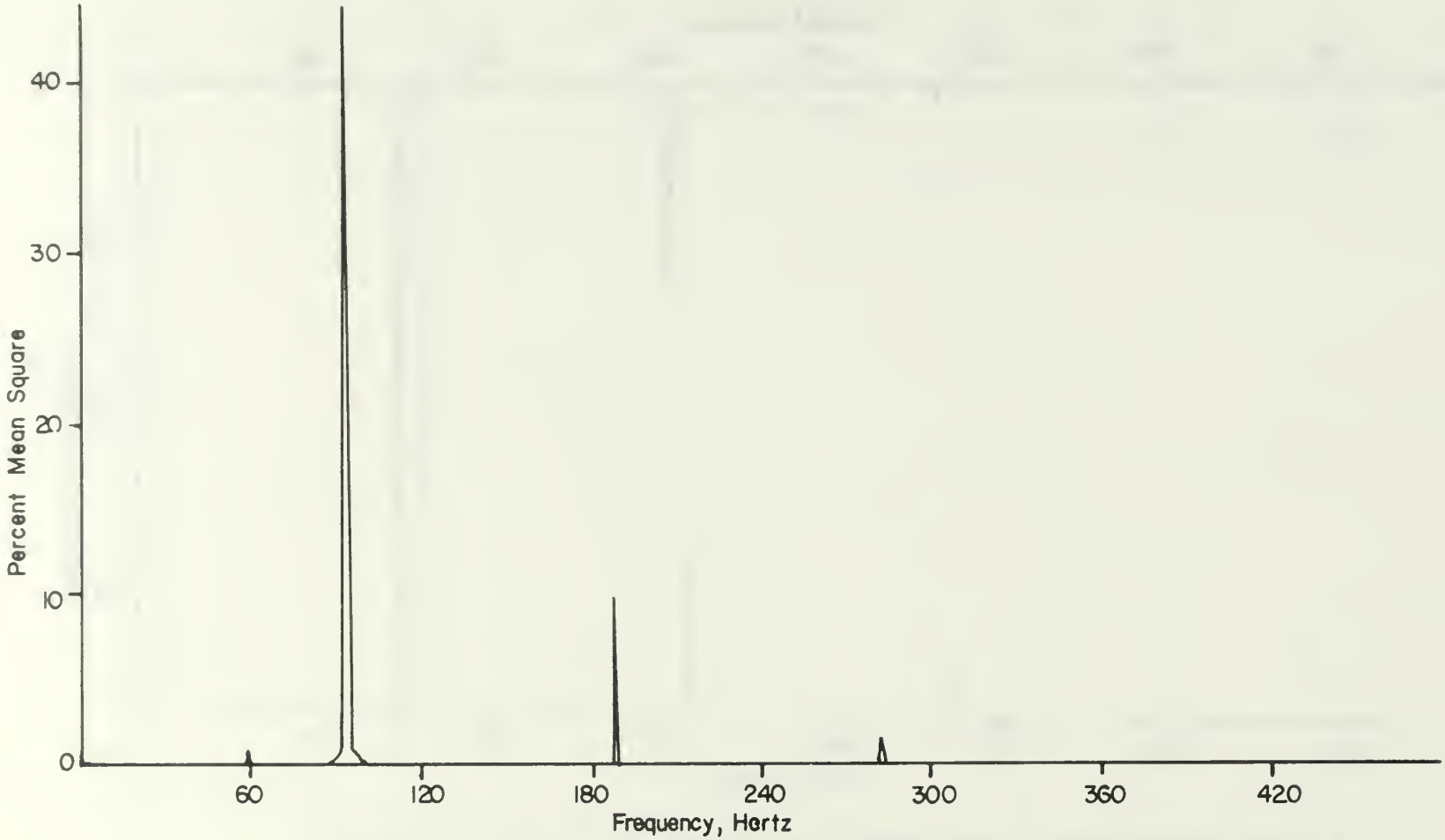

FIGURE 64. PSD OF UNSTEADY PRESSURE COEFFICIENT, RUN 5

ξ=0.950 LOWER SURFACE

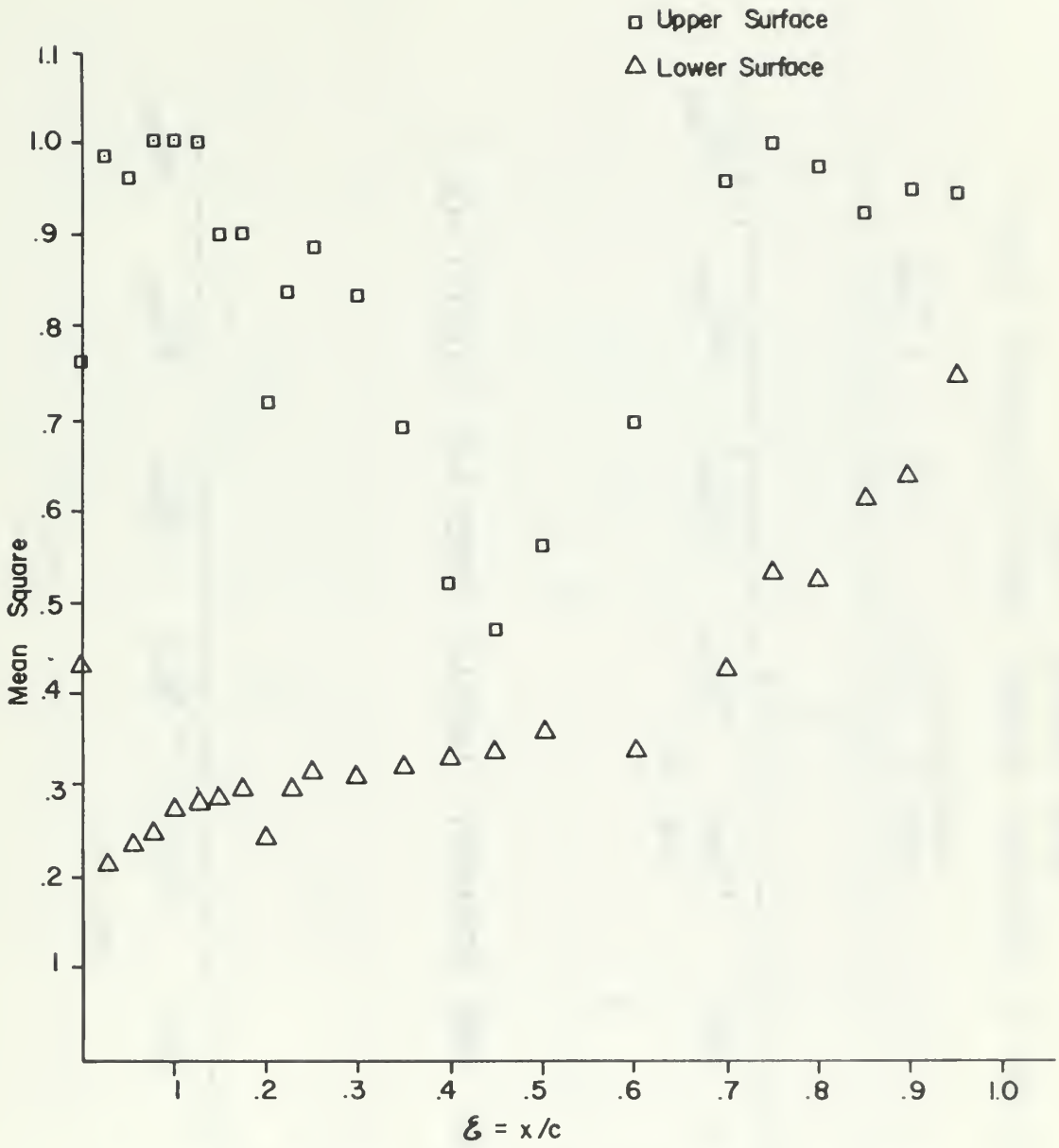

FIGURE 65. MEAN SQUARE OF UNSTEADY PRESSURE COEFFICIENTS ON AIRFOIL

RUN 5 $\alpha = 15$ $f_0 = 94$ Hz $\overline{U} = 102.66$ $\varepsilon = 0.0854$

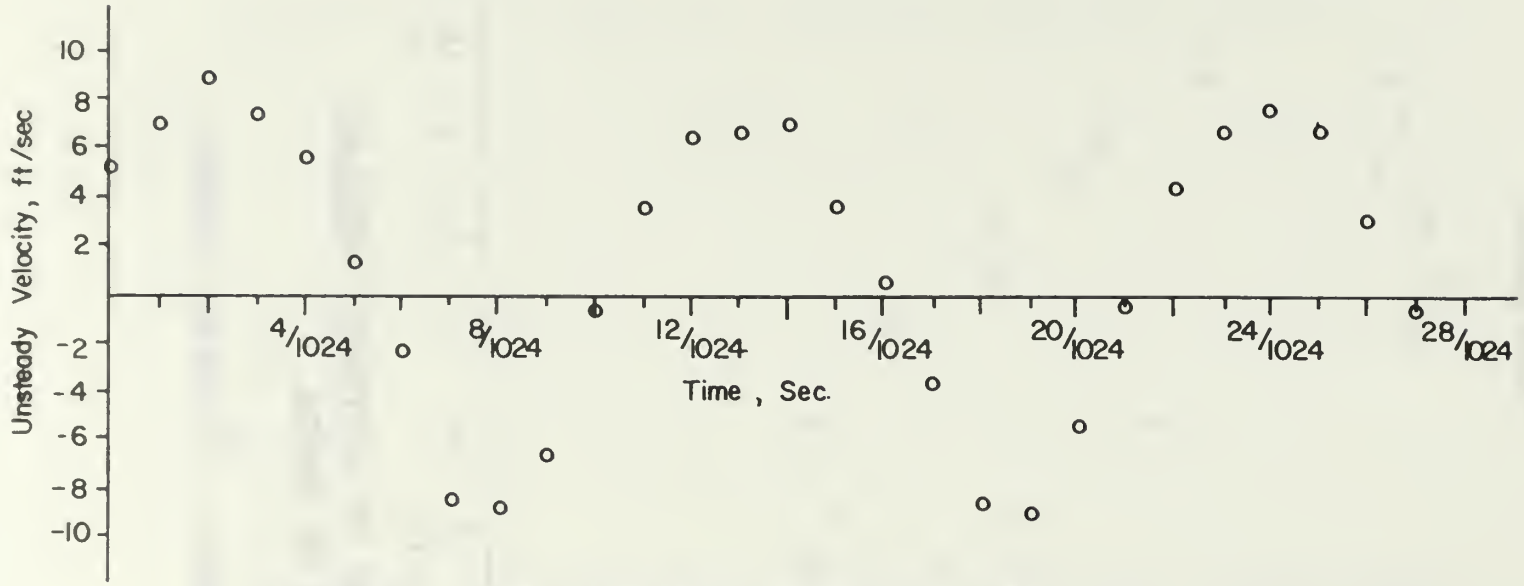

FIGURE 66. TIME DEPENDENT NORMAL FORCE AND VELOCITY, RUN 5

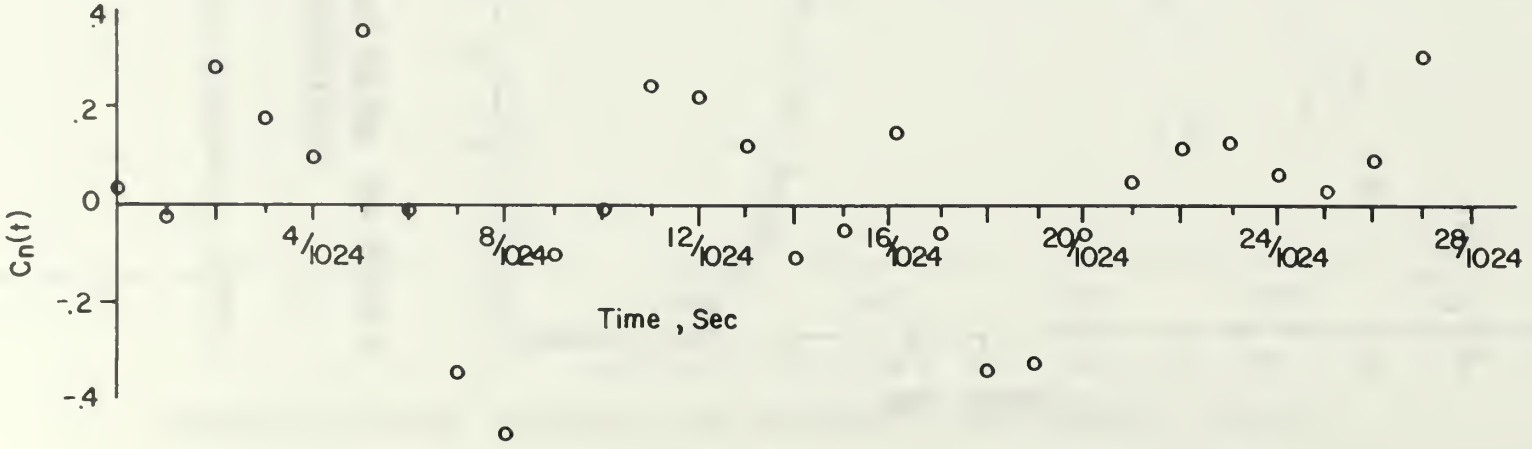

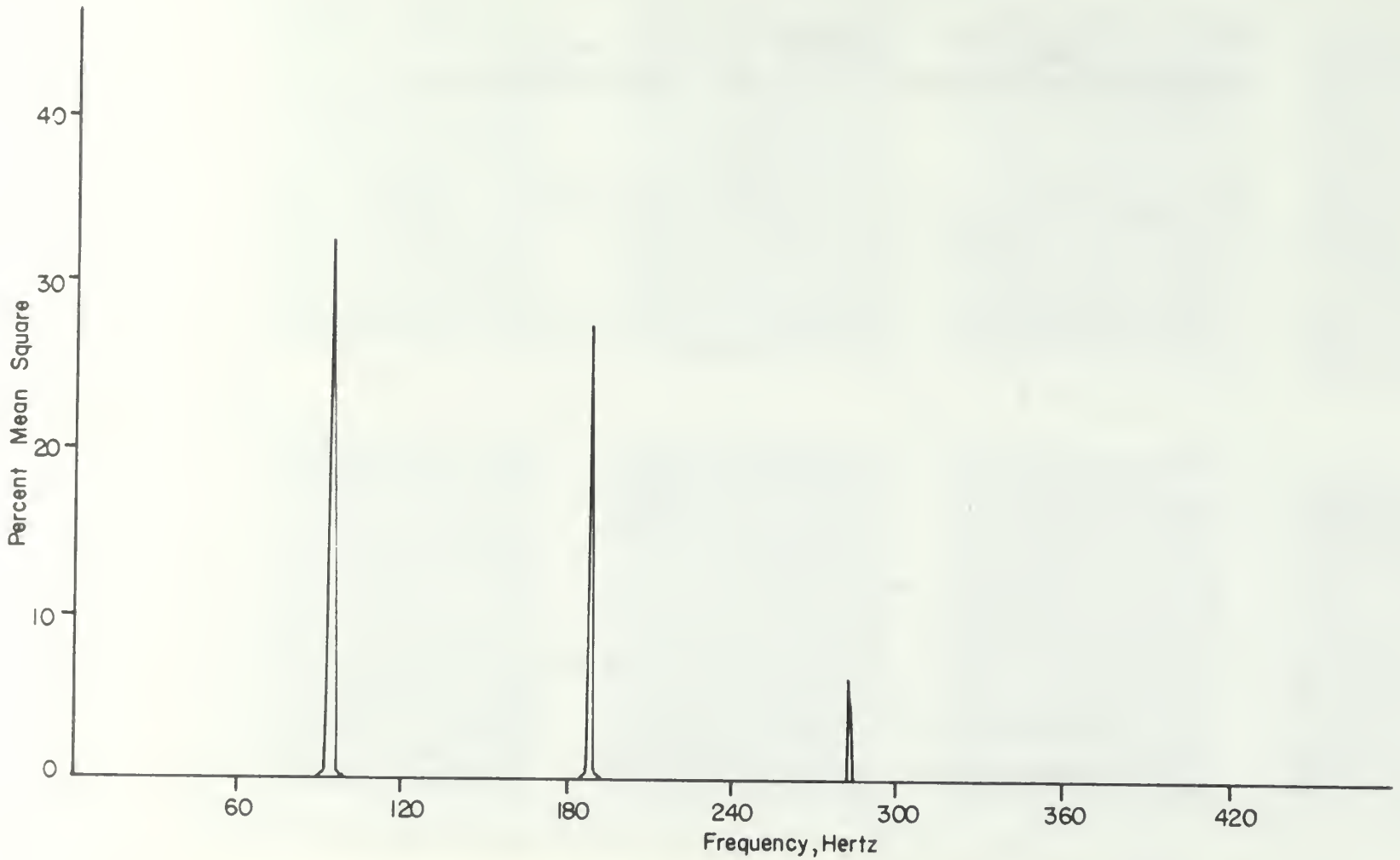

FIGURE 67. PSD OF UNSTEADY NORMAL FORCE COEFFICIENT, RUN 5
MEAN SQUARE =0.100

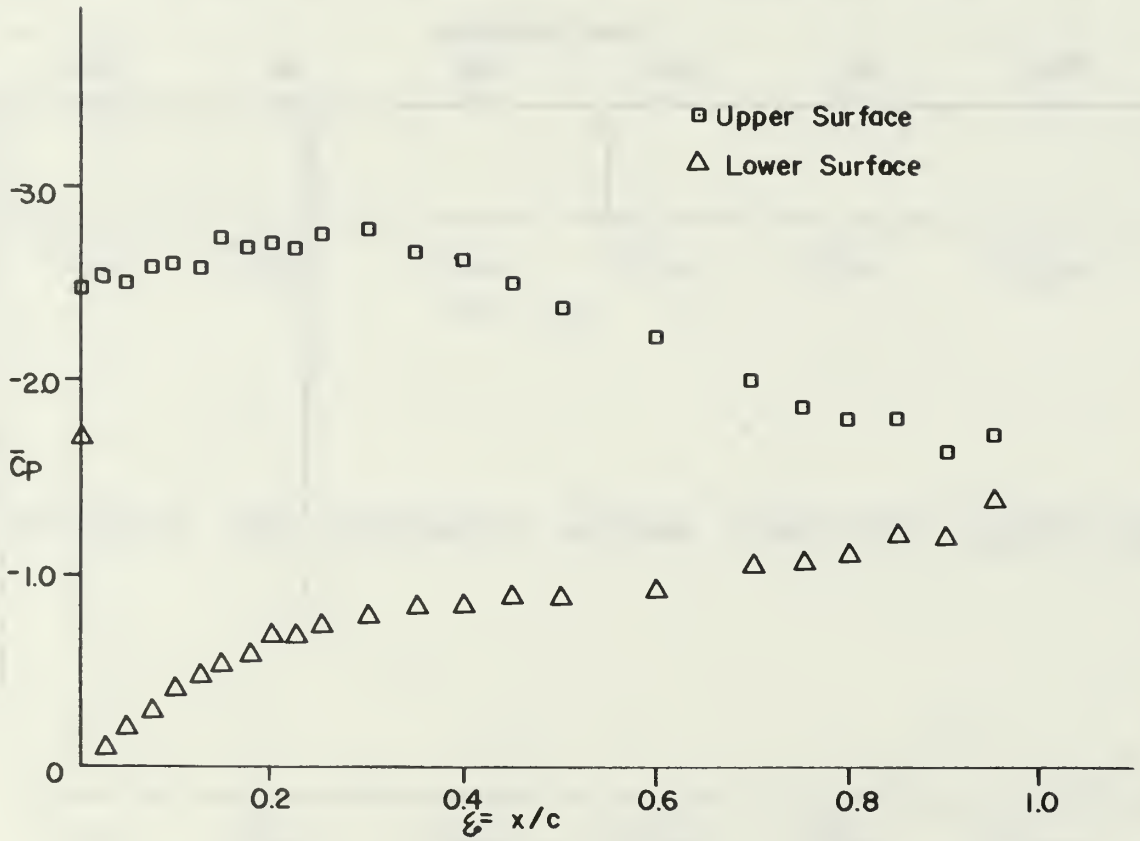

FIGURE 68. MEAN PRESSURE DISTRIBUTION ON AIRFOIL
$\alpha = 15°$ $f_0 = 94$ Hz $\varepsilon = 0.085$

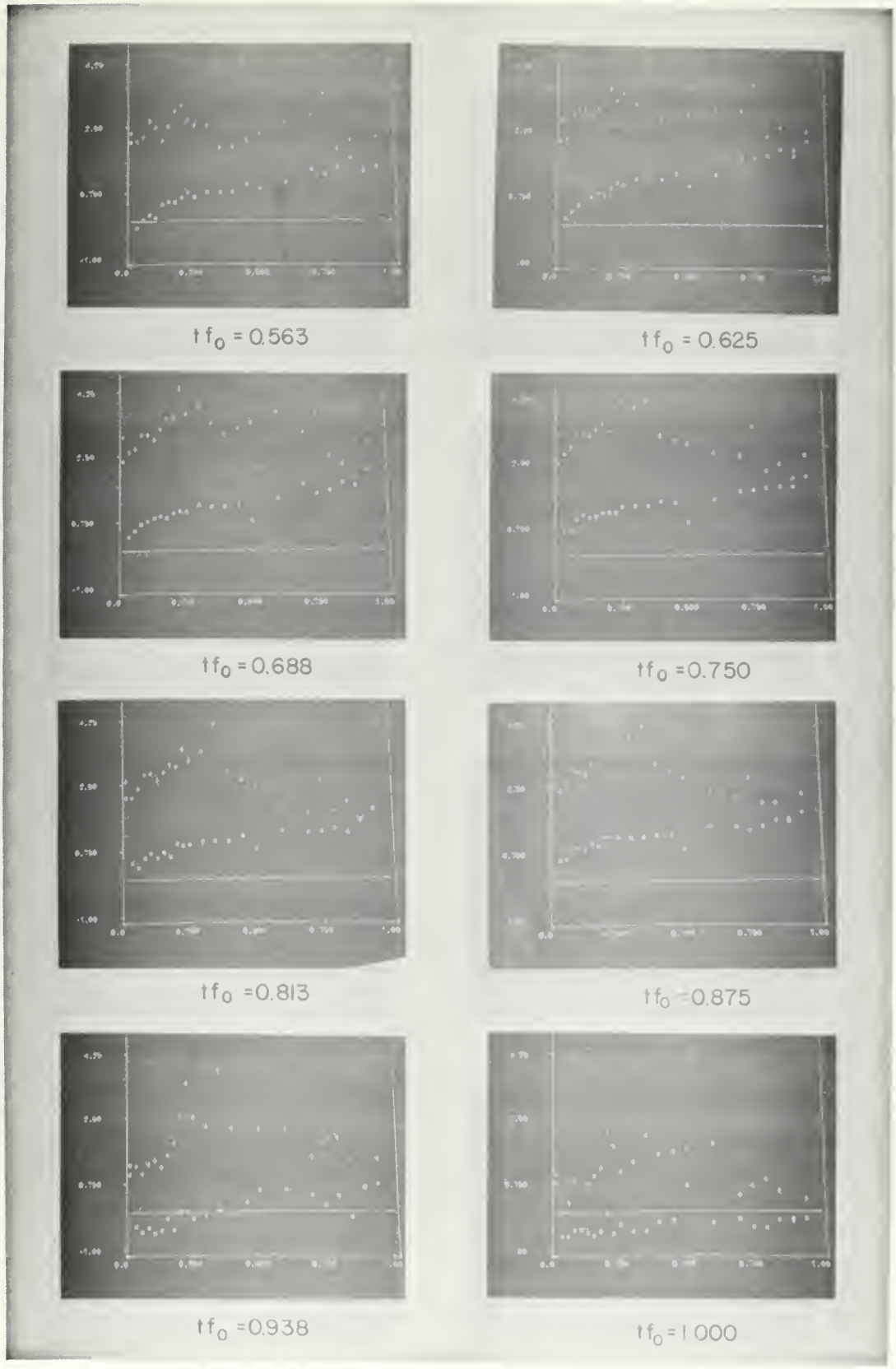

Figure 69. Time Dependent Pressure, Run 5

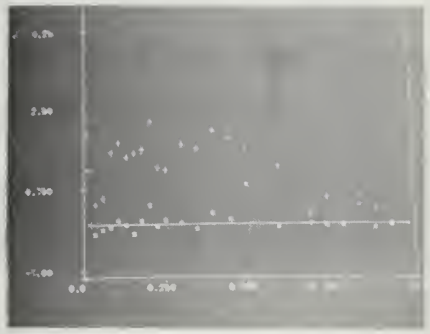

$tf_0 = 0.0625$

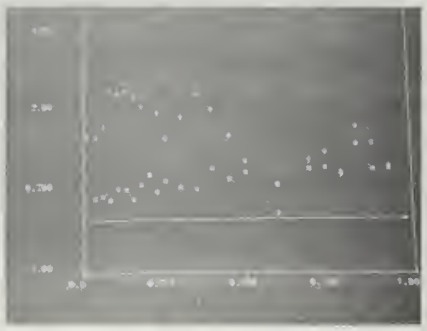

$tf_0 = 0.125$

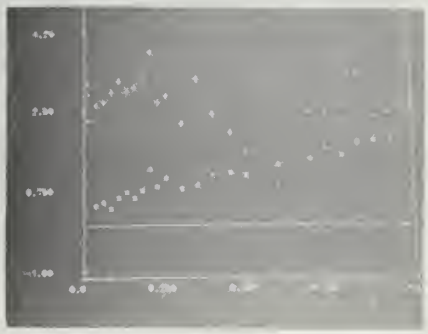

$tf_0 = 0.188$

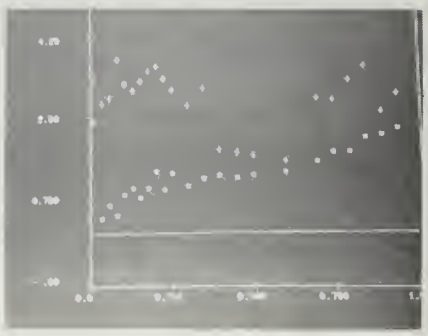

$tf_0 = 0.250$

$tf_0 = 0.313$

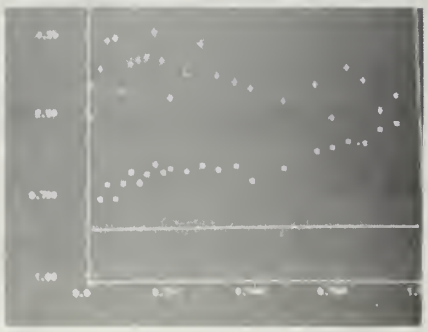

$tf_0 = 0.375$

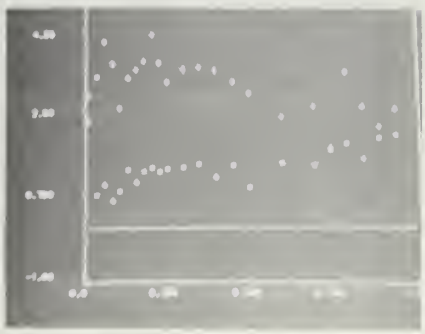

$tf_0 = 0.438$

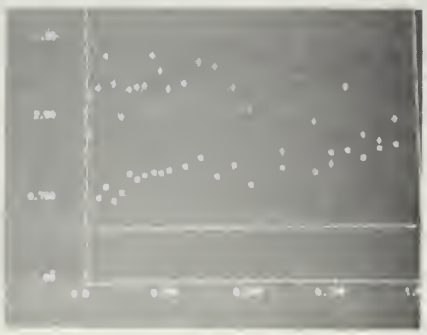

$tf_0 = 0.500$

Figure 70. Time Dependent Pressure Distribution, Run 5

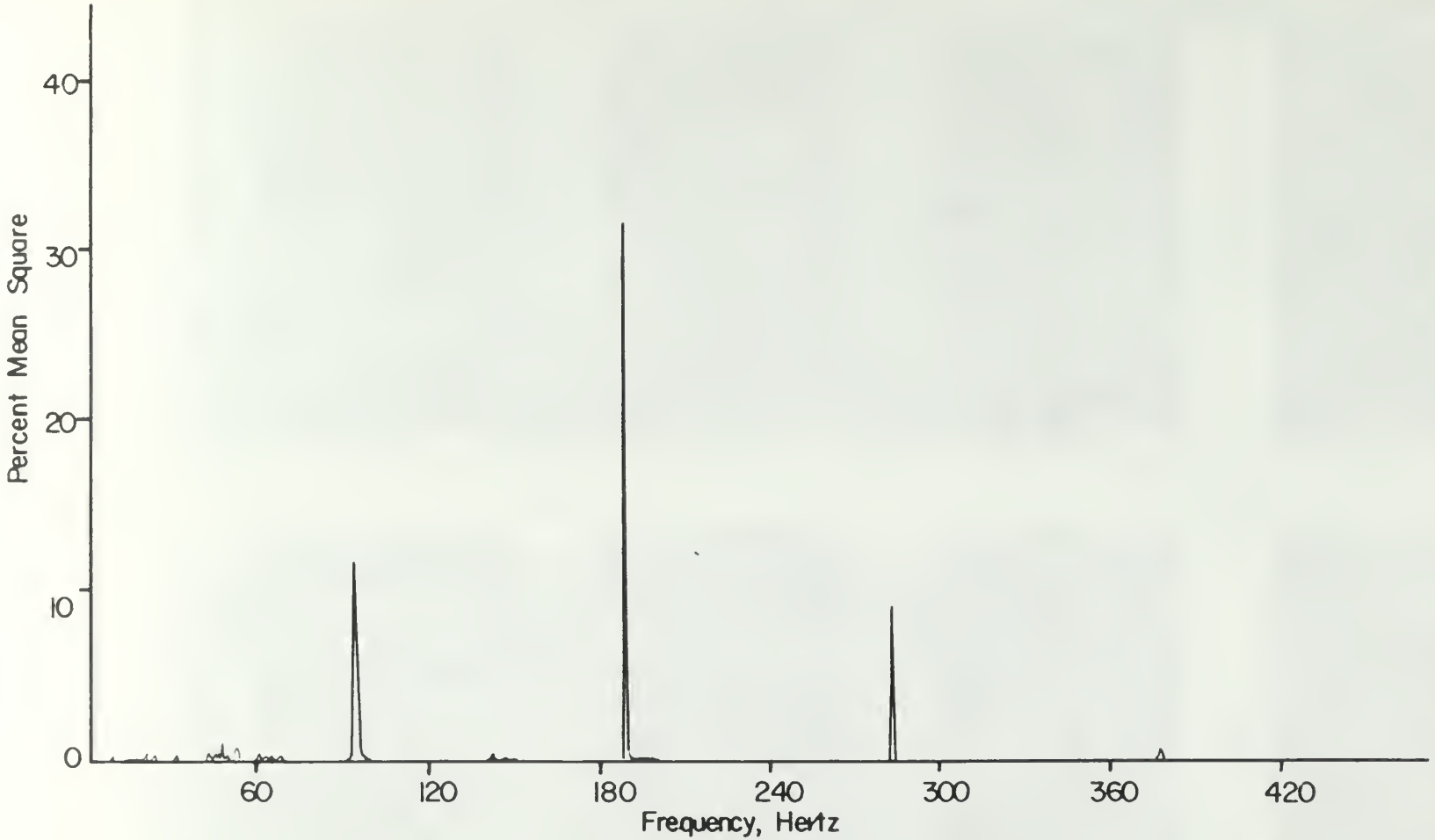

FIGURE 71. PSD OF UNSTEADY PRESSURE AT THE CENTER OF PRESSURE, RUN 5, MEAN SQUARE = 0.003

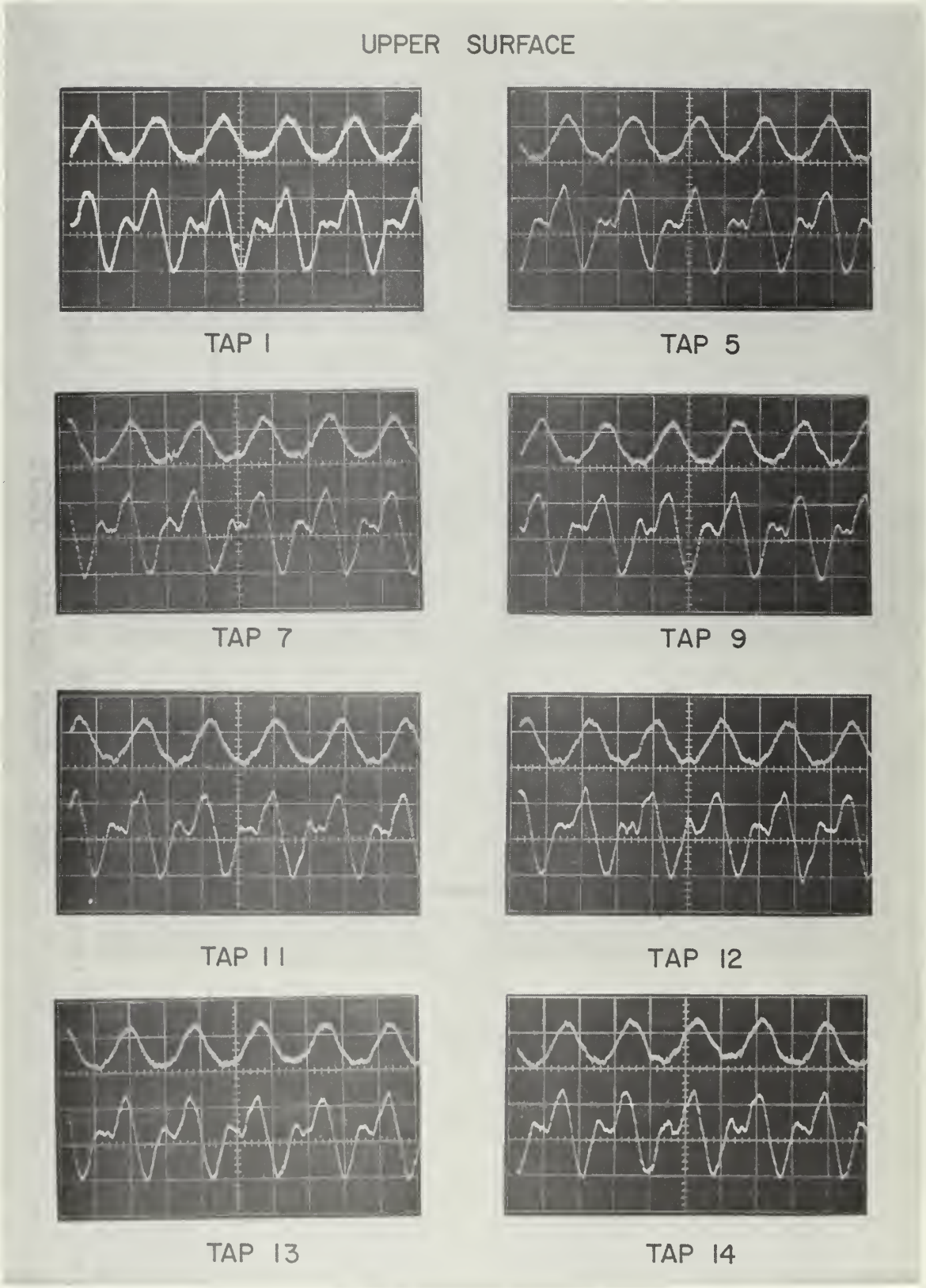

Figure 72. Pictures, Run 7, Pressure, Velocity

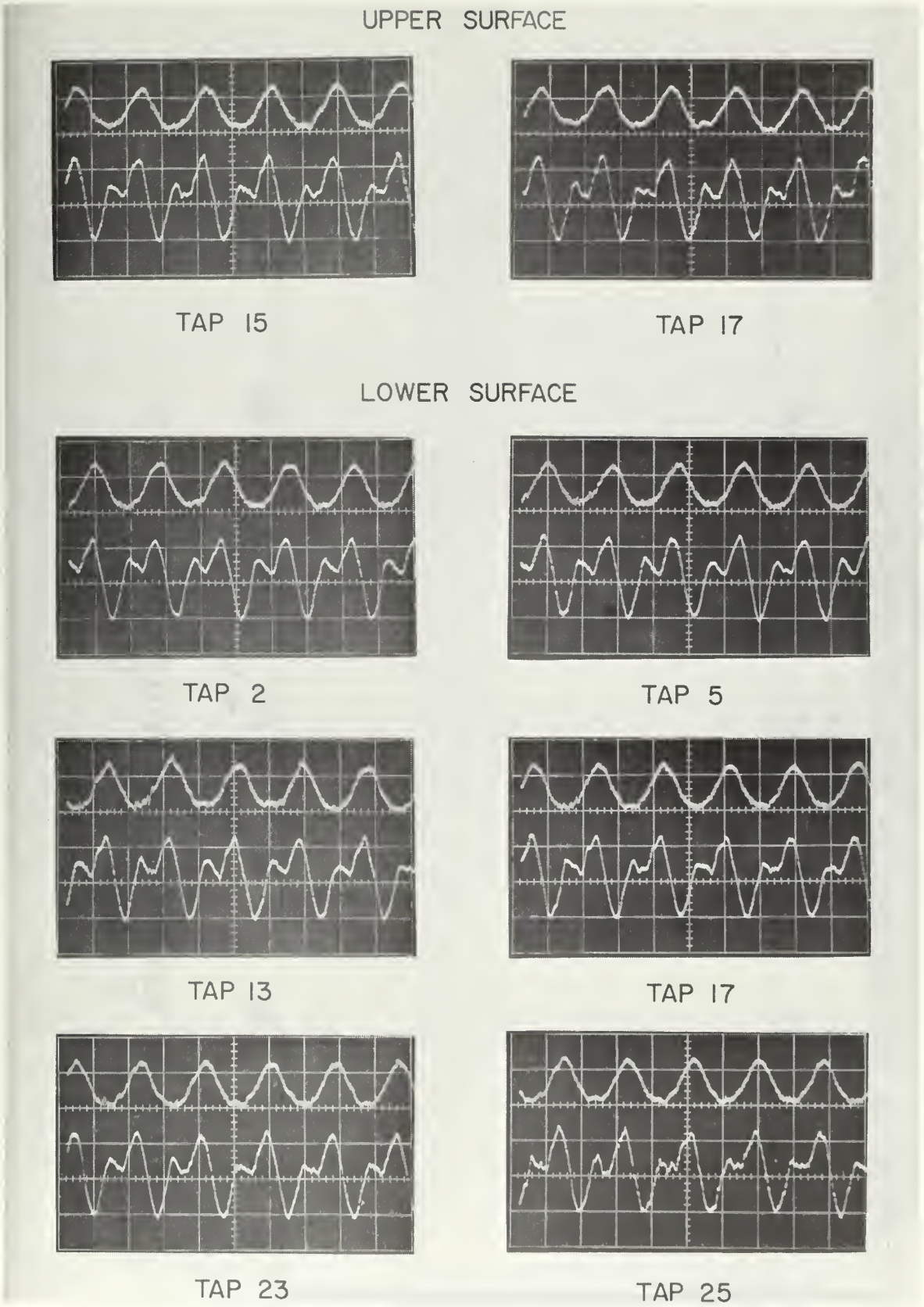

Figure 73. Pictures, Run 7, Pressure, Velocity

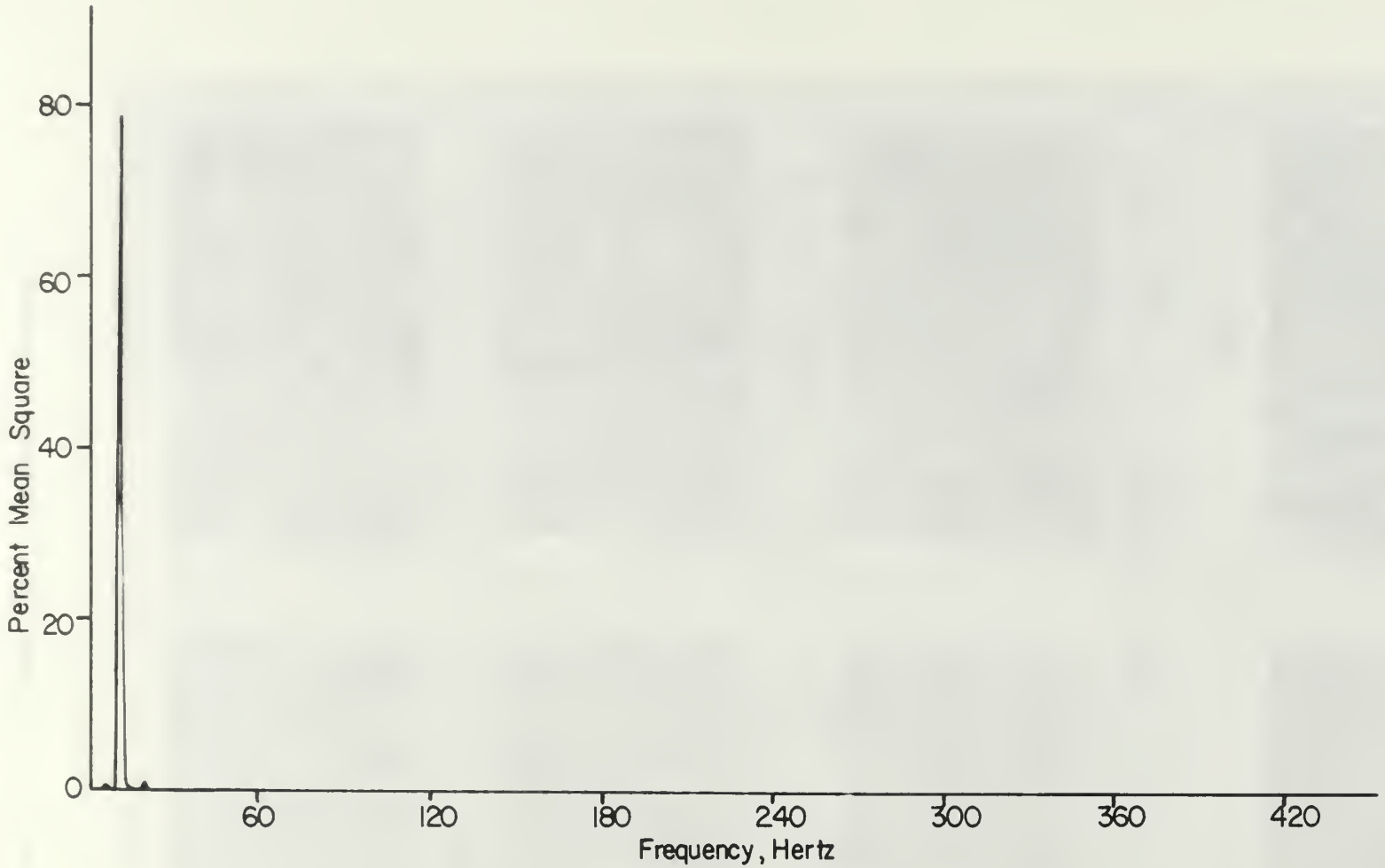

FIGURE 74. PSD OF UNSTEADY VELOCITY, RUN 7

$\bar{U}$ = 100.46 $\bar{U}^2$ = 25.99

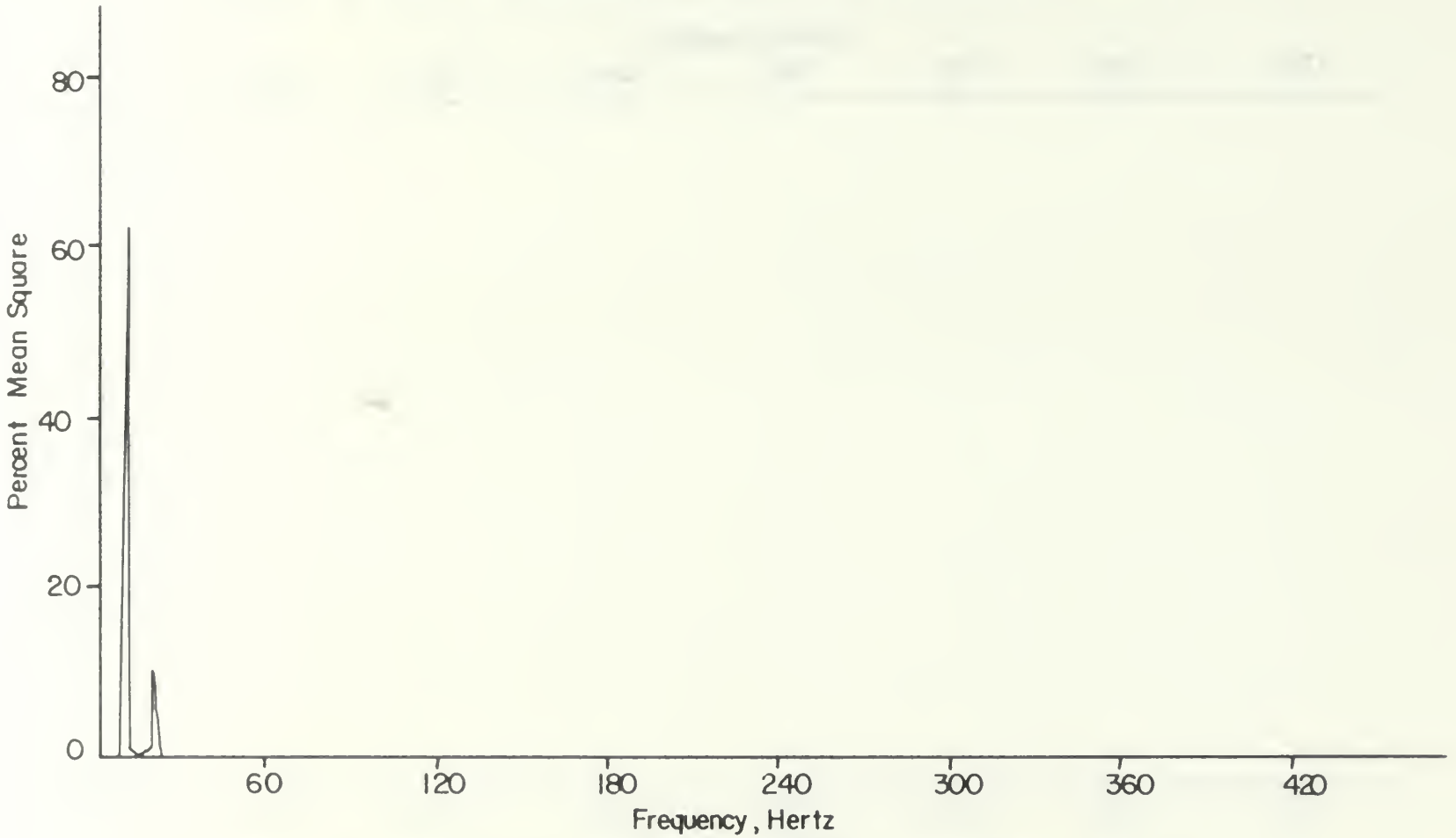

FIGURE 75 PSD OF UNSTEADY PRESSURE COEFFICIENT, RUN 7

$\xi = 0.0$ UPPER SURFACE

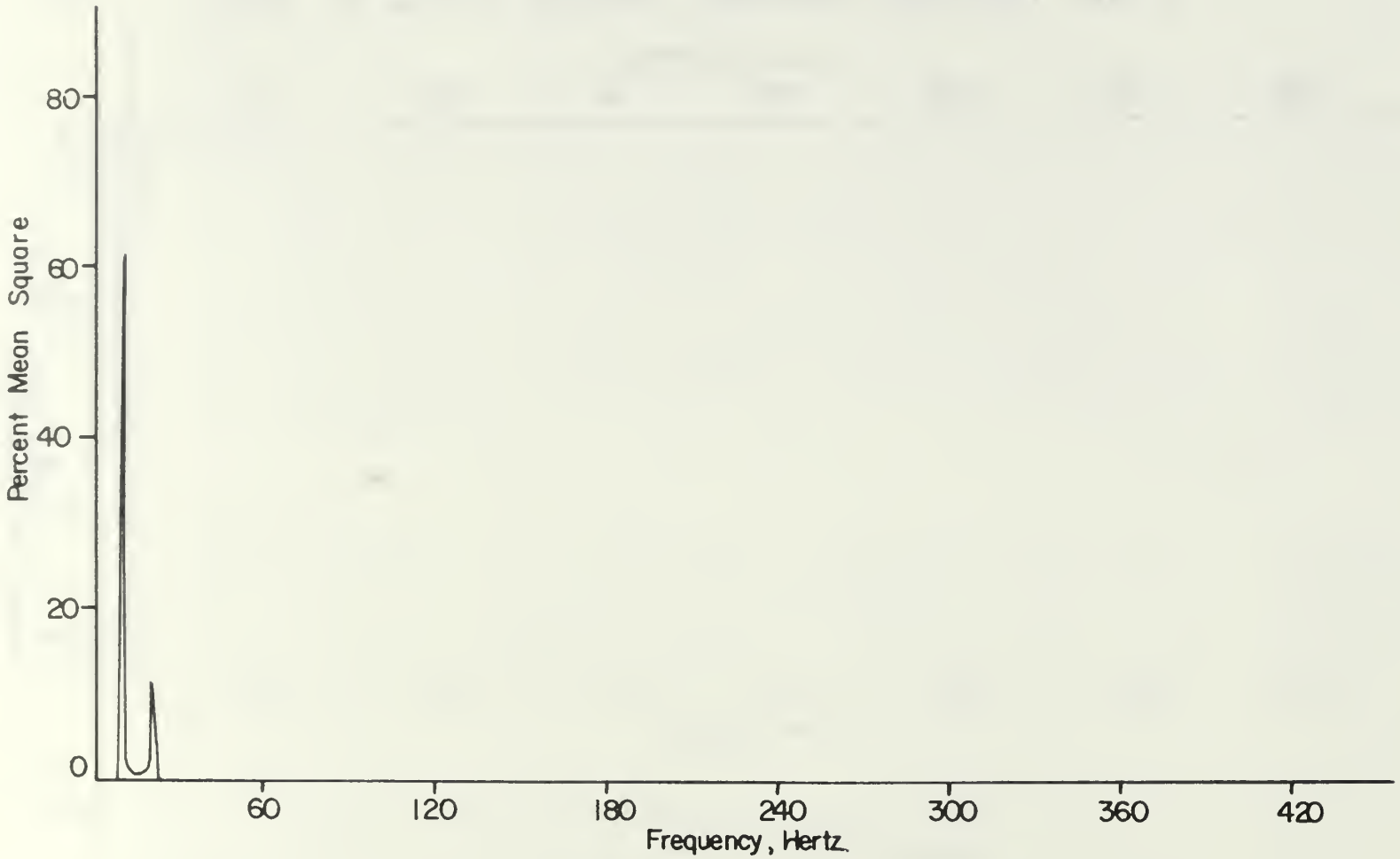

FIGURE 76. PSD OF UNSTEADY PRESSURE COEFFICIENT, RUN 7
$\varepsilon = 0.100$ UPPER SURFACE

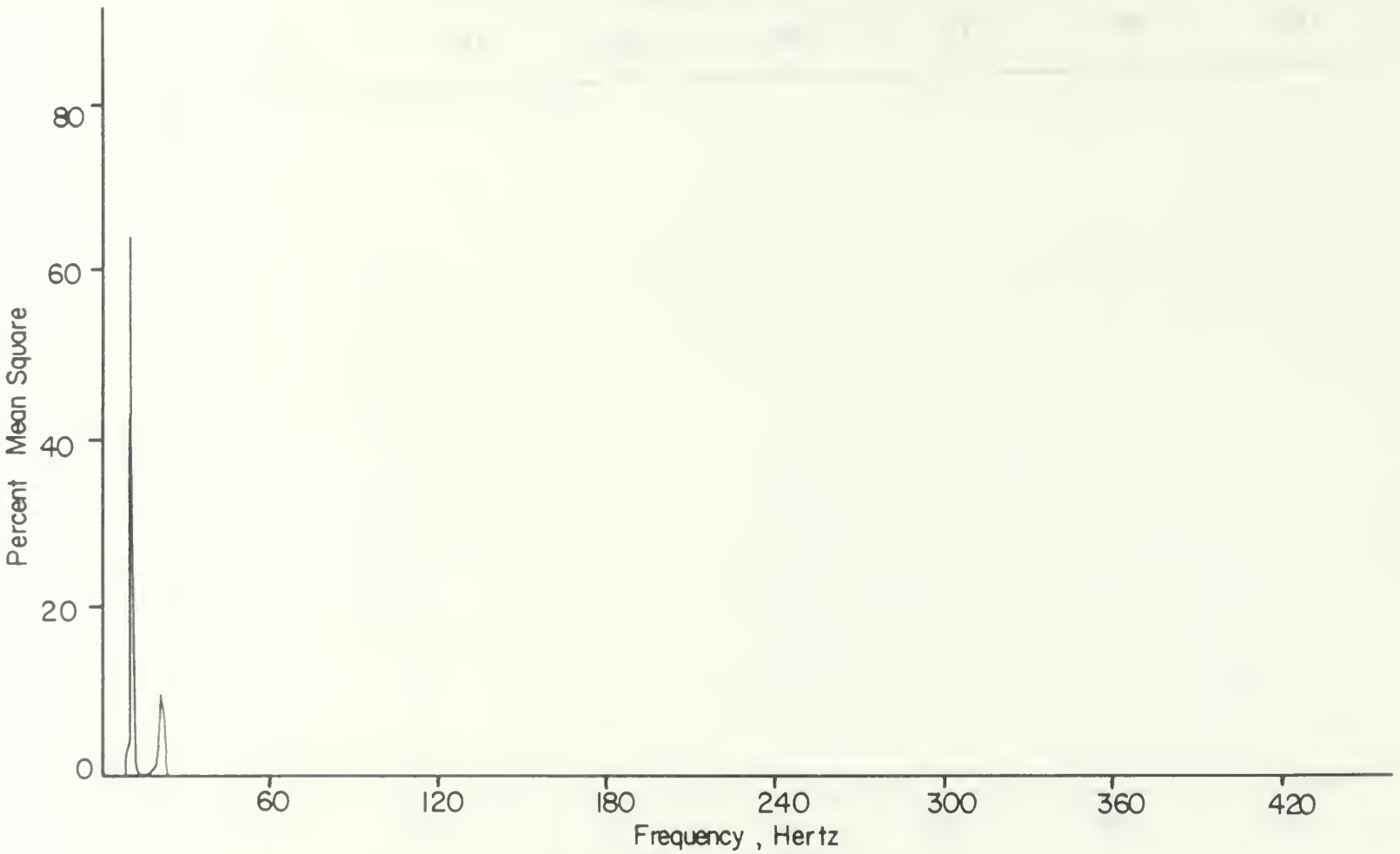

FIGURE 77. PSD OF UNSTEADY PRESSURE COEFFICIENT , RUN 7

$\xi = 0.500$ UPPER SURFACE

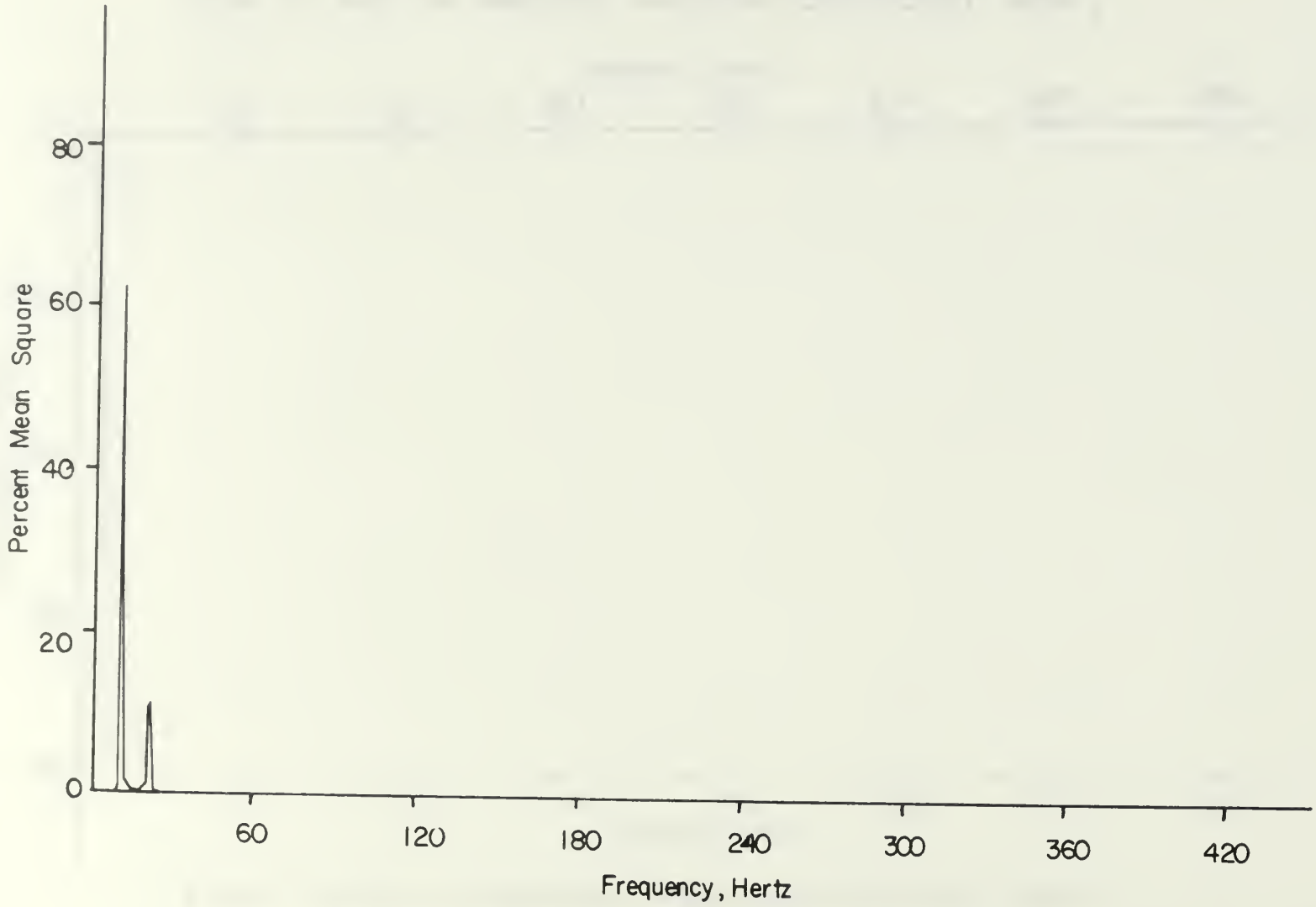

FIGURE 78. PSD OF UNSTEADY PRESSURE COEFFICIENT, RUN 7

$\varepsilon = 0.900$ UPPER SURFACE

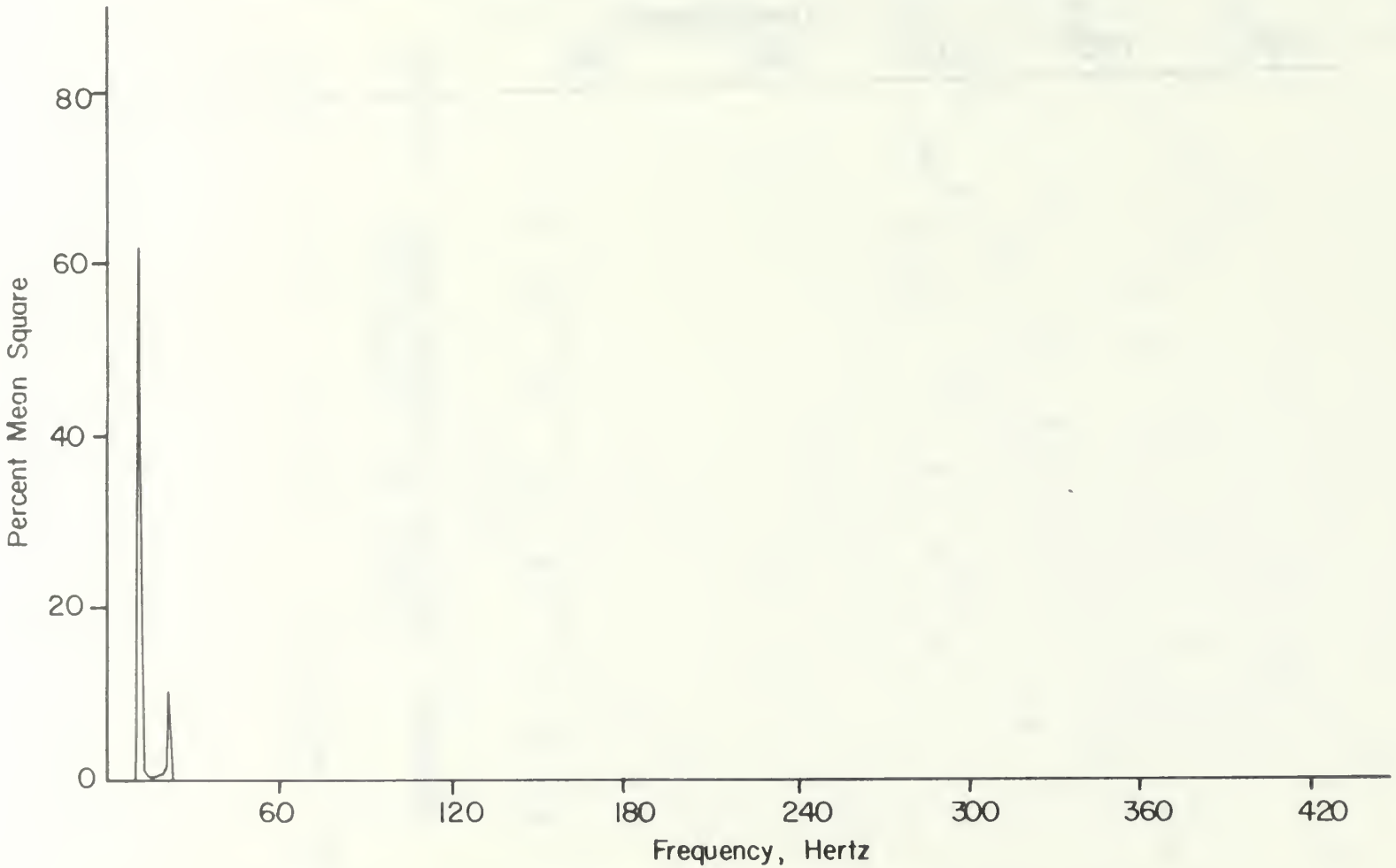

FIGURE 79. PSD OF UNSTEADY PRESSURE COEFFICIENT, RUN 7
$\epsilon = 0.100$ LOWER SURFACE

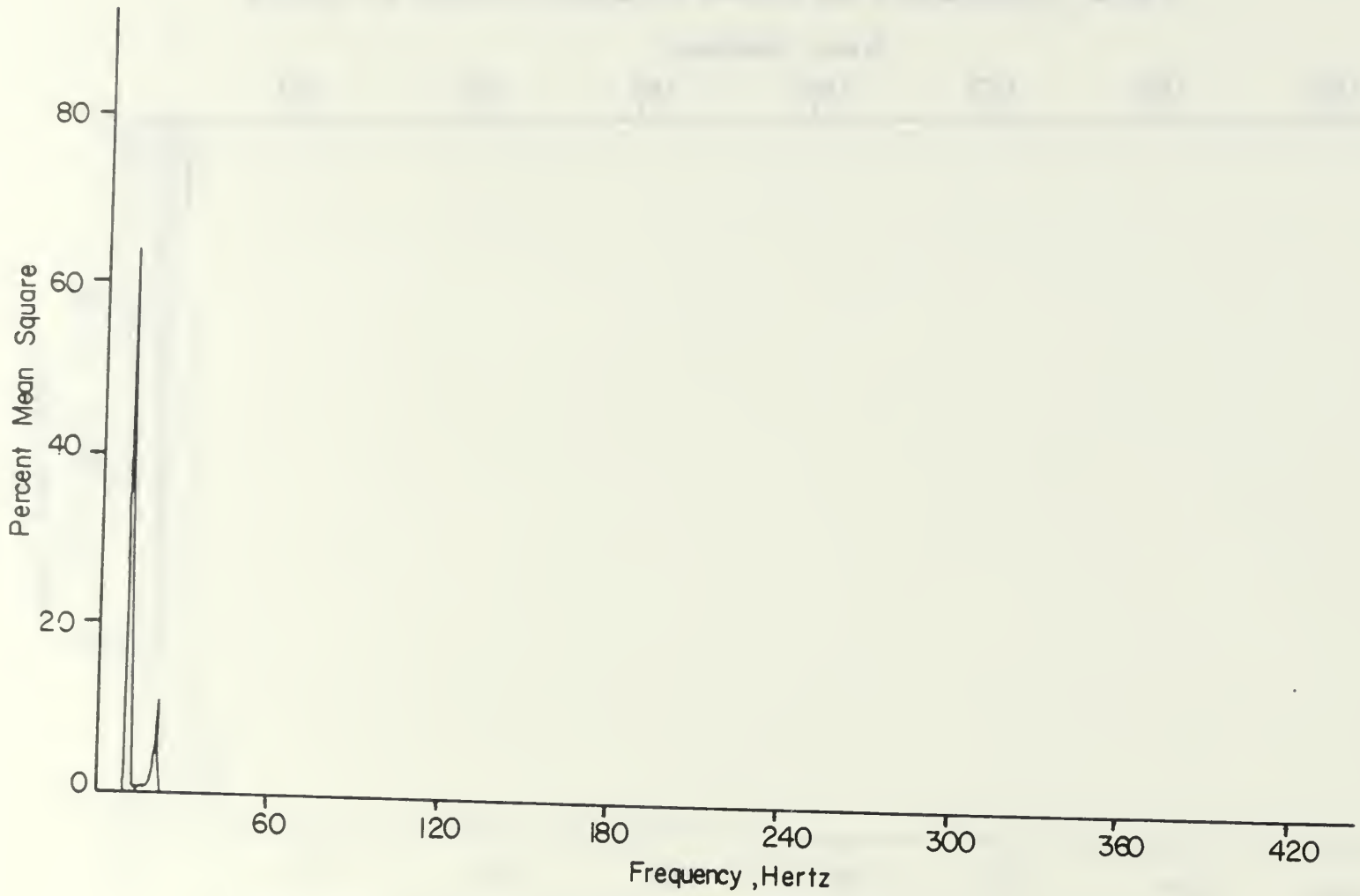

FIGURE 80. PSD OF UNSTEADY PRESSURE COEFFICIENT, RUN 7
$\zeta = 0.500$
LOWER SURFACE

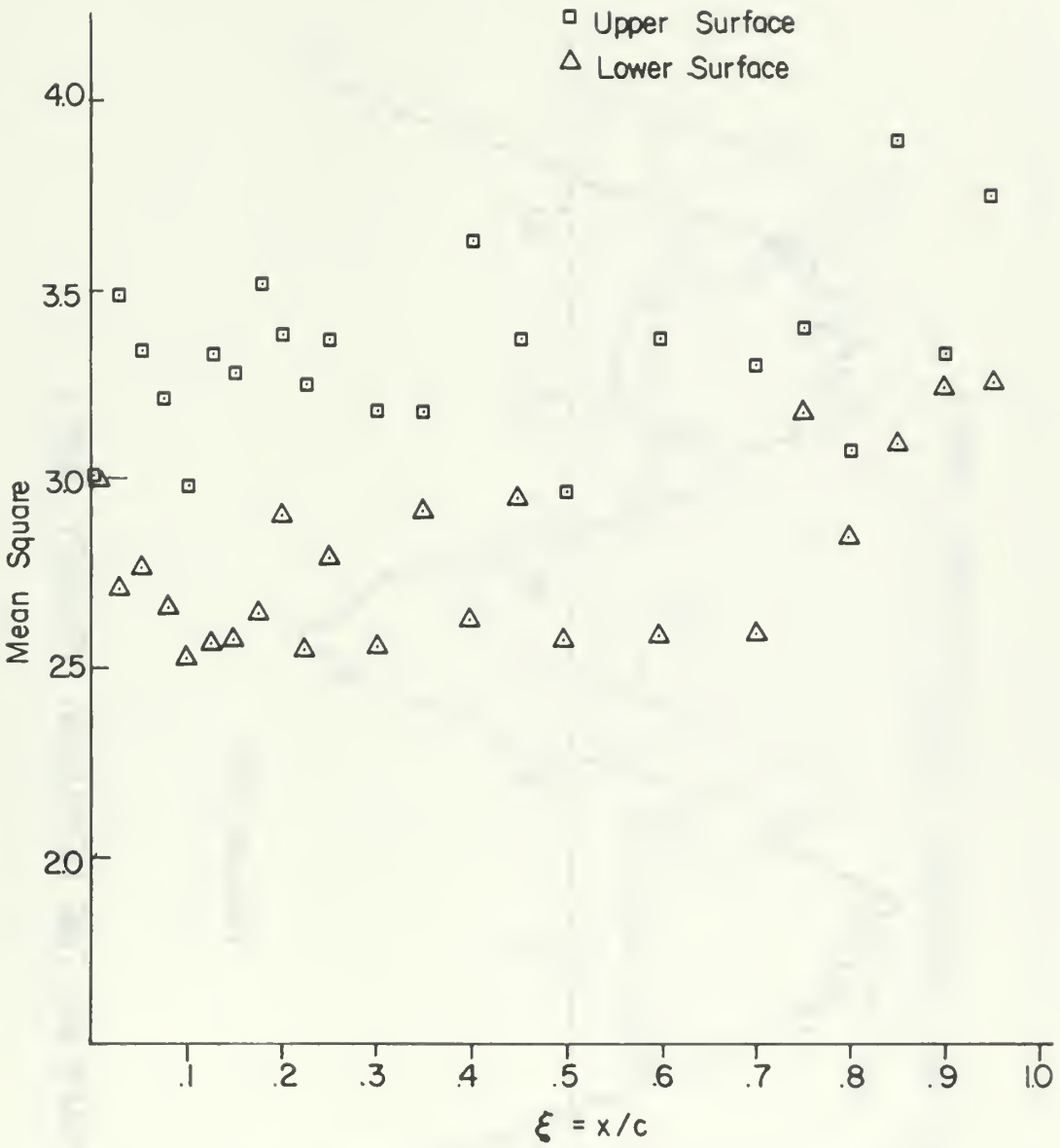

FIGURE 81. MEAN SQUARE OF UNSTEADY PRESSURE COEFFICIENTS ON AIRFOIL

RUN 7. $\alpha = 15°$ $f_o = 11$ Hz $\bar{U} = 100$ ft/sec $\varepsilon = 0.0718$

FIGURE 82. TIME DEPENDENT VELOCITY, RUN 7

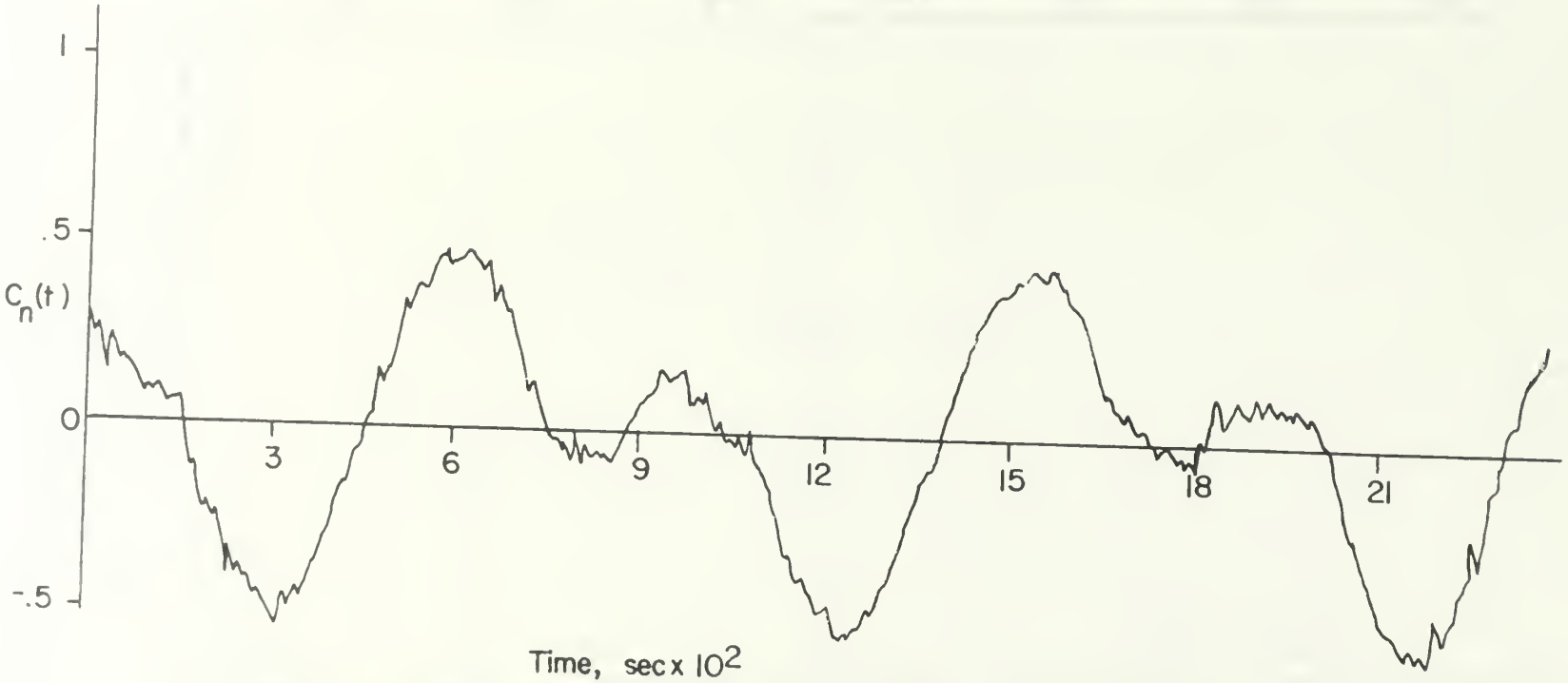

FIGURE 83. TIME DEPENDENT NORMAL FORCE, RUN 7

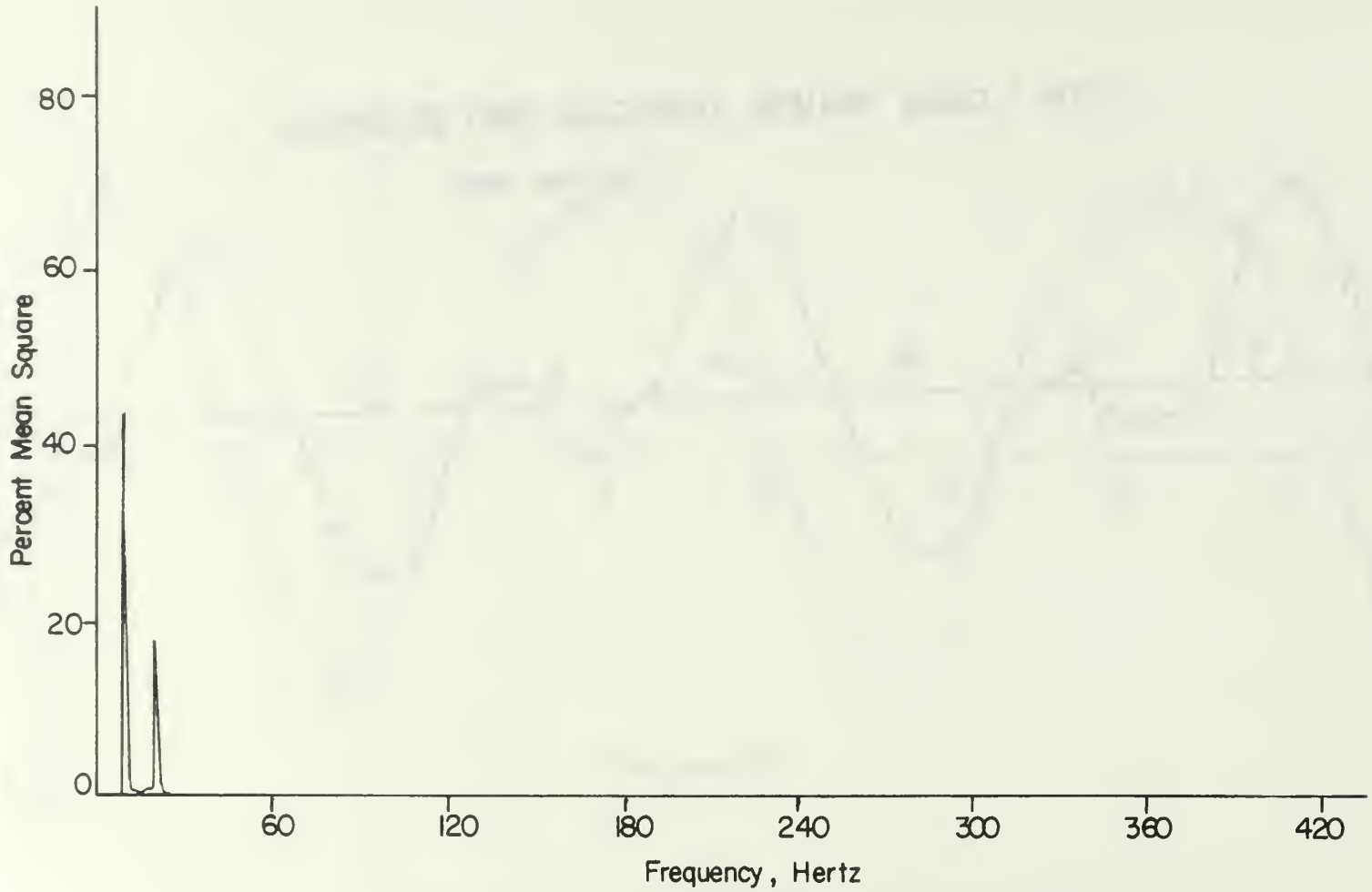

FIGURE 84. PSD OF UNSTEADY NORMAL FORCE COEFFICIENT, RUN 7
MEAN SQUARE = 0.075

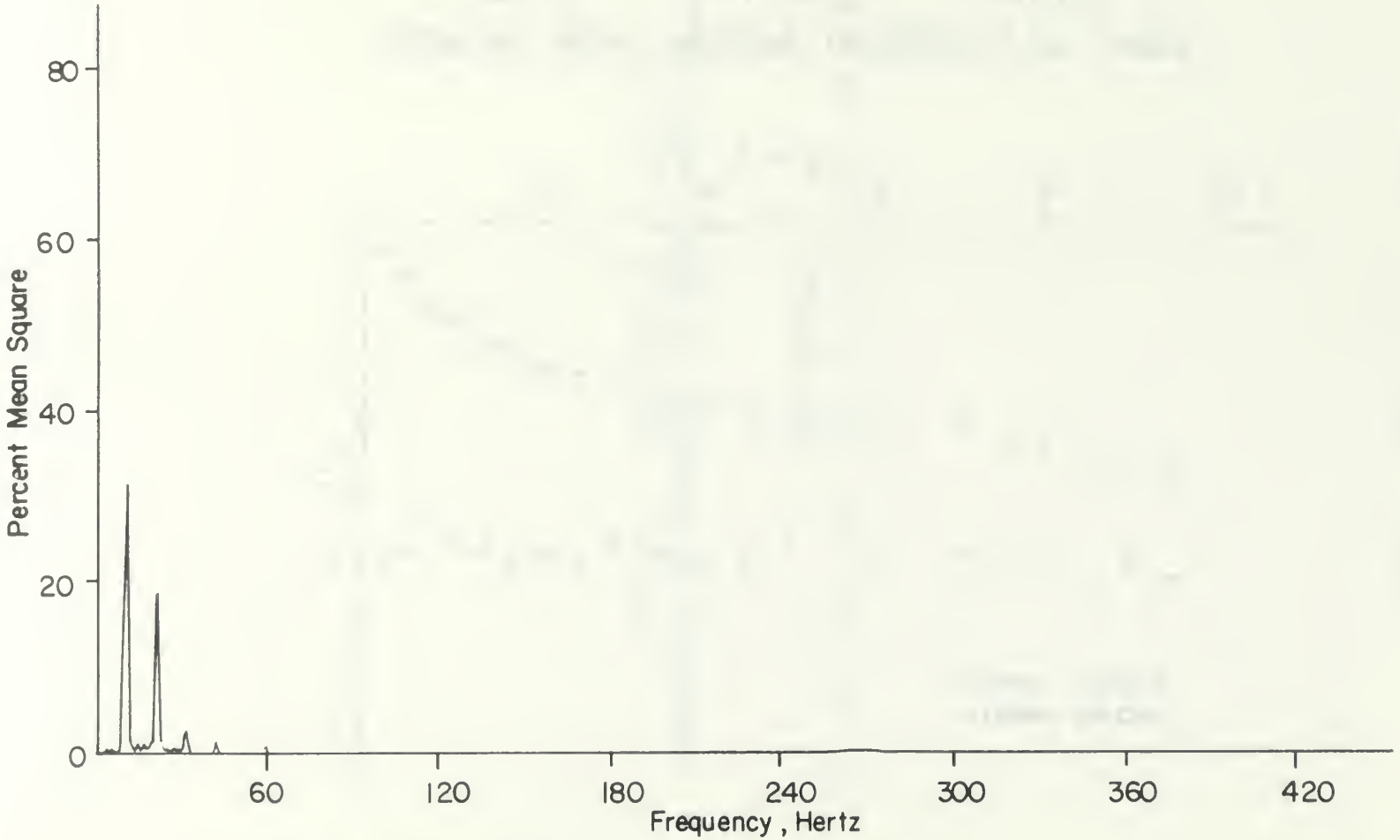

FIGURE 85. PSD OF UNSTEADY PRESSURE AT THE CENTER OF PRESSURE, RUN 7
MEAN SQUARE =0.010

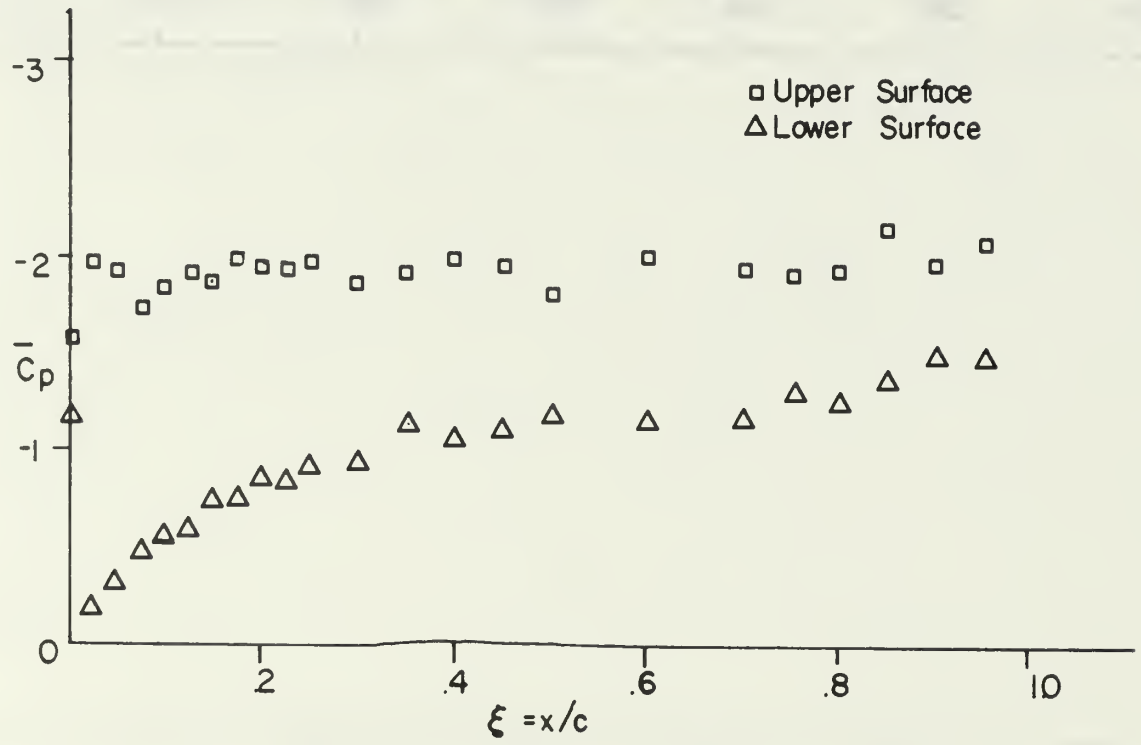

FIGURE 86. MEAN PRESSURE DISTRIBUTION ON AIRFOIL
$\alpha = 15°$ $f_o = 11$ Hz $\zeta = 0.072$

FIGURE 87. MEAN NORMAL FORCE COEFFICIENT VS. FREQUENCY

$\alpha = 15°$ $\bar{U} = 100$ ft/sec $\zeta \approx 0.08$

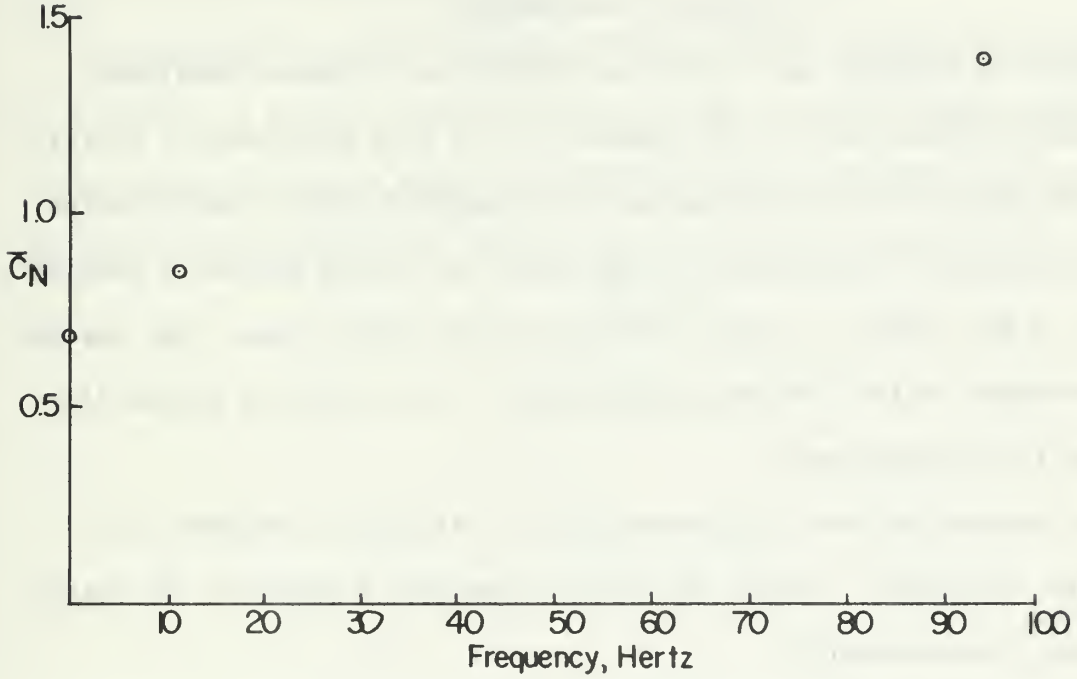

FIGURE 88. MEAN CENTER OF PRESSURE VS. FREQUENCY

$\alpha = 15°$ $\bar{U} = 100$ ft/sec $\zeta \approx 0.08$

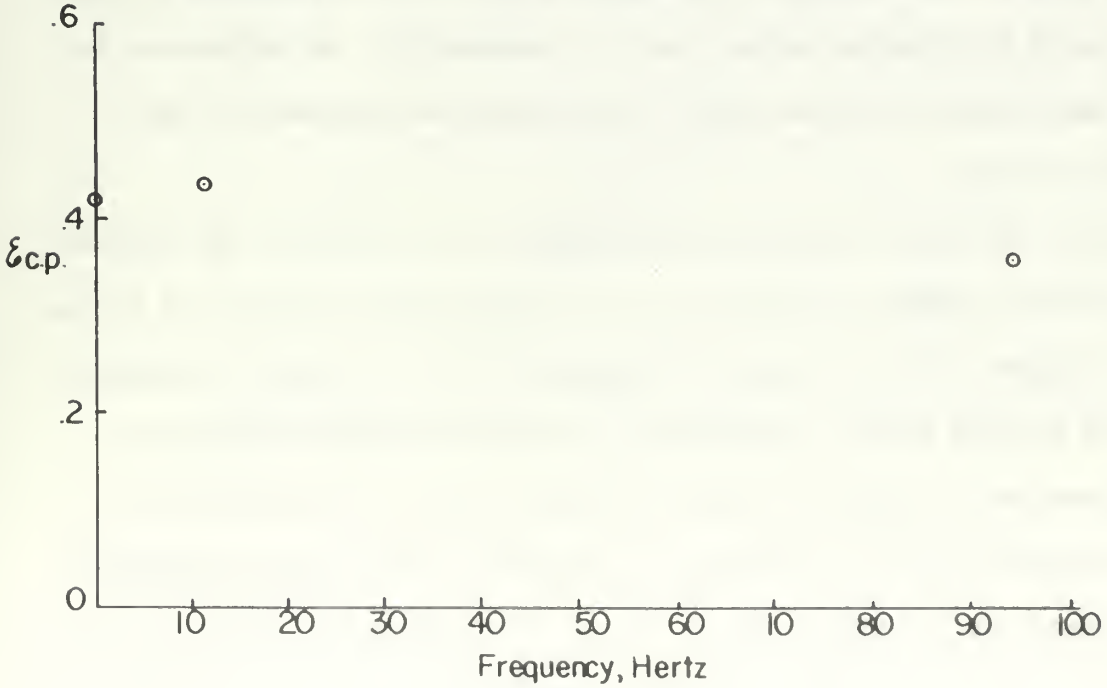

APPENDIX A

TRANSDUCER CALIBRATION

Dyanmic calibration was carried out using the procedure developed by Johnson in Reference 14. The results of his work were used to select the inside diameter of the tubing and tube length for this investigation. The stainless steel tubing used in the model was 0.0625 inches in outside diameter, 0.047 inches in inside diameter and 24 inches long. The plastic tubing attached to the transducer housing was 0.49 inches in inside diameter and 11.5 inches long.

Both transducers were first mounted in a calibration chamber and statically calibrated. Figure 89 shows a schematic diagram of the static calibration instrumentation.

A sound driver was then mounted on the calibration chamber and driven at known frequencies by the amplified output of an audio oscillator. The spectrum from 0 to 500 hertz was scanned to see if any difference in phase or gain could be detected between the two transducers. No difference in phasing was detected and the ratio of the gains was constant for the observed spectrum.

The next step was to remove the transducer to be used for the investigation from the chamber, install it in its housing and reconnect it to the chamber through steel and plastic tubing identical in length and diameter to that to be used in the experiment. The values of phase difference and wave analyzer readings for each transducer were then recorded at 5 hertz increments from 0 to 400 hertz. The gain of the remote transducer was then taken as the product of the ratio of static gains and the ratio of the wave analyzer readings. The amplifiers used to amplify the two

transducer outputs were switched and the procedure was repeated. No differences in results were noted. Figure 90 shows a schematic of the dynamic calibration instrumentation.

The spectral interval subsequently used in the analysis of results was 1 hertz. A linear interpolation was used to obtain intermediate points in the frequency range 0 to 400 hertz and a simple linear extrapolation made from 400 to 512 hertz. The results are shown in Fig. 10 and 11.

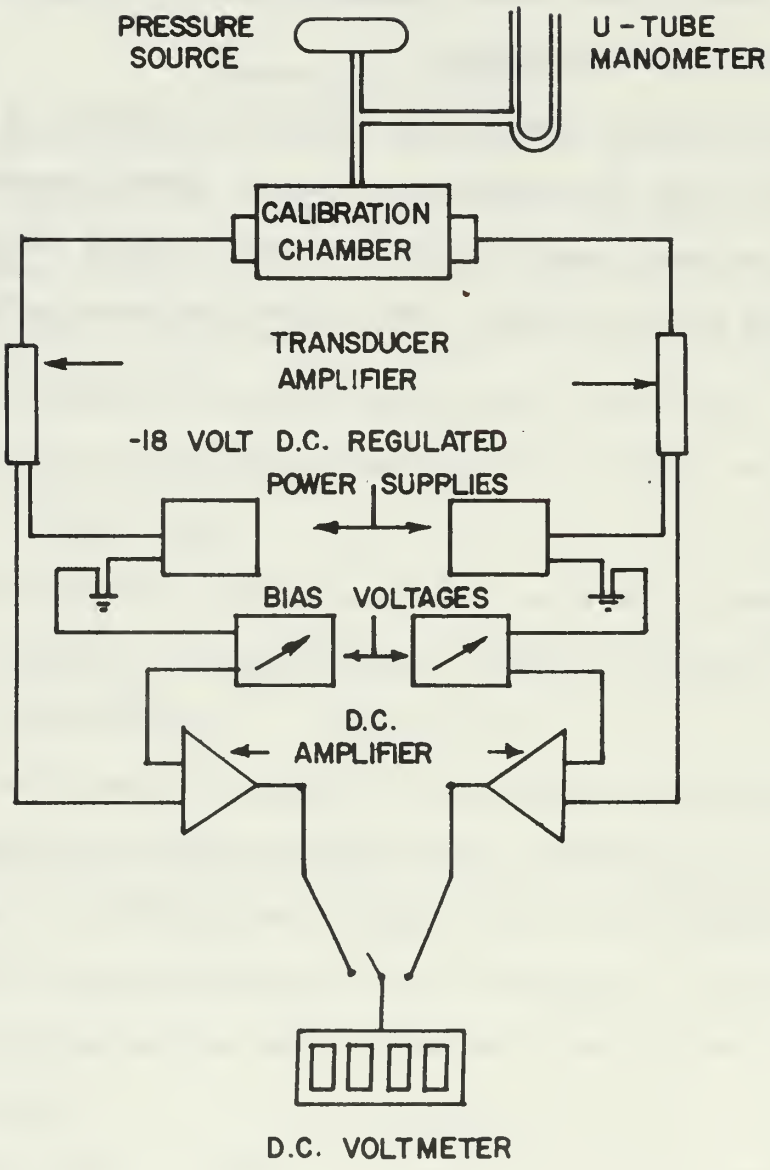

FIGURE 89. STATIC CALIBRATION INSTRUMENTATION

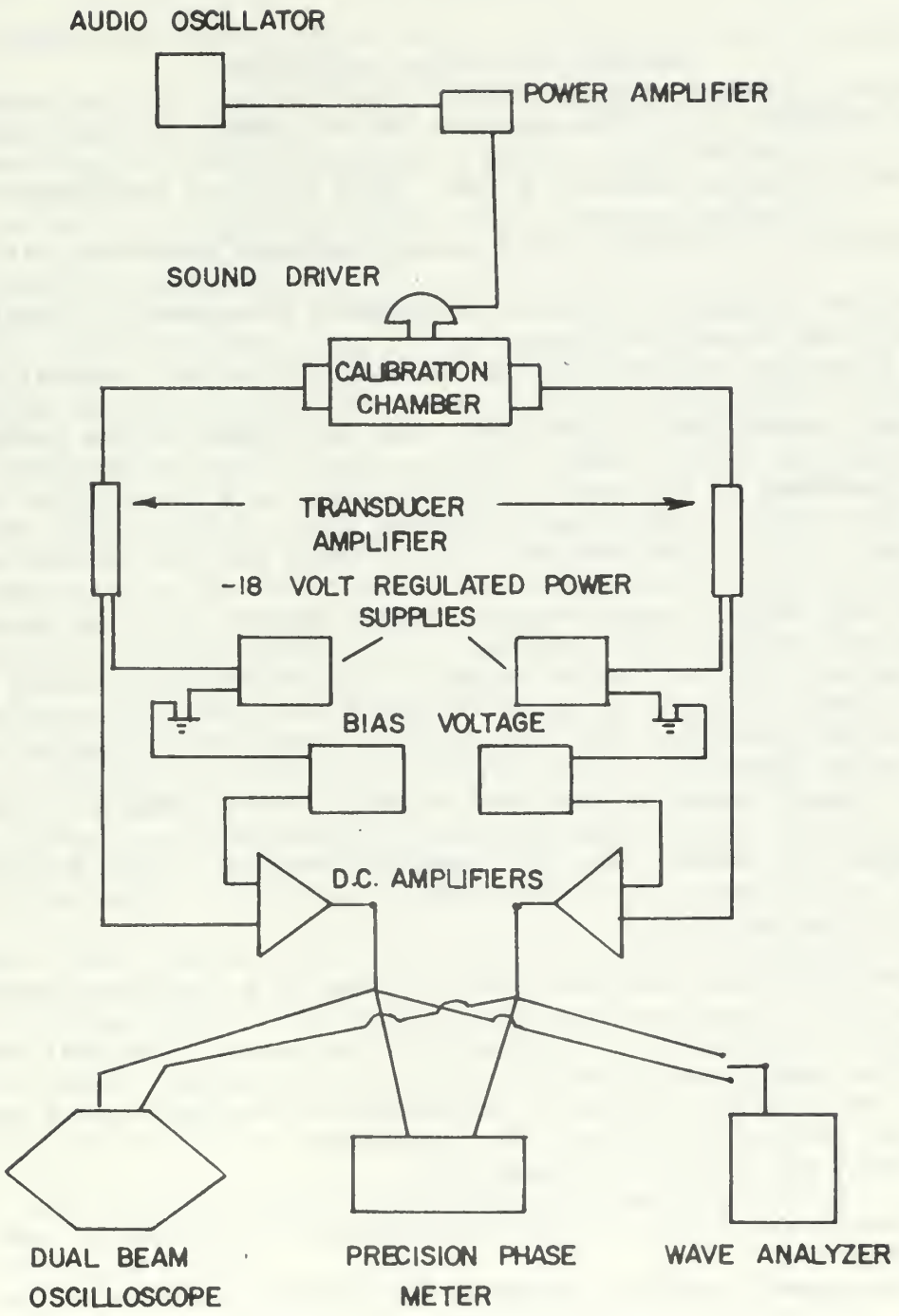

FIGURE 90. DYNAMIC CALIBRATION INSTRUMENTATION

APPENDIX B

ANALOGUE TO DIGITAL CONVERSION

The available digitizing equipment was not capable of digitizing more than one analog signal at a time. This precluded simultaneous digitization of the velocity and pressure analogues associated with a given tap and ultimately required photographic measurement of phasing.

The procedure used was based on an available digital computer program. The program takes binary words from one channel of the analogue to digital interface of the hybrid and stores them in a given buffer until the buffer is full. The contents of that buffer are then written on magnetic tape while a second buffer is being filled. When the second buffer is full it is written on magnetic tape and the first buffer takes on the storage function. The cycle repeats itself for the sample length desired. Sample length is expressed in terms of the number of blocks of 1024 samples per record. The 1024 samples correspond to the storage capacity of the buffers.

The analogue signal to be digitized is taken by a designated trunk line from the analogue side of the hybrid to the analog to digital converter. The sampling interval is controlled by interupts into a trunk line on the logic board of the analogue.

For this investigation a sampling frequency of 1024 samples per second was chosen in order to simplify the computer analysis of the data. For minimum scale error in the conversion process it was desirable that the digitized signal be as large as possible. A compromise between the desired amplitude of the digitized signal and numerical convenience was worked out by making the filter gain be of the order of 100.

The filter was used to improve signal to noise-plus-signal ratios of the analogue data. Preliminary investigations had shown that some high frequency noise was picked up in the data recording process from both the transducer and the tape recorder. ("High frequency" for the purpose of this investigation meaning frequencies greater than 500 hertz.) Filtering prevented this high frequency noise from distorting the resulting spectral estimates.

For the steady flow runs it was not necessary to preserve any phase information and the analogue circuitry used is shown schematically in Fig. 91. The conversion process in this case was commenced when the "Master Clock" on the analogue computer was switched from "Reset" to "Run" with the analogue computer in the "Compute" mode. In more specific terms, switching the master clock to "Run" enabled the interrupts to the digital computer.

The unsteady flow runs were digitized using the circuitry shown in Fig. 92. A 1000 hertz sine wave was recorded on a third track of the data tape. This signal was used to start the interrupts to the digital computer at the point on the tape corresponding to the start of the 1000 hertz signal. The idea was that the velocity and pressure analogues corresponding to a given pressure tap would be digitized starting at the same point on the tape. The large gain on the 1000 hertz signal was used to get maximum rise time to the comparator. Utilizing the circuitry shown in Fig. 92 also allowed control of the digitizing process from the digital side of the hybrid.

The procedure described above was not adequate to preserve the phase information between the velocity and pressure analogue signals, Possible reasons include variabilities in the response times of the comparator and/or the delay flop in the logic circuitry and/or recording

data at too slow a tape speed to be able to get the rise time necessary to insure adequate responses of the above analogue devices.

A method that was not tried would be to use the 1000 hertz signal to put the analogue into "Compute" rather than utilizing the delay flop and comparator circuitry shown in Fig. 92. This would eliminate at least one of the elements in the circuit and possibly both.

The hybrid has the capability of converting 32 analogue channels with only a slight time skew. The conversion process is limited by buffer size and the speed at which the filled buffers can be written on magnetic tape. The time it takes to fill a buffer cannot be less than the time it takes to write the contents of a buffer on magnetic tape. This limits the sampling frequency.

In order to sample more than one track at a time the digital computer program would have had to be written to store the sampled analogue signals alternately in the buffers. The author did not have the time available to rewrite the program and the Electrical Engineering Department Computer Laboratory does not have the programming support available to rewrite it.

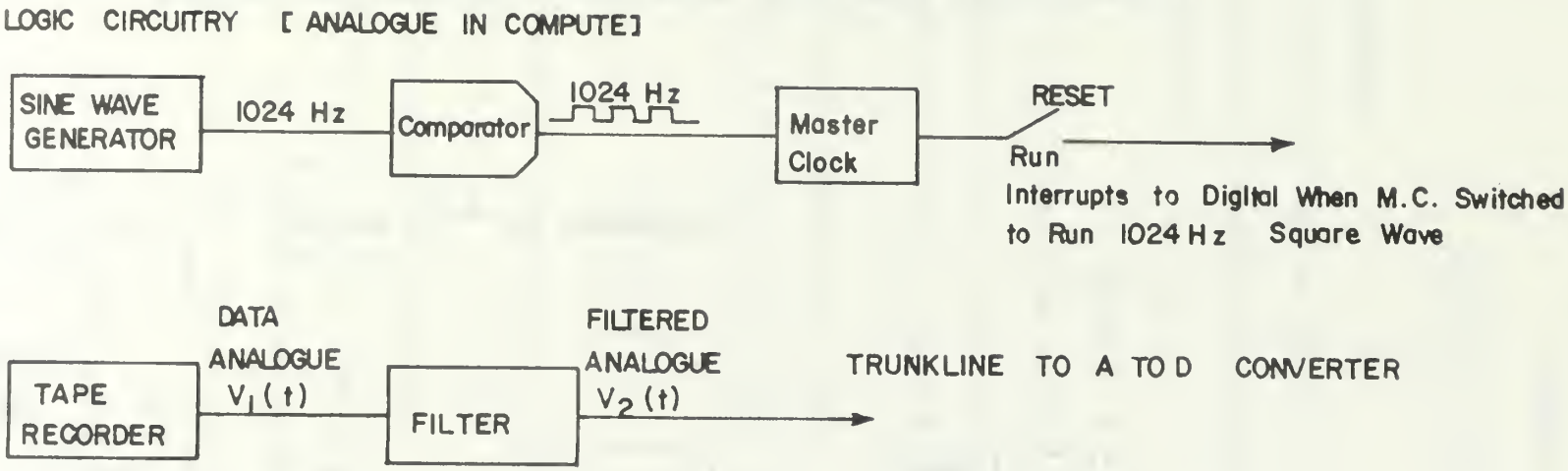

FIGURE 91. LOGIC AND ANALOGUE CIRCUITRY FOR STEADY FLOW CONVERSION

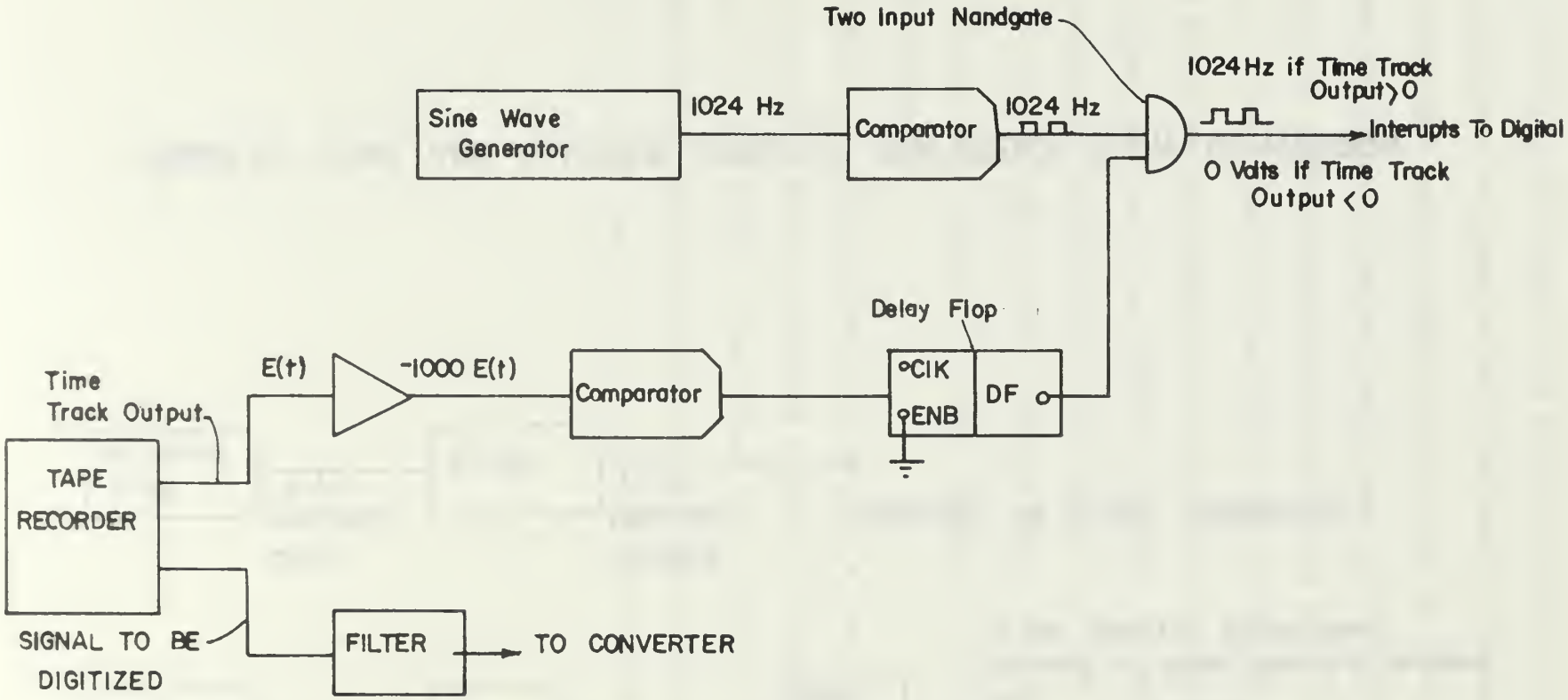

FIGURE 92. LOGIC AND ANALOGUE CIRCUITRY FOR UNSTEADY FLOW CONVERSION

APPENDIX C

NUMERICAL ANALYSIS OF DATA

A. ASSUMPTIONS

The digital analysis was based on the assumption that the pressure at any point on the surface of the airfoil was a parametric function of the free stream velocity, i.e.,

$$P = P(x,y,U),\ U = U(t)$$

The oscilloscope traces shown in Fig. 36 and Fig. 72 indicate the validity of this assumption which allowed the establishment of a common time base for each pressure analogue sample.

B. MEAN AND MEAN SQUARE CALCULATIONS

The mean of a digital array $\left\{V_n\right\}$, n = 1,N was calculated from the relation:

$$\overline{V} = \left(\frac{1}{N}\right) \sum_{n=1}^{N} V_n$$

where V_n corresponds physically to a quantity measured at time t_n and N is the number of samples in the array. For spectral calculations, it was desirable that the arrays subjected to spectral analysis have a zero mean. This prevents distortion at the low frequency end of the spectrum [Ref. 13]. Consequently, the mean was subtracted from the initial array $\left\{V_n\right\}$ to form a new digital array $\left\{U_n\right\}$. This new array corresponded to the unsteady part of the analogue signal.

The mean square of $\left\{U_n\right\}$ was calculated from the relation:

$$\overline{U}^2 = \frac{1}{N} \sum_{n=1}^{N} U_n^{\,2}$$

C. SPECTRAL CALCULATIONS

1. Fourier Transforms

All sampling for this investigation was done at the rate of 1024 samples per second. Spectral analysis was performed on arrays of 1024 samples each. This procedure yields a Nyquist Cutoff Frequency of 512 hertz and an equivalent spectral bandwidth of 1 hertz [Ref. 13].

The complex Fourier Transform of the digital array under consideration was calculated using the relation:

$$U_K = \frac{1}{N} \sum_{n=0}^{N-1} U_{n+1} \, e^{-2\pi i \frac{nK}{N}}$$

where:

U_K = spectral component at frequency $\frac{K \cdot F_C}{N/2}$, K = 1, ... N/2

i = V-T

e = 2.7183...

The inverse transfer functions of the tubing and filter were applied to the pressure analogues in complex form in order to get the Fourier Transform of the pressure at the surface of the airfoil, i.e.,

$$P_K = \frac{U_K}{G_K H_K}$$

The Fourier Transform of the unsteady velocity was found by simply dividing the Fourier Transform of the velocity analogue by the transfer function of the filter.

The inverses of the pressure and velocity transforms were taken using the same subroutine as was used to take the transform of the original analogue array. Details of the capabilities of this subroutine, called "HARM" in the data analysis program, are given by Cooley and Tukey in Reference 15.

2. Power Spectral Densities

The power spectral density of $\{U_n\}$ and the Fourier Transform of $\{U_n\}$ are related by:

$$G_{U_K} = 2U_K, U_K^*$$

The power spectral density of a function describes the general frequency composition of the function in terms of the spectral density of its mean square. Thus the mean square of $\{P_n\}$ was calculated from:

$$\overline{P}^2 = \sum_{K=0}^{\infty} G_{P_K} \Delta f_B$$

where the equivalent spectral bandwidth, Δf_B, was 1 hertz for this investigation. Reference 13 has a complete discussion of the properties of the power spectral density and its uses.

D. NORMAL FORCE AND CENTER OF PRESSURE

The integral relations given in Chapter IV, D, were approximated by a simple trapezoidal summation. For example, the mean normal force coefficient, defined as

$$\overline{C}_N = \int_0^1 [\overline{C}_P(\xi, -\eta) - \overline{C}_P(\xi, +\eta)]\, d\xi$$

was approximated by:

$$\overline{C}_N \approx \sum_{n=1}^{23} \frac{[\Delta\overline{C}_P(n+1) + \Delta\overline{C}_P(n)]}{2} \Delta\xi_n$$

where:

$$\Delta\overline{C}_P(n) = \overline{C}_{P_u}(n) - \overline{C}_{P_L}(n).$$

APPENDIX D

EVALUATION OF EXPERIMENTAL TECHNIQUES

A. PRESSURE MEASURING SYSTEM

Dynamic calibration of the transducer and pressure tap leads was accomplished using a sound driver to produce reference pressure fluctuations, (Appendix A). The lower frequency bound on the flat portion of the dynamic response curve of the sound driver was 160 hertz with detectable response of decreasing amplitude to 25 hertz.

Below 25 hertz, both the gain of the amplifier used to drive the sound driver and the gain of the sound driver were very small. The power required to produce any output response from the sound driver below 25 hertz caused saturation of the amplifier with the result that the output of the sound driver was a distorted signal rather than a simple sine wave. The combination of a complex signal, decreasing interval between harmonics, and low gain made the wave analyzer more difficult to read and the resulting gains subject to greater uncertainty than gains measured at higher frequencies.

Defining error in terms of a maximum percentage of deviation from a true value, the estimated error in the system transfer function was 5 per cent above 25 hertz and 10 per cent below 25 hertz.

B. TAPE RECORDER AND ANALOGUE TO DIGITAL CONVERSION

Table II gives examples of the differences between measured recorded voltages and their digital equivalents. The differences were considered to be insignificant.

C. SPECTRAL ANALYSIS

The power spectral density estimates of the unsteady pressures and velocities are considered by the author to be reasonable estimates to their true power spectral densities. A detailed discussion of error criteria in spectral calculations is given by Bendat and Piersol in Reference 13.

D. NORMAL FORCE AND CENTER OF PRESSURE

The inability to preserve phase information in the analogue to digital conversion process and subsequent measurement of time differences from oscilloscope traces made error in the normal force calculations difficult to evaluate.

It was estimated that phasing between the pressure and velocity analogues associated with a given tap could be measured to within 1/2 sample time increment or approximately 17 degrees at 94 hertz and 2 degrees at 11 hertz. The quality of these measurements would establish minimum error bounds on the normal force and center of pressure calculations.

E. EXPERIMENTAL ENVIRONMENT

The variation in the ratio of the unsteady to steady components of the velocity associated with individual taps for Runs 5 and 7 are given in Tables IV and V. The pressure coefficients associated with a given tap were calculated using the measured mean velocity associated with that tap in an effort to minimize the effect of the variations on the normal force and center of pressure calculations. These variations in free stream velocity apparently were due to fluctuations in line voltage and atmospheric disturbances.

TABLE IX

RATIO OF SQRT(2)*SQRT(VELOCITY MEAN SQUARE) TO MEAN VELOCITY

RUN 5

TAP	LOCATION	UPPER	LOWER
1	0.0	0.088	0.078
2	0.025	0.091	0.081
3	0.050	0.090	0.080
4	0.075	0.089	0.080
5	0.100	0.089	0.080
6	0.125	0.089	0.080
7	0.150	0.086	0.083
8	0.175	0.090	0.083
9	0.200	0.088	0.080
10	0.225	0.090	0.079
11	0.250	0.088	0.080
12	0.300	0.087	0.081
13	0.350	0.091	0.081
14	0.400	0.088	0.081
15	0.450	0.089	0.082
16	0.500	0.091	0.082
17	0.600	0.087	0.081
18	0.700	0.091	0.084
19	0.750	0.090	0.086
20	0.800	0.087	0.084
21	0.850	0.086	0.086
22	0.900	0.089	0.086
23	0.950	0.087	0.087
24	0.250	0.088	0.086
25	0.500	0.090	0.086

THE AVERAGE MEAN VELOCITY FOR RUN 5
WAS 102.66
THE AVERAGE MEAN SQUARE WAS 38.43
THE RATIO OF UNSTEADY TO STEADY WAS 0.0854
THE AVERAGE Q WAS 12.05

TABLE V

RATIO OF SQRT(2)*SQRT(VELOCITY MEAN SQUARE) TO MEAN VELOCITY

RUN 7

TAP	LOCATION	UPPER	LOWER
1	0.0	0.069	0.073
2	0.025	0.072	0.071
3	0.050	0.072	0.073
4	0.075	0.071	0.072
5	0.100	0.070	0.073
6	0.125	0.072	0.071
7	0.150	0.072	0.071
8	0.175	0.074	0.072
9	0.200	0.071	0.073
10	0.225	0.072	0.071
11	0.250	0.071	0.071
12	0.300	0.070	0.071
13	0.350	0.071	0.074
14	0.400	0.073	0.071
15	0.450	0.071	0.073
16	0.500	0.071	0.071
17	0.600	0.074	0.071
18	0.700	0.072	0.071
19	0.750	0.069	0.071
20	0.800	0.070	0.072
21	0.850	0.073	0.073
22	0.900	0.071	0.074
23	0.950	0.070	0.072
24	0.250	0.071	0.072
25	0.500	0.072	0.074

THE AVERAGE MEAN VELOCITY FOR RUN 7
WAS 100.46
THE AVERAGE MEAN SQUARE WAS 25.99
THE RATIO OF UNSTEADY TO STEADY WAS 0.0718
THE AVERAGE Q WAS 11.63

```
                AN EXPERIMENTAL INVESTIGATION
                        INTO THE
                   UNSTEADY NORMAL FORCE
                        ON AN
          AIRFOIL IN AN OSCILLATING FREE STREAM

  PROGRAMMED BY M. R. BANNING, CAPT. USMC. AUG-SEP. 1969


      DIMENSION P(4096),U(4096),CN(1024),BMP(2,25),
     *BMSP(2,25),BMU(2,25),BMSU(2,25),DATA(1024),S(256),
     *INV(256),M(3),Y(50),ETA(25),GX(512),X(25),KPHASE(2,25)
     *FREQ(512),TIMEIT(512),RANGE(4)
      COMPLEX*8 A(1024,1,1),G(512),H(512),CON
      INTEGER SIDE,HOLE,SF,FRUN,ALPHA
C
      REAL*8 ITIL1(12)/'UNSTEADY PRESSURE COEFFICIENTS VS TI
     *RUN 6                                    M.R.BANNING'/
      REAL*8 ITIL2(12)/'UNSTEADY VELOCITY VS TIME
     *RUN 6                                    M.R.BANNING'/
      REAL*8 ITIL3(12)/'PSD OF UNSTEADY PRESSURE
     *RUN 6                                    M.R.BANNING'/
      REAL*8 ITIL4(12)/'PSD OF UNSTEADY VELOCITY
     *RUN 6                                    M.R.BANNING'/
      REAL*8 ITIL5(12)/'MEAN PRESSURE COEFFICIENTS VS ETA
     *RUN 6                                    M.R.BANNING'/
      REAL*8 ITIL6(12)/'PSD OF UNSTEADY NORMAL FORCE
     *RUN 6                                    M.R.BANNING'/
      REAL*8 ITIL7(12)/'UNSTEADY NORMAL FORCE VS TIME
     *RUN 6                                    M.R.BANNING'/
      REAL*8 ITIL8(12)/'PSD OF UNSTEADY CENTER OF PRESSURE
     *RUN 6                                    M.R.BANNING'/
      REAL LABEL /4H    /
      REAL*8 LABEL /8H        /
      REAL LABC(50)
C
      DEFINE FILE 1(51200,2,U,IB)
C
      READ(5,501) NRUN,NBSKIP,IFFIL,FRUN,ALPHA
      READ(5,503) PSLOPE,UMVOLT,QFO,TEMP,PATM
      READ(5,502)(ETA(I),I=1,25)
      READ(5,504)(G(I),I=1,512)
      READ(5,504)(H(I),I=1,512)
      READ(5,505)(LABC(I),I=1,50)
C
      GASCON=2116.0/(.0023769*518.688)
      TEMPR=TEMP+459.688
      RHO=PATM*70.73/(GASCON*TEMPR)
      UMEAN=SQRT(2.0*QFO*5.202/(2.54*RHO))
C
      WRITE(6,701) NRUN,NBSKIP,PSLOPE,UMVOLT,UMEAN
  701 FORMAT(1H1, ///,T32,'INPUT PARAMETERS FOR RUN',I3,/,
     *T32,'NO. OF BLOCKS SKIPPED BEFORE READING FIRST',
     *' RECORD=',I4,/,
     *T32,'TRANSDUCER SLOPE=',F5.3,' VOLTS/IN. OF H2O',/,
     *T32,'HOT WIRE OUTPUT OF ',F3.1,' VOLTS CORRESPONDS TO'
     */,T35,'A VELOCITY OF ',F6.2,' FEET/SEC')
      WRITE(6,702) FRUN,TEMP,PATM,RHO,UMEAN
  702 FORMAT(T32,'FREE STREAM OSCILLATION=',I4,' HERTZ',/,
     *T32,'ATMOSPHERIC TEMPERATURE=',F5.1,' DEGREES F',/,
     *T32,'ATMOSPHERIC PRESSURE=',F6.2,' IN. OF HG',/,
     *T32,'ATMOSPHERIC DENSITY=',F8.5,' SLUGS/FT**3',/,
     *T32,'MEAN VELOCITY=',F7.2,' FT/SEC')
      WRITE(6,703) ALPHA
  703 FORMAT(T32,'ANGLE OF ATTACK=',I3,' DEGREES')
C
      REWIND 4
C
      NOBLKS=4
      KIN=140
      IFSET=-1
      NTOT=1024
```

```
      NDIM=23
      IFFIL=0
      KK=10
      M(1)=KK
      M(2)=0
      M(3)=0
      FAC1=5.202/(.5*RHO*PSLOPE)
      FAC2=UMEAN/UMVCLT
      FAC3=CABS(H(1))
      FAC4=FAC1/FAC3
      FAC5=FAC2/FAC3
      FAC6=FAC2/(CABS(H(FRUN+1)))
C
      RANGE(1)=0.05
      RANGE(2)=0.0
      RANGE(3)=15.0
      RANGE(4)=-15.0
C
      DO 1002 I=1,512
      FREQ(I)=I-1
 1002 TIMEIT(I)=(I-1)*1.0/1024.
      DO 1 I=1,NBSKIP
    1 CALL INDATA(DATA)
      L=0
C
      DO 11 SIDE=1,2
      DO 11 HOLE=1,25
      L=L+1
C
      DO 3 IBLK=1,4
      J=(IBLK-1)*1024
      CALL INDATA(DATA)
      DO 3 JJ=1,1024
      I=J+JJ
    3 U(I)=DATA(JJ)
C
      CALL BMEAN(U,NOBLKS,BMU(SIDE,HOLE),BMSU(SIDE,HOLE))
C
      CALL BZERO(U,KIN,KOUT)
C
      KPHASE(SIDE,HOLE)=KOUT
      KSTART=KOUT
      KLAST=KSTART+1023
C
      BMU(SIDE,HOLE)=FAC5*BMU(SIDE,HOLE)
      BMSU(SIDE,HOLE)=(FAC6**2)*BMSU(SIDE,HOLE)
C
      DO 6 K=KSTART,KLAST
      I=K-KSTART+1
    6 A(I,1,1)=FAC2*U(K)
C
      IFSET=-1
      CALL HARM(A,M,INV,S,IFSET,IFERR)
C
      A(513,1,1)=A(513,1,1)/H(512)
      A(1,1,1)=A(1,1,1)/H(1)
      GX(1)=2.0*A(1,1,1)*CONJG(A(1,1,1))
      DO 21 I=2,512
      KCONJG=NTOT-I+2
      A(I,1,1)=A(I,1,1)/H(I)
      CON=CONJG(A(I,1,1))
      A(KCONJG,1,1)=CON
   21 GX(I)=2.0*A(1,1,1)*CON
C
      SUM=0.0
      DO 22 I=2,511
   22 SUM=SUM+GX(I)
      SUM=SUM+.5*GX(1)+.5*GX(512)
C
      IFSET=1
      CALL HARM(A,M,INV,S,IFSET,IFERR)
      DO 7 I=1,1024
```

```
    7 U(I)=A(I,1,1)
C
      WRITE(6,122)
      WRITE(6,102)
      WRITE(6,104) NRUN,SIDE,HOLE
      WRITE(6,120) BMU(SIDE,HOLE)
      CALL UTPLOT(TIMEIT,U,50,RANGE,1,0)
C
   11 CONTINUE
C
      WRITE(6,100)
      WRITE(6,102)
      WRITE(6,104) NRUN,SIDE,HOLE
      WRITE(6,105) SUM
      DO 61 LINE=1,128
      IX1=(LINE-1)*4+1
      IX2=IX1+3
      IF((LINE.EQ.44).OR.(LINE.EQ.89)) WRITE(6,107)
   61 WRITE(6,106)(IX,GX(IX),IX=IX1,IX2)
C
      WRITE(6,119)
      WRITE(6,102)
      WRITE(6,104) (NRUN,SIDE,HOLE)
      WRITE(6,120) BMU(SIDE,HOLE)
      DO 8001 LINE=1,89
      IX1=(LINE-1)*4+1
      IX2=IX1+3
      IF(L.EQ.44) WRITE(6,107)
 8001 WRITE(6,121)(IX,U(IX),IX=IX1,IX2)
C
      DO 1001 J=1,512
 1001 GX(J)=GX(J)/SUM
      CALL DRAW(480,FREQ,GX,0,0,LABC(L),ITIL4,60.0,0.2,
     *0,0,0,0,8,5,0,LAST)
      CALL DRAW(30,TIMEIT,U,0,2,LABEL, ITIL2,0.004,0.0,
     *0,0,0,0,8,4,0,LAST)
C
      RANGE(3)=9.0
      RANGE(4)=-.90
C
      L=0
C
      DO 13 SIDE=1,2
      DO 13 HOLE=1,25
C
      L=L+1
C
      DO 2 IBLK=1,4
      J=(IBLK-1)*1024
      CALL INDATA(DATA)
      DO 2 JJ=1,1024
      I=J+JJ
    2 P(I)=DATA(JJ)
C
      CALL BMEAN(P,NOBLKS,BMP(SIDE,HOLE),BMSP(SIDE,HOLE))
C
      CALL BZERO(P,KIN,KOUT)
      KSTART=KOUT+1
      KLAST=KSTART+1023
C
      FAC7=FAC1/(BMU(SIDE,HOLE)**2)
      BMP(SIDE,HOLE)=FAC4*BMP(SIDE,HOLE)/(BMU(SIDE,HOLE)**2)
C
      DO 4 K=KSTART,KLAST
      I=K-KSTART+1
    4 A(I,1,1)=FAC7*P(K)
C
      IFSET=-1
      CALL HARM(A,M,INV,S,IFSET,IFERR)
      A(513,1,1)=A(513,1,1)/(G(512)*H(512))
      A(1,1,1)=A(1,1,1)/(G(1)*H(1))
      GX(1)=2.0*A(1,1,1)*CONJG(A(1,1,1))
```

```
C
      DO 19 I=2,512
      A(I,1,1)=A(I,1,1)/(G(I)*H(I))
      KCONJG=NTOT-I+2
      CON=CONJG(A(I,1,1))
      A(KCONJG,1,1)=CON
   19 GX(I)=2.0*A(I,1,1)*CON
C
      SUM=0.0
      DO 20 I=2,511
   20 SUM=SUM+GX(I)
      SUM=.5*GX(1)+.5*GX(512)+SUM
C
      IFSET=1
      CALL HARM(A,M,INV,S,IFSET,IFERR)
      DO 5 I=1,1024
      P(I)=A(I,1,1)
    5 P(I)=P(I)+BMP(SIDE,HOLE)
C
      DO 12 I=1,1024
      IB=(L-1)*1024+I
   12 WRITE(1'IB) P(I)
C
      WRITE(6,119)
      WRITE(6,101)
      WRITE(6,104) NRUN,SIDE,HOLE
      WRITE(6,120) BMP(SIDE,HOLE)
      DO 8000 LINE=1,89
      IX1=(LINE-1)*4+1
      IX2=IX1+3
      IF(LINE.EQ.44) WRITE(6,107)
 8000 WRITE(6,114)(IX,P(IX),IX=IX1,IX2)
C
      DO 8002 I=1,1024
 8002 P(I)=P(I)-BMP(SIDE,HOLE)
      WRITE(6,122)
      WRITE(6,101)
      WRITE(6,104) NRUN,SIDE,HOLE
      WRITE(6,120) BMP(SIDE,HOLE)
      CALL UTPLOT(TIMEIT,P,50,RANGE,1,0)
C
      WRITE(6,100)
      WRITE(6,101)
      WRITE(6,104) NRUN,SIDE,HOLE
      WRITE(6,105) SUM
      DO 60 LINE=1,128
      IX1=(LINE-1)*4+1
      IX2=IX1+3
      IF((LINE.EQ.44).OR.(LINE.EQ.89)) WRITE(6,107)
   60 WRITE(6,106)(IX,GX(IX),IX=IX1,IX2)
C
      DO 8050 I=1,512
 8050 GX(I)=GX(I)/SUM
      CALL DRAW(480,FREQ,GX,0,0,LABC(L),ITIL3,60.0,0.2,
     *0,0,0,0,8,4,0,LAST)
C
   13 CONTINUE
C
      WRITE(2,5000) BMP
C
      DO 50 IT=1,1024
       DO 51 HOLE=1,50
      ID=(HOLE-1)*1024+IT
      READ(1'IB) Y(HOLE)
      SIDE=1
      IHOLE=HOLE
      IF(HOLE.GT.25) IHOLE=HOLE-25
      IF(HOLE.GT.25) SIDE=2
   51 Y(HOLE)=Y(HOLE)-BMP(SIDE,IHOLE)
C
      WRITE(2,5000) Y
C
```

```
      DO 52 HOLE=1,25
      Y(HOLE)=Y(HOLE+25)-Y(HOLE)
   52 X(HOLE)=Y(HOLE)*ETA(HOLE)
      CALL QTFG(ETA,Y,Y,NDIM)
      CN(IT)=Y(NDIM)
      CALL QTFG(ETA,X,X,NDIM)
      DATA(IT)=X(NDIM)
   50 CONTINUE
C
      SUM1=0.0
      SUM2=0.0
      DO 27 SIDE=1,2
      DO 27 HOLE=1,25
      SUM1=SUM1+BMU(SIDE,HOLE)
      SUM2=SUM2+BMSU(SIDE,HOLE)
   27 CONTINUE
      DO 36 SIDE=1,2
      DO 36 HOLE=1,25
   36 BMSU(SIDE,HOLE)=SQRT(2.0)*SQRT(BMSU(SIDE,HOLE))/
     *BMU(SIDE,HOLE)
      BMUA=SUM1/50.0
      BMSUA=SUM2/50.0
      UMA=BMUA
      UMSA=BMSUA
      RATIO=SQRT(2.0*UMSA)/UMA
      QMEAN=.5*RHO*UMA**2
C
      DO 29 HOLE=1,23
      Y(HOLE)=BMP(2,HOLE)-BMP(1,HOLE)
   29 X(HOLE)=Y(HOLE)*ETA(HOLE)
      CALL QTFG(ETA,Y,Y,NDIM)
      FNMEAN=Y(NDIM)
      CALL QTFG(ETA,X,X,NDIM)
      CMMEAN=X(NDIM)
      DO 31 I=1,1024
   31 DATA(I)=(CMMEAN+DATA(I))/(FNMEAN+CN(I))
C
      NOBLKS=1
      CALL BMEAN(DATA,NOBLKS,CPM,CPMS)
C
      WRITE(6,108)
      WRITE(6,110) NRUN,FRUN,RATIO,UMA,ALPHA
      WRITE(6,112) FNMEAN
      DO 32 LINE=1,89
      ICN1=(LINE-1)*4+1
      ICN2=ICN1+3
      IF(LINE .EQ. 44) WRITE(6,107)
   32 WRITE(6,113)(ICN,CN(ICN),ICN=ICN1,ICN2)
C
      WRITE(6,109)
      WRITE(6,110) NRUN,FRUN,RATIO,UMA,ALPHA
      WRITE(6,111) CPM
      DO 33 LINE=1,89
      ICP1=(LINE-1)*4+1
      ICP2=ICP1+3
      IF(LINE .EQ. 44) WRITE(6,107)
   33 WRITE(6,114)(ICP,DATA(ICP),ICP=ICP1,ICP2)
C
      WRITE(6,218) NRUN
      DO 37 HOLE=1,25
   37 WRITE(6,214) HOLE,ETA(HOLE),(BMSU(SIDE,HOLE),SIDE=1,2)
      WRITE(6,208)NRUN,UMA,UMSA,RATIO,QMEAN
      WRITE(6,213) NRUN
      DO 28 HOLE=1,25
   28 WRITE(6,214) HOLE,ETA(HOLE),(BMP(SIDE,HOLE),
     *SIDE=1,2)
      WRITE(6,215) NRUN,FNMEAN
C
      DO 34 I=1,1024
   34 A(I,1,1)=CN(I)
      IFSET=-1
      CALL HARM(A,M,INV,S,IFSET,IFERR)
```

```
      SUM=0.0
      DO 35 I=1,512
      GX(I)=2.0*A(I,1,1)*CONJG(A(I,1,1))
   35 SUM=SUM+GX(I)
      SUM=SUM-.5*GX(1)-.5*GX(512)
C
      WRITE(6,100)
      WRITE(6,115)
      WRITE(6,110) NRUN,FRUN,RATIO,UMA,ALPHA
      WRITE(6,105) SUM
      DO 38 LINE=1,128
      ICN1=(LINE-1)*4+1
      ICN2=ICN1+3
      IF((LINE.EQ.44).OR.(LINE.EQ.89)) WRITE(6,107)
   38 WRITE(6,106)(ICN,GX(ICN),ICN=ICN1,ICN2)
C
      DO 1004 HOLE=1,23
 1004 Y(HOLE)=-BMP(1,HOLE)
      CALL DRAW(23,ETA,Y,1,3,LABEL,ITIL5,0.2,1.0,
     *0,0,0,0,8,4,0,LAST)
      DO 1005 HOLE=1,23
 1005 Y(HOLE)=-BMP(2,HOLE)
      CALL DRAW(23,ETA,Y,3,5,LABEL,ITIL5,0.2,1.0,
     *0,0,0,0,8,4,0,LAST)
C
      CALL DRAW(30,TIMEIT,CN,0,2,LABEL,ITIL7,0.004,0.0,
     *0,0,0,0,8,4,0,LAST)
      DO 1006 I=1,512
 1006 GX(I)=GX(I)/SUM
      CALL DRAW(480,FREQ,GX,0,0,LABEL,ITIL6,60.0,0.2,
     *0,0,0,0,8,5,0,LAST)
C
      DO 39 I=1,1024
   39 A(I,1,1)=DATA(I)
      IFSET=-2
      CALL HARM(A,M,INV,S,IFSET,IFERR)
      SUM=0.0
      DO 40 I=1,512
      GX(I)=2.0*A(I,1,1)*CONJG(A(I,1,1))
   40 SUM=SUM+GX(I)
      SUM=SUM-.5*GX(1)-.5*GX(512)
C
      WRITE(6,100)
      WRITE(6,116)
      WRITE(6,110) NRUN,FRUN,RATIO,UMA,ALPHA
      WRITE(6,105) SUM
      DO 41 LINE=1,128
      ICP1=(LINE-1)*4+1
      ICP2=ICP1+3
      IF((LINE.EQ.44).OR.(LINE.EQ.89)) WRITE(6,107)
   41 WRITE(6,106)(ICP,GX(ICP),ICP=ICP1,ICP2)
C
      DO 1008 I=1,512
 1008 GX(I)=GX(I)/SUM
      CALL DRAW(480,FREQ,GX,0,0,LABEL,ITIL8,60.0,0.2,
     *0,0,0,0,8,5,0,LAST)
C
      DO 42 I=1,1024
   42 P(I)=CN(I)
      KKR=9
      CALL RHARM(P,KKR,INV,S,IFERR)
      WRITE(6,100)
      WRITE(6,117)(P(I),I=1,1026)
      DO 43 I=1,1024
   43 P(I)=DATA(I)
      CALL RHARM(P,KKR,INV,S,IFERR)
      WRITE(6,100)
      WRITE(6,117)(P(I),I=1,1026)
      CALL RHARM(U,KKR,INV,S,IFERR)
      WRITE(6,100)
      WRITE(6,117)(U(I),I=1,1026)
C
```

```
100 FORMAT(1H1,///////,T53,'TABLE',/,
   *T46,'POWER SPECTRAL DENSITY')
101 FORMAT(T42,'UNSTEADY PRESSURE COEFFICIENT')
102 FORMAT(T49,'UNSTEADY VELOCITY')
104 FORMAT(T42,'RUN',I2,T53,'SIDE',I2,T66,'TAP',I3)
105 FORMAT(T48,'MEAN SQUARE=',F7.3)
106 FORMAT(13X,4('GX(',I3,')=',E10.3,4X))
107 FORMAT(1H1,///////,T47,'TABLE    (CONTINUED)',/)
108 FORMAT(1H1,///////,T53,'TABLE',/,
   *T41,'UNSTEADY NORMAL FORCE COEFFICIENTS')
109 FORMAT(1H1,///////,T53,'TABLE',/,
   *T43,'UNSTEADY CENTER OF PRESSURE')
110 FORMAT(T12,'RUN',I2,2X,'FREQUENCY=',I2,' HZ',2X,
   *'EPS=',F5.3,2X,'MEAN VELOCITY=',F6.2,' FT/SEC',
   *2X,'ALPHA=',I2,' DEG',2X,'SF=1024 HZ')
111 FORMAT(T42,'MEAN CENTER OF PRESSURE=',F6.3)
112 FORMAT(T39,'MEAN NORMAL FORCE COEFFICIENT=',F6.3)
113 FORMAT(11X,4('CN(',I3,')=',F6.3,11X))
114 FORMAT(11X,4('CP(',I3,')=',F6.3,11X))
115 FORMAT(T41,'UNSTEADY NORMAL FORCE COEFFICIENT')
116 FORMAT(T43,'UNSTEADY CENTER OF PRESSURE')
117 FORMAT(1X,10E10.2)
119 FORMAT(1H1,///////,T53,'TABLE')
120 FORMAT(T50,'MEAN=',F8.3)
121 FORMAT(11X,4('U(',I3,')=',F7.3,10X))
122 FORMAT(1H1)
200 FORMAT(T32,'THE AVERAGE MEAN VELOCITY FOR RUN',I3,/,
   *T32,'WAS',F7.2,/,
   *T32,'THE AVERAGE MEAN SQUARE WAS',F7.2,/,
   *T32,'THE RATIO OF UNSTEADY TO STEADY WAS',F7.4,/,
   *T32,'THE AVERAGE Q WAS',F7.2)
213 FORMAT(1H1,///////,T53,'TABLE',/,
   *T32,'MEAN PRESSURE COEFFICIENTS',/,
   *T32,'RUN',I3,/,
   *T32,'TAP',T39,'LOCATION',T50,'CP UPPER',
   *     T60,'CP LOWER')
214 FORMAT(32X,I2,6X,F5.3,6X,F6.3,5X,F6.3)
215 FORMAT(//,T32,'THE MEAN NORMAL FORCE COEFFICIENT FOR'
   *,' RUN',I3,/,
   *T32,'IS',F6.3)
218 FORMAT(1H1,///////,T53,'TABLE',/,
   *T32,'RATIO OF SQRT(2)*SQRT(VELOCITY',
   *' MEAN SQUARE) TO MEAN VELOCITY',/,
   *T32,'RUN',I3,/,
   *T32,'TAP',T39,'LOCATION',T50,'UPPER',T60,'LOWER')
501 FORMAT(5I5)
503 FORMAT(5F10.0)
502 FORMAT(16F5.2)
504 FORMAT(8E10.3)
505 FORMAT(20A4)
5100 FORMAT(50A4)
     STOP
     END


     SUBROUTINE QTFG(X,Y,Z,NDIM)
     DIMENSION X(1),Y(1),Z(1)
     SUM2=0.
     DO 2 I=2,NDIM
     SUM1=SUM2
     SUM2=SUM2+0.5*(X(I)-X(I-1))*(Y(I)+Y(I-1))
   2 Z(I-1)=SUM1
   3 Z(NDIM)=SUM2
   4 RETURN
     END
```

```
      SUBROUTINE BMEAN(P,NOBLKS,BM,BMS)
      DIMENSION P(1)
      MK=0
      BMS=0.0
      BM=0.0
    1 DO 5 I=1,NOBLKS
      J=(I-1)*1024
      SUM=0.0
      DO 3 II=1,1024
      JJ=J+II
      IF(MK .EQ. 0) GO TO 2
      SUM=SUM+P(JJ)**2
      GO TO 3
    2 SUM=SUM+P(JJ)
    3 CONTINUE
      SUM=SUM/1024
      IF (MK .EQ. 0)          GO TO 4
      BMS=BMS+SUM
      GO TO 5
    4 BM=BM+SUM
    5 CONTINUE
      IF (MK .EQ. 2)  GO TO 6
      BMS=BMS/NOBLKS
      GO TO 8
    6 BM=BM/NOBLKS
      DO 7 I=1,JJ
    7 P(I)=P(I)-BM
      MK=1
      GO TO 1
    8 CONTINUE
  101 FORMAT    (20X,'NOBLKS=',I2,/,20X,'MEAN=',F10.4,/,20X,
     *'=',F10.4,//)
  103 FORMAT(20X,'THE FOLLOWING ARRAY LISTS THE INPUT TIME H
     *,/,   20X,'ZERO MEAN AND NORMALIZED WITH RESPECT TO TH
     *E',//)
  102 FORMAT(1X,10E11.3)
      RETURN
      END


      SUBROUTINE INDATA(DATA)
      DIMENSION DATA(1024)
    1 FORMAT(16(64A4))
      READ(4,1) DATA
      RETURN
      END


      SUBROUTINE BZERO(X,KIN,KOUT)
      DIMENSION X(1)
      XZERO=1.0
      KOUT=1
       DO 1 K=21,KIN
      IF(X(K).GT. 0.0) GO TO 1
      IF(X(K+1) .LT. 0.0) GO TO 1
      IF((X(K-1).GT.0.0).OR.(X(K-2).GT.0.0)) GO TO 1
      CK=ABS(X(K))
      CKP1=ABS(X(K+1))
      IF(CK.LT.CKP1) GO TO 2
      KTRY=K+1
      XTRY=CKP1
      IF(XTRY.LT.XZERO) GO TO 3
      GO TO 1
    2 KTRY=K
      XTRY=CK
      IF(XTRY.LT.XZERO) GO TO 3
      GO TO 1
    3 KOUT=KTRY
```

```
      ENTRY LTHOLD(X,Y,NDATA,RANGE,KKZ,MODCUR)
  444 IF(MODCUR.EQ.2.OR.MODCUR.EQ.1)JSET=0
      JSET=JSET+1
      IF(JSET.GT.4) JSET=1
      DO 700 I=1,NDATA,KKZ
      IPTX=60.*(YMAX-Y(I))/YRANGE+1.5
      IPTY=80.*(X(I)-XMIN)/XRANGE+1.5
      IF(IPTX.GT.61.OR.IPTY.GT.81) GO TO 70
      IF(IPTX.LE.0.OR.IPTY.LE.0)GO TO 70
      GRID(IPTX,IPTY) = XCHAR(JSET)
      GO TO 700
   70 IERR=IERR+1
  700 CONTINUE
C
C     COMPUTE PROPER SCALE NUMBERS
C
      IF(MODCUR.EQ.0.OR.MODCUR.EQ.1) GO TO 8000
      IF(MODCUR.EQ.2) RETURN
      GO TO 922
 8000 XINCR=XRANGE/4.
      YINCR=YRANGE/6.
      XSCALE(1)=XMAX
      YSCALE(1)=YMAX
      DO 80 I=2,5
   80 XSCALE(I)=XSCALE(I-1)-XINCR
      DO 81 I=2,7
   81 YSCALE(I)=YSCALE(I-1)-YINCR
C
C     OUTPUT SECTION WITH GRAPH
C
      IF(MODCUR.EQ.0.OR.MODCUR.EQ.3)GO TO 922
      RETURN
   17 FORMAT(12X,
     1          1P E10.3,4(10X,E10.3)/15X,2H**,8(10H**********
  922 WRITE(6,17) XSCALE(5),XSCALE(4),XSCALE(3),XSCALE(2),XS
      II=1
      I=0
      DO 101 IK=1,61
      IF(I)91,91,92
   91 WRITE(6,18) YSCALE(II),(GRID(IK,IX),IX=1,81),YSCALE(II
   18 FORMAT(3X,1P
     1           E10.3,2X,1H+,1X,81A1,1X,1H+,2X,F10.3)
      II=II+1
      GOTO 102
   92 WRITE(6,19) (GRID(IK,IX),IX=1,81)
   19 FORMAT(15X,1H*,1X,81A1,1X,1H*)
  102 I=I+1
      IF(I-10)101,103,103
  103 I=0
  101 CONTINUE
      WRITE(6,22) XSCALE(5),XSCALE(4),XSCALE(3),XSCALE(2),XS
   22 FORMAT(15X,2H**,8(10H**********),3H***/  1P
     1                                        12X,E10.3,4(10X
      IF(IERR) 1000,1000,1001
 1001 WRITE(6,20) IERR
   20 FORMAT(10X 'NUMBER OF POINTS OUT OF RANGE ='  I4)
 1000 RETURN
      END
```

```
      INV(1)=0
      DO 980 L=1,MT
      INV(LM1EXP+1) = MTLEXP
      DO 970 J=2,LM1EXP
      JJ=J+LM1EXP
  970 INV(JJ)=INV(J)+MTLEXP
      MTLEXP=MTLEXP/2
  980 LM1EXP=LM1EXP*2
  982 IF(IFSET)12,895,12
      END


      SUBROUTINE UTPLOT (X   ,Y   ,NDATA,RANGE,KKZ,MODCUR)
      DIMENSION GRID(61,81),XSCALE(5),YSCALE(7)
      DIMENSION X   (1),Y   (1),RANGE(4)
      INTEGER*2 GRID,BLANK,DOT,XCHAR(4)/1H.,1H+,1H*,1HX/
      DATA DOT,BLANK/Z4B40,Z4040/
C
C     GRID IS THE MATRIX USED TO PLOT THE POINTS
C
      IERR=0
      XMAX=RANGE(1)
      XMIN=RANGE(2)
      YMAX=RANGE(3)
      YMIN=RANGE(4)
C
C     CHECKING X AND Y POINTS AND PLOTTING THOSE OUT OF RANG
C     AT THE MARGIN
C
      DO 30  I=1,NDATA,KKZ
      IF(X   (I)-XMAX) 205,205,220
  220 X   (I)=XMAX
      IERR=IERR+1
      GOTO 210
  205 IF(X   (I)-XMIN)203,210,210
  203 X   (I)=XMIN
      IERR=IERR+1
  210 IF(Y   (I)-YMAX)215,215,212
  212 Y   (I)=YMAX
      IERR=IERR+1
      GOTO 30
  215 IF(Y   (I)-YMIN)217,  30,30
  217 Y   (I)=YMIN
      IERR=IERR+1
C
   30 CONTINUE
C
C     PLOTTING X AND Y AXIS , IF NECESSARY
C
      XRANGE=XMAX-XMIN
      YRANGE=YMAX-YMIN
C
C     BLANKING OUT MATRIX-(GRID)
C
      DO 300 I=1,61
      DO 301 JJ=1,81
301   GRID(I,JJ)=BLANK
  300 CONTINUE
      YTEST=YMAX*YMIN
      XTEST=XMAX*XMIN
      IF(XTEST)1,222,222
  222 IF(YTEST)333,444,444
    1 IYAXIS=80.*(-XMIN)/XRANGE+1.5
      DO 40  I=1,61
   40 GRID(I,IYAXIS)=DOT
      GOTO 222
  333 IXAXIS=60.*YMAX/YRANGE+1.5
      DO 60  I=1,81
   60 GRID(IXAXIS,I)=DOT
C
C     PLACING POINTS IN THEIR PROPER GRID POSITIONS
C
```

```
      GO TO 830
  820 IP1=INV(JP1)/NTVN1
  830 I=2*(IPP1+IP1)+1
      IF (J-I) 840,845,845
  840 T=A(I)
      A(I)=A(J)
      A(J)=T
      T=A(I+1)
      A(I+1)=A(J+1)
      A(J+1)=T
  845 CONTINUE
  850 J=J+2
  860 JJ1=JJ1+JJD1
C     END OF JPP1 AND JP2
C
  870 JJ2=JJ2+JJD2
C     END OF JPP2 AND JP3 LOOPS
C
  880 JJ3 = JJ3+JJD3
C     END OF JPP3 LOOP
C
  890 IF(IFSET)891,895,895
  891 DO 892 I = 1,NX
  892 A(2*I) = -A(2*I)
  895 RETURN
C
C     THE FOLLOWING PROGRAM COMPUTES THE SIN AND INV TABLES.
C
  900 MT=MAXO(M(1),M(2),M(3)) -2
      MT = MAXO(2,MT)
  904 IF (MT-18)906,906,905
  905 IFERR = 1
      GO TO 895
  906 IFERR=0
      NT=2**MT
      NTV2=NT/2
C
C     SET UP SIN TABLE
C     THETA=PIE/2**(L+1) FOR L=1
  910 THETA=.7853981634
C
C     JSTEP=2**(MT-L+1) FOR L=1
      JSTEP=NT
C
C     JDIF=2**(MT-L) FOR L=1
C     JDIF=2**(MT-L) FOR L=1
      JDIF=NTV2
      S(JDIF)=SIN(THETA)
      DO 950 L=2,MT
      THETA=THETA/2.
      JSTEP2=JSTEP
      JSTEP=JDIF
      JDIF=JSTEP/2
      S(JDIF)=SIN(THETA)
      JC1=NT-JDIF
      S(JC1)=COS(THETA)
      JLAST=NT-JSTEP2
      IF(JLAST - JSTEP) 950,920,920
  920 DO 940 J=JSTEP,JLAST,JSTEP
      JC=NT-J
      JD=J+JDIF
  940 S(JD)=S(J)*S(JC1)+S(JDIF)*S(JC)
  950 CONTINUE
C
C     SET UP INV(J) TABLE
C
  960 MTLEXP=NTV2
C
C     MTLEXP=2**(MT-L). FOR L=1
      LM1EXP=1
C
C     LM1EXP=2**(L-1). FOR L=1
```

```
C       BIT-REVERSED.  THE FOLLOWING ROUTINE PUTS THEM IN ORDE
        NTSQ=NT*NT
        M3MT=M3-MT
  350   IF(M3MT) 370,360,360
C
C       M3 GR. OR EQ. MT
  360   ICC3=1
        N3VNT=N3/NT
        MINN3=NT
        GO TO 380
C
C       M3 LESS THAN MT
  370   ICC3=2
        N3VNT=1
        NTVN3=NT/N3
        MINN3=N3
  380   JJD3 = NTSQ/N3
        M2MT=M2-MT
  450   IF (M2MT)470,460,460
C
C       M2 GR. OR EQ. MT
  460   IGC2=1
        N2VNT=N2/NT
        MINN2=NT
        GO TO 480
C
C       M2 LESS THAN MT
  470   IGC2 = 2
        N2VNT=1
        NTVN2=NT/N2
        MINN2=N2
  480   JJD2=NTSQ/N2
        M1MT=M1-MT
  550   IF(M1MT)570,560,560
C
C       M1 GR. OR EQ. MT
  560   IGC1=1
        N1VNT=N1/NT
        MINN1=NT
        GO TO 580
C
C       M1 LESS THAN MT
  570   IGC1=2
        N1VNT=1
        NTVN1=NT/N1
        MINN1=N1
  580   JJD1=NTSQ/N1
  600   JJ3=1
        J=1
        DO 880 JPP3=1,N3VNT
        IPP3=INV(JJ3)
        DO 870 JP3=1,MINN3
        GO TO (610,620),IGC3
  610   IP3=INV(JP3)*N3VNT
        GO TO 630
  620   IP3=INV(JP3)/NTVN3
  630   I3=(IPP3+IP3)*N2
  700   JJ2=1
        DO 870 JPP2=1,N2VNT
        IPP2=INV(JJ2)+I3
        DO 860 JP2=1,MINN2
        GO TO (710,720),IGC2
  710   IP2=INV(JP2)*N2VNT
        GO TO 730
  720   IP2=INV(JP2)/NTVN2
  730   I2=(IPP2+IP2)*N1
  800   JJ1=1
        DO 860 JPP1=1,N1VNT
        IPP1=INV(JJ1)+I2
        DO 850 JP1=1,MINN1
        GO TO (810,820),IGC1
  810   IP1=INV(JP1)*N1VNT
```

```
  170 I3C=-I3C
      W3(1)=-S(I3C)
      W3(2)=S(I3CC)
      GO TO 200
  180 W3(1)=-1.
      W3(2)=0.
      GO TO 200
C
C     3*I IN THIRD QUADRANT
  190 I3CCC=NT+I3CC
      I3CC = -I3CC
      W3(1)=-S(I3CCC)
      W3(2)=-S(I3CC)
  200 ILAST=IL+JJ
      DO 220 I=JJ,ILAST,IDIF
      KLAST=KL+I
      DO 220 K=I,KLAST,2
      K1=K+KBIT
      K2=K1+KBIT
      K3=K2+KBIT
C
C     DO TWO STEPS WITH J NOT 0
C     A(K)=A(K)+A(K2)*W2
C     A(K2)=A(K)-A(K2)*W2
C     A(K1)=A(K1)*W+A(K3)*W3
C     A(K3)=A(K1)*W-A(K3)*W3
C
C     A(K)=A(K)+A(K1)
C     A(K1)=A(K)-A(K1)
C     A(K2)=A(K2)+A(K3)*I
C     A(K3)=A(K2)-A(K3)*I
C
      R=A(K2)*W2(1)-A(K2+1)*W2(2)
      T=A(K2)*W2(2)+A(K2+1)*W2(1)
      A(K2)=A(K)-R
      A(K)=A(K)+R
      A(K2+1)=A(K+1)-T
      A(K+1)=A(K+1)+T
C
      R=A(K3)*W3(1)-A(K3+1)*W3(2)
      T=A(K3)*W3(2)+A(K3+1)*W3(1)
      AWR=A(K1)*W(1)-A(K1+1)*W(2)
      AWI=A(K1)*W(2)+A(K1+1)*W(1)
      A(K3)=AWR-R
      A(K3+1)=AWI-T
      A(K1)=AWR+R
      A(K1+1)=AWI+T
      T=A(K1)
      A(K1)=A(K)-T
      A(K)=A(K)+T
      T=A(K1+1)
      A(K1+1)=A(K+1)-T
      A(K+1)=A(K+1)+T
      R=-A(K3+1)
      T=A(K3)
      A(K3)=A(K2)-R
      A(K2)=A(K2)+R
      A(K3+1)=A(K2+1)-T
  220 A(K2+1)=A(K2+1)+T
C     END OF I AND K LOOPS
C
  230 JJ=JJDIF+JJ
C     END OF J-LOOP
C
  235 JLAST=4*JLAST+3
  240 CONTINUE
C     END OF  L  LOOP
C
  250 CONTINUE
C     END OF  ID  LOOP
C
C     WE NOW HAVE THE COMPLEX FOURIER SUMS BUT THEIR ADDRESS
```

```
      R =-A(K2+1)
      T = A(K2)
      A(K2) = A(K)-R
      A(K) = A(K)+R
      A(K2+1)=A(K+1)-T
      A(K+1)=A(K+1)+T
C
      AWR=A(K1)-A(K1+1)
      AWI = A(K1+1)+A(K1)
      R=-A(K3)-A(K3+1)
      T=A(K3)-A(K3+1)
      A(K3)=(AWR-R)/ROOT2
      A(K3+1)=(AWI-T)/ROOT2
      A(K1)=(AWR+R)/ROOT2
      A(K1+1)=(AWI+T)/ROOT2
      T= A(K1)
      A(K1)=A(K)-T
      A(K)=A(K)+T
      T=A(K1+1)
      A(K1+1)=A(K+1)-T
      A(K+1)=A(K+1)+T
      R=-A(K3+1)
      T=A(K3)
      A(K3)=A(K2)-R
      A(K2)=A(K2)+R
      A(K3+1)=A(K2+1)-T
   35 A(K2+1)=A(K2+1)+T
      IF(JLAST-1) 235,235,90
   90 JJ= JJ + JJDIF
C
C     NOW DO THE REMAINING J'S
      DO 230 J=2,JLAST
C
C     FETCH W'S
C     DEF- W=W**INV(J), W2=W**2, W3=W**3
   96 I=INV(J+1)
   98 IC=NT-I
      W(1)=S(IC)
      W(2)=S(I)
      I2=2*I
      I2C=NT-I2
      IF(I2C)120,110,100
C
C     2*I IS IN FIRST QUADRANT
  100 W2(1)=S(I2C)
      W2(2)=S(I2)
      GO TO 130
  110 W2(1)=0.
      W2(2)=1.
      GO TO 130
C
C     2*I IS IN SECOND QUADRANT
  120 I2CC = I2C+NT
      I2C=-I2C
      W2(1)=-S(I2C)
      W2(2)=S(I2CC)
  130 I3=I+I2
      I3C=NT-I3
      IF(I3C)160,150,140
C
C     I3 IN FIRST QUADRANT
  140 W3(1)=S(I3C)
      W3(2)=S(I3)
      GO TO 200
  150 W3(1)=0.
      W3(2)=1.
      GO TO 200
C
  160 I3CC=I3C+NT
      IF(I3CC)190,180,170
C
C     I3 IN SECOND QUADRANT
```

```
      KBIT=KBIT/4
      KL=KBIT-2
C
C     DO FOR J=0
      DO 80  I=1,IL1,IDIF
      KLAST=I+KL
      DO 80  K=I,KLAST,2
      K1=K+KBIT
      K2=K1+KBIT
      K3=K2+KBIT
C
C     DO TWO STEPS WITH J=0
C     A(K)=A(K)+A(K2)
C     A(K2)=A(K)-A(K2)
C     A(K1)=A(K1)+A(K3)
C     A(K3)=A(K1)-A(K3)
C
C     A(K)=A(K)+A(K1)
C     A(K1)=A(K)-A(K1)
C     A(K2)=A(K2)+A(K3)*I
C     A(K3)=A(K2)-A(K3)*I
C
      T=A(K2)
      A(K2)=A(K)-T
      A(K)=A(K)+T
      T=A(K2+1)
      A(K2+1)=A(K+1)-T
      A(K+1)=A(K+1)+T
C
      T=A(K3)
      A(K3)=A(K1)-T
      A(K1)=A(K1)+T
      T=A(K3+1)
      A(K3+1)=A(K1+1)-T
      A(K1+1)=A(K1+1)+T
C
      T=A(K1)
      A(K1)=A(K)-T
      A(K)=A(K)+T
      T=A(K1+1)
      A(K1+1)=A(K+1)-T
      A(K+1)=A(K+1)+T
C
      R=-A(K3+1)
      T = A(K3)
      A(K3)=A(K2)-R
      A(K2)=A(K2)+R
      A(K3+1)=A(K2+1)-T
   80 A(K2+1)=A(K2+1)+T
      IF (JLAST) 235,235,82
   82 JJ=JJDIF    +1
C
C     DO FOR J=1
      ILAST= IL  +JJ
      DO 85  I = JJ,ILAST,IDIF
      KLAST = KL+I
      DO 85 K=I,KLAST,2
      K1 = K+KBIT
      K2 = K1+KBIT
      K3 = K2+KBIT
C
C     LETTING W=(1+I)/ROOT2,W3=(-1+I)/ROOT2,W2=I,
C     A(K)=A(K)+A(K2)*I
C     A(K2)=A(K)-A(K2)*I
C     A(K1)=A(K1)*W+A(K3)*W3
C     A(K3)=A(K1)*W-A(K3)*W3
C
C     A(K)=A(K)+A(K1)
C     A(K1)=A(K)-A(K1)
C     A(K2)=A(K2)+A(K3)*I
C     A(K3)=A(K2)-A(K3)*I
C
```

```
      XZERO=XTRY
      IF(XZERO.LT.0.00001) GO TO 5
    1 CONTINUE
    5 RETURN
      END


      SUBROUTINE HARM(A,M,INV,S,IFSET, IERR)
      DIMENSION A(1),INV(1),S(1),N(3),M(3),NP(3),W(2),W2(2),
      EQUIVALENCE (N1,N(1)),(N2,N(2)),(N3,N(3))
   10 IF( IABS(IFSET) - 1) 900,900,12
   12 MTT=MAXO(M(1),M(2),M(3)) -2
      ROOT2 = SQRT(2.)
      IF (MTT-MT ) 14,14,13
   13 IERR=1
      RETURN
   14 IERR=0
      M1=M(1)
      M2=M(2)
      M3=M(3)
      N1=2**M1
      N2=2**M2
      N3=2**M3
   16 IF(IFSET) 18,18,20
   18 NX= N1*N2*N3
      FN = NX
      DO 19 I = 1,NX
      A(2*I-1) = A(2*I-1)/FN
   19 A(2*I) = -A(2*I)/FN
   20 NP(1)=N1*2
      NP(2)= NP(1)*N2
      NP(3)=NP(2)*N3
      DO 250 ID=1,3
      IL = NP(3)-NP(ID)
      IL1 = IL+1
      MI = M(ID)
      IF (MI)250,250,30
   30 IDIF=NP(ID)
      KBIT=NP(ID)
      MEV = 2*(MI/2)
      IF (MI - MEV )60,60,40
C
C     M IS ODD. DO L=1 CASE
   40 KBIT=KBIT/2
      KL=KBIT-2
      DO 50 I=1,IL1,IDIF
      KLAST=KL+I
      DO 50 K=I,KLAST,2
      KD=K+KBIT
C
C     DO ONE STEP WITH L=1,J=0
C     A(K)=A(K)+A(KD)
C     A(KD)=A(K)-A(KD)
C
      T=A(KD)
      A(KD)=A(K)-T
      A(K)=A(K)+T
      T=A(KD+1)
      A(KD+1)=A(K+1)-T
   50 A(K+1)=A(K+1)+T
      IF (MI - 1)250,250,52
   52 LFIRST =3
C
C     DEF - JLAST = 2**(L-2) -1
      JLAST=1
      GO TO 70
C
C     M IS EVEN
   60 LFIRST = 2
      JLAST=0
   70 DO 240 L=LFIRST,MI,2
      JJDIF=KBIT
```

TAPE CONVERSION PROGRAM

THE ASSEMBLER LANGUAGE PROGRAM 'FORM' THAT DOES THE
ACTUAL BIT CONVERSION WAS WRITTEN BY PIMCORN C. ZELENY
OF THE NAVAL POSTGRADUATE SCHOOL COMPUTER FACILITY STAFF

```
C   THIS PROGRAM CONVERTS 7 TRACK, 24 BIT WORD TAPE
C   TO 9 TRACK 32 BIT WORD TAPE.
      DIMENSION INDATA(1024),DATA(1024)
      FACTOR=100.0/(2**31-1)
      REWIND 2
      REWIND 4
      NOBLKS=1
C     DO J=1,K     WHERE K IS THE NUMBER OF BLOCKS OF 1024 EAC
      DO 31 J=1,1000
      READ(2,3,ERR=50) INDATA
      CALL FORM(INDATA)
      DO 1 I=1,1024
    1 DATA(I)=INDATA(I)*FACTOR
      WRITE (4,3) DATA
      CALL BMEAN(DATA,NOBLKS,BM,BMS)
      WRITE(6,70)J,BM,BMS
      GO TO 31
   50 WRITE (6,51) J
   31 CONTINUE
    3 FORMAT(16(64A4))
   51 FORMAT ('0',5X,'READ ERROR, RECORD NO.=',I6)
   66 FORMAT(1X,10E10.2)
   70 FORMAT(10X,'RECORD NO=',I6,'    MEAN=',F8.3,'    MEAN SQ
     *F10.3)
      STOP
      END


      SUBROUTINE BMEAN(P,NOBLKS,BM,BMS)
      DIMENSION P(1)
      MK=0
      BMS=0.0
      BM=0.0
    1 DO 5 I=1,NOBLKS
      J=(I-1)*1024
      SUM=0.0
      DO 3 II=1,1024
      JJ=J+II
      IF(MK .EQ. 0) GO TO 2
      SUM=SUM+P(JJ)**2
      GO TO 3
    2 SUM=SUM+P(JJ)
    3 CONTINUE
      SUM=SUM/1024
      IF (MK .EQ. 0)          GO TO 4
      BMS=BMS+SUM
      GO TO 5
    4 BM=BM+SUM
    5 CONTINUE
      IF (MK .EQ. 0)  GO TO 6
      BMS=BMS/NOBLKS
      GO TO 8
    6 BM=BM/NOBLKS
      DO 7 I=1,JJ
    7 P(I)=P(I)-BM
      MK=1
      GO TO 1
    8 CONTINUE
      RETURN
      END
```

```
      SUBROUTINE FORM(INDATA)
FORM      START 0
*         SUBROUTINE FORM(INDATA)
*
* THIS SUBROUTINE WILL CONVERT 24 BIT BINARY WORDS STORED IN
* AN ARRAY LENGTH SPECIFIED BY THE INDEX VALUE TO 32 BIT BIN
* AND PLACE THESE SAME WORDS BACK INTO INDATA
*
*
*
          STM    14,12,12(13)        THIS SUBROUTINE CONVERTS
          BALR   6,0                 24 BIT BINARY WORDS TO
          USING  *,6                 32 BIT WORDS
          USING  DATA,7
          SR     7,7
          L      11,=F'1024'         THIS IS THE INDEX VALUE
          L      12,0(1)
LOOP      L      2,NUM(12)
          LR     3,7
          SRDL   2,8
          SRL    2,3
          SRDL   2,8
          SRL    2,2
          SRDL   2,8
          SRL    2,2
          SRDL   2,8
          ST     3,NUM(12)
          LA     12,4(12)
          BCT    11,LOOP
          LM     2,12,28(13)
          MVI    12(13),X'FF'
          BCR    15,14
DATA      DSECT
NUM       DS     1F
          END
```

DISPLAY PROGRAM

THE SUBROUTINES THAT GIVE THE POINT PLOT ON THE IBM 2250
DISPLAY UNIT WERE WRITTEN BY LT.(JG) G.J. VORHOFF,
DEPARTMENT OF AERONAUTICAL ENGINEERING,
NAVAL POSTGRADUATE SCHOOL

```
      INTEGER HOLE
      DIMENSION Y(50),CPU(25),CPL(25),RANGE(4),ETA(25),
     *CPM(2,25)
      REAL*4 TITLE(15)/'UNSTEADY PRESSURE COEFFICIENTS VS ET
     *          '/
      NDIM=23
      RANGE(1)=1.
      RANGE(2)=0.
      RANGE(3)=6.
      RANGE(4)=-1.
      READ(5,101)(ETA(I),I=1,25)
  101 FORMAT(16F5.0)
      CALL GGSP
9997  CONTINUE
      DO 1 IT=1,1 24
      READ(4,102) Y
  102 FORMAT(50A4)
      IF(IT.NE.1) GO TO 3
      L=0
      DO 2 I=2,50,2
      L=L+1
      CPL(L)=-Y(I-1)
      CPM(1,L)=CPU(L)
      CPL(L)=-Y(I)
    2 CPM(2,L)=CPL(L)
      GO TO 6
    3 DO 4 I=1,25
    4 CPU(I)=-Y(I)+CPM(1,I)
      DO 5 I=26,5
      J=I-25
    5 CPL(J)=-Y(I)+CPM(2,J)
    6 CONTINUE
      CALL UTPCRT(ETA,CPU,NDIM,RANGE,1,1,TITLE,&9998,&9999)
      CALL UPHCRT(ETA,CPL,NDIM,RANGE,1,3,TITLE,IJ,IK,&9998,&
    1 CONTINUE
9998  CONTINUE
      CALL GGSP
      GO TO 9997
9999  CONTINUE
      STOP
      END


      SUBROUTINE UTPCRT(U,V,NDATA,RANGE,KKZ,MODCUR,TITLE,*,*
C
C  UTPCRT PRODUCES A POINT-PLOT ON THE 2250 GRAPHIC DISPLAY.
C  U IS THE VECTOR OF ABSCISSAE
C  V IS THE VECTOR OF ORDINATES
C  NDATA IS THE LENGTH OF VECTORS U, AND V  (THE NUMBER OF P
C  RANGE IS THE SCALING VECTOR:
C    RANGE(1) = MAXIMUM DESIRED X VALUE PLOTTED
C    RANGE(2) = MINIMUM DESIRED X VALUE PLOTTED
C    RANGE(3) = MAXIMUM DESIRED Y VALUE PLOTTED
C    RANGE(4) = MINIMUM DESIRED Y VALUE PLOTTED
C  EVERY KKZ'TH ELEMENT OF THE INPUT LISTS WILL BE PLOTTED
C  USER SETS MODCUR = 0
C  TITLE IS EITHER THE NAME OF A 60-BYTE ARRAY OR A 60-CHARA
C  CONSTANT.
C  DATA SET FT09F001 MUST BE PROVIDED, DCB=(RECFM=F,LRECL=80
C  FIRST RETURN IS FOR RESTART, SECOND FOR TERMINATION
C
      COMMON/IGNORE/NULL,IDEV,IGSPNM
C
      DIMENSION A(4),B(4)  ,XSCALE(5),YSCALE(5)
```

```
     1,NULL(1),AREA(19),TITLE(15)
      DIMENSION U(1),V(1),X(100),Y(100),RANGE(4)
      REAL*4                    XCHAR(4)/1H+,1H*,1HX,1H./
      INTEGER A,B
      IF(MODCUR.EQ.1)WRITE(6,4)TITLE
    4 FORMAT('1',15A4///)
      CALL UTPLOT(U,V,NDATA,RANGE,KKZ,MODCUR)
      DO 2 I=1,NDATA
      X(I)=U(I)
      Y(I)=V(I)
    2 CONTINUE
C
C   INITIALIZE GRAPHIC DATA SETS
C
      CALL INGDS(IDEV,IGDSNM)
      CALL SDATM(IGDSNM    ,1)
      CALL SGDSL(IGDSNM,1.8,1.64,11.3,11.5  ,0.,0.,12.,12.)
      XMAX=RANGE(1)
      XMIN=RANGE(2)
      YMAX=RANGE(3)
      YMIN=RANGE(4)
      XRANGE=XMAX-XMIN
      YRANGE=YMAX-YMIN
      DX=XRANGE/56.
      DY=YRANGE/40.
      XLL=XMIN-DX
      XUR=XMAX+DX
      YLL=YMIN-DY
      YUR=YMAX+DY
      CALL SDATL(IGDSNM,XLL,YLL,XUR,YUR)
      CALL INGDS(IDEV,IGDSNN)
      CALL SDATM(IGDSNN    ,3)
      CALL SDATL(IGDSNN    ,0,0,73,51)
C
C   PLOT TITLE
C
      CALL PTEXT(IGDSNN    ,TITLE,60,NULL,NULL,NULL,0,51)
      CALL EXEQ(IGDSNN,&9998,&9999)
C
C   PLOT GRAPH FRAME
C
      A(1)=11
      B(1)=7
      A(2)=11
      B(2)=49
      A(3)=69
      B(3)=49
      A(4)=69
      B(4)=7
      CALL STPOS(IGDSNN    ,69,7)
      CALL PLINE(IGDSNN    ,A,B,NULL,NULL,NULL,4)
      CALL EXEQ(IGDSNN,&9998,&9999)
C
C   COMPUTE PROPER SCALE NUMBERS
C
 8000 XINCR=XRANGE/4.
      YINCR=YRANGE/4.
      XSCALE(1)=XMAX
      YSCALE(1)=YMAX
      DO 80 I=2,5
   80 XSCALE(I)=XSCALE(I-1)-XINCR
      DO 81 I=2,5
   81 YSCALE(I)=YSCALE(I-1)-YINCR
C
C   PLOTTING X AND Y AXIS, IF NECESSARY
C
      YTEST=YMAX*YMIN
      XTEST=XMAX*XMIN
      IF(XTEST)1,222,222
  222 IF(YTEST)333,444,444
    1 CONTINUE
      CALL STPOS(IGDSNM    ,0.,YMIN)
```

```
      CALL PLINE(IGDSNM    ,0.,YMAX)
      CALL EXEQ(IGDSNM,&9998,&9999)
      GOTO 222
  333 CONTINUE
      CALL STPOS(IGDSNM    ,XMIN,0.)
      CALL PLINE(IGDSNM    ,XMAX,0.)
      CALL EXEQ(IGDSNM,&9998,&9999)
  444 CONTINUE
C
C   PLOT SCALE NUMBERS
C
      REWIND 9
      DO 102 I=1,5
      WRITE(9,18)YSCALE(I)
   18 FORMAT(G1^.3,' - ')
  102 CONTINUE
      WRITE(9,54)
   54 FORMAT(12X,'|',4(13X,'|'))
      WRITE(9,22)XSCALE(5), XSCALE(4),XSCALE(3),XSCALE(2),XS
   22 FORMAT(4X,5(4X,G1^.3))
      END FILE 9
      REWIND 9
      DO 101 I=1,5
      READ(9,53)(AREA(K),K=1,19)
   53 FORMAT(19A4)
      LINE=48-(I-1)*1^
      CALL PTEXT(IGDSNN    ,AREA,12,NULL,NULL,NULL,0,LINE)
      CALL EXEQ(IGDSNN,&9998,&9999)
  101 CONTINUE
      DO 103 I=1,2
      READ(9,53)(AREA(K),K=1,19)
      LINE=8-I
      CALL PTEXT(IGDSNN    ,AREA,74,NULL,NULL,NULL,0,LINE)
      CALL EXEQ(IGDSNN,&9998,&9999)
  103 CONTINUE
      ITEMP1=IGDSNM
      ITEMP2=IGDSNN
      IERR=0
      GO TO 5
C
C   (NOTE:  ENTRY UPHCRT ALLOWS FOR ADDING CURVES TO GRAPH WH
C    HAS ALREADY BEEN LAID OUT -- CALLED BY PRNCRT)
C
      ENTRY UPHCRT(U,V,NDATA,RANGE,KKZ,MODCUR,TITLE,IGDSNM,I
C
      IF(MODCUR.EQ.3)WRITE(6,4)TITLE
      CALL UTHOLD(U,V,NDATA,RANGE,KKZ,MODCUR)
      DO 3 I=1,NDATA
      X(I)=U(I)
      Y(I)=V(I)
    3 CONTINUE
    5 CONTINUE
      IGDSNM=ITEMP1
      IGDSNN=ITEMP2
C
C   CHECKING X AND Y POINTS AND PLOTTING THOSE OUT OF RANGE A
C
      DO 2^  I=1,NDATA,KKZ
      IF(X   (I)-XMAX) 205,205,220
  220 X   (I)=XMAX +DX
      IERR=IERR+1
      GOTO 21^
  205 IF(X   (I)-XMIN)2^3,210,21^
  203 X   (I)=XMIN -DX
      IERR=IERR+1
  210 IF(Y   (I)-YMAX)215,215,212
  212 Y   (I)=YMAX +DY
      IERR=IERR+1
      GO TO 3^
  215 IF(Y   (I)-YMIN)217,  30,30
  217 Y   (I)=YMIN -DY
      IERR=IERR+1
```

```
   30 CONTINUE
C
C   PLACING POINTS IN THEIR PROPER POSITIONS
C
       IF(MODCUR.EQ.0.OR.MODCUR.EQ.1)JSET=0
       JSET=JSET+1
       IF(JSET.GT.4) JSET=1
       DO 91 I=1,NDATA,KKZ
       RXCHAR=XCHAR(JSET)
       XI=X(I)
       YI=Y(I)
       CALL PTEXT(IGDSNM,RXCHAR,1,NULL,NULL,NULL,XI,YI)
       CALL EXEQ(IGDSNM,&9998,&9999)
   91  CONTINUE
       IF(MODCUR.EQ.0.OR.MODCUR.EQ.3)GO TO 922
       RETURN
  922  CONTINUE
C
       IF(IERR) 1000,1000,1001
 1001  CONTINUE
       REWIND 9
       WRITE(9,20) IERR
   20  FORMAT( 'NUMBER OF POINTS OUT OF RANGE = ',I4)
       END FILE 9
       REWIND 9
       READ(9,53)(AREA(K),K=1,19)
       CALL PTEXT(IGDSNN   ,AREA,40,NULL,NULL,NULL,0,4)
       CALL EXEQ(IGDSNN,&9998,&9999)
 1000  CONTINUE
C      IF(MODCUR.EQ.3)RETURN
C
C   WAIT FOR END-KEY ATTENTION
C
       CALL CREATN(IATTN)
       CALL RQATT(IATTN,ICODE,NULL,&9998,&9999)
       CALL MPATL(IATTN,-1)
       CALL FNATL(IATTN)
       CALL TMGDS(IGDSNM)
       CALL TMGDS(IGDSNN)
       RETURN
 9998  CONTINUE
       RETURN 1
 9999  CONTINUE
       RETURN 2
       END


       SUBROUTINE PRNCRT(X,Y,NN,MODCUR,TITLE,*,*)
C
C   PRNCRT PRODUCES A POINT-PLOT ON THE 2250 DISPLAY.  IT CAN
C   SEVERAL CURVES ON THE SAME GRAPH, DEPENDING ON THE CALLED
C   MODCUR:
C      =0,   THIS IS THE ONLY CURVE FOR GRAPH
C      =1,   THIS IS THE FIRST OF SEVERAL CURVES FOR GRAPH
C      =2,   THIS IS AN INTERMEDIATE CURVE FOR GRAPH
C      =3,   THIS IS THE LAST OF MANY CURVES FOR GRAPH
C   X IS THE VECTOR OF ABSCISSAE
C   Y IS THE VECTOR OF ORDINATES
C   NN IS THE LENGTH OF VECTORS X AND Y (THE NUMBER OF POINTS
C   TITLE IS EITHER THE NAME OF A 60-BYTE ARRAY OR A 60-CHARA
C   CONSTANT.
C     PRNCRT CREATES THE PROPER RANGE VECTOR AND CALLS UTPCRT
C   POINTS OF THE FIRST CURVE ON A GRAPH.  SUCCEEDING CURVES
C   ARE TRUNCATED TO THE SAME RANGE AND PLOTTED WITH DIFFEREN
C   FIRST RETURN IS FOR RESTART, SECOND FOR TERMINATION
C   DATA SET FT09F001 MUST BE PROVIDED, DCB=(RECFM=F,LRECL=80
C
       COMMON/IGNORE/NULL,IDEV,IGSPNM
C
       DIMENSION X(51), Y(51), RANGE(4)
      1,NULL(1),AREA(19),TITLE(15)
       EQUIVALENCE (RANGE(1),XMAX), (RANGE(2),XMIN),(RANGE(3)
```

```
     1          (RANGE(4),YMIN)
C
C   BRANCH ON MODCUR
C
        IF(MODCUR.EQ.2.OR.MODCUR.EQ.1) GO TO 40
        GO TO 400
C
C   GAUGE INPUT DATA AND COMPUTE RANGE FOR FIRST OR ONLY CURV
C
   40   XMAX=-1.E20
        XMIN=1.E20
        YMAX=-1.E20
        YMIN=1.E20
C
        DO 1 I=1,NN
C
        IF(X(I)-XMAX) 6,6,2
  2     XMAX=X(I)
        YXMAX=Y(I)
  6     IF(X(I)-XMIN) 3,3,7
  3     XMIN=X(I)
        YXMIN=Y(I)
  7     IF(Y(I)-YMAX) 8,8,4
  4     YMAX=Y(I)
        XYMAX=X(I)
  8     IF(Y(I)-YMIN) 5,5,1
  5     YMIN=Y(I)
        XYMIN=X(I)
C
  1     CONTINUE
C
C   CALL UTPCRT PROPERLY
C
  400   IF(MODCUR.EQ.2.OR.MODCUR.EQ.3) GO TO 50
        CALL UTPCRT(X,Y,NN,RANGE,1,MODCUR,TITLE,&9998,&9999)
        GO TO 70
   50   CALL UPHCRT(X,Y,NN,RANGE,1,MODCUR,TITLE,IGD,IGD1,&9998
   70   IF(MODCUR.NE.3)RETURN
C
C   LIST TRUNCATION RANGE AFTER END OF MULTI-CURVE PLOT
C
        REWIND 9
        WRITE(9,101) YMAX, XYMAX,YMIN,XYMIN
 101    FORMAT( 'MAX Y = ',G14.7,' AT X = ',G14.7/
     1          'MIN Y = ',G14.7,' AT X = ',G14.7)
        WRITE(9,102) XMAX, YXMAX, XMIN, YXMIN
 102    FORMAT( 'MAX X = ',G14.7,' AT Y = ',G14.7/
     1          'MIN X = ',G14.7,' AT Y = ',G14.7)
        END FILE 9
        IGDSNM=IGD1
        REWIND 9
        DO 60 I=49,52
        READ(9,61)                  (APEA(K),K=1,19)
  61    FORMAT(19A4)
        J=52-I
        CALL PTEXT(IGDSNM,APEA,74,NULL,NULL,1,0,J)
        CALL EXEQ(IGDSNM,&9998,&9999,&62)
  60    CONTINUE
C
C   WAIT FOR END-KEY ATTENTION
C
        CALL CREATN(IATTN)
        CALL RQATT(IATTN,ICODE,NULL,&9998,&9999)
        CALL MPATL(IATTN,-1)
        CALL ENATL(IATTN)
  62    CONTINUE
        CALL TMGDS(IGD)
        CALL TMGDS(IGD1)
        RETURN
9998    CONTINUE
        RETURN 1
9999    CONTINUE
```

```
      RETURN 2
      END

      SUBROUTINE DELAY(N)
C
C   CAUSE TIME LAPSE OF N HUNDREDTHS OF A SECOND (REAL TIME)
C
      INTEGER TIME,DT
      TIME=ITIME(0)
    1 CONTINUE
      DT=ITIME(0)-TIME
      IF(DT.LT.N)GO TO 1
      RETURN
      END

      SUBROUTINE EXEQ(IGOSNM,*,*,*)
C
C   CONTROL DISPLAY REGENERATION -- HOLD FURTHER GRAPHIC DATA
C   BUFFER IS READY
C
      COMMON/ATTENT/IATNL
      COMMON/IGNORE/NULL,IDEV,IGSPNM
      CALL EGATN(IATNL,ICODE,1,NULL,0,31,32)
      IF(ICODE.EQ.-1)CALL START(&9998)
      IF(ICODE.EQ.31)CALL FINISH(&9998,&9999)
      IF(ICODE.EQ.32)RETURN 3
      CALL EXEC(IGOSNM)
      CALL DELAY(5)
      RETURN
9998  CONTINUE
      RETURN 1
9999  CONTINUE
      RETURN 2
      END

      SUBROUTINE GOGSP
C
C   INITIALIZE GSP, 2250, AND SEVERAL WORK-DATA-SETS
C
      COMMON/ATTENT/IATNL
      COMMON/IGNORE/NULL,IDEV,IGSPNM
C
      NULL=-5
C
      CALL INGSP(IGSPNM,NULL)
      GO TO 1
C
C   ENTRY PROVIDES FOR RE-INITIALIZATION
C
      ENTRY GGSP
      CALL TMDEV(IDEV)
C
    1 CONTINUE
      CALL INDEV(IGSPNM,22,IDEV)
      CALL SALRM(IDEV)
      CALL MLITS(IDEV,3)
      CALL CRATL(IDEV,IATNL)
      CALL ENATN(IATNL,0,31,32)
      RETURN
      END

      SUBROUTINE START(*)
C
C   RESPONSE TO RE-INITIALIZATION COMMAND DURING EXECUTION
C
      COMMON/IGNORE/NULL,IDEV,IGSPNM
C
      CALL SALRM(IDEV)
```

```
      CALL TMDEV(IDEV)
      CALL INDEV(IGSPNM,22,IDEV)
      CALL INITDS(IGDPGL,3,2,0.,0.,1.,1.,0.,0.,48.,34.,.TRUE
      DO 1 I=1,10
      CALL PTEXT(IGDPGL,'RESTARTING GSP...',17,NULL,NULL,NUL
    1 CONTINUE
      CALL EXEC(IGDPGL)
      CALL DELAY(100)
      RETURN 1
      END


      SUBROUTINE FINISH(*,*)
C
C   RESPONSE TO TERMINATION REQUEST DURING EXECUTION
C   (ALLOW ONE CHANCE TO CHANGE MIND)
C
      COMMON/IGNORE/NULL,IDEV,IGSPNM
C
      DIMENSION FMT(13)
      DATA FMT/'('1********** EXECUTION ABORTED BY USER ***
      CALL SALRM(IDEV)
      CALL TMDEV(IDEV)
      CALL INDEV(IGSPNM,22,IDEV)
      CALL INITDS(IGDPGL,3,2,0.,0.,1.,1.,0.,0.,48.,34.,.TRUE
C
C   INTENSIFY MESSAGE
C
      CALL BGSEQ(IGDPGL)
      DO 2 I=1,10
      CALL PTEXT(IGDPGL,'LAST CHANCE... START OR FINISH?',31
     1NULL,9,17)
    2 CONTINUE
      CALL ENSEQ(IGDPGL,KEY)
      CALL EXEC(IGDPGL)
      CALL CRATL(IDEV,IATNL)
      CALL ENATN(IATNL,0,31)
C
C   FLASH ENKB LIGHTS AND CRT DISPLAY
C
    1 CONTINUE
      CALL DELAY(50)
      CALL CMIT(IGDPGL,NULL,KEY)
      CALL MLITS(IATNL,2)
      CALL DELAY(50)
      CALL INCL(IGDPGL,NULL,KEY)
      CALL MLITS(IATNL,3)
      CALL RQATN(IATNL,ICODE,1,NULL ,0,-35)
      IF(ICODE.EQ.0)GO TO 1
      CALL MLITS(IATNL,1)
      IF(ICODE.EQ.-1)CALL START(&9998)
      CALL RESET(IGDPGL)
C
C   CONFIRM TERMINATION
C
      DO 3 I=1,10
      CALL PTEXT(IGDPGL,FMT(2),44,NULL,NULL,NULL, 3,17)
    3 CONTINUE
      CALL EXEC(IGDPGL)
      WRITE(6,FMT)
      CALL DELAY(500)
      CALL TMDEV(IDEV)
      RETURN 2
9998  CONTINUE
      RETURN 1
      END
```

```
      SUBROUTINE INITDS(IGDSNM,IDATM,ICHAM,X1,Y1,X2,Y2,X3,Y3
C
C   INTERFACE TO GSP GDS-CREATION AND OPTION-DEFINITION ROUTI
C
      COMMON/IGNORE/NULL,IDEV,IGSPNM
C
      LOGICAL LP
      CALL INGDS(IDEV,IGDSNM)
      CALL SGDSL(IGDSNM,X1,Y1,X2,Y2,0.,0.,1.,1.)
      CALL SDATL(IGDSNM,X3,Y3,X4,Y4)
      CALL SDATM(IGDSNM,IDATM)
      CALL SCHAM(IGDSNM,ICHAM)
      IF(LP)CALL SLPAT(IGDSNM,1)
      RETURN
      END


      SUBROUTINE CREATN(IATTN)
C
C   INTERFACE TO GSP 'CRATL'
C   MAINTAIN RESTART/ABORT LEVEL AS ACTIVE
C
      COMMON/IGNORE/NULL,IDEV,IGSPNM
C
      CALL CRATL(IDEV,IATTN)
      CALL MLPEO(IATTN,1,2,1)
      CALL MLPEO(IATTN,2,4,1)
      CALL MPATL(IATTN, 1)
      CALL ENATN(IATTN,0,31,32)
      RETURN
      END


      SUBROUTINE RQATT(IATTN,ICODE,/IRRAY/,*,*)
C
C   INTERFACE TO GSP 'RQATN'
C   RESTART OR ABORT ATTENTIONS TAKE PRECEDENCE
C
      COMMON/ATTENT/IATNL
      COMMON/IGNORE/NULL,IDEV,IGSPNM
C
      DIMENSION IRRAY(1)
      CALL RQATN(IATNL,ICODE,1,NULL,0,31,32)
      IF(ICODE.EQ.-1)CALL START(&9998)
      IF(ICODE.EQ.31)CALL FINISH(&9998,&9999)
      IF(ICODE.EQ.32)RETURN
      CALL MPATL(IATTN,-1)
      CALL RQATN(IATTN,ICODE,2    ,IRRAY,0,-35)
      CALL MPATL(IATNL,-1)
      IF(ICODE.EQ.-1)CALL START(&9998)
      IF(ICODE.EQ.31)CALL FINISH(&9998,&9999)
      RETURN
9998  CONTINUE
      RETURN 1
9999  CONTINUE
      RETURN 2
      END
```

LIST OF REFERENCES

1. Aeronautical Research Com. R and M 1561, The Flow Near a Wing Which Starts Suddenly from Rest and then Stalls, by R. H. Francis and J. Cohen, 1933.

2. Liiva, Jaan, Unsteady Aerodynamic and Stall Effects on Helicopter Rotor Blade Sections, paper presented at 6th Aerospace Sciences Meeting, New York, N. Y., January 1968.

3. Liiva, Jaan and Davenport, Franklyn J., Dynamic Stall of Airfoil Sections for High Speed Rotors, paper presented at 24th American Helicopter Society, Inc., Annual National Forum, Washington, D. C., May 1968.

4. N.A.C.A. Technical Note Number 1326, Airfoil in Sinusoidal Motion in a Pulsating Stream, by J. Mayo Greenberg, June 1947.

5. Isaacs, Rufas, "Airfoil Theory for Flows of Variable Velocity", Journal of Aeronautical Sciences, V. 12, p. 113-117, January 1945.

6. Nickerson, R. J., The Effect of Free Stream Oscillations on the Laminar Boundry Layer on a Flat Plate, Sc.D. Thesis, Massachusetts Institute of Technology, 1957.

7. Hori, E., "Experiments on the Boundry Layer of an Oscillating Circular Cylinder", Bulletin of the Japan Society of Mechanical Engineers, V. 6, n. 22, p. 201-209, 1963.

8. Hill, P. G., Laminar Boundry Layers in Oscillatory Flow, Sc.D. Thesis, Massachusetts Institute of Technology, 1958.

9. Karlsson, S. F., An Unsteady Turbulent Boundry Layer, Ph.D. Thesis, Johns Hopkins University, 1958.

10. Miller, J. A., Transition in Oscillating Blasius Flow, Ph.D. Thesis, Illinois Institute of Technology, June 1963.

11. Allen, T. J., Pressure Distribution on an Airfoil in Oscillating Flow, M.S. Thesis, Naval Postgraduate School, Monterey, California, June 1969.

12. N.A.C.A. Technical Report Number 824, Summary of Airfoil Data, by Ira H. Abbott, Albert E. von Doenhoft, and Louis S. Stivers, Jr., 1945.

13. Bendat, J. S. and Piersol, A. G., Measurement and Analysis of Random Data, John Wiley and Sons, Inc., 1966.

14. Johnson, R. B., A Technique for Measuring Unsteady Pressures, A.E. Thesis, Naval Postgraduate School, Monterey, California, September 1968.

15. Cooley, J. W. and Tukey, J. W., "An Alogrithm for the Machine Calculation of Complex Fourier Series", Mathematics of Computations, V. 19, (April 1965), p. 297.

INITIAL DISTRIBUTION LIST

		No. Copies
1.	Defense Documentation Center Cameron Station Alexandria, Virginia 22314	2
2.	Library, Code 0212 Naval Postgraduate School Monterey, California 93940	2
3.	Commander, Naval Air Systems Command Department of the Navy Washington, D. C. 20360	10
4.	Dean of Research Administration Naval Postgraduate School Monterey, California 93940	2
5.	Chairman, Department of Aeronautics Naval Postgraduate School Monterey, California 93940	1
6.	Professor James A. Miller Department of Aeronautics Naval Postgraduate School Monterey, California 93940	10
7.	Captain Maurice R. Banning, USMC 2525 Walnut Street Orange, California 92668	1
8.	Commandant of the Marine Corps (Code AO3C) Headquarters, U. S. Marine Corps Washington, D. C. 20380	1
9.	James Carson Breckinridge Library Marine Corps Development and Educational Command Quantico, Virginia 22134	1

Security Classification

DOCUMENT CONTROL DATA - R & D

(Security classification of title, body of abstract and indexing annotation must be entered when the overall report is classified)

ORIGINATING ACTIVITY *(Corporate author)*

Naval Postgraduate School
Monterey, California 93940

2a. REPORT SECURITY CLASSIFICATION

Unclassified

2b. GROUP

REPORT TITLE

The Unsteady Normal Force on an Airfoil in Oscillating Flow

DESCRIPTIVE NOTES *(Type of report and, inclusive dates)*

Aeronautical Engineer; December 1969

AUTHOR(S) *(First name, middle initial, last name)*

Maurice Ray Banning

REPORT DATE	7a. TOTAL NO. OF PAGES	7b. NO. OF REFS
December 1969	171	15

a. CONTRACT OR GRANT NO.	9a. ORIGINATOR'S REPORT NUMBER(S)
b. PROJECT NO.	
c.	9b. OTHER REPORT NO(S) *(Any other numbers that may be assigned this report)*
d.	

0. DISTRIBUTION STATEMENT

This document has been approved for public release and sale; its distribution is unlimited.

1. SUPPLEMENTARY NOTES	12. SPONSORING MILITARY ACTIVITY
	Naval Postgraduate School Monterey, California 93940

3. ABSTRACT

The effects of oscillating flow on the pressure force normal to the chord of a symmetrical airfoil were investigated experimentally employing a remote pressure transducer to measure the instantaneous pressure distribution.

An open circuit wind tunnel having a set of rotating shutter blades located down stream of the test section was used to produce the oscillating flow. Electrical signals analogous to the free stream velocity and surface pressure were recorded simultaneously on separate tracks of a magnetic tape. The recorded data were converted to digital representation, and numerical techniques utilized to evaluate the spectral composition of the measured pressure distribution, from which the normal force was calculated.

It was found that the magnitude of the total normal force at high angles of attack is significantly greater in oscillating flow than in steady flow and is frequency dependent; while at low angles of attack no significant differences were observed. Moreover it was found that higher order harmonics of the fundamental free-stream frequency constitute a significant fraction of the normal force, and these fractions are also frequency dependent. The observed results are not adequately predicted by quasi-steady aerodynamic analysis.

DD FORM 1 NOV 65 1473 (PAGE 1)

S/N 0101-807-6811

Security Classification

A-31408

14 KEY WORDS	LINK A		LINK B		LINK C	
	ROLE	WT	ROLE	WT	ROLE	WT
Airfoil						
Oscillating Flow						
Unsteady Normal Force						

DD FORM 1 NOV 65 1473 (BACK)

S/N 0101-807-6821

thesB214
The unsteady normal force on an airfoil
3 2768 002 01389 8
DUDLEY KNOX LIBRARY